EPA-650/2-74-086-a

SEPTEMBER 1974

Environmental Protection Technology Series

PROCEDURES FOR MEASUREMENT IN STRATIFIED GASES VOLUME I

Office of Research and Development
U.S. Environmental Protection Agency
Washington, DC 20460

EPA-650/2-74-086-a

PROCEDURES FOR MEASUREMENT IN STRATIFIED GASES VOLUME I

by

A. Zakak, R. Siegel, J. McCoy, S. Arab-Ismali,
J. Porter, L. Harris, L. Forney, and R. Lisk

Walden Research Division of Abcor, Inc.
201 Vassar St.,
Cambridge, Massachusetts 02139

Contract No. 68-02-1306
Program Element No. 1AB013
ROAP No. 21ACX-092

EPA Project Officer: William B. Kuykendal

Control Systems Laboratory
National Environmental Research Center
Research Triangle Park, North Carolina 27711

Prepared for

OFFICE OF RESEARCH AND DEVELOPMENT
U.S. ENVIRONMENTAL PROTECTION AGENCY
WASHINGTON, D.C. 20460

September 1974

This report has been reviewed by the Environmental Protection Agency and approved for publication. Approval does not signify that the contents necessarily reflect the views and policies of the Agency, nor does mention of trade names or commercial products constitute endorsement or recommendation for use.

TABLE OF CONTENTS

TABLE OF CONTENTS (continued)

APPENDIX A through J - See Volume II

LIST OF FIGURES

LIST OF FIGURES (continued)

LIST OF FIGURES (continued)

LIST OF FIGURES (continued)

LIST OF TABLES

LIST OF TABLES (continued)

SECTION I

CONCLUSIONS

Results from the literature and field surveys indicate that gas stratification exists, but it is likely to be less general and less severe than particulate stratification. For a given gas stream, it is necessary to make a preliminary gas concentration survey to determine the existance of spatial stratification.

Where stratification exists, we have concluded as a result of this program, that there are two methods of obtaining representative gas samples. Where conditions permit, we recommend a system of monitoring the ratio of pollutants such as SO_2, NO_x, etc. to CO_2 from a single location. Then from the measured fuel flow and chemistry of the process, the mass flow of CO_2 is the mass flow of the pollutant. Where conditions do not permit such a system, we recommend a schedule of manual surveys and installation of a multi-element proportional sampler and gas velocity array.

We also examined the use of devices to mix stratified gas streams. Our conclusion is that passive mixing devices are unlikely to be useful mixing devices due to the practical problem of retrofitting high pressure drop devices to existing boiler duct work. An active mixing device using jet of flue gas was theoretically examined and appears promising; however, definite conclusions on the effectiveness of this approach is withheld in the observance of an experimental evaluation.

SECTION II

RECOMMENDATIONS

In the course of this project, areas requiring further development were identified. These are as follows:

A. A program is needed to develop an automatic instrumentation system for extracting continuous representative gas samples from stratified gas streams, for example, a multi-probe automatic proportional gas sampler which would be practical in terms of cost and adaptability to various process streams.

B. A program is needed to develop techniques for determining the total gas flow profile or velocity vector in process streams. It is likely that in practice a significant fraction of errors in emission measurements are attributable to errors in gas velocity/flow determination. (It is understood that development in this area is in progress.)

C. Further documentation of the extent and frequency of gas stratification in process streams together with statistical analyses of data would be helpful in refining sampling methodologies. (It is understood that a program to gather some of this data will be starting soon.)

D. An experimental program is required to assess fully the practicality of using jets to mix flue gases.

SECTION III
INTRODUCTION

This final report marks the conclusion of a ten-month program, the object of which was to develop methods for the continuous extraction of a representative gas sample from stratified streams. A representative sample is one which permits an accurate deduction of a gaseous pollutant emission or mass flow through a test section. This program is the first study known to us involving theoretical and experimental investigation into the problem of gas sampling in stratified flow. However, the concept of accounting for stratification in the determination of particulate emission is well known and appreciated. In the course of this program, we found that there is little documentation on the extent of spatial variations of gas concentrations in full-scale power plant effluent streams. Nevertheless, the available documentation as well as our program data indicate that such stratification exists, although it is unlikely that gas stratification is as widespread or as severe as particulate stratification. One of the results of this program was the formulation of procedures for obtaining representative gas samples in the presence of gas concentration stratification.

The program was organized into three tasks, viz.:

- Task I - Survey
- Task II - Development
- Task III - Demonstration

Task I activities were divided into literature and field survey sub-tasks. The first sub-task involved a literature and personal contact survey to obtain and evaluate: 1) documentation of gas concentration and velocity profiles for process streams, 2) information on sampling procedures, 3) information on mixing process streams, and, 4) information on sampling devices. The second sub-task involved the performance of field measurements on four ducts of two power plants to obtain information on gas stratification.

Task II was divided into an analytical development sub-task and an experimental sub-task. In the analytical sub-task, sampling methodologies were investigated and a method of mixing flue gases using gas jets was examined. In the experimental sub-task, laboratory experiments using various measurement techniques were conducted in a wind tunnel. The results of these sub-tasks indicate several approaches to the problem of obtaining emission measurements in stratified flow.

Task III was a demonstration task. Based on the results of Tasks I and II, procedures for extracting representative gas samples from stratified process streams were identified and the most potentially reliable of these were further developed. Different steps utilized in these favored procedures were then demonstrated on a full-scale power plant.

SECTION IV

PROGRAM

A. TASK I - LITERATURE AND FIELD SURVEY

1. LITERATURE SEARCH

The literature survey involved an examination of the open literature as well as a personal inquiry into the present knowledge of flue gas stratification and the state of existing technology for sampling stratified gases. Approaches to sampling flue gases are evaluated for sampling in stratified gas streams.

a. Background and Summary

The problem of sampling stratified gas streams for gases has not been as universally appreciated by practitioners as has the problem of sampling for particulate matter. However, where investigators have been concerned with gas stratification, the approach has been to mimic the spatial methodology used for the sampling of particulate matter, viz., to sub-divide the sampling plane of the test duct into a number of equal sub-areas and to extract samples from the centroids of the sub-areas.

This search found documentation for only single arbitrary point sampling and the centroid of equal approach mentioned above. No recommended methodology was found such as those commonly reported for velocity and particulate sampling.

It was found that people experienced in the sampling of effluent from boilers recognize a rule of thumb in regard to the composition of gas streams. This rule is not documented but is in accord with intuitive notions of air in-leakage, i.e., high gas velocity gives low O_2 concentration.[1]

No instrumentation designed for obtaining a representative sample of gases was found which samples gases representatively for emission, although multipoint gas samplers have been reported which account for spatial variation over the sampling plane. In the following section (Section IV, B.1.b., Sampling Methodologies), it is shown by mathematic development that to obtain a representative gas sample, certain sampling parameters must be made proportional

to the gas stream velocity (speed) at the sampling location. While no instrumentation intended for proportional sampling of gas was found, there are available a number of descriptions of actual and conceptual instruments for the isokinetic sampling of particulate matter. Since isokinetic sampling is a special case of proportional sampling, these instruments are described and evaluated in terms of applicability to gas sampling with consideration for simplicity, hence economy of implementation.

Other schemes which obviate traversing techniques are evaluated. A method using a diffusion tube(s) across the sampling plane was examined. In principle, this device can obtain a spatial average of the concentration along the tube and an emission average for the special case of a flat (constant value) velocity profile. However, in practice, it is expected that a temperature profile in the sampling plane would also effect the sample. For these reasons an in-stack diffusion tube technique is not a promising area for development.

Another technique examined was the use of a tracer gas to obtain a representative sample from a single point stack gas extraction. Two general approaches to this method are to introduce a special tracer gas into the gas stream or to use an intrinsic gas in the effluent. The approach of using special tracer gases is, in principle, an unreasonable approach. On the other hand, the use of an intrinsic tracer, e.g., CO_2, has no obvious technological problems and thus warrants further developmental work (see section IV, A.2., Field Survey).

This search found reports of gas mixing using mixing orifices or baffles (usually half area). The devices are for use on laboratory or pilot plant scale experiments. This approach is not practical for retrofitting to full-scale systems because of the obvious adverse pressure drop which would be produced in the flue gas stream.

b. Sampling Systems

b.1. General

Given a suitable sampling methodology, certain resolutions must be made as to which approach will be used to implement sampling. As shown in the analytical section for sampling methodologies, a sample must be extracted which is volumetrically proportional to the stack gas velocity. The first resolution to be made is whether to use a single traversing (moving) sampling nozzle or a fixed array of sampling nozzles. A combination of these approaches, i.e., a moving array, would compound the disadvantages of both methods with little advantage over either method.

While the single traversing nozzle reduces the complications of building an array with a multitude of proportional sampling nozzles, the expense is incurred of building a complicated in-stack mechanism for moving the nozzle about. Additionally, the single probe approach is intrinsically unable to obtain a simultaneous measurement over the sampling plane. Without a formal cost effectiveness analysis, it seems that a fixed array of sampling probes would be the most satisfactory approach.

The practical choice of the type of proportional sampling system is between sampling at a flow rate proportional to the local stack gas velocity or at a fixed flow rate for all nozzles in the array but at times proportional to the stack gas velocity. Both of these approaches, of course, require a sample integrating scheme to operate. The approach in which the sampling time is proportional to the stack gas velocity will not provide a rigorous simultaneous measurement. However, the whole array could be sampled in a short time compared to process times, e.g., 1 minute. Therefore, if the whole array is sampled cyclically, the measurement would be virtually simultaneous. This technique requires that the gas analyzer has a response time much shorter than the scan time over the array.

b.2. Proportional Samplers

Regardless of the choice (type of methodology employed) of methodology (probe location and number), it is necessary that gas concentration measurements at a sampling point be weighted by the local gas velocity and the area ascribed to that probe. In the common methodologies, where each sample is taken to represent an equal area of the duct, it is required that all samples extracted be volumetrically proportional to the local stack gas velocity. The obvious ways to satisfy these conditions are the following:

(a) sample flow rate proportioned to the local stack gas velocity for equal times

(b) sample equal flow rates for times proportioned to the local stack gas velocity

The approach indicated by (a) is used in the isokinetic sampling of particulate matter. A variety of devices has been proposed and employed for the automatic collection of particulates. Before discussing these devices, additional requirements for isokinetic sampling which do not apply to proportional sampling should be indicated. By definition isokinetic sampling denotes that the stack gas stream is not accelerated in the vicinity of the inlet to the nozzle. This requirement involves constraints applicable only to ioskinetic sampling, viz.:

- the axis of the sampling nozzle must be parallel to the stack gas stream with the nozzle facing into the stream

- the gas velocity (vector) at the face of the nozzle must be identical to the stack gas velocity in the neighborhood of the nozzle

It is seen that when (b) above is satisfied, the requirements for proportional sampling are satisfied. The proportionality of the sample flow to the stack gas velocity is the nozzle area.

This search found no reports of automatic proportional samplers; however, documentation of several isokinetic samplers was found. Descriptions of particular automatic isokinetic instruments are presented in Appendix A.

Three general approaches have been used in automatic isokinetic samplers. These are the following:

(1) null balance probe

(2) computation and adjustment of sample flow rate based on information from a velocity measurement in the neighborhood of the sampling nozzle

(3) passive, gas stream driven sampler

In the null balance nozzle, the flow (velocity) of the sample through the nozzle is matched to the stack gas flow (velocity) just outside the nozzle. In this approach, the temperature and pressure of the sample stream at the sample sensor are assumed to be (or made to be) identical to the temperature and pressure of the stack gas stream at the reference sensor. Sensors which have been or could be used include:

- static pressure probes
- temperature probes
- thermal anemometers

Examples of the null static pressure types are described in Volume II, on pages 1 through 3 and Reference 50. An example of a null temperature probe type is shown on page 4. Thermal anemometers located in the sampling nozzle and just outside the nozzle are straightforward applications of a null approach. An attractive feature of this approach is the simplicity with which an error signal is obtained to operate a closed-loop servo-mechanism for flow control. It is significant that the only reference to a system implementing automatic multi-point isokinetic sampling was of the null balance type (see page 3).

Computation of the sample flow rate from a velocity measurement made in the neighborhood of the sampling nozzle involves the automation of the usual manual procedure for isokinetic sampling. Examples of instruments using this approach are shown in Volume II, on pages 5 through 9. Even to the casual glance this approach is more complex than the null balance approach, and hence, it is not attractive for a multi-point sampling system.

The last approach for discussion is a passive device which is operated, hence adjusted, by the gas flow. This is an attractive approach since it eliminates the need for a servomechanism for control. A particular example of this type of device is shown on page 10 in Volume II.

b.3. Arrays and Traversing Mechanisms

Probe arrays and mechanical traversing mechanisms may be used to implement sampling methodology. Shown in Appendix B are some examples of these approaches. Generally, the arrays have been used to obtain a spatial average of concentration over the sampling plane. The array system (Volume II, P. 13) could have an interesting extension if the sample time for each probe were adjusted to be proportional to the stack gas velocity. This would of course require a companion array of velocity sensors and a logic system for control.

It was suggested that a gas sample be extracted from an Annubar instrument[2] (Volume II, p. 16). However, sampling from this instrument did not lead to a representative sample. Sampling conditions and results are reported in the laboratory tests section.

Mechanical systems which move a single sensor over a sampling plane have been constructed, but these devices can become very complex.[18] A simpler system which is mechanically driven, is commercially available for a particulate analyzer. This system is shown in Volume II, p. 17. Inquiry into the rationale for the trajectory of this system revealed that it was designed principally for convenience and based on the assumption that it was an improvement over a single point measurement.

It is significant to note that in rectangular ducts, averaging was recommended (Volume II, p. 18) along the diagonal axis of the test section, including the corner points and sampling through a common manifold. By this method, a true average can be obtained only when a uniform flow exists across the duct cross section.

b.4. Diffusion Tube Samplers

The use of diffusion tubes located over the sampling plane has been suggested as a method for obtaining a representative gas sample from flue gas. It is shown in Appendix C that this approach will, in principle, give a spatial sample average, but is unlikely to give a representative sample for emissions except in the special but trivial case of virtually constant gas velocity over the sampling plane. Diffusion tubes have been used in stack sampling[3] where the intent has been only to separate the sample gas from moisture and particulate matter. Diffusion tube devices are temperature dependent; hence, in applications where a spatial average is sought, an erroneous answer is obtained where gas temperatures are stratified over the sampling plane.

A reference to a proposed method for controlling temperature of a diffusion sampling tube using a heat pipe was found (see Appendix D). However, the fact that diffusion tubes will only provide a spatial average and not an emission average makes this approach unpromising and would not warrant the temperature stabilizing development effort.

A sampling scheme using an out-of-stack diffusion tube is outlined in Appendix C, Figures C-1 and C-3. This conceptual design eliminates the need for a servo-mechanism for proportional control and is similar to the device shown in Appendix A, Figure A-10. Preliminary calculations were made in order to estimate the length of diffusion tubes required. The detailed calculations are shown in Appendix C. Results show that the length of Teflon PTFE necessary to permeate 5,000 ppm at 100°C

from a 50×10^{-6} m^3/sec. stream flow is 2.8×10^5 m. While this length may be reduced by increasing the tube permeability (using silicon rubber and raising the temperature) and by decreasing the flow to a minute amount, obtaining a tube of reasonable length does not appear promising.

b.5. Tracer Techniques

It is almost a classical idea to use a tracer material to measure volumetric flow of fluids (see Appendix E). For an example, see reference 4. Tracers may be of two types, viz.:

- introduced to the process stream
- intrinsic to the process stream

An approach to representative sampling using a tracer introduced into the gas stream is, in principle, an unreasonable approach. Setting aside the practical concerns of what material to use as a tracer, volumes required, etc., it is obvious that to be of an advantage, the tracer must be well mixed with the gas stream. It is obvious that any effort to mix the tracer might as well be directed toward homogenizing the gas stream. This, however, would eliminate the need for a tracer.

The use of an intrinsic tracer, e.g., CO_2, is theoretically applicable. However, there may be some philosophical resistance to this approach, since process data such as fuel rate and analysis must be obtained external to the direct sample measurement. This approach has proven to be viable for many locations and is a recommended procedure.

In the field survey subtask of this program, field data from coal and oil power plants were taken on the ratio of SO_2 to CO_2 across the sampling planes. The low amount of gas stratification in all cases was such that no comprehensive test of the method was made.

c. Gas Mixing Systems

A system which mixes the flue gases would reduce the sampling procedure to a simple single point gas concentration measurement, providing emission data when multiplied by the total flow. The flow measurement may be made anywhere along the duct system. Baffles, usually one-half area plates, have been used for mixing gas streams[5,6]. This approach is incompatible with retrofitting to full scale systems because intolerable pressure drops are produced in the process stream.

The method of using jets to mix the gas streams was examined analytically (see jet mixing section, Section IV, B.c.). Preliminary results indicated that the power required for the mixing jet can be modest as compared to the power required to drive flue gas through the duct. However, scaled laboratory experiments should be performed to test the analytical results prior to any full-scale demonstration of this approach.

d. Conclusions and Recommendations

This search found that there is no generally recognized or specifically reported sampling methodology (sampling strategy) for stratified gases. When the problem of measuring stratified gases has occurred, it has been handled on an ad hoc basis, frequently by the use of rakes or probe arrays which account only for spatial variations of gas concentrations with no consideration of velocity, hence emission. Development of a rational sampling methodology is a promising analytical approach. Such an approach was undertaken as a part of this study and is reported elsewhere in this report.

No reports of automatic proportional gas samplers were found. However, three general approaches to isokinetic sampling have been identified, which could form the conceptual basis for automatic proportional sampler design. Of the three approaches, null balance and the gas driven approach seem most promising for instrument development, since these devices appear to offer some simplicity of implementation. A conceptual example is given in Figure 1. A null probe is shown using either a thermal anemometer or a

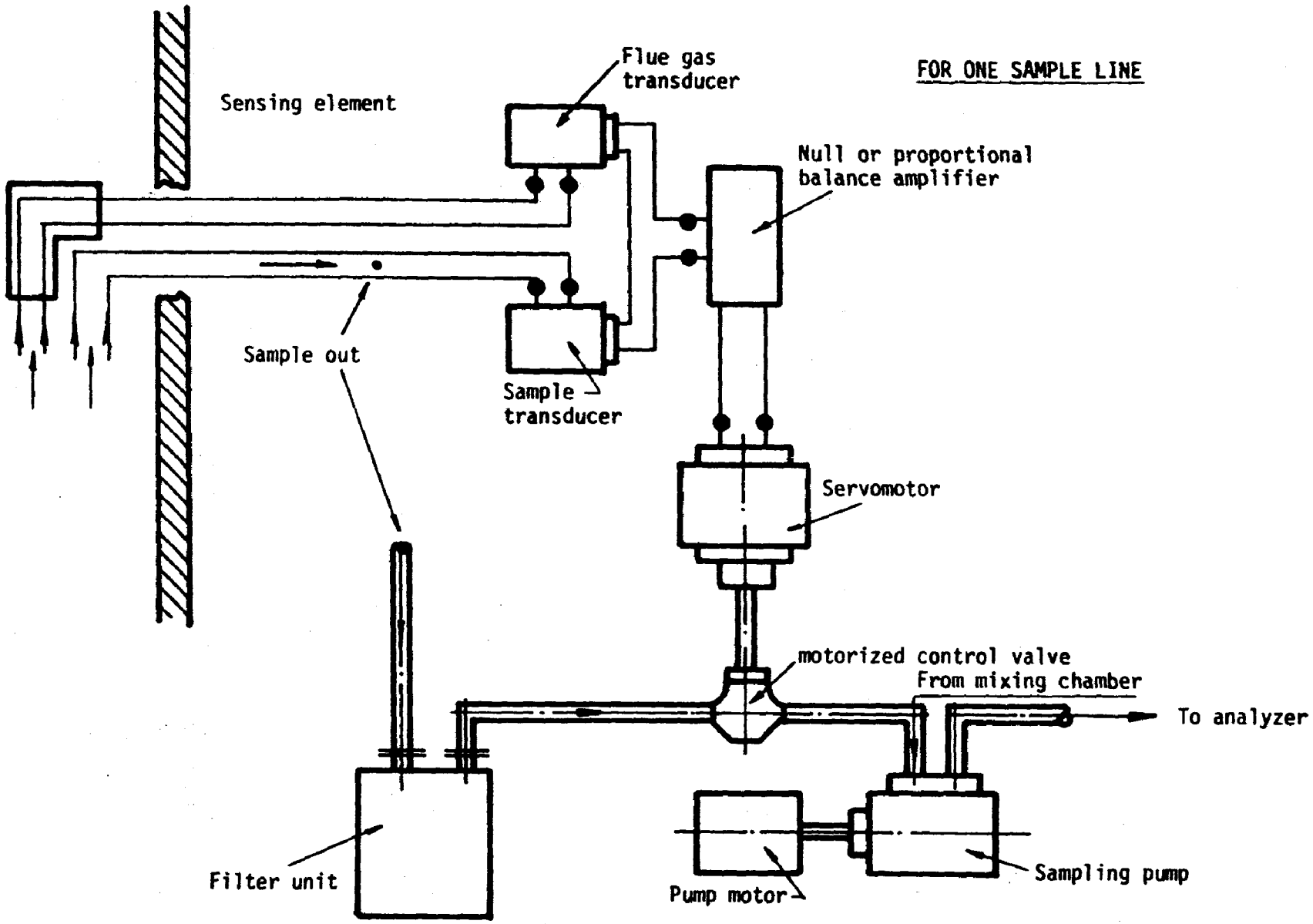

Figure 1. A Null Probe

thermocouple sensor approach[7,8,9,10]. The null probe method is a straightforward application of servo-mechanisms. For multi-point arrays the sensors and servomechanisms would, of course, have to be repeated for each element of the sample array. The development of this concept is promising but requires an extensive program.

The conclusions reached from examining mechanical traversing schemes is that a considerable effort with a large amount of complicated machinery is necessary to achieve a rational traversing plan. From a common sense point of view, mechanical traversing schemes appear complex compared to the more promising fixed array of probes.

A possible area for development of the probe array approach is to use both a sampling nozzle array system (conventional gas-extractive probes) with an associated velocity array. The data from the velocity array would be used to control the sampling time (the volume by design) sequentially for each probe proportional to the local stack gas velocity. A logic controlled system for this approach, though straightforward, is not trivial. It has been reported by Grandville[13] that at locations remote from bends or obstruction and where the mean velocities are greater than about 20 ft. per sec., the flow distribution patterns are often similar, although the total flow rate may vary. Given these conditions, a simple control system using a timer program could be implemented which would be dependent only on the velocity profile (relative velocity) and not the value of total flow. On installation of the system, the timer would be adjusted for the particular flow profile. The total flow may be determined by a single, independent velocity measurement. This appears to be a very promising area for development; however, more substantial evidence on the behavior of flow profile preservation under fluctuations of total flow would be necessary before pursuing this approach.

The use of a tracer introduced to the gas stream is not a promising approach. The use of an intrinsic tracer, e.g., CO_2, is a recommended approach. The scheme of producing a constant gas concentration over the sampling plane by use of an upstream mixing device is not promising for when

devices such as baffles are used, intolerable pressure drops are introduced into the system. The approach which involves using a jet mixing scheme is promising. However, before attempting a full-scale application, scaled laboratory experiments are recommended to validate the analytical results indicated in this report.

2. FIELD SURVEY

The results of the field survey are presented herein. Data were taken from a total of four sampling planes using NDIR analyzers for SO_2 and CO_2 concentrations and an S-type pitot tube for velocity. Two of the sampling planes were located across the ductwork of a coal-fired power plant (Bow, New Hampshire), and two were located across the ductwork of an oil-fired power plant (Weymouth, Massachusetts). The data from the coal-fired power plant were taken from locations just before and just after the electrostatic precipitator. The data from the oil-fired plant were taken from locations on ductwork just before the stack breaching. In all cases, existing sampling ports were used; hence, no special efforts (other than inspection) or costs were made to obtain sampling planes in locations of known gas stratification.

a. Sampling Procedure

The data taken were simultaneous concentrations of SO_2 and CO_2 by NDIR analysis and pitot tube heads. Attempts were made to collect information on gas temperature and angle of attach but instrumental problems precluded reliable data. A fine sampling mesh (2 inches) was used near the walls but somewhat further apart (on some locations) near the center (6-inch mesh). Because of the fine sampling mesh, several hours were necessary to traverse a duct; hence, temporal variations in concentration may effect the data.

b. Results

The data have been reduced and normalized to the following forms:

$$(a)\quad \frac{SO_2 \text{ concentration}}{\text{average } SO_2 \text{ concentration}}$$

$$(b)\quad \frac{\dfrac{SO_2 \text{ concentration}}{CO_2 \text{ concentration}}}{\text{average } \dfrac{SO_2}{CO_2} \text{ concentration}}$$

$$(c)\quad \frac{\sqrt{\Delta P}}{\text{average } \sqrt{\Delta P}} \approx \frac{\text{velocity}}{\text{average velocity}}$$

The set of points represented by (a) and (c) describe the SO_2 and velocity profiles over the sampling planes. The set of points represented by (b) describe the differences between the SO_2 concentration profile and the CO_2 profile.

Tables 1 through 4 present the normalized data. The distance values denote the insertion depth of the probes. The standard deviation (S.D.), the mean (average) and the coefficient of variation (CV) have been calculated for both the set of points associated with a port and the set of points associated with the whole sampling plane. This breakdown was done because the total time to traverse the whole sampling plane took several hours (approximately a work day in some cases) and no fixed-point reference probes were used to gather correction data to account for temporal variation in the process stream. Therefore, the set of points associated with a port are more closely related in time than the set for a whole sampling plane.

A summary of the amount of gas stratification for all sampling planes is shown in Table 5, along with the amount of velocity stratification. The amount of gas stratification shown for the coal-fired power plant data is so low that it probably reflects the precision of the analyzers as much as the amount of gas stratification. The amount of SO_2 stratification for the oil-fired power plant data is higher than the suspected precision of the analyzers, but the magnitudes represent only a moderate amount of stratification.

TABLE 1

COAL-FIRED "OUTLET"

$\frac{\sqrt{\Delta P}}{\sqrt{\Delta P}}$	$\frac{\overline{SO_2}}{\overline{CO_2}}\ \frac{SO_2}{CO_2}$	$\frac{SO_2}{\overline{SO_2}}$	Distance (Inch)		$\frac{\sqrt{\Delta P}}{\sqrt{\Delta P}}$	$\frac{\overline{SO_2}}{\overline{CO_2}}\ \frac{SO_2}{CO_2}$	$\frac{SO_2}{\overline{SO_2}}$	Distance (Inch)	
0.48	0.983	1.016	0		0.47	0.868	1.016	0	
0.93	0.970	1.029	2		0.95	0.900	1.054	2	
0.98	0.983	1.016	4		0.93	0.911	1.079	4	
1.05	0.952	1.029	6		0.95	0.932	1.104	6	
1.09	0.963	1.041	8		0.95	0.922	1.092	8	
1.09	0.963	1.041	10		1.02	0.922	1.092	10	
1.12	0.963	1.041	12		1.05	0.932	1.079	12	
1.12	0.966	1.054	14		1.02	0.932	1.079	14	
1.14	0.968	1.066	16		1.05	0.932	1.079	16	
1.14	0.974	1.073	18		1.02	0.932	1.079	18	
1.14	0.961	1.079	20		1.02	0.932	1.079	20	
1.14	0.955	1.073	22		1.02	0.932	1.079	22	
1.14	0.955	1.079	24		1.02	0.922	1.066	24	
1.09	0.966	1.092	26		1.05	0.922	1.066	26	
1.09	0.966	1.092	28		1.05	0.916	1.054	28	
1.09	0.961	1.085	30		1.05	0.916	1.054	30	
1.12	0.955	1.079	32		1.02	0.938	1.079	32	
1.09	0.955	1.079	34		1.05	0.956	1.054	34	
1.11	0.961	1.085	36		1.09	0.933	1.054	36	
1.11	0.966	1.092	38		1.09	0.933	1.054	38	
1.13	1.058	1.079	40		1.07	0.945	1.041	40	
1.13	1.066	1.073	42		1.09	0.944	1.054	42	
1.13	1.058	1.079	44		1.14	0.944	1.054	44	
1.11	1.058	1.079	46		1.12	0.944	1.066	46	
1.11	1.071	1.092	48		1.09	0.933	1.054	48	
1.11	1.069	1.098	50		1.09	0.927	1.066	50	
1.11	1.057	1.085	52		1.07	0.933	1.054	52	
1.09	1.051	1.079	54		1.07	0.922	1.066	54	
1.14	1.045	1.079	56		1.05	0.933	1.079	56	
0.89	1.045	1.079	58		0.98	0.911	1.079	58	
--	--	--	60		--	--	--	60	
0.127	0.045	0.023			0.115	0.016	0.0176	SD	
1.073	0.995	1.068			1.021	.927	1.0668	AVG	
11.84%	4.52%	2.15%			11.26%	1.73%	1.65%	C V*	

Bow Outlet #2 Port (Coal Fired)

Bow Outlet #1 Port (Coal Fired)

AVG SIX PORT

	S.D.	AVG.	C V*
$SO_2/\overline{SO_2}$	0.0205	1.000	2.05%
$SO_2/CO_2/\overline{SO_2}/\overline{CO_2}$	0.0263	1.005	2.62%
$\sqrt{\Delta P}/\sqrt{\overline{\Delta P}}$	0.1156	0.991	11.68%

* Coefficient of variation

TABLE 1 CONT'

$\frac{\sqrt{\Delta P}}{\sqrt{\Delta P}}$	$\frac{\overline{SO_2}}{\overline{CO_2}}\ \frac{SO_2}{CO_2}$	$\frac{SO_2}{\overline{SO_2}}$	Distance (Inch)		$\frac{\sqrt{\Delta P}}{\sqrt{\Delta P}}$	$\frac{\overline{SO_2}}{\overline{CO_2}}\ \frac{SO_2}{CO_2}$	$\frac{SO_2}{\overline{SO_2}}$	Distance (Inch)	
0.00	0.965	0.885	0		0.23	1.009	0.966	0	
0.70	1.000	0.916	2		0.81	1.009	0.966	2	
0.81	1.023	0.916	4		1.04	1.022	0.979	4	
0.93	1.014	0.928	6		1.12	1.022	0.979	6	
0.93	1.021	0.928	8		1.12	1.022	0.979	8	
0.93	1.021	0.928	10		1.09	1.022	0.979	10	
0.93	1.058	0.947	12		1.09	1.035	0.991	12	
0.93	1.041	0.954	14		1.09	1.022	0.979	14	
0.91	1.047	0.960	16		1.07	1.028	0.991	16	
0.91	1.041	0.954	18		1.09	1.017	0.960	18	
0.86	1.047	0.960	20		1.07	1.022	0.979	20	
0.91	1.047	0.960	22	Bow Outlet #4 Port (Coal Fired)	1.09	1.028	0.985	22	Bow Outlet #3 Port (Coal Fired)
0.86	1.063	0.966	24		1.19	1.035	0.991	24	
0.86	1.055	0.966	26		1.19	1.037	0.979	26	
0.86	1.055	0.960	28		1.14	1.035	0.991	28	
0.91	1.065	0.954	30		1.14	1.026	1.004	30	
0.91	1.065	0.954	32		1.16	1.028	0.991	32	
0.91	1.072	0.960	34		1.16	1.014	0.991	34	
0.93	1.079	0.966	36		1.19	1.014	0.991	36	
0.91	1.072	0.960	38		1.19	1.026	1.004	38	
0.95	1.065	0.954	40		1.19	1.026	1.004	40	
0.93	1.093	0.979	42		1.19	1.026	1.004	42	
0.93	1.069	0.972	44		1.16	0.984	1.004	44	
0.95	1.072	0.960	46		1.16	0.984	1.004	46	
0.95	1.063	0.966	48		1.16	0.997	1.016	48	
0.93	1.079	0.966	50		1.16	0.984	1.004	50	
0.93	1.079	0.966	52		1.14	0.984	1.004	52	
0.93	1.072	0.960	54		1.12	0.978	0.997	54	
0.93	1.065	0.954	56		1.12	0.978	0.997	56	
0.93	1.072	0.960	58		0.98	0.991	1.010	58	
0.86	1.096	0.966	60		--	--	--	60	
0.051	0.028	0.019			0.179	0.018	0.013	$\pm$.D.	
0.904	1.054	.952			1.088	1.013	.99	AVG	
5.64%	2.66%	1.99%			16.45%	1.78%	1.31%	C.V*	

* Coefficient of variation

TABLE 1 CONT'

$\frac{\sqrt{\Delta P}}{\sqrt{\Delta P}}$	$\frac{\overline{SO_2}}{\overline{CO_2}}$ $\frac{SO_2}{CO_2}$	$\frac{SO_2}{\overline{SO_2}}$	Distance (Inch)		$\frac{\sqrt{\Delta P}}{\sqrt{\Delta P}}$	$\frac{\overline{SO_2}}{\overline{CO_2}}$ $\frac{SO_2}{CO_2}$	$\frac{SO_2}{\overline{SO_2}}$	Distance (Inch)	
0.47	0.937	0.885	0		0.33	0.976	0.928	0	
0.74	0.943	0.891	2		0.74	0.990	0.941	2	
0.86	0.943	0.891	4		0.74	0.990	0.941	4	
0.91	0.977	0.922	6		0.93	1.032	0.960	6	
0.91	0.964	0.914	8		0.93	1.032	0.972	8	
0.91	0.971	0.916	10		0.93	1.037	0.979	10	
0.91	0.977	0.922	12		0.93	1.024	0.966	12	
0.93	0.971	0.916	14		0.93	1.024	0.966	14	
0.95	0.964	0.916	16		0.93	1.024	0.966	16	
0.93	0.964	0.916	18		0.93	1.037	0.979	18	
0.93	0.964	0.916	20		0.93	1.065	0.991	20	
0.93	0.976	0.928	22		0.95	1.109	1.016	22	
0.93	0.984	0.928	24	Bow Outlet # 6 Port (Coal Fired)	0.95	1.107	1.023	24	Bow Outlet # 5 Port (Coal Fired)
0.93	0.996	0.941	26		0.95	1.099	1.023	26	
0.95	0.990	0.941	28		0.95	1.099	1.023	28	
0.95	0.976	0.928	30		0.95	1.094	1.010	30	
0.93	0.970	0.922	32		0.95	1.094	1.010	32	
0.91	0.976	0.928	34		0.95	1.082	0.991	34	
0.98	0.975	0.941	36		0.93	1.082	0.991	36	
1.02	0.983	0.947	38		0.95	1.075	0.985	38	
1.02	0.989	0.957	40		0.95	1.088	0.997	40	
1.02	1.001	0.979	42		0.98	1.087	1.004	42	
0.98	0.988	0.966	44		1.02	1.087	1.004	44	
0.98	0.988	0.956	46		1.02	1.087	1.004	46	
1.02	1.000	0.985	48		1.05	1.079	1.004	48	
0.98	0.994	0.972	50		1.02	1.074	0.991	50	
0.98	0.988	0.966	52		1.02	1.074	0.991	52	
0.98q	0.974	0.954	54		1.02	1.087	1.004	54	
0.95	0.989	0.954	56		0.98	1.081	0.997	56	
0.93	1.003	0.954	58		1.02	1.073	0.997	58	
--	--	--	60		0.95	1.093	1.016	60	
0.102	0.016	0.026			0.129	0.036	0.024	S.D.	
0.927	0.977	0.935			0.929	1.063	0.989	AVG	
11.0%	1.64%	2.78%			13.88%	3.39%	2.43	C V*	

*Coefficient of variation

TABLE 2

COAL-FIRED "INLET"

$\frac{\sqrt{\Delta P}}{\sqrt{\Delta P}}$	$\frac{\overline{SO_2}}{\overline{CO_2}} \frac{SO_2}{CO_2}$	$\frac{SO_2}{\overline{SO_2}}$	Distance (Inch)	Inlet Southside #2 Port (Coal Fired)	$\frac{\sqrt{\Delta P}}{\sqrt{\Delta P}}$	$\frac{\overline{SO_2}}{\overline{CO_2}} \frac{SO_2}{CO_2}$	$\frac{SO_2}{\overline{SO_2}}$	Distance (Inch)	Inlet Southside #1 Southport (Coal Fired)
0.83	0.877	0.860	0		0.94	0.943	0.978	0	
0.92	0.950	0.939	3		0.98	0.956	0.991	3	
0.97	0.989	0.978	6		1.05	0.943	0.965	6	
0.95	0.989	0.978	9		1.08	0.930	0.952	9	
0.95	0.996	0.984	12		1.06	0.943	0.952	12	
0.94	1.003	0.984	15		1.10	0.963	0.965	15	
1.05	0.983	0.965	18		1.06	0.963	0.952	18	
1.06	0.990	0.958	21		1.06	0.911	0.913	21	
1.06	0.990	0.952	24		1.05	0.957	0.939	24	
1.08	0.990	0.952	27		1.03	0.963	0.965	27	
1.05	0.997	0.965	30		1.02	0.943	0.926	30	
1.05	0.991	0.939	33		1.02	0.957	0.939	33	
1.05	0.977	0.939	36		0.97	0.996	0.978	36	
1.02	0.964	0.926	39		0.95	1.003	0.991	39	
1.02	0.971	0.932	42		0.97	1.002	1.004	42	
0.97	0.985	0.932	45		0.97	1.002	1.004	45	
0.90	0.985	0.932	48		0.98	0.989	1.004	48	
0.87	0.978	0.913	51		0.98	1.002	0.991	51	
0.86	0.972	0.900	54		0.98	0.994	1.017	54	
0.81	0.978	0.906	57		0.97	0.994	1.017	57	
0.76	0.979	0.900	60		0.95	0.988	1.017	60	
0.75	0.979	0.900	63		0.95	0.988	1.017	63	
0.75	0.972	0.893	66		0.97	1.000	1.030	66	
			69		0.98	1.008	1.030	69	
			70		0.76	0.994	1.017	70	
0.108	0.024	0.032			0.067	0.027	0.033	±STD.D.	
0.942	0.977	0.935			0.993	0.973	0.982	AVG.	
(0.1146)	(0.0246)	(0.0342)			(0.0674)	(0.0277)	(0.0336)	C V*	
11.46%	2.46%	3.42%			6.74%	2.77%	3.36%		

AVG. OF SEVEN PORT

	S.D.	AVG	C V*
$SO_2/\overline{SO_2}$	0.0319	1.005	3.88%
$SO_2/CO_2 \mid SO_2/CO_2$	0.0247	1.002	2.47%
$\sqrt{\Delta P}/\sqrt{\Delta P}$	0.1360	1.016	13.38%

* Coefficient of Variation

TABLE 2 CONT'

$\frac{\sqrt{\Delta P}}{\sqrt{\Delta P}}$	$\frac{\overline{SO_2}}{\overline{CO_2}}\frac{SO_2}{CO_2}$	$\frac{SO_2}{\overline{SO_2}}$	Distance (Inch)	Inlet Southside #4 Port (Coal Fired)	$\frac{\sqrt{\Delta P}}{\sqrt{\Delta P}}$	$\frac{\overline{SO_2}}{\overline{CO_2}}\frac{SO_2}{CO_2}$	$\frac{SO_2}{\overline{SO_2}}$	Distance (Inch)	Inlet Southside #3 Port (Coal Fired)
1.05	0.969	1.004	0		1.00	0.892	1.004	0	
1.10	0.956	1.004	2		1.13	0.932	1.056	2	
1.16	0.987	1.037	4		1.14	0.915	1.056	4	
1.16	0.986	1.050	6		1.16	0.926	1.069	6	
1.19	0.993	1.043	8		1.16	0.943	1.069	8	
1.19	1.006	1.056	10		1.19	0.938	1.082	10	
1.19	1.006	1.056	12		1.19	0.966	1.095	12	
1.19	1.025	1.063	24		1.19	0.966	1.095	24	
1.13	1.026	1.050	36		1.16	0.978	1.108	36	
0.98	1.013	1.037	48		1.11	0.997	1.082	48	
0.95	1.020	1.050	60		1.05	1.009	1.095	60	
0.81	1.025	1.056	62		0.97	1.016	1.095	62	
0.90	1.020	1.050	64		1.00	0.997	1.082	64	
1.00	1.020	1.050	66		0.97	1.009	1.095	66	
0.94	1.001	1.023	68		0.98	0.997	1.082	68	
0.86	0.994	1.017	70		1.00	1.009	1.095	70	
0.130	0.020	0.018			0.007	0.039	0.024		Std.D
1.050	1.002	1.04			1.087	0.968	1.078		Avg.
(0.0124)	(0.02)	(0.0173)			(0.08)	(0.040)	(0.0223)		C V*
12.4%	2.0%	1.73%			8%	4.0%	2.23%		

* Coefficient of variation

TABLE 2 CONT'

$\frac{\sqrt{\Delta P}}{\sqrt{\Delta P}}$	$\frac{\overline{SO_2}}{\overline{CO_2}}\frac{SO_2}{CO_2}$	$\frac{SO_2}{\overline{SO_2}}$	Distance (Inch)		$\frac{\sqrt{\Delta P}}{\sqrt{\Delta P}}$	$\frac{\overline{SO_2}}{\overline{CO_2}}\frac{SO_2}{CO_2}$	$\frac{SO_2}{\overline{SO_2}}$	Distance (Inch)	
1.08	1.019	1.056	0	Inlet Southside #6 Port (Coal-Fired)	1.05	0.984	0.952	0	Inlet Southside #5 Port (Coal-Fired)
1.16	1.031	1.069	2		1.13	1.005	0.965	2	
1.14	1.057	1.095	4		1.19	1.032	0.991	4	
1.17	1.057	1.095	6		1.21	1.065	1.030	6	
1.19	1.057	1.095	8		1.22	1.042	1.030	8	
1.22	1.042	1.095	10		1.24	1.037	1.017	10	
1.21	1.055	1.108	12		1.24	1.029	1.017	12	
1.22	1.058	1.082	24		1.21	1.046	0.991	24	
1.02	1.051	1.082	36		1.10	1.005	0.965	36	
0.98	1.076	1.108	48		1.10	1.029	0.939	48	
0.86	1.020	1.043	60		0.84	1.032	0.913	60	
0.81	1.034	1.043	62		0.83	1.017	0.900	62	
0.83	1.028	1.030	64		0.79	1.032	0.913	64	
0.83	1.015	1.017	66		0.78	1.047	0.926	66	
0.81	1.015	1.017	68		0.78	1.087	0.939	68	
0.78	1.028	1.030	70		0.76	1.041	0.900	70	
0.173	0.018	0.032			0.194	0.024	0.046	$\pm$ S.D.	
1.019	1.040	1.066			1.029	1.033	0.961	Avg.	
(0.1697) 16.97%	(0.0173) 1.73%	(0.030) 3.0%			(0.1885) 18.85%	(0.0232) 2.32%	(0.0479) 4.79%	C V *	

* Coefficient of Variation

TABLE 2 CONT'

$\frac{\sqrt{\Delta P}}{\sqrt{\Delta P}}$	$\frac{\overline{SO_2}}{\overline{CO_2}} \frac{SO_2}{CO_2}$	$\frac{SO_2}{\overline{SO_2}}$	Distance (Inch)
0.94	0.969	0.991	0
1.08	1.007	1.017	2
1.10	1.007	1.017	4
1.06	1.015	1.017	6
1.10	1.016	1.004	8
1.10	1.023	1.004	10
1.10	1.018	0.978	12
1.13	1.034	0.965	24
1.13	1.034	0.965	36
1.06	1.034	0.965	48
--	--	--	60
0.75	1.045	0.939	62
0.83	1.045	0.939	64
0.81	1.016	0.913	66
0.75	1.032	0.913	68
0.68	1.061	0.939	70
0.194	0.021	0.036	Std. Devn.
0.997	1.023	0.971	Avg.
0.195	0.02	0.037	C V*
99.5%	2%	3.7%	

Inlet Southside #7 Port (Coal-Fired)

* Coefficient of Variation

TABLE 3

OIL-FIRED "WEST"

$\frac{\sqrt{\Delta P}}{\sqrt{\Delta P}}$	$\frac{\overline{SO_2}}{\overline{CO_2}}\frac{SO_2}{CO_2}$	$\frac{SO_2}{\overline{SO_2}}$	Distance (Inch)		$\frac{\sqrt{\Delta P}}{\sqrt{\Delta P}}$	$\frac{\overline{SO_2}}{\overline{CO_2}}\frac{SO_2}{CO_2}$	$\frac{SO_2}{\overline{SO_2}}$	Distance (Inch)
0.86	0.993	1.065	0	Edgar Station West Duct Mid Port	0.65	0.788	0.789	0
0.84	0.993	1.065	2		0.60	0.938	0.907	2
0.84	1.027	1.065	4		0.60	1.002	0.986	4
0.84	1.027	1.065	6		0.60	1.002	0.986	6
0.86	1.084	1.104	8		0.56	1.002	0.986	8
0.84	1.084	1.104	10		0.56	1.041	1.025	10
0.93	1.123	1.143	12		0.56	1.023	1.025	12
1.02	1.162	1.143	14		0.60	1.059	1.025	14
1.09	1.162	1.143	16		0.65	1.018	0.986	16
1.05	1.141	1.143	18		0.65	1.059	1.025	18
1,14	1.141	1.143	20		0.65	1.041	1.025	20
1.19	1.123	1.143	22		0.81	1.059	1.025	22
1.19	1.123	1.143	24		0.84	1.018	0.986	24
1.28	1.121	1.104	30		0.93	1.018	0.986	30
1.35	1.063	1.065	36		0.93	1.059	1.025	36
1.37	1.041	1.025	42		0.95	1.018	0.986	42
1.37	1.063	1.065	48		0.98	1.002	0.986	48
1.37	1.082	1.065	50		1.07	1.059	1.025	50
1.39	1.082	1.065	52		1.16	1.034	0.946	52
1.37	1.041	1.025	54		1.19	1.009	0.907	54
1.35	1.018	0.986	56		1.21	1.009	0.907	56
1.37	1.059	1.025	58		1.28	1.050	0.907	58
1.35	1.059	1.025	60		1.32	1.004	0.867	60
1.35	1.018	0.986	62		1.30	1.025	0.867	62
1.39	1.018	0.986	64		1.40	1.000	0.828	64
1.39	1.018	0.986	66		1.44	1.000	0.828	66
1.39	1.039	0.986	68		1.30	1.000	0.828	68
1.42	1.039	0.986	70		1.30	0.979	0.828	70
1.35	1.059	1.025	71		1.14	0.979	0.828	71
0.219	0.049	0.057			0.305	0.051	0.079	S.D.
1.191	1.069	1.064			0.938	1.010	0.942	Avg.
18.38%	4.58%	5.36%			32.51%	5.05%	8.38%	C V*

	Avg. West Ports		
	S.D.	Avg.	C V*
$SO_2/\overline{SO_2}$	0.0622	1.000	6.22%
$SO_2/CO_2 \mid \overline{SO_2}/\overline{CO_2}$	0.0530	1.001	5.30%
$\sqrt{\Delta P}/\sqrt{\Delta P}$	0.2731	1.01	27.04%

* Coefficient of Variation

TABLE 3 CONT'

$\frac{\sqrt{\Delta P}}{\sqrt{\Delta P}}$	$\frac{\overline{SO_2}}{\overline{CO_2}}$ $\frac{SO_2}{CO_2}$	$\frac{SO_2}{\overline{SO_2}}$	Distance (Inch)
0.56	0.740	0.867	0
0.58	0.817	0.946	2
0.60	0.856	0.946	4
0.60	0.870	0.946	6
0.60	0.906	0.986	8
0.60	0.906	0.986	10
0.60	0.906	0.986	12
0.65	0.927	1.025	14
0.70	0.943	1.025	16
0.74	0.943	1.025	18
0.77	0.943	1.025	20
0.74	0.979	1.065	22
0.77	0.963	1.065	24
0.77	1.000	1.104	30
0.86	0.927	1.025	36
0.95	0.842	0.946	42
1.05	0.870	0.946	48
1.07	0.906	0.986	50
1.07	0.957	1.025	52
1.07	0.957	1.025	54
1.09	0.952	0.986	56
1.09	0.945	0.946	58
1.14	0.929	0.946	60
1.19	0.961	0.946	62
1.23	0.929	0.946	64
1.30	0.973	1.025	66
1.35	0.957	1.025	68
1.44	1.007	1.025	70
1.32	0.988	1.025	71
0.276	0.058	0.049	S.D.
0.913	0.924	0.993	Avg.
30.23%	6.28%	4.93%	C V*

Edgar Station West Duct Bot. Port

* Coefficient of variation

TABLE 4

OIL-FIRED "EAST"

$\frac{\sqrt{\Delta P}}{\sqrt{\Delta P}}$	$\frac{\overline{SO_2}}{\overline{CO_2}}\ \frac{SO_2}{CO_2}$	$\frac{SO_2}{\overline{SO_2}}$	Distance (Inch)		$\frac{\sqrt{\Delta P}}{\sqrt{\Delta P}}$	$\frac{\overline{SO_2}}{\overline{CO_2}}\ \frac{SO_2}{CO_2}$	$\frac{SO_2}{\overline{SO_2}}$	Distance (Inch)	
0.76	0.718	0.796	0		0.30	0.749	0.995	0	
0.89	0.881	0.961	2		0.59	0.932	1.127	2	
0.94	0.988	1.061	4		0.64	1.000	1.194	4	
0.96	1.050	1.127	6		0.64	1.029	1.227	6	
0.98	1.050	1.127	8		0.62	1.056	1.260	8	
0.98	1.082	1.160	10		0.59	1.099	1.293	10	
0.98	1.117	1.160	12		0.66	1.148	1.194	12	
1.00	1.084	1.127	14		0.68	1.173	1.160	14	
1.02	1.103	1.127	16		0.70	1.159	1.127	16	
1.00	1.103	1.127	18		0.76	1.159	1.127	18	
1.02	1.121	1.127	20		0.83	1.181	1.127	20	
1.00	1.103	1.127	22	Edgar Station East Duct Mid Port	0.85	1.146	1.094	22	Edgar Station East Duct Top Port
1.00	1.121	1.127	24		0.87	1.191	1.127	24	
0.98	1.121	1.127	30		0.87	1.146	1.094	30	
0.98	1.121	1.127	36		0.85	1.111	1.061	36	
0.94	1.087	1.094	42		0.83	1.111	1.061	42	
0.96	1.107	1.094	48		0.89	1.126	1.094	48	
0.94	1.126	1.094	50		0.91	1.111	1.061	50	
0.94	1.091	1.061	52		0.96	1.111	1.061	52	
0.94	1.091	1.061	54		0.98	1.132	1.061	54	
0.94	1.111	1.061	56		1.02	1.154	1.061	56	
0.89	1.097	1.028	58		1.08	1.175	1.061	58	
0.89	1.097	1.028	60		1.08	1.154	1.061	60	
0.91	1.060	0.995	62		1.08	1.111	1.061	62	
0.89	1.082	0.995	64		1.13	1.132	1.061	64	
0.94	1.082	0.995	66		1.15	1.060	0.995	66	
0.94	1.082	0.995	68		1.21	1.078	1.028	68	
0.94	1.060	0.995	70		1.21	1.082	0.995	70	
0.94	1.025	0.961	71		1.19	1.082	0.995	71	
0.052	0.083	0.080			0.226	0.088	0.077	S.D.	
.947	1.066	1.064			0.867	1.099	1.098	Avg.	
5.5%	7.79%	7.5%			26.06%	8.0%	7.0%	C V *	

Avg. East Ports

	S.D.	Avg.	C V*
$SO_2/\overline{SO_2}$	0.0730	1.000	7.3%
$SO_2/CO_2 \mid \overline{SO_2}/\overline{CO_2}$	0.0762	1.000	7.62%
$\sqrt{\Delta P}/\sqrt{\Delta P}$	0.1250	.999	12.51%

* Coefficient of Variation

TABLE 4 CONT'

$\frac{\sqrt{\Delta P}}{\sqrt{\Delta P}}$	$\frac{\overline{SO_2}}{\overline{CO_2}}$ $\frac{SO_2}{CO_2}$	$\frac{SO_2}{\overline{SO_2}}$	Distance (Inch)
1.02	0.617	0.663	0
1.13	0.753	0.796	2
1.13	0.803	0.862	4
1.13	0.846	0.895	6
1.11	0.879	0.928	8
1.11	0.893	0.928	10
1.08	0.879	0.928	12
1.11	0.893	0.928	14
1.11	0.908	0.928	16
1.11	0.875	0.895	18
1.13	0.875	0.895	20
1.15	0.903	0.862	22
1.15	0.848	0.796	24
1.17	0.848	0.796	30
1.13	0.819	0.796	36
1.19	0.805	0.796	42
1.21	0.792	0.796	48
1.23	0.805	0.796	50
1.21	0.792	0.796	52
1.21	0.805	0.796	54
1.21	0.805	0.796	56
1.21	0.805	0.796	58
1.25	0.805	0.796	60
1.25	0.819	0.796	62
1.25	0.819	0.796	64
1.30	0.854	0.829	66
1.30	0.872	0.862	68
1.30	0.887	0.862	70
1.21	0.903	0.862	71
0.070	0.059	0.062	S.D.
1.175	0.834	0.836	Avg.
5.96%	7.07%	7.41%	C V*

Edgar Station East Duct Bottom Port

* Coefficient of variation

TABLE 5

SUMMARY TABLE OF COEFFICIENT OF VARIATION* (%) FOR THE SAMPLING PLANES

	$SO_2/\overline{SO_2}$	$(SO_2/CO_2) / (\overline{SO_2/CO_2})$	$\sqrt{\Delta P} / \overline{\sqrt{\Delta P}}$
Coal-Fired			
Inlet	3.2	2.5	13
Outlet	2.1	2.6	12
Oil-Fired **			
West	6.2	5.3	27
East	7.3	7.6	13

* NOTE: As a rule of thumb the range of a set of numbers is about 3 to 6 times the standard deviation. Therefore, the range of stratification about the average value, represented in percent, is ± 3 to 6 times the C.V. with ± 4-1/2 times as typical. For example, in the case of the coal-fired inlet duct, one would expect extreme deviation for the SO_2 concentration values to be in the neighborhood of ± 14% for the mean.

** This oil fired plant is Edgar Station. The field demonstration, TASK III, was performed at Mystic Station, also an oil fired plant.

The reason that the concentration ratios of SO_2 to CO_2 vary about the same amount as the SO_2 concentration is not obvious. Clearly, this result is not in accord with the hypothesis which predicts that SO_2 and CO_2 are stratified in the same way, i.e., ratios are preserved through dilution, etc. One could look to the effect of the analysis technique itself for a possible explanation. In any case, further experiments described under Task II are in accord with the above-stated hypothesis.

c. Conclusion

If one assumes that the precision of the analyzer is ± 2 to ± 5 percent, the amount of gas stratification for the coal-fired power plant is almost negligible (range for all SO_2 data points is + 7% and - 8% from the average of the reading for respective parts).

The data for the oil-fired plant do show noticeable stratification with a range for SO_2 from - 25% to + 18% (from the average for a port) for all SO_2 concentrations.

The ratio data of SO_2/CO_2 are not consistent with the theory which predicts that this ratio should be a constant over the sampling plane. It is expected that this inconsistency is the result of the sampling technique used, since subsequent measurements during Task III show a constant ratio.

3. GAS STRATIFICATION DOCUMENTATION

During the literature search task of this program, data were sought on the existence of stratification in gas streams for both gas concentration and the associated gas velocity. It was discovered that this type of data are scarce; however, a few examples were found and are presented below.

No data with both velocity and concentration were obtained from the literature search. However, some data showing gas concentration stratification were found. Data supplied by the Bureau of Mines are shown in Figure 2. The CO_2 concentration ranges approximately 40% from the mean at a location at the

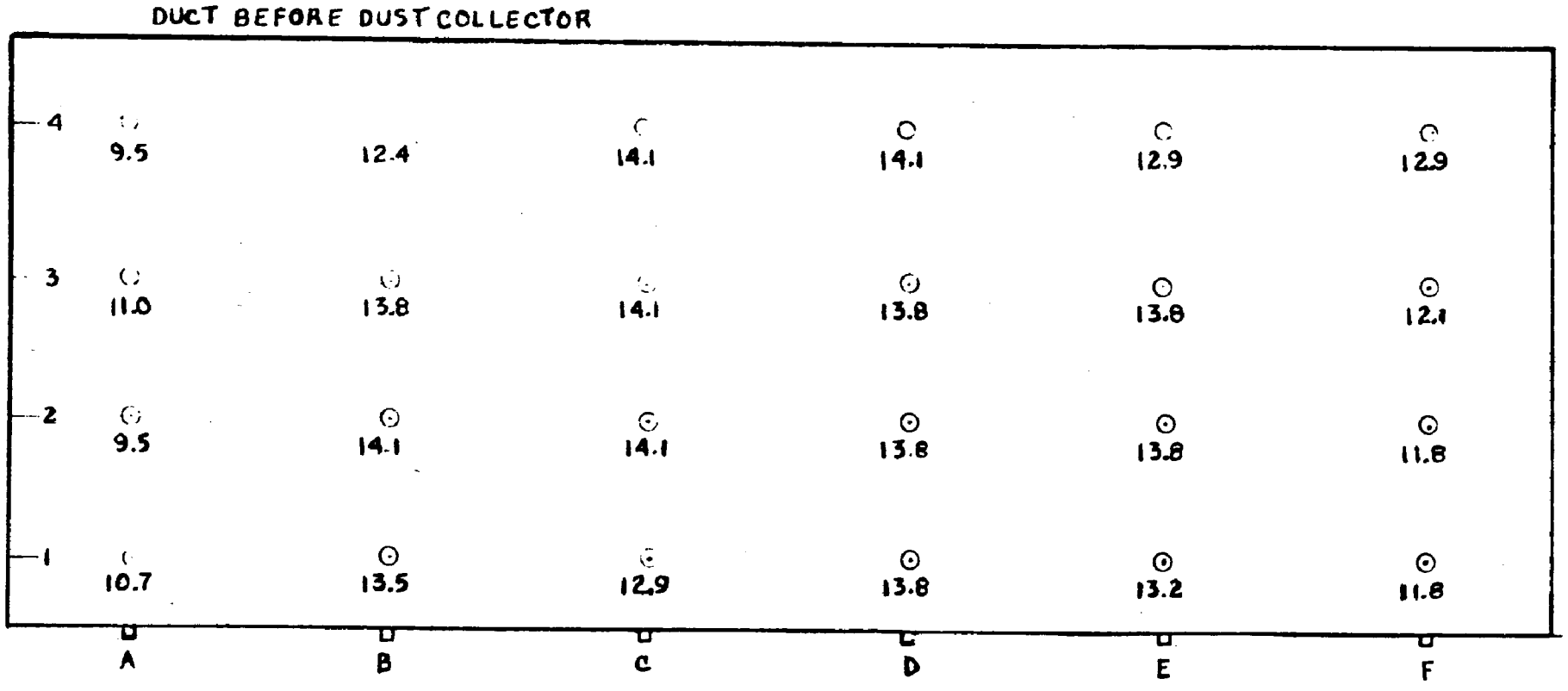

FIGURE 2

CO_2 CONCENTRATIONS BEFORE DUST COLLECTOR

inlet to a dust collector. Data supplied by TVA are shown in Figures 3 through 6 and show various degrees of SO_2 stratification at a test section following a furnace of a coal-fired power plant (Shawnee, Kentucky). Additional data on CO_2 and SO_2 stratification were obtained from the field survey and the final field demonstration tasks, which were collected from oil-fired power plants. These data are documented below. Evidence of gas stratification was also presented on Page 44 of Walden Research's final report entitled "Improved Chemical Methods for Sampling and Analysis of Gaseous Pollutants from the Combustion of Fossil Fuels.[3]

4. CONCEPTUAL OCCURENCE OF GAS STRATIFICATION

As an aid in the investigation of the problem of conducting emission measurements on process streams, some conceptual processes are presented which could lead to gas stratification. These are presented not as locations of assured stratification, but as possible locations where stratification can be expected.

Various conceptual designs forecasting the probable occurrence of gas stratification are shown in Figures 7, a,b,c, and d. Figure 7a shows two different streams joining a common stream. The stratified plane can occur downstream of the junction. In Figure 7b, two identical streams branch out from the main then meet again in one stream. One branch has air in leakage causing a stratified plant to occur downstream of the junction. Figure 7c depicts the same condition as Figure 7b, except a different degree of air in leakage occurs in the two identical streams. A stratified plane can occur after the air in leakage location. Figure 7d shows the condition of a by-pass branching that follows a different process than the main stream. In this case the stratified plane can occur after the junction.

PLANE A-A WEST SIDE 3-16-70

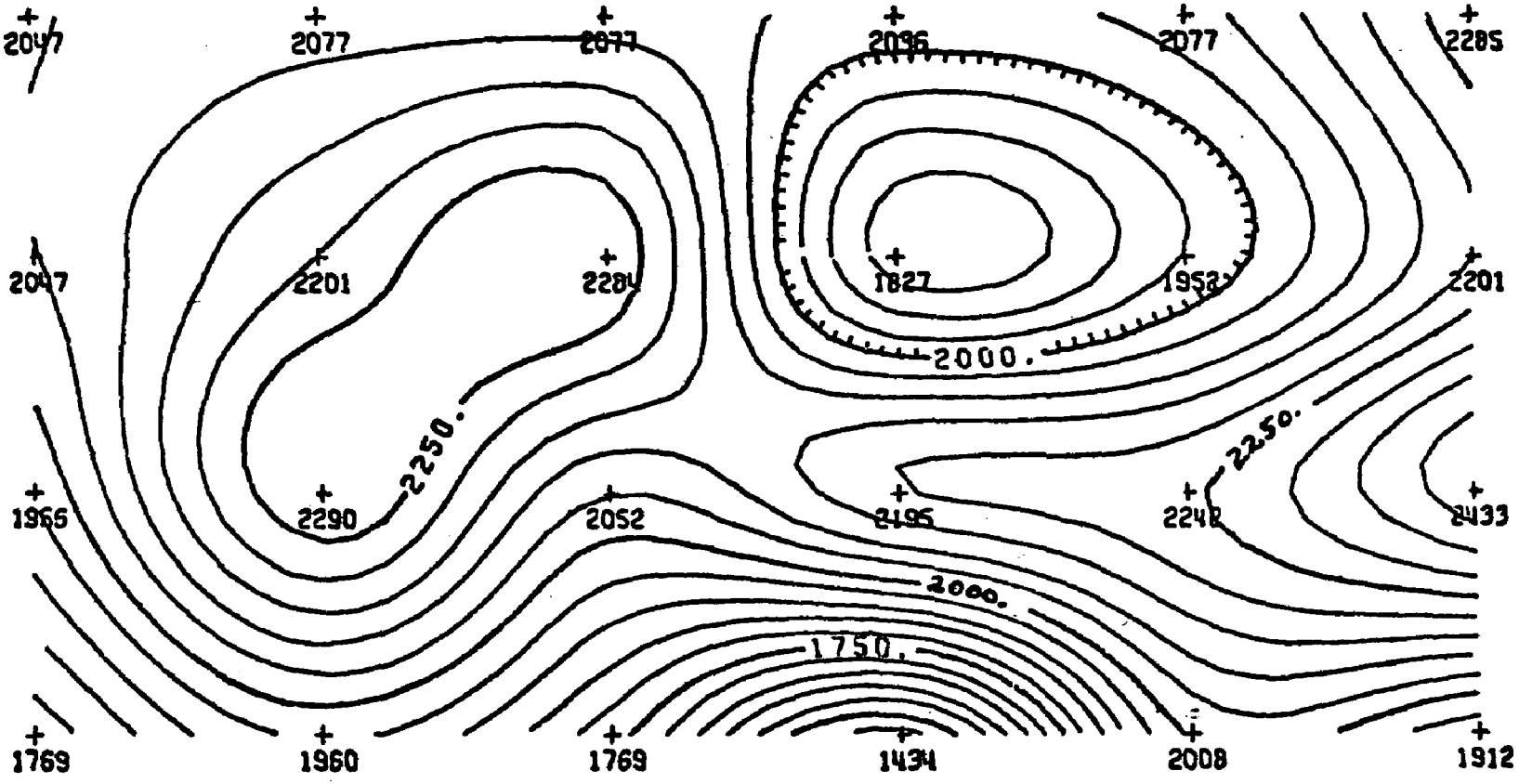

Figure 3 (TVA) 46 feet x 24 feet

SO2 DISTRIBUTION - INT =50 PPM

PLANE A-A WEST SIDE

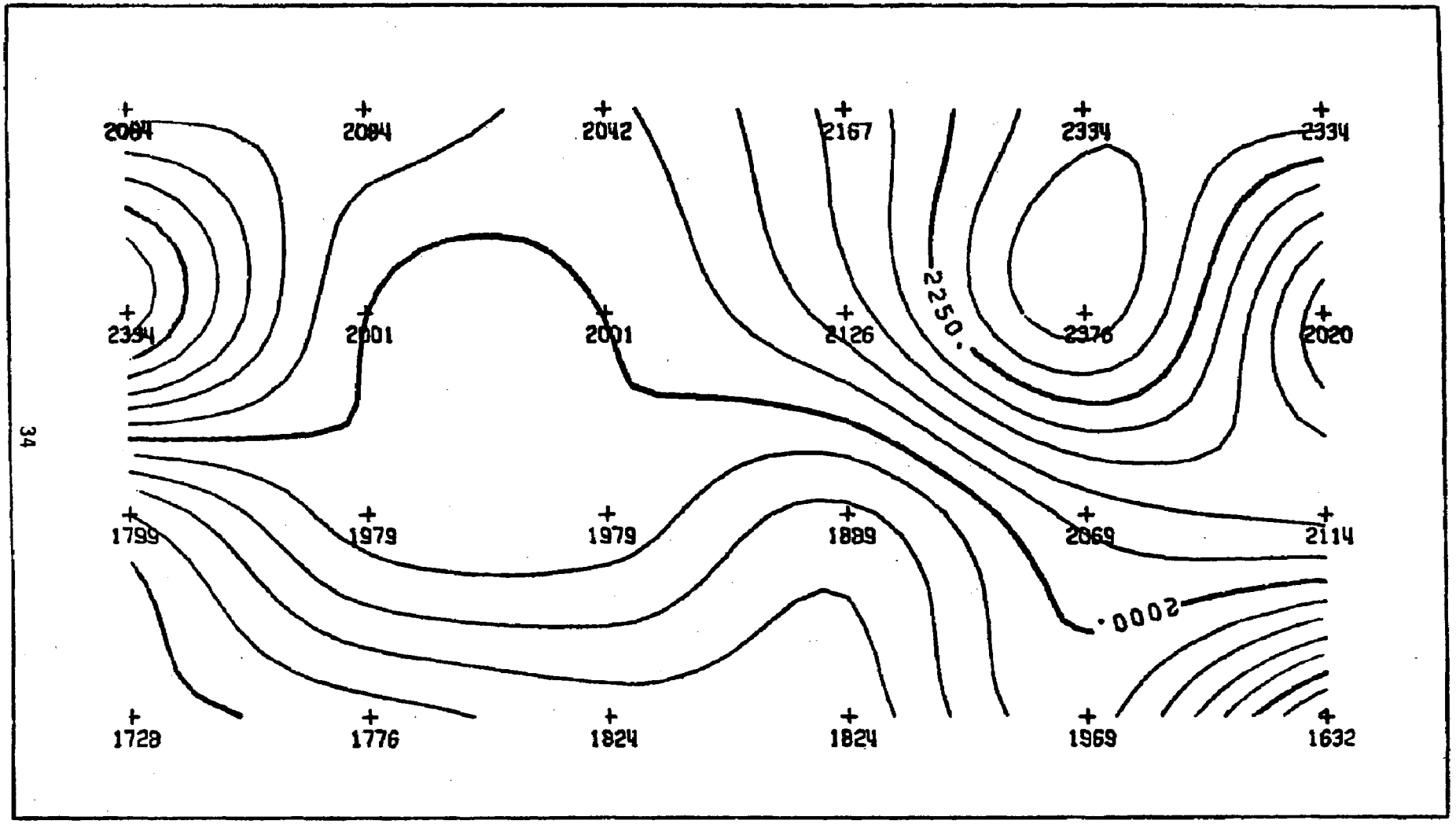

SO2 DISTRIBUTION - INT.=50 PPM

Figure 4.

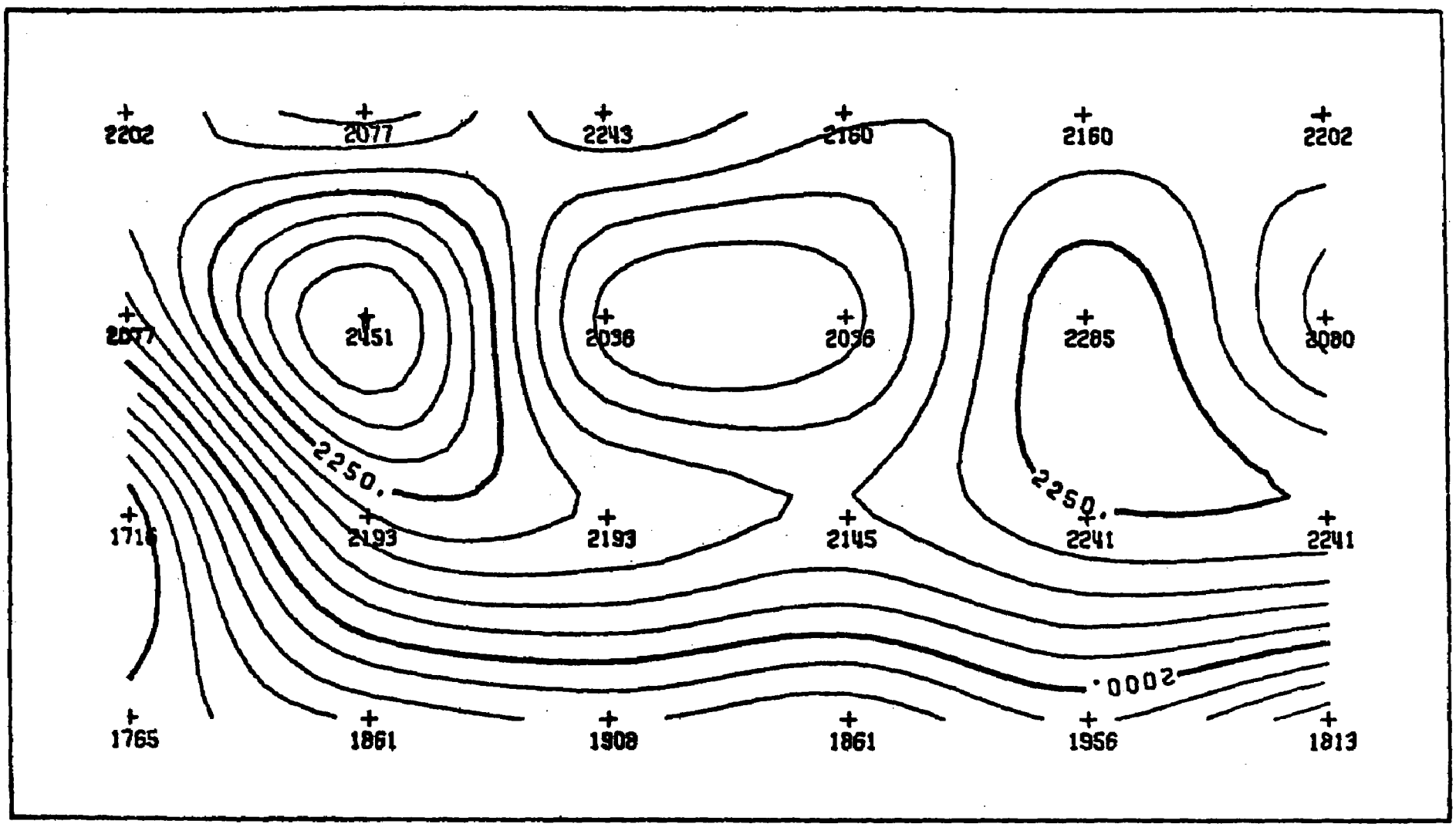
PLANE A-A WEST SIDE
2202
2077
2243
2160
2160
2202
2077
2451
2036
2036
2285
2080
2250.
2250.
1716
2193
2193
2145
2241
2241
.0002
1765
1861
1908
1861
1956
1813
SO2 DISTRIBUTION - INT.=50 PPM

Figure 5.

PLANE A-A WEST SIDE

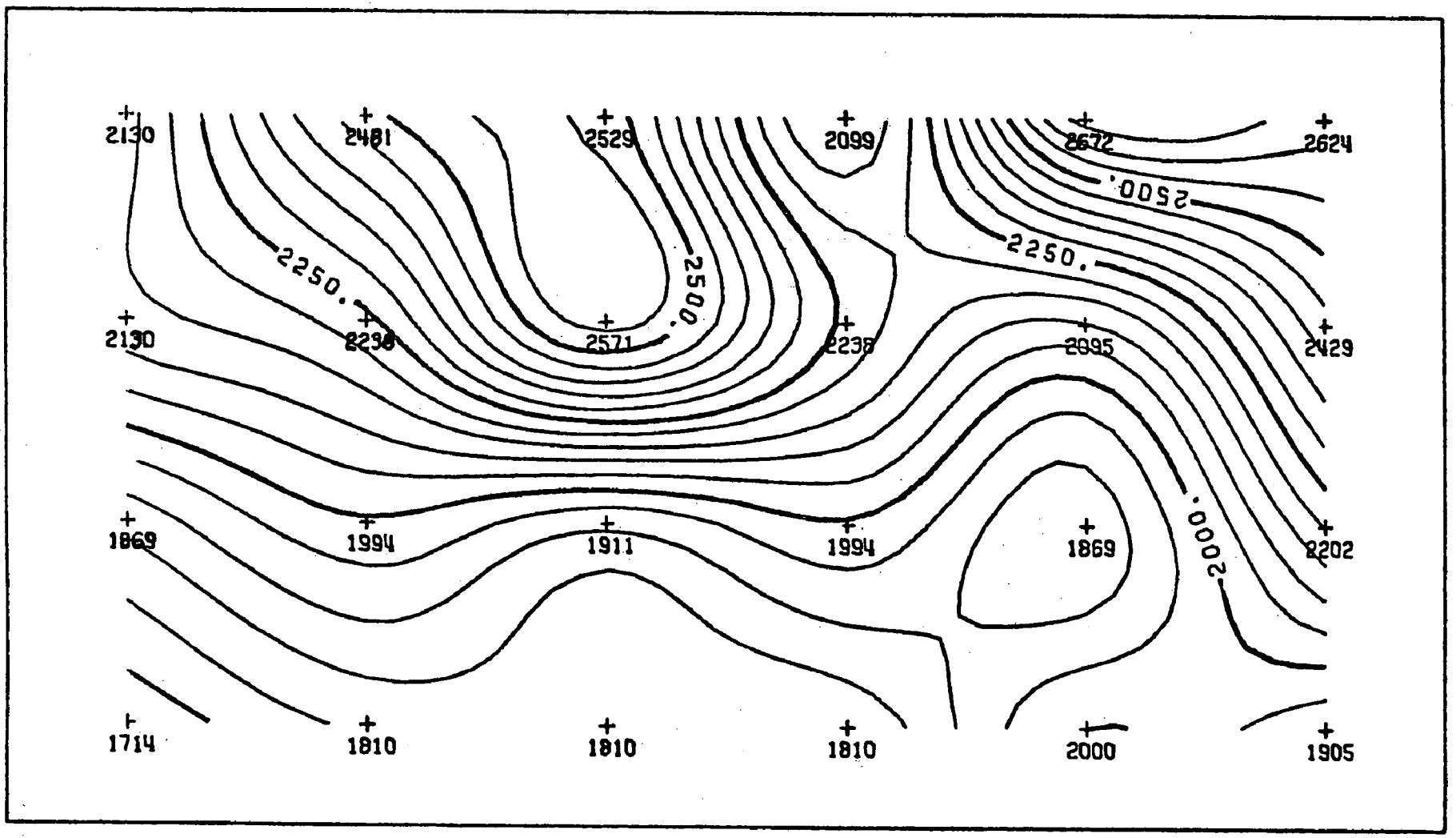

SO2 DISTRIBUTION - INT.=50 PPM

Figure 6.

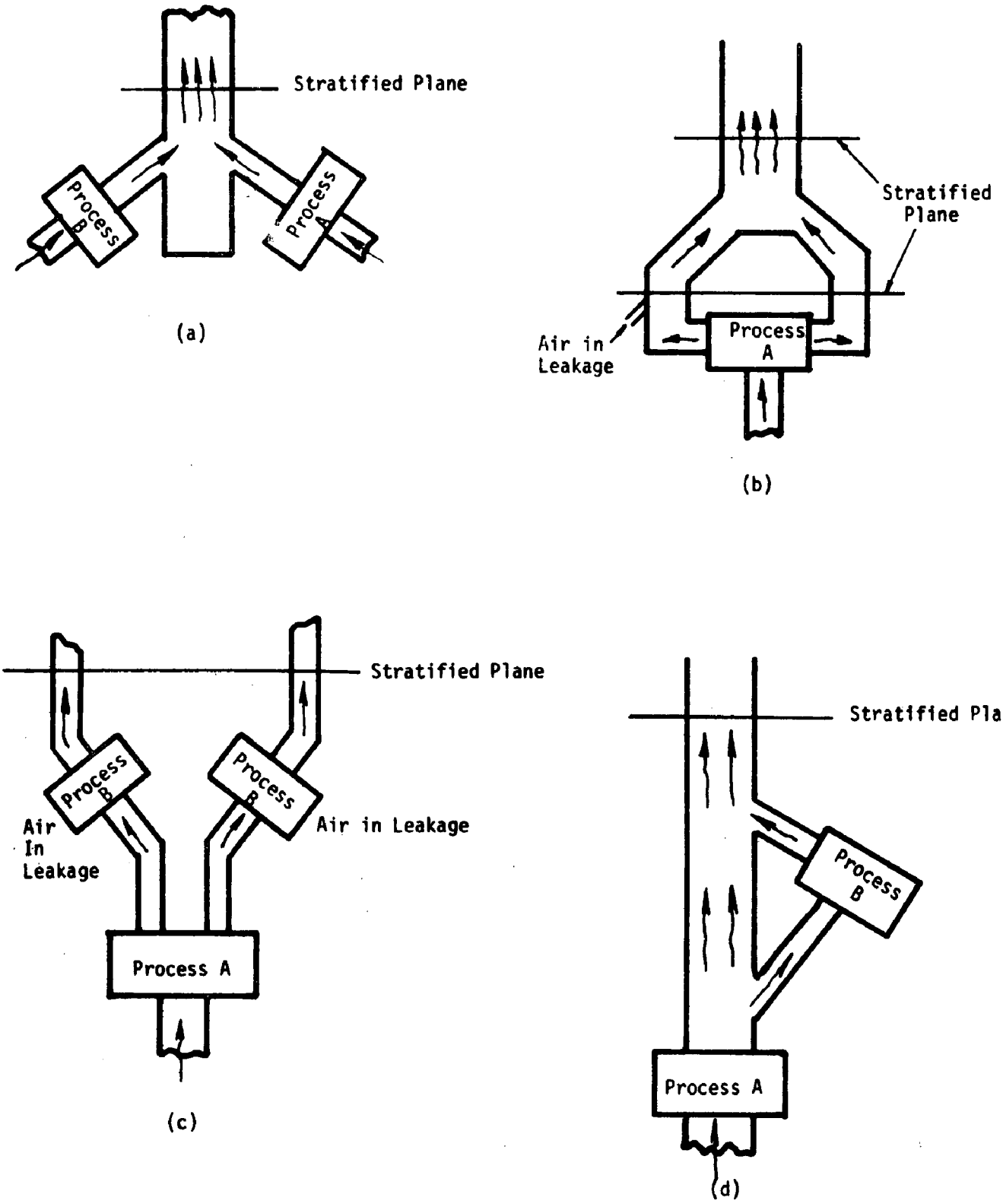

Figure 7. Conceptual Occurrence of Gas Stratification

B. TASK II - ANALYTICAL ACTIVITIES AND LABORATORY EXPERIMENTS

1. ANALYTICAL ACTIVITIES

a. Analytical Simulation

The results of the analytical simulation sub-task are presented below. The purpose of this sub-task was to develop procedures for emission measurements for flow of stratified gases in rectangular and circular ducts.

a.1 Background

(a) Representative Stack Sampling for Gases

The classical problem of stack sampling for gases is to associate the (average) samples taken generally at different times and positions with either an average concentration or, with greater difficulty, an average throughput. The collection of a gas sample which accurately represents the flow at a given point is far simpler than the complexities of representative particulate sampling. Isokinetic sampling rates are not a requirement since the (thermal and turbulent) eddy diffusivities are far too large to permit significant moelcular fractionation in the very weak centrifugal fields imposed by any velocity mismatch attainable in sampling. The precision and accuracy of the determination are a function of the method(s) employed, the experimental design, and the variability of the source. There is very little information extant on sampling methodologies for continuously extracting a representative gas sample from a non-uniform stream. There is, however, considerable background on sampling with manual analytic methods.

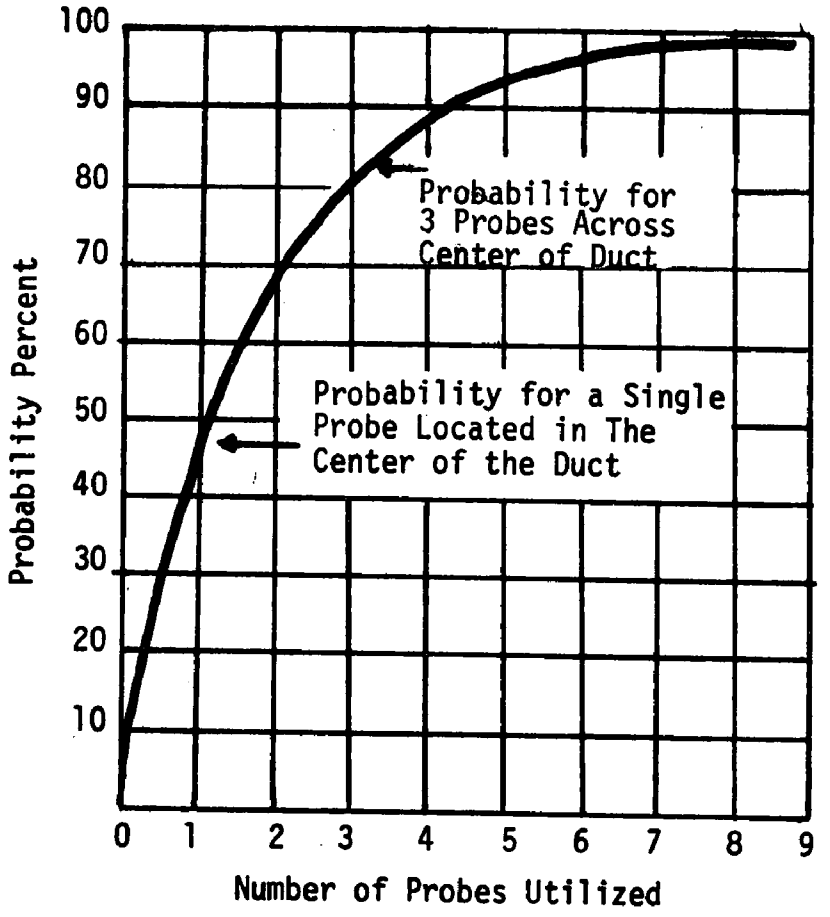

Figure 1. Probability of obtaining an accuracy within 15% of 9-point analysis for O_2 in a large duct[31]

Literature is scarce on sampling locations for obtaining representative average concentrations of gases with ducts. Although this subject is frequently discussed in the literature on particulate sampling, the discussions are concerned with inertial separation of particles from the gas stream. Since inertial separation of pollutant gases from carrier gases does not occur, the particulate sampling discussions are not generally applicable (i.e., isokinetic sampling is not necessary and stratification due to duct bends, etc., is not present).

It is a commonly held belief that gas stratification is not present in ducts with turbulent gas flow[29]. However, eddy diffusion studies[30] show that a straight duct length of the order of 100 duct diameters is required for good mixing of a highly stratified gas. It follows that in many large-scale combustion systems where infiltration air is known to occur, there is no direct location where the gas is well mixed. Luxl carried out a total of 792 Orsat oxygen traverses in ten different ducts of fossil fuel combination sources. He found (Figure 1) that stratification is generally present and that single point samples are usually nonrepresentative in large ducts.

ASME[32] specifies a multi-point sampling system for Orsat analysis of flue gases and a single point sampling system for SO_3 and SO_2, but there is no explanation of this apparent inconsistency. The multi-point locations specified are also selected by ASME for velocity traverse. It may be argued that velocity traverse schemes can give representative average velocities in a duct where the velocity profile is not generally flat; hence the same techniques should give representative values of emissions. However, until a careful study is made, the accuracy of this technique cannot be established.

The emission of material from a combustion source is described by the general equation:

$$E_a = \int_A C_a \vec{v} \cdot \vec{n} \, dA \qquad (1)$$

where E_a is the emission of material (a), C_a is the concentration of (a), $\vec{v}$ the flue gas velocity along the duct, A is the cross sectional area of the duct, and $\vec{n}$ the unit vector normal to A. It follows from Equation (1) that C_a and $\vec{v}$ are coupled if neither is constant across the duct; hence, they should be measured together.

A traverse using a continuous oxygen or carbon dioxide analyzer can quickly determine the extent of infiltration air stratification. If the gases are not significantly stratified, the pollutant gases may be assumed to be well mixed and the concentration can be determined from a single sampling point. However, it is more prudent to sample at more than one point as a check on the mixing of the pollutant gases.

For rigorous measurements, a set of replicate samples should be taken at traverse points and a statistical analysis performed in order to establish the flow pattern and an estimate of residual error. For subsequent measurements in this duct, fewer sampling points can be used and the accuracy predicted[33].

(b) Variance of Concentration in Large Ducts

A major problem in the high precision determination of pollutant emissions is the variation in species concentration which may exist in a large duct as a result of air infiltration and poor mixing (stratification). In the course of NAPCA's (now EPA) extensive studies of coal-fired power plant effluents[34], many CO_2 concentration profiles were obtained by traverse of large ducts at different sampling locations. The following discussion, based on a random selection of this test data and, therefore, incomplete, outlines the magnitude of the problem and the influence of both sampling location and equipment type on the results obtained.

Typical sampling locations are illustrated in the power plant schematic (Figure 2). The most common locations are at the entrance and exit of the duct collection equipment. The statistical method adopted was to calculate the mean CO_2 concentration for each traverse plane, the standard deviation from the mean, and the coefficient of variation (CV*= 100 σ/mean). Two examples, illustrating relatively homogeneous and stratified flows, are given in Figure 3. The observed coefficient of variation of the CO_2 concentration is given in Table 1 as a function of sampling location. The relatively low value of CV*at the outlet of the dust collector, presumably the result of good mixing, suggests this to be the location of choice for both simplicity and high precision. The relatively high value of CV*at the inlet to the dust collector may be associated with air infiltration at the air preheater, which is a common occurrence.

The most frequently used sampling locations for emissions determinations are the inlet and outlet of the dust collectors. The coefficient of variation of the CO_2 concentration at these locations is given in Table 2 as a function of equipment type. With the exception of Plant No. 3, CV*at the inlet is relatively large compared to the outlet values.

Conclusions which may be drawn from these data are: CO_2 (or O_2) traverses are extremely valuable for selection of sampling locations and determination of the number of samples required for a high precision emissions determination.

(c) Flue Gas Flow Measurement Methods

Although this report is directed to the problems of gas sampling, an understanding of velocity and total flow measurements is essential to the development and analysis of representative sampling systems. The discussion that follows summarizes the general methodology in practice today, which is used to infer velocity profiles and total flow from a finite number of point measurements.

* Coefficient of variation

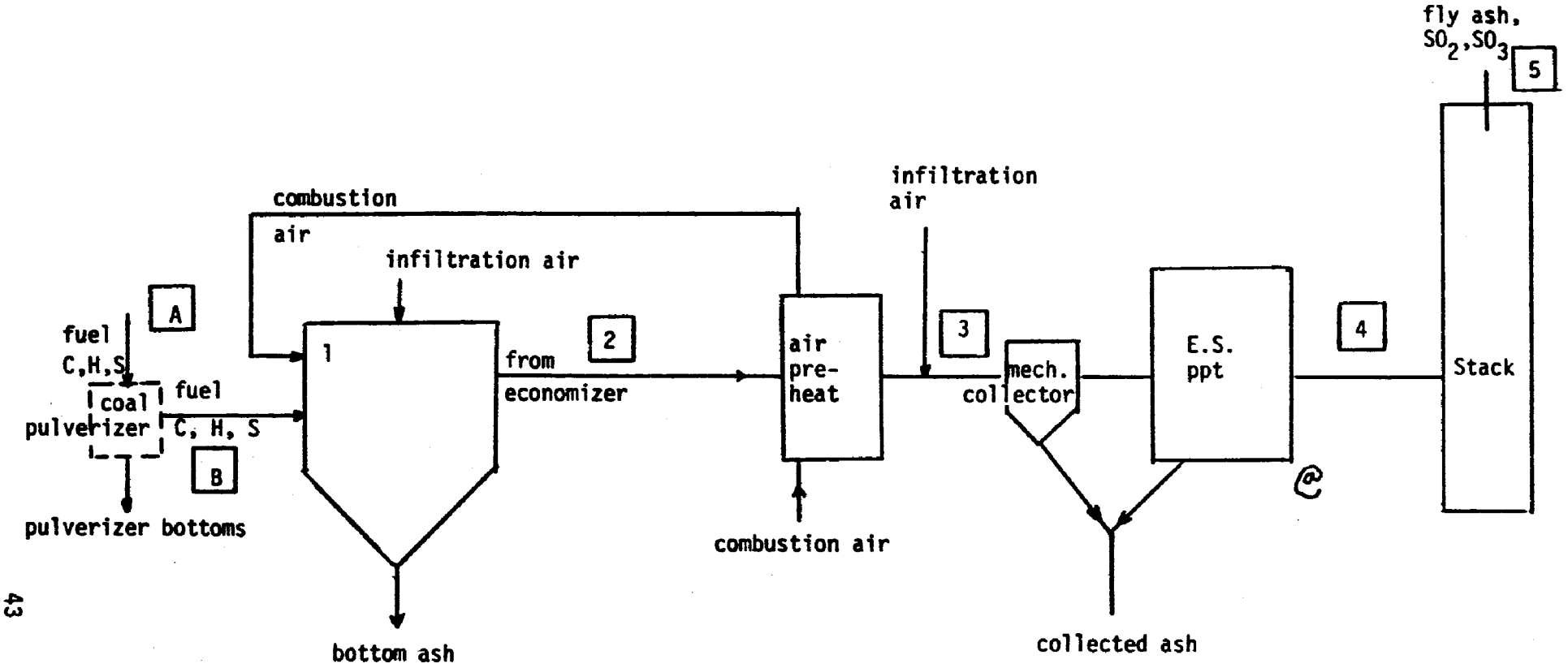

@ occasionally the E.S. precipitator may be upstream of the air-preheater

A Plant input data

1 Flue gas sampling points

Figure 2. Schematic - Large Combustion Unit.

"HOMOGENEOUS"

1.03	1.00	0.98	1.00	1.01
1.03	1.01	0.98	1.00	1.01
1.00	1.01	0.98	1.01	1.01

3"3"

22'

Ave CO_2 = 11.7%

CV* = 1.5%

"STRATIFIED"

.74	.92	1.0	1.0	.97	.95
.82	1.01	1.02	1.01	1.00	.90
.75	1.05	.99	1.02	1.01	.90
.82	1.00	.93	.93	1.01	.86

4'8"

14'10"

Ave CO_2 = 12.6

CV* = 9.3%

* Coefficient of variation

Random selection from six plants.

Figure 3. Normalized CO_2 Traverse Data at Dust Collector of Coal-Fired Power Plants.

OBSERVED COEFFICIENT OF VARIATION FOR CO_2 TRAVERSE AT VARIOUS SAMPLING LOCATIONS

Sampling Position	T°(F)	No. of Traverse Points	CO_2 (CV), %	
Furnace (1)*	2400	12 12	4.0 5.2	>4.6
Economizer Inlet (2)	860	8 8	3.8 3.8	>3.8
Economizer Outlet (3) (Dust Collector Inlet)	360	24 24	7.1 5.4	>6.2
Outlet of Dust Collector (4)	350	18 18	3.2 3.2	>3.2

(2) Sampling should be conducted at the outlet of dust collectors in the absence of other information.

(3) For simplified methods, single point sampling at the dust collector outlet appear to be feasible (Coefficient of Variation < 5%).

*See Figure 2.

TABLE 2

OBSERVED COEFFICIENT OF VARIATION FOR CO_2 TRAVERSE
FOR VARIOUS COAL-FIRED PLANTS

Plant No.	Type of Boiler Firing	Dust Collection Equipment	Sampling Location	No. of Traverse Points	CO_2(CV), %
1	Horizontally Opposed	C	I	24	9.3
			O	12	2.3,1.4
2	Cyclone	E	I	24	4.6
			O	24	3.2
3	Spreader Stoker	C	I	18	1.5
			O	9	1.02
4	Corner	C,E	I	18	8.8
			O	12	0.97
5	Vertical	C,E	I	24	7.1
			O	12	3.2

C = cyclone
E = electrostatic precipitator
I = dust collector inlet
O = dust collector outlet

Total flow (Q) across a cross section of a duct can be described by an equation similar to Equation (1) above, as an integral over the area:

$$Q = \int_A v \cdot dA \qquad (2)$$

where v is the velocity normal to a differential area, dA.

Measuring gas stream velocities at various points across a flue or duct is a velocity traverse. From the geometry of the ducts and the geometry of the traverse point, the gas velocities may be used to calculate the volumetric flow. This calculation is the evaluation of the integral in Equation (2). The integral may be evaluated graphically; however, the most common technique is to divide the test section into a number of equal area zones and determine the mean velocity in each zone. The velocities for each zone are averaged and the volumetric flow is given by:

$$V = \bar{v}A \qquad (3)$$

where $\bar{v}$ is the average velocity and A is the area of the test section.

Discussion of techniques for dividing test sections into equal area zones will be limited to ducts of circular and rectangular cross sections, since sampling in ducts of other forms is rare. For ducts of unusual shape, the volumetric flow should be determined by graphic integration for accurate results.

The number of test zones into which a flue is divided will depend upon the uniformity of velocity distribution and the accuracy desired, and not upon the size of the duct, since for any two similar ducts (different only in size) with similar velocity distributions, an equal number of velocity readings will be required to determine the average velocities with equal accuracy. However, in practice, the size of the pitot tube will limit the number of velocity measurements in small ducts.

The tangential method divides a duct of circular cross section into n equal zones, a circular central zone and (n-1) annular zones (Figure 4). Each zone is divided into two equal area annular parts and the velocity measurement is made at the radius of the boundary between the equal area parts. The mathematical derivation of the division of a circular cross section by this technique is found in Ower[35]. The method of dividing a circular duct by this technique is shown in Figure 4. The EPA sampling procedure uses this technique[36], as shown in Figure 5.

The log-linear method is an alternative which gives higher accuracy. The circular cross section is again divided into equal area annular zones, but the velocity is not arbitrarily measured at the center of area of each zone. Instead, the measurement points are calculated on the basis of an empirical analysis of the flow through circular pipes. The development of this method, including the determination of the measurement points, may be found in Ower[35]. The results are summarized in Table 3.

For fully developed flow, Winternitz[37] found that a four point log-linear traverse gave an error of less than 0.5%; whereas the ten point tangential method overestimated the mean velocity by about 1%. For nonfully developed flow, the ten point tangential technique was somewhat better than the four point log-linear, but an eight point log-linear method was superior to the ten point tangential method. The six point log-linear method will give results with an error of less than 1% in flow distributions as asymmetric as that shown in curve A[35] of Figure 6.

Because the log-linear method provides better accuracy than the tangential method for an equal number of measurements, it is recommended for velocity traverses in ducts of circular cross section. At the present time, the log-linear method is in general use in the United Kingdom[33,38].

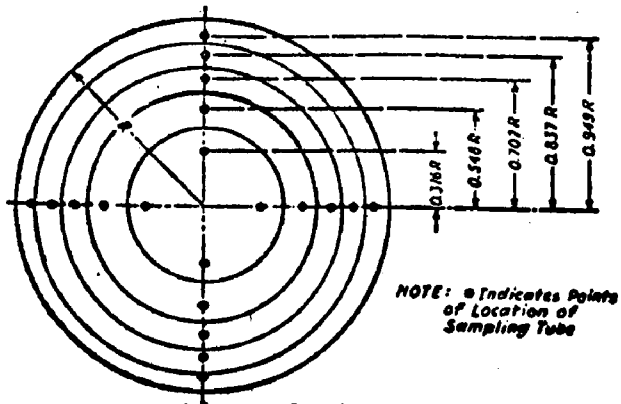

cross section of circular duct

Formula for determining location of points in circular duct

$$r_p = \sqrt{\frac{2R^2(2p-1)}{n}}$$

where r_p = distance from center of duct to point p
R = radius of duct
p = sampling point number. To be numbered from center of duct outward. All four points on same circumference have same number.
n = total number of points

NOTE: r_p will be in same units as R.

Example: Duct radius = R; 20 points total.
Distance to point 3 = r_3.

$$r_3 = \sqrt{\frac{2R^2(2\cdot 3-1)}{n}} = \sqrt{\frac{2R^2 5}{20}} = \sqrt{.5R^2}$$

$r_3 = 0.707R$

Figure 4. Tangential Method for Duct Division[31]

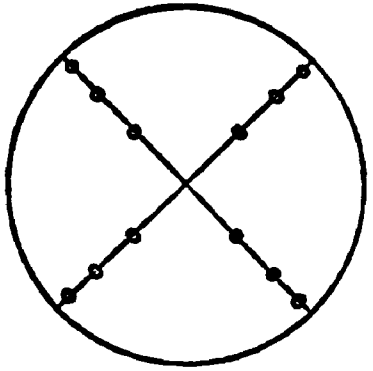

Cross section of circular stack divided into 12 equal areas, showing location of traverse points at centroid of each area.

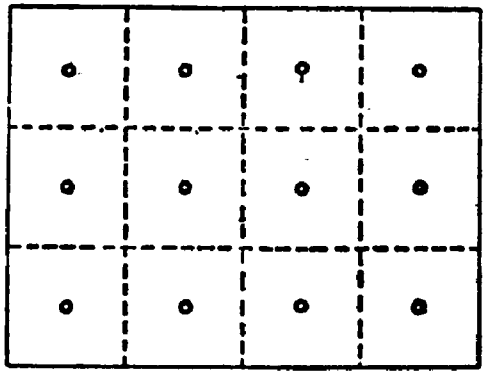

Cross section of rectangular stack divided into 12 equal areas, with traverse points at centroid of each area.

Location of traverse points in circular stacks
(Percent of stack diameter from inside wall to traverse point)

Traverse point number on a diameter	Number of traverse points on a diameter											
	2	4	6	8	10	12	14	16	18	20	22	24
1	14.6	6.7	4.4	3.3	2.5	2.1	1.8	1.6	1.4	1.3	1.1	1.1
2	85.4	25.0	14.7	10.5	8.2	6.7	5.7	4.9	4.4	3.9	3.5	3.2
3		75.0	29.5	19.4	14.6	11.8	9.9	8.5	7.5	6.7	6.0	5.5
4		93.3	70.5	32.3	22.6	17.7	14.6	12.5	10.9	9.7	8.7	7.9
5			85.3	67.7	34.2	25.0	20.1	16.9	14.6	12.9	11.6	10.5
6			95.6	80.6	65.8	35.5	26.9	22.0	18.8	16.5	14.6	13.2
7				89.5	77.4	64.5	36.6	28.3	23.6	20.4	18.0	16.1
8				96.7	85.4	65.0	63.4	37.5	29.6	25.0	21.8	19.4
9					91.8	82.3	73.1	62.5	38.2	30.6	26.1	23.0
10					97.5	88.2	79.9	71.7	61.8	38.8	31.5	27.2
11						93.3	85.4	78.0	70.4	61.2	39.3	32.3
12						97.9	90.1	83.1	76.4	69.4	60.7	39.8
13							94.3	87.5	81.2	75.0	68.5	60.2
14							98.2	91.5	85.4	79.6	73.9	67.7
15								95.1	89.1	83.5	78.2	72.8
16								98.4	92.5	87.1	82.0	77.0
17									95.6	90.3	85.4	80.6
18									98.6	93.3	88.4	83.9
19										96.1	91.3	86.8
20										98.7	94.0	89.5
21											96.5	92.1
22											98.9	94.5
23												96.8
24												98.9

Figure 5. EPA Sampling Point Locations.

TABLE 3

LOCATION OF MEASURING POINTS FOR LOG-LINEAR METHOD [37]

No. of Measuring Points Per Diameter	Distance from Wall in Pipe Diameters
4	0·043, 0·290, 0·710, 0·957
6	0·032, 0·135, 0·321, 0·679, 0·865, 0·968
8	0·021, 0·117, 0·184, 0·345 0·655, 0·816, 0·883, 0·979
10	0·019, 0·076, 0·153, 0·217, 0·361 0·639, 0·783, 0·847, 0·924, 0·981

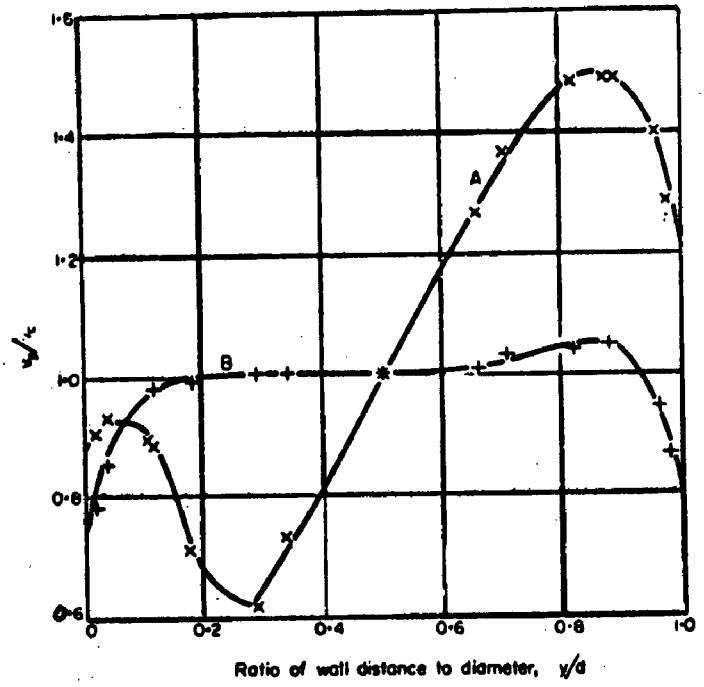

Figure 6. Types of Asymmetric Velocity Distribution in Pipes

The technique used for dividing a rectangular duct into equal area zones is to divide the section into a number of geometrically similar rectangular zones and to measure the velocity at the centroid of each zone. The rules regarding the number of zones are more arbitrary than for circular ducts. As in the case of circular ducts, the accuracy of the traverse will depend on the uniformity of the flow and the number of velocity measurements. However, it is a convention to increase the number of sampling points with duct size. The recommended number of test points in two different procedures are given in Table 4 as a function of the cross section area of the duct. The EPA method contains a similar formulation[36].

British Standards[39] 1042 recommends a division into at least 16 zones, with five velocity measurements in each corner zone, and three velocity measurements on each wall zone. The velocity in each zone is averaged before averaging the velocities over the duct. No zone should be greater than 36 inches^2, which means that more than 16 zones are necessary for ducts with cross sectional areas over 4 feet^2. The BSI Traverse Plan is shown in Figure 7.

The National Engineering Laboratory (U.K.) has found that errors of 2% or more can occur for certain types of asymmetric flow distributions when the 16 part, 48 point traverse is used[37].

A variety of sample point location methods based on other mathematical formulae have been presented by ASME[42]. A table of these methods is shown in Table 5. Figure 8 gives a comparison of these methods when applied to some hypothetical flow proflies.

(d) Summary

The main point of this discussion relevant to the development of procedures to obtain representative samples for gas flow is the intrinsic coupling of velocity and concentration in the area integral (Equation 1) describing the total emission in a general non-uniform system. If we are to obtain a representative value for concentration, it must be

TABLE 4

TEST POINTS FOR RECTANGULAR DUCTS

A. Haaland [40]

Cross Section Area Square Feet	Number of Test Points
Less than 2	4
2 to 25	12
Greater than 25	20 or more

B. ASTM [41]

Inside Cross Sectional Area of Flue, ft^2	Minimum Number of Test Points
1* to 3	4
2< to 12	6 - 24
12<	More than 24

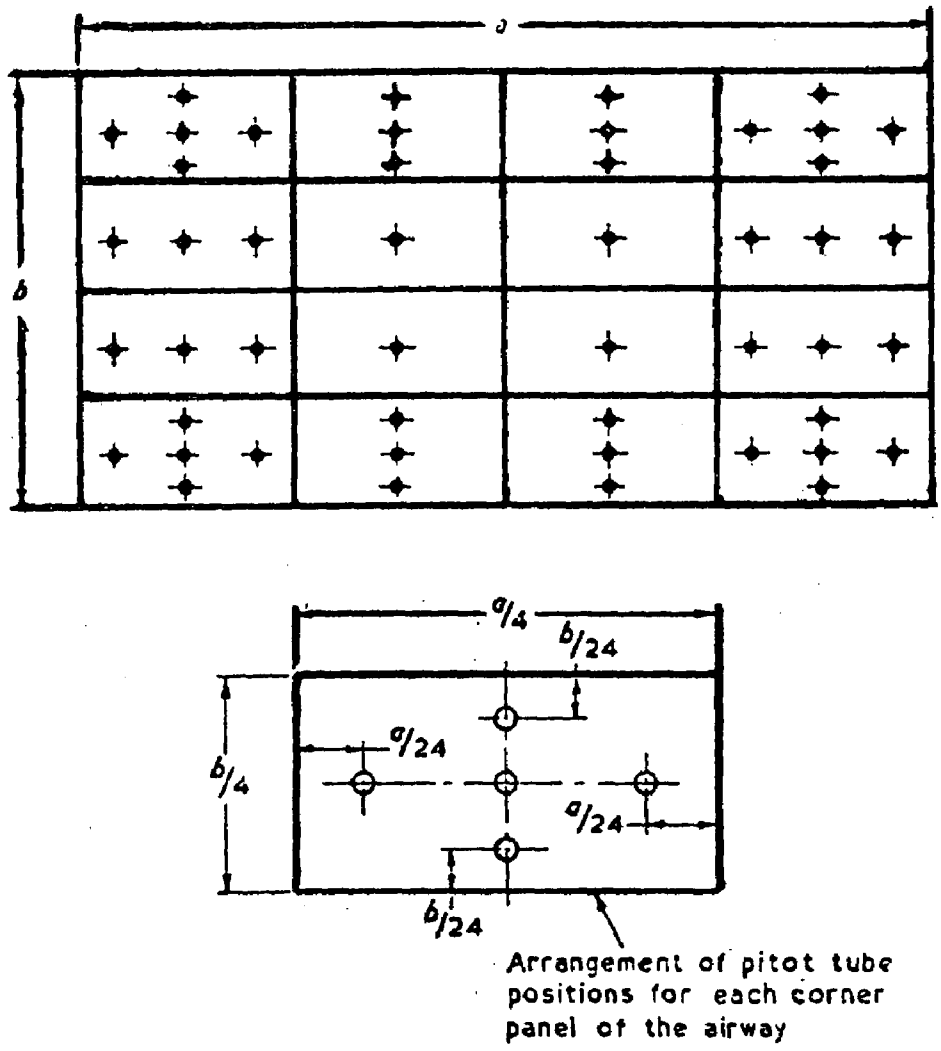

Figure 7. Traverse Plan for Rectangular Duct[38]

TABLE 5.

STATION LOCATIONS AND WEIGHTS FOR AVERAGING

Averaging for linear interval $0 \leq x \leq 1$

Averaging in a circular duct, in interval $0 \leq r \leq 1$

NUMBER OF STATIONS	METHOD											
	CENTROID OF EQUAL AREAS (a)			NEWTON-COTES			CHEBYSHEF (a)			GAUSS		
n	x	r	w	x	r	w	x	r	w	x	r	w
2	0.2500 .7500	0.5000 .8660	1/2	(b) 0 1	(b) 0 1	(b) 1/2	(e) 0.2113 .7887	(e) 0.4597 .8881	(e) 1/2	(e) 0.2113 .7887	(e) 0.4597 .8881	(e) 1/2
3	0.1667 .5000 .8333	0.4082 .7071 .9129	1/3	(c) 0 0.5 1	(c) 0 0.7071 1	(c) 0.1667 .6667 .1667	0.1464 .5000 .8536	0.3827 .7071 .9239	1/3	0.1127 .5000 .8873	0.3357 .7071 .9420	0.2778 .4444 .2778
4	0.1250 .3750 .6250 .8750	0.3536 .6124 .7906 .9354	1/4	(d) 0 0.3333 .6667 1	(d) 0 0.5774 .8165 1	(d) 0.1250 .3750 .3750 .1250	0.1027 .4072 .5928 .8973	0.3203 .6382 .7699 .9473	1/4	0.0694 .3300 .6700 .9306	0.2635 .5745 .8185 .9647	0.1739 .3261 .3261 .1739
5	0.1000 .3000 .5000 .7000 .9000	0.3162 .5477 .7071 .8367 .9487	1/5	0 0.25 .50 .75 1	0 .5000 .7071 .8660 1	0.0778 .3556 .1333 .3556 .0778	0.0838 .3127 .5000 .6873 .9162	0.2891 .5592 .7071 .8290 .9572	1/5	0.0469 .2308 .5000 .7692 .9531	0.2166 .4804 .7071 .8771 .9763	0.1185 .2393 .2844 .2393 .1185
6	0.0833 .2500 .4167 .5833 .7500 .9167	0.2887 .5000 .6455 .7638 .8660 .9574	1/6	0 0.2 .4 .6 .8 1	0 0.4472 .6325 .7746 .8944 1	0.0660 .2604 .1736 .1736 .2604 .0660	0.0669 .2887 .3667 .6333 .7113 .9331	0.2586 .5373 .6057 .7958 .8434 .9660	1/6			
7	0.0714 .2143 .3571 .5000 .6429 .7857 .9286	0.2673 .4629 .5976 .7071 .8018 .8864 .9636	1/7	0 0.1667 .3333 .5000 .6667 .8333 1	0 0.4082 .5774 .7071 .8165 .9129 1	0.0488 .2571 .0321 .3238 .0321 .2571 .0488	0.0581 .2352 .3381 .5000 .6619 .7648 .9419	0.2410 .4849 .5814 .7071 .8136 .8745 .9705	1/7			
8	0.0625 .1875 .3125 .4375 .5625 .6875 .8125 .9375	0.2500 .4330 .5590 .6614 .7500 .8292 .9014 .9682	1/8	0 0.1429 .2857 .4286 .5714 .7143 .8571 1	0 0.3780 .5345 .6547 .7559 .8452 .9258 1	0.0435 .2070 .0766 .1730 .1730 .0766 .2070 .0435	(f) 0.0513 .2036 .2964 .4487 .5513 .7036 .7964 .9487	(f) 0.2266 .4513 .5444 .6698 .7425 .8388 .8924 .9740	(f) 1/8			
9	0.0556 .1667 .2778 .3889 .5000 .6111 .7222 .8333 .9444	0.2357 .4082 .5270 .6236 .7071 .7817 .8498 .9129 .9718	1/9	0 0.1250 .2500 .3750 .5000 .6250 .7500 .8750 1	0 0.3536 .5000 .6124 .7071 .7906 .8660 .9354 1	0.0349 .2077 -.0327 .3702 -.1601 .3702 -.0327 .2077 .0349	0.0442 .1995 .2356 .4160 .5000 .5840 .7644 .8005 .9558	0.2103 .4466 .4854 .6450 .7071 .7642 .8743 .8947 .9776	1/9			
10	0.05 .15 .25 .35 .45 .55 .65 .75 .85 .95	0.2236 .3873 .5000 .5916 .6708 .7416 .8062 .8660 .9220 .9747	1/10	0 0.1111 .2222 .3333 .4444 .5556 .6667 .7778 .8889 1	0 0.3333 .4714 .5774 .6667 .7454 .8165 .8819 .9428 1	0.0319 .1757 .0121 .2159 .0645 .0645 .2159 .0121 .1757 .0319	(g) 0.0419 .1564 .2500 .3436 .4581 .5419 .6564 .7500 .8436 .9581	(g) 0.2046 .3954 .5000 .5862 .6768 .7361 .8102 .8660 .9185 .9788	(g) 1/10			
n	x	r	w	x	r	w	x	r	w			
	CENTROID OF EQUAL AREAS			NEWTON-COTES			CHEBYSHEF					

NOTES

(a) All measurements of equal weight

(b) Trapezoidal rule

(c) Parabolic rule (Simpson's rule)

(d) Three-eighths rule

(e) 0.2 - 0.8 rule

(f) Two 4-station intervals

(g) Two 5-station intervals

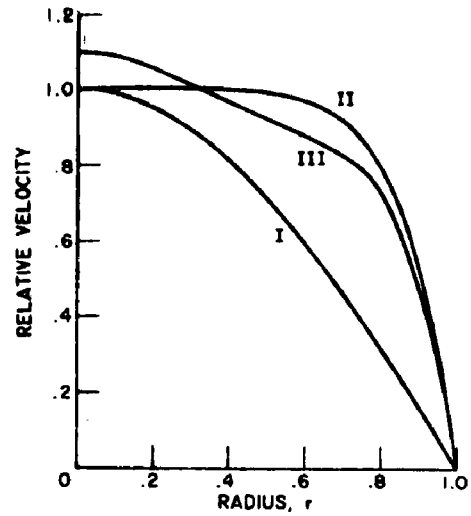

(a) VELOCITY DISTRIBUTIONS

	DISTRIBUTION		
	I	II	III
CENTROID OF EQUAL AREAS	−0.26	+1.16	+0.77
NEWTON-COTES	-0.00_5	−0.20	−0.08
CHEBYSHEF	-0.00_4	+0.02	+0.01
GAUSS	-0.00_8	-0.00_1	-0.00_2

(b) ERROR, %, IN 4-POINT APPROXIMATION

ERROR IN 4-POINT AVERAGING OF SOME ARBITRARY AXIALLY-SYMMETRIC VELOCITY DISTRIBUTIONS.

Figure 8.

weighted by the velocity at the sampling point, unless either the velocity or the concentration is uniform or can be made uniform by the sampling system.

It is interesting to note that the conditions which often lead to stratification[33] of particulate matter are often the most favorable for gas sampling. Components such as fans impart high shears and mix the gases passing through, tending to reduce stratification and non-uniform profiles. Particles which are subject to non-uniform inertia forces in the same processes are, in contrast, often segregated and consequently, large concentration gradients develop.

a.2 Simulation

The objective of the analytical simulation was to develop a measure of accuracy for the extraction of representative samples for several measurement strategies as a function of hypothetical and actual flow and concentration profiles, and specific system parameters, such as number and location of sampling points. Based on these results, we have attempted to develop a set of statistics that could be used to establish generalized sampling strategies.

To predict concentration and velocity profiles in ducts would require enormous effort, considering that the errors generated by the computational techniques and the unknown initial condition at the upstream end of the duct system would render the model virtually useless in predicting stack gas effluent rates. To apply this approach, some of the problems that would have to be overcome are the following:

(a) Numerical solution methods must be developed for the simultaneous solution of the three-dimensional forms of:

(1) the continuity equation
(2) the equations of motion (Navier-Stokes Equations)
(3) energy equation
(4) equations of state for the fluid phase
(5) viscosity dependence on temperature

(b) The geometric configuration of the stack and the conditions existing at the duct walls must be specified.

(c) The initial condition in the fire box must be specified.

The boundary conditions on the duct walls depend, in general, on prevailing weather conditions such as wind and humidity. The initial condition in the fire box depends on the reaction rate in coal burning, and a variety of other conditions which affect coal combustion. Since these effects are not generally known, it would be futile to attempt to simulate the flow, heat and mass transport through the network of ducts and equipment leading to the stack.

Therefore, in this study we adopted an approach such that one specifies duct geometry, actual concentration and velocity profiles in the duct, and the number of probes and location and area associated with each probe. The model, which has been programmed for digital solution, will then compute the actual effluent rates, viz.:

$$\frac{\int_A CV\,dA}{\int_A dA} \quad \text{and} \quad \frac{\int_A V\,dA}{\int_A dA}$$

The error in the measured and actual effluent rate is then calculated as:

$$\varepsilon_1 = \frac{\left| \int_A CV\,dA - \sum_i C_i V_i A_i \right|}{\int_A CV\,dA}$$

$$\varepsilon_2 = \frac{\left| \int_A V\,dA - \sum_i V_i A_i \right|}{\int V\,dA}$$

By calculating a series of such cases, graphs have been produced showing the error in stack gas measurement (i.e., average velocity effluent emission rate) as a function of number of probes, probe location, strategy, and specified concentration and velocity profiles. These graphs serve as guidelines for determining the best number, location, and strategy for placing probes in a specific duct if some a priori estimate for measurement (survey) of the duct profiles is available.

a.3 Simulation Results

Sixteen fictitious and actual stratification profile sets were identified and prepared for sampling strategy evaluation. (See Appendix G for figures 9-a through 21-b and Table 6.) These cases included the analytic functions:

CASE I

$$u(x,y) = \frac{90}{4ab}\left[1 - \left(\frac{2x}{a}\right)^2\right]\left[1 - \left(\frac{2y}{b}\right)^2\right]$$

$$c(x,y) = C_o\left[1 + \frac{1}{4}\left(1 + \frac{2x}{a}\right)\left(1 + \frac{2y}{b}\right)\right]$$

for a rectangular duct where a and b are ducts dimensions and Q is the volumetric flow rate; and

CASE II

$$U(r,\theta) = \frac{2Q}{\pi a^2}\left[1 - \frac{r^2}{a}\right]$$

$$c(r,\theta) = C_o\left(\frac{r}{a}\right)\sin^2\theta$$

for a circular duct of radius a.

Case III (Figures 9-a and 9-b) consists of normalized velocity and concentration (CO_2) profiles derived from exhaust emission measurements of a T-53 aircraft gas turbine combustor at idle setting (circular duct). Case IV (Figures 10-a and 10-b) consists of velocity and temperature profiles taken from an EPA test of a coal fired boiler sampled at a precipitator inlet (rectangular duct). For test purposes, the temperature profile in degrees Fahrenheit has been taken as the concentration profile for the duct. Case V, also a rectangular duct and shown in Figures 11-a and 11-b, illustrates actual velocity and SO_2 stratification immediately downstream of a coal-fired TVA boiler. Cases VI - IX, shown in Figures 12-a and 12-b , 13-a and 13-b, 14-a and 14-b and 15-a and 15-b, are hypothetical concentration and velocity profiles for circular ducts as defined by Walden staff. Cases X and XI, shown in Figures 16-a and 16-b and 17-a and 17-b, respectively, are also hypothetical profiles but for rectangular ducts. Cases XIII-1 to XIII-4, shown in Figures 18-a,b to 21-a,b are actual concentration velocity data obtained from a TVA duct immediately downstream of a coal-fired power plant furnace. Case XII, shown in Table 6, is for an experimental wind tunnel test conducted at Walden.

Strategies selected for testing of the rectangular duct cases include: equal area (1, 9, 16, 49, 100 probes); British Standard 1042 (48 probes); Newton Cotes* (9, 16, 49, 100 probes); Gauss* (9, 16 probes); Chebyshef (9, 16, 49, 100 probes); equal area with square area segments (50 probes); and an equal area circular ring analog (8, 16, 24 probes) defined by the sketch below (4 zones, 16 probes).

---

* points weighed equally <u>not</u> appropriate weighting factors

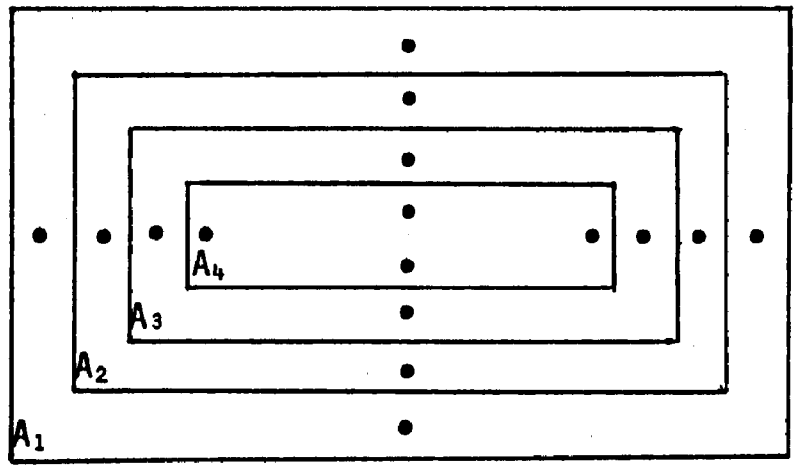

$A_1=A_2=A_3=A_4$

This latter procedure is applicable when two ports are located perpendicular to one another at the center points of adjacent sides in a rectangular duct. Traverse positions for the zones are listed in Table 7. Note that probes located according to the Chebyshef procedure for zones of this type were analyzed for Case XII.

Strategies selected for testing of the circular duct cases include: the centroid of the duct (1 probe); tangential (2, 4, 6 points per diameter; 2 diameters* and 4 diameters**); and log linear (4, 6, 8 points per diameter; 2 diameters* and 4 diameters**). In addition, both the log-linear and tangential strategies have been investigated with orthogonal probes, containing 6 probes per diameter with the diameters rotated so that additional probe sampling locations of 30° and 120°; 45° and 135°; and 60° and 150° can be simulated.

Test results for the 16 sample cases are shown in Tables 8 and 9-1 thru 9-15 and are summarized in Tables 10-1 thru 11-4, Figures 22 thru 29, Tables 12-1 thru 12-5 and Figures 30 thru 33. In Tables 10-1 thru 10-7 the left most entry for the average error in emission or velocity has been

---

* Probes oriented at 0° and 90°

** Probes oriented at 9°, 45°, 90°, and 135°

TABLE 7

VELOCITY TRAVERSE POINTS IN RECTANGULAR DUCTS
WITH PERPENDICULAR PORTS

PERCENT OF DISTANCE ACROSS DUCT

Traverse Point	Number of Zones Across Duct				
	2	3	4	5	6
1	7.3	4.6	3.4	2.6	2.2
2	17.7	15.2	10.7	8.3	6.8
3	82.3	35.6	19.8	14.8	12.0
4	92.7	64.4	36.0	23.1	17.8
5	--	84.8	64.0	38.8	25.4
6	--	95.4	80.2	61.2	39.8
7	--	--	89.3	76.9	60.2
8	--	--	96.6	85.2	74.6
9	--	--	--	91.7	82.2
10	--	--	--	97.4	88.0
11	--	--	--	--	93.2
12	--	--	--	--	97.8

TABLE 8

TEST RESULTS FOR A RECTANGULAR DUCT (5' x 10')

WITH VELOCITY AND CONCENTRATION PROFILES OF THE FORM:

$$U(x,y) = \frac{9Q}{4ab}\left[1 - \left(\frac{2x}{a}\right)^2\right]\left[1 - \left(\frac{2y}{b}\right)^2\right]$$

$$C(x,y) = C_o\left[1 + \frac{1}{4}\left(1 + \frac{2x}{a}\right)\left(1 + \frac{2y}{b}\right)\right]$$

Strategy: Equal Area with Square Equal Area Segments

	Error (ε) Computed by Program		Error (ε) Hand Calculated	
# Probes	$\varepsilon_{emission}$	$\varepsilon_{ave.\ velocity}$	$\varepsilon_{emission}$	$\varepsilon_{ave.\ velocity}$
50	+ 2.52%	+ 2.52%	n.c.**	+ 2.5%

Strategy: Newton-Cotes*

	Error (ε) Computed by Program		Error (ε) Hand Calculated	
# Probes	$\varepsilon_{emission}$	$\varepsilon_{ave.\ velocity}$	$\varepsilon_{emission}$	$\varepsilon_{ave.\ velocity}$
9	- 74.9%	- 75.0%	- 75.0%	- 75.0%
16	- 55.5%	- 55.6%	- 55.5%	- 55.5%
49	- 30.6%	- 30.6%	n.c.	- 30.5%
100	- 21.0%	- 21.0%	n.c.	- 21.0%

TABLE 8 (continued)

Strategy: Chebyshef

# Probes	Error (ε) Computed by Program		Error (ε) Hand Calculated	
	$\varepsilon_{emission}$	$\varepsilon_{ave.\ velocity}$	$\varepsilon_{emission}$	$\varepsilon_{ave.\ velocity}$
9	- .012%	- .013%	0%	- .034%
16	+ .124%	+ .124%	n.c.	+ .117%
49	+ .020%	+ .021%	n.c.	+ .013%
100	+ .007%	+ .008%	n.c.	+ .0004%

Strategy: British Standards 1042

# Probes	Error (ε) Computed by Program		Error (ε) Hand Calculated	
	$\varepsilon_{emission}$	$\varepsilon_{ave.\ velocity}$	$\varepsilon_{emission}$	$\varepsilon_{ave.\ velocity}$
48	+ 3.85%	+ 3.85%	n.c.	3.97%

Strategy: Gauss*

# Probes	Error (ε) Computed by Program		Error (ε) Hand Calculated	
	$\varepsilon_{emission}$	$\varepsilon_{ave.\ velocity}$	$\varepsilon_{emission}$	$\varepsilon_{ave.\ velocity}$
9	- 19.0%	- 19.0%	- 20.4%	- 19.0%
16	- 26.5%	- 26.5%	n.c.	- 26.6%

TABLE 8 (continued)

Strategy: Equal Area

# Probes	Error (ε) Computed by Program		Error (ε) Hand Calculated	
	$\varepsilon_{emission}$	$\varepsilon_{ave.\ velocity}$	$\varepsilon_{emission}$	$\varepsilon_{ave.\ velocity}$
1	+ 124.9%	+ 125.0%	n.c.	+ 125.0%
9	+ 11.4%	+ 11.4%	n.c.	+ 11.4%
16	+ 6.36%	+ 6.36%	n.c.	+ 6.34%
49	+ 2.04%	+ 2.04%	n.c.	+ 2.03%
100	+ 1.00%	+ 1.00%	n.c.	+ 0.99%

Strategy: Circular Analog-Equal Area

# Probes	Error (ε) Computed by Program		Error (ε) Hand Calculated	
	$\varepsilon_{emission}$	$\varepsilon_{ave.\ velocity}$	$\varepsilon_{emission}$	$\varepsilon_{ave.\ velocity}$
8	- 3.98%	- 3.98%	n.c.	- 4.0%
16	+ 16.5%	+ 16.5%	n.c.	+ 16.5%
24	+ 14.9%	+ 14.9%	n.c.	+ 14.9%

* Points weighted equally not by appropriate weighting factors

** n.c. means not calculated

Test Results for Case II

Strategy: Centroid

# Probes	Error (ε) Computed by Program	
	$\varepsilon_{emission}$	$\varepsilon_{ave.\ velocity}$
1	- 51.3 %	+ 99.4 %

Strategy: Log Linear

# Probes	Error (ε) Computed by Program	
	$\varepsilon_{emission}$	$\varepsilon_{ave.\ velocity}$
4 probes/diameter-2 diameters*	- 23.1 %	- 1.19%
4 probes/diameter-4 diameters**	- 11.1 %	- 1.20%
6 probes/diameter-2 diamerers*	- 18.4 %	- 2.5 %
6 probes/diameter-4 diameters**	- 7.9 %	- 2.5 %
8 probes/diameter-2 diameters*	- 15.9 %	- .001%
8 probes/diameter-4 diameters**	- 5.2 %	- .004%
6 probes/diameter-2 diameters(30° and 120°)	+ 3.8 %	- 2.5 %
6 probes/diameter-2 diameters(45° and 135°)	+ 2.5 %	- 2.5 %
6 probes/diameter-2 diameters(60° and 150°)	- 21.0 %	- 2.5 %

Strategy: Tangential

# Probes	Error (ε) Computed by Program	
	$\varepsilon_{emission}$	$\varepsilon_{ave.\ velocity}$
2 probes/diameter-2 diameter*	+ 26.1 %	- 0.22%
2 probes/diameter-4 diameters**	+ 31.3 %	- 0.22%
4 probes/diameter-2 diameters*	- 1.24%	+ 0.005%
4 probes/diameter-4 diameters**	+ 8.2 %	+ 0.005%
6 probes/diameter-2 diameters*	- 7.2 %	+ 0.119%
6 probes/diameter-4 diameters**	+ 2.8 %	+ 0.117%
6 probes/diameter-2 diameters(30° and 120°)	+ 15.5 %	+ 0.116%
6 probes/diameter-2 diameters(45° and 135°)	+ 12.8 %	+ 0.115%
6 probes/diameter-2 diameters(60° and 150°)	- 15.2 %	+ 0.115%

* 0° and 90° ** 0°, 45°, 90°, 135°

TABLE 9-2

Test Results for Case III

Strategy: Centroid

# Probes	Error (ε) Computed by Program	
	$\varepsilon_{emission}$	$\varepsilon_{ave.\ velocity}$
1	+ 8.6 %	- 10.0 %

Strategy: Log Linear

# Probes	Error (ε) Computed by Program	
	$\varepsilon_{emission}$	$\varepsilon_{ave.\ velocity}$
4 probes/diameter-2 diameters*	- 1.60%	- 1.98%
4 probes/diameter-4 diameters**	- 0.91%	- 1.85%
6 probes/diameter-2 diamerers*	- 1.62%	- 2.04%
6 probes/diameter-4 diameters**	- .74%	- 1.9 %
8 probes/diameter-2 diameters*	+ .145%	- .191%
8 probes/diameter-4 diameters**	+ 1.08%	.059%
6 probes/diameter-2 diameters(30° and 120°)	+ .48%	- 1.77%
6 probes/diameter-2 diameters(45° and 135°)	+ .137%	- 1.78%
6 probes/diameter-2 diameters(60° and 150°)	- 1.17%	- 1.81%

Strategy: Tangential

# Probes	Error (ε) Computed by Program	
	$\varepsilon_{emission}$	$\varepsilon_{ave.\ velocity}$
2 probes/diameter-2 diameter*	+ 10.1 %	+ 10.5 %
2 probes/diameter-4 diameters**	+ 12.0 %	+ 10.7 %
4 probes/diameter-2 diameters*	+ 4.2 %	+ 4.2 %
4 probes/diameter-4 diameters**	+ 5.4 %	+ 4.4 %
6 probes/diameter-2 diameters*	+ 2.7 %	+ 2.5 %
6 probes/diameter-4 diameters**	+ 3.8 %	+ 2.7 %
6 probes/diameter-2 diameters(30° and 120°)	+ 5.2 %	+ 2.9 %
6 probes/diameter-2 diameters(45° and 135°)	+ 4.8 %	+ 2.9 %
6 probes/diameter-2 diameters(60° and 150°)	+ 3.5 %	+ 2.8 %

* 0° and 90° ** 0°, 45°, 90°, 135°

TABLE 9-3

Test Results for Case IV

Strategy: British Standards 1042

# Probes	Error (ε) Computed by Program	
	$\varepsilon_{emission}$	$\varepsilon_{ave.\ velocity}$
48	+ 5.4 %	+ 5.4 %

Strategy: Equal Area

# Probes	Error (ε) Computed by Program	
	$\varepsilon_{emission}$	$\varepsilon_{ave.\ velocity}$
1	+ 37.7 %	+ 36.0 %
9	+ 8.4 %	+ 8.2 %
16	+ 13.4 %	+ 13.4 %
49	+ 7.7 %	+ 7.8 %

Strategy: Circular Analog-Equal Area

# Probes	Error (ε) Computed by Program	
	$\varepsilon_{emission}$	$\varepsilon_{ave.\ velocity}$
8	- 2.8 %	- 2.9 %
16	- 2.6 %	- 3.0 %
24	- 3.6 %	- 4.0 %

Strategy: Newton-Cotes*

# Probes	Error (ε) Computed by Program	
	$\varepsilon_{emission}$	$\varepsilon_{ave.\ velocity}$
9	- 84.2 %	- 84.3 %
16	- 70.9 %	- 70.9 %
49	- 41.5 %	- 41.6 %

* Points weighted equally not by appropriate weighting factors

TABLE 9-3(cont.)

Strategy: Gauss*

# Probes	Error (ε) Computed by Program	
	$\varepsilon_{emission}$	$\varepsilon_{ave.\ velocity}$
9	+ 7.2 %	+ 7.1 %
16	+ 3.3 %	+ 3.9 %

Strategy: Chebyshef

# Probes	Error (ε) Computed by Program	
	$\varepsilon_{emission}$	$\varepsilon_{ave.\ velocity}$
9	+ 8.0 %	+ 7.8 %
16	+ 11.4 %	+ 11.2 %
49	+ 4.0 %	+ 4.1 %

* Points weighted equally not by appropriate weighting factors

TABLE 9-4

Test Results for Case V

Strategy: British Standards 1042

# Probes	Error (ε) Computed by Program	
	$\varepsilon_{emission}$	$\varepsilon_{ave.\ velocity}$
48	+ 1.15%	+ 3.54%

Strategy: Equal Area

# Probes	Error (ε) Computed by Program	
	$\varepsilon_{emission}$	$\varepsilon_{ave.\ velocity}$
1	+ 3.13%	+ 7.44%
9	+ 21.8 %	+ 22.9 %
16	+ 11.4 %	+ 14.7 %
49	+ 6.0 %	+ 5.3%

Strategy: Circular Analog-Equal Area

# Probes	Error (ε) Computed by Program	
	$\varepsilon_{emission}$	$\varepsilon_{ave.\ velocity}$
8	- .72%	+ 7.5 %
16	- 7.8 %	+ 0.81%
24	- 8.4 %	- .088%

Strategy: Newton-Cotes*

# Probes	Error (ε) Computed by Program	
	$\varepsilon_{emission}$	$\varepsilon_{ave.\ velocity}$
9	- 88.1 %	- 87.3 %
16	- 66.1 %	- 68.1 %
49	- 37.9 %	- 36.4 %

* Points weighted equally not by appropriate weighting factors

TABLE 9-4 (cont.)

Strategy: Gauss*

# Probes	Error (ε) Computed by Program	
	$\varepsilon_{emission}$	$\varepsilon_{ave.\ velocity}$
9	- .685%	+ 6.1 %
16	+ 2.2 %	- 7.0 %

Strategy: Chebyshef

# Probes	Error (ε) Computed by Program	
	$\varepsilon_{emission}$	$\varepsilon_{ave.\ velocity}$
9	+ 16.9 %	+ 18.5 %
16	+ .63%	+ 5.3 %
49	+ 6.3 %	+ .012%

* Points weighted equally not by appropriate weighting factors

TABLE 9-5

Test Results for Case VI

Strategy: Centroid

# Probes	Error (ε) Computed by Program εemission	εave. velocity
1	+ 115.5 %	+ 68.6 %

Strategy: Log Linear

# Probes	Error (ε) Computed by Program εemission	εave. velocity
4 probes/diameter-2 diameters*	- 24.5 %	- 13.2 %
4 probes/diameter-4 diameters**	- 18.3 %	- 8.0 %
6 probes/diameter-2 diamerers*	- 15.9 %	- 9.3 %
6 probes/diameter-4 diameters**	- 9.1 %	- 4.1 %
8 probes/diameter-2 diameters*	- 9.5 %	- 6.9 %
8 probes/diameter-4 diameters**	- 2.3 %	- 1.66%
6 probes/diameter-2 diameters(30° and 120°)	- 4.7 %	+ .29%
6 probes/diameter-2 diameters(45° and 135°)	- 2.3 %	+ 1.11%
6 probes/diameter-2 diameters(60° and 150°)	+ 1.66%	+ 4.6 %

Strategy: Tangential

# Probes	Error (ε) Computed by Program εemission	εave. velocity
2 probes/diameter-2 diameter*	+ 24.9 %	+ 14.9 %
2 probes/diameter-4 diameters**	+ 35.4 %	+ 21.5 %
4 probes/diameter-2 diameters*	- 6.3 %	- 1.14%
4 probes/diameter-4 diameters**	+ 1.68%	+ 4.7 %
6 probes/diameter-2 diameters*	- 7.9 %	- 3.5 %
6 probes/diameter-4 diameters**	.27%	+ 2.1 %
6 probes/diameter-2 diameters(30° and 120°)	+ 4.7 %	+ 6.9 %
6 probes/diameter-2 diameters(45° and 135°)	+ 7.4 %	+ 7.7 %
6 probes/diameter-2 diameters(60° and 150°)	+ 11.8 %	+ 11.7 %

* 0° and 90° ** 0°, 45°, 90°, 135°

TABLE 9-6

Test Results for Case VII

Strategy: Centroid

# Probes	Error (ε) Computed by Program $\varepsilon_{emission}$	$\varepsilon_{ave.\ velocity}$
1	+ 129.6 %	+ 68.6 %

Strategy: Log Linear

# Probes	Error (ε) Computed by Program $\varepsilon_{emission}$	$\varepsilon_{ave.\ velocity}$
4 probes/diameter-2 diameters*	- 11.1 %	- 13.2 %
4 probes/diameter-4 diameters**	- 6.6 %	- 8.0 %
6 probes/diameter-2 diamerers*	- 9.9 %	- 9.3 %
6 probes/diameter-4 diameters**	- 5.5 %	- 4.1 %
8 probes/diameter-2 diameters*	- 5.8 %	- 6.9 %
8 probes/diameter-4 diameters**	- 1.26%	- 1.66%
6 probes/diameter-2 diameters(30° and 120°)	- 2.7 %	+ 0.29%
6 probes/diameter-2 diameters(45° and 135°)	- 1.10%	+ 1.11%
6 probes/diameter-2 diameters(60° and 150°)	+ 4.3 %	+ 4.6 %

Strategy: Tangential

# Probes	Error (ε) Computed by Program $\varepsilon_{emission}$	$\varepsilon_{ave.\ velocity}$
2 probes/diameter-2 diameter*	+ 10.1 %	+ 14.9 %
2 probes/diameter-4 diameters**	+ 15.2 %	+ 21.5 %
4 probes/diameter-2 diameters*	- 1.82%	- 1.14%
4 probes/diameter-4 diameters**	+ 3.1 %	+ 4.7 %
6 probes/diameter-2 diameters*	- 3.7 %	- 3.5 %
6 probes/diameter-4 diameters**	+ 1.11%	+ 2.1 %
6 probes/diameter-2 diameters(30° and 120°)	+ 4.1 %	+ 6.9 %
6 probes/diameter-2 diameters(45° and 135°)	+ 5.9 %	+ 7.7 %
6 probes/diameter-2 diameters(60° and 150°)	+ 11.8 %	+ 11.7 %

* 0° and 90° ** 0°, 45°, 90°, 135°

TABLE 9-7

Test Results for Case VIII

Strategy: Centroid

# Probes	Error (ε) Computed by Program: εemission	εave. velocity
1	+ 1078.7 %	+ 429 %

Strategy: Log Linear

# Probes	Error (ε) Computed by Program: εemission	εave. velocity
4 probes/diameter-2 diameters*	- 13.0 %	- 22.5 %
4 probes/diameter-4 diameters**	+ 12.1 %	- 8.5 %
6 probes/diameter-2 diamerers*	- 23.0 %	- 18.8 %
6 probes/diameter-4 diameters**	- 1.24%	- 7.8 %
8 probes/diameter-2 diameters*	- 19.4 %	- 15.4 %
8 probes/diameter-4 diameters**	+ 2.7 %	- 4.8 %
6 probes/diameter-2 diameters(30° and 120°)	+ 17.4 %	+ 1.95%
6 probes/diameter-2 diameters(45° and 135°)	+ 20.5 %	+ 3.2 %
6 probes/diameter-2 diameters(60° and 150°)	+ 18.7 %	- 6.9 %

Strategy: Tangential

# Probes	Error (ε) Computed by Program: εemission	εave. velocity
2 probes/diameter-2 diameter*	- 36.4 %	+ 2.6 %
2 probes/diameter-4 diameters**	- 19.6 %	+ 5.7 %
4 probes/diameter-2 diameters*	- 19.3 %	- 12.1 %
4 probes/diameter-4 diameters**	+ 3.5 %	- 1.92%
6 probes/diameter-2 diameters*	- 20.1 %	- 13.8 %
6 probes/diameter-4 diameters**	+ 2.4 %	- 3.2 %
6 probes/diameter-2 diameters(30° and 120°)	+ 22.4 %	+ 6.5 %
6 probes/diameter-2 diameters(45° and 135°)	+ 25.0 %	+ 7.3 %
6 probes/diameter-2 diameters(60° and 150°)	+ 23.5 %	- 3.5 %

* 0° and 90° ** 0°, 45°, 90°, 135°

TABLE 9-8

Test Results for Case IX

Strategy: Centroid

# Probes	Error (ε) Computed by Program	
	εemission	εave. velocity
1	+676.5 %	+429.2 %

Strategy: Log Linear

# Probes	Error (ε) Computed by Program	
	εemission	εave. velocity
4 probes/diameter-2 diameters*	- 18.3 %	- 22.5 %
4 probes/diameter-4 diameters**	- 2.1 %	- 8.5 %
6 probes/diameter-2 diamerers*	- 20.7 %	- 18.8 %
6 probes/diameter-4 diameters**	- 7.9 %	- 7.8 %
8 probes/diameter-2 diameters*	- 18.8 %	- 15.4 %
8 probes/diameter-4 diameters**	- 6.5 %	- 4.8 %
6 probes/diameter-2 diameters(30° and 120°)	+ 1.00%	+ 1.95%
6 probes/diameter-2 diameters(45° and 135°)	+ 4.8 %	+ 3.2 %
6 probes/diameter-2 diameters(60° and 150°)	+ .52%	- 6.9 %

Strategy: Tangential

# Probes	Error (ε) Computed by Program	
	εemission	εave. velocity
2 probes/diameter-2 diameter*	- 19.7 %	+ 2.6 %
2 probes/diameter-4 diameters**	- 15.2 %	+ 5.7 %
4 probes/diameter-2 diameters*	- 17.2 %	- 12.1 %
4 probes/diameter-4 diameters**	- 4.7 %	- 1.92%
6 probes/diameter-2 diameters*	- 18.0 %	- 13.8 %
6 probes/diameter-4 diameters**	- 5.5 %	- 3.2 %
6 probes/diameter-2 diameters(30° and 120°)	+ 3.5 %	+ 6.5 %
6 probes/diameter-2 diameters(45° and 135°)	+ 7.0 %	+ 7.3 %
6 probes/diameter-2 diameters(60° and 150°)	+ 2.6 %	- 3.5 %

* 0° and 90° ** 0°, 45°, 90°, 135°

TABLE 9-9

Test Results for Case X

Strategy: British Standards 1042

# Probes	Error (ε) Computed by Program	
	$\varepsilon_{emission}$	$\varepsilon_{ave.\ velocity}$
48	- .40%	- .42%

Strategy: Equal Area

# Probes	Error (ε) Computed by Program	
	$\varepsilon_{emission}$	$\varepsilon_{ave.\ velocity}$
1	+140.7 %	+108.8 %
9	+ 14.3 %	+ 12.9 %
16	+ 6.2 %	+ 7.2 %
49	+ 1.33%	+ 2.3 %

Strategy: Circular Analog-Equal Area

# Probes	Error (ε) Computed by Program	
	$\varepsilon_{emission}$	$\varepsilon_{ave.\ velocity}$
8	- 3.1 %	- 2.3 %
16	+ 19.8 %	+ 14.4 %
24	+ 18.4 %	+ 12.9 %

Strategy: Newton-Cotes*

# Probes	Error (ε) Computed by Program	
	$\varepsilon_{emission}$	$\varepsilon_{ave.\ velocity}$
9	- 73.3 %	- 77.3 %
16	- 54.6 %	- 57.2 %
49	- 29.0 %	- 31.2 %

* Points weighted equally not by appropriate weighting factors

TABLE 9-9(cont.)

Strategy: Gauss*

# Probes	Error (ε) Computed by Program	
	$\varepsilon_{emission}$	$\varepsilon_{ave.\ velocity}$
9	- 19.2 %	- 17.0 %
16	- 53.3 %	- 43.1 %

Strategy: Chebyshef

# Probes	Error (ε) Computed by Program	
	$\varepsilon_{emission}$	$\varepsilon_{ave.\ velocity}$
9	+ 1.80%	+ 1.84%
16	+ .190%	+ 0.101%
49	- 1.32%	+ .019%

* Points weighted equally not by appropriate weighting factors

TABLE 9-10

Test Results for Case XI

Strategy: British Standards 1042

# Probes	Error (ε) Computed by Program	
	$\varepsilon_{emission}$	$\varepsilon_{ave.\ velocity}$
48	+ 0.20%	+ 0.24%

Strategy: Equal Area

# Probes	Error (ε) Computed by Program	
	$\varepsilon_{emission}$	$\varepsilon_{ave.\ velocity}$
1	+ 55.6 %	+ 34.5 %
9	+ 20.7 %	+ 17.9 %
16	+ 10.3 %	+ 10.2 %
49	+ 2.3 %	+ 3.4 %

Strategy: Circular Analog-Equal Area

# Probes	Error (ε) Computed by Program	
	$\varepsilon_{emission}$	$\varepsilon_{ave.\ velocity}$
8	+ 9.7 %	+ 8.4 %
16	+ 12.6 %	+ 7.9 %
24	+ 11.7 %	+ 6.9 %

Strategy: Newton-Cotes*

# Probes	Error (ε) Computed by Program	
	$\varepsilon_{emission}$	$\varepsilon_{ave.\ velocity}$
9	- 79.0 %	- 82.3 %
16	- 58.4 %	- 60.9 %
49	- 29.6 %	- 32.2 %

* Points weighted equally not by appropriate weighting factors

TABLE 9-10 (cont.)

Strategy: Gauss*

# Probes	Error (ε) Computed by Program	
	εemission	εave. velocity
9	- 10.0 %	- 8.43%
16	- 35.8 %	- 25.8 %

Strategy: Chebyshef

# Probes	Error (ε) Computed by Program	
	εemission	εave. velocity
9	+ 10.4 %	+ 9.1 %
16	0.074%	0.005%
49	- 1.8 %	0.014%

* Points weighted equally not by appropriate weighting factors

TABLE 9-11

Test Results for Case XII

Strategy: British Standards 1042

# Probes	Error (ε) Computed by Program	
	$\varepsilon_{emission}$	$\varepsilon_{ave.\ velocity}$
48		

Strategy: Equal Area

# Probes	Error (ε) Computed by Program	
	$\varepsilon_{emission}$	$\varepsilon_{ave.\ velocity}$
1	+ 172.0 %	+ 27.4 %
9	+ 58.9 %	+ 15.5 %
16	+ 68.6 %	+ 16.1 %
25	+ 64.5%	+ 11.4%

Strategy: Circular Analog-Equal Area

# Probes	Error (ε) Computed by Program	
	$\varepsilon_{emission}$	$\varepsilon_{ave.\ velocity}$
8	+ 78.4 %	+ 16.7 %
16	+ 113.0 %	+ 8.2 %

Strategy: Circular Analog-Equal Area-Chebyshef Locations

# Probes	Error (ε) Computed by Program	
	$\varepsilon_{emission}$	$\varepsilon_{ave.\ velocity}$
8	+ 100.0 %	+ 24.2 %
16	+ 123.0 %	+ 13.8%

TABLE 9-11 (cont.)

Strategy: Chebyshef

# Probes	Error (ε) Computed by Program	
	$\varepsilon_{emission}$	$\varepsilon_{ave.\ velocity}$
9	+ 59.6%	+ 16.1 %
16	+ 65.7%	+ 14.7 %
25	+ 61.4%	+ 9.2 %

TABLE 9-12

Test Results for Case XIII-1

Strategy: British Standards 1042

# Probes	Error (ε) Computed by Program	
	εemission	εave. velocity
48	+ 2.2 %	+ 4.0 %

Strategy: Equal Area

# Probes	Error (ε) Computed by Program	
	εemission	εave. velocity
1	+ 5.7 %	+ 7.4 %
9	+ 9.9 %	+ 13.5 %
16	+ 11.2 %	+ 14.8 %
49	+ 7.9 %	+ 8.2 %

Strategy: Circular Analog-Equal Area

# Probes	Error (ε) Computed by Program	
	εemission	εave. velocity
8	+ 3.5 %	+ 5.9 %
16	+ 5.3 %	+ 2.8 %
24	+ 6.3 %	+ 3.6 %

Strategy: Chebyshef

# Probes	Error (ε) Computed by Program	
	εemission	εave. velocity
9	+ 9.9 %	+ 13.6 %
16	+ 8.7 %	+ 12.7 %
49	+ 6.6 %	+ 3.5 %

TABLE 9-13

Test Results for Case XIII-2

Strategy: British Standards 1042

# Probes	Error (ε) Computed by Program	
	$\varepsilon_{emission}$	$\varepsilon_{ave.\ velocity}$
48	+ 4.6 %	+ 4.0 %

Strategy: Equal Area

# Probes	Error (ε) Computed by Program	
	$\varepsilon_{emission}$	$\varepsilon_{ave.\ velocity}$
1	+ 11.1 %	+ 7.4 %
9	+ 16.5 %	+ 13.5 %
16	+ 18.6 %	+ 14.8 %
49	+ 10.2 %	+ 8.2 %

Strategy: Circular Analog-Equal Area

# Probes	Error (ε) Computed by Program	
	$\varepsilon_{emission}$	$\varepsilon_{ave.\ velocity}$
8	+ 4.1 %	+ 5.9 %
16	- 6.6 %	- 2.8 %
24	- 7.4 %	- 3.6 %

Strategy: Chebyshef

# Probes	Error (ε) Computed by Program	
	$\varepsilon_{emission}$	$\varepsilon_{ave.\ velocity}$
9	+ 16.8 %	+ 13.6 %
16	+ 16.4 %	+ 12.7 %
49	+ 2.8 %	+ 3.5 %

TABLE 9-14

Test Results for Case XIII-3

Strategy: British Standards 1042

# Probes	Error (ε) Computed by Program	
	$\varepsilon_{emission}$	$\varepsilon_{ave.\ velocity}$
48	+ 2.5 %	+ 3.5 %

Strategy: Equal Area

# Probes	Error (ε) Computed by Program	
	$\varepsilon_{emission}$	$\varepsilon_{ave.\ velocity}$
1	+ 2.4 %	+ 7.1 %
9	+ 15.5 %	+ 17.9 %
16	+ 12.8 %	+ 16.0 %
49	+ 6.4 %	+ 7.4 %

Strategy: Circular Analog-Equal Area

# Probes	Error (ε) Computed by Program	
	$\varepsilon_{emission}$	$\varepsilon_{ave.\ velocity}$
8	+ 10.3 %	+ 11.0 %
16	+ 1.2 %	+ 1.4 %
24	+ 0.33%	+ 0.60 %

Strategy: Chebyshef

# Probes	Error (ε) Computed by Program	
	$\varepsilon_{emission}$	$\varepsilon_{ave.\ velocity}$
9	+ 14.1 %	+ 17.5 %
16	+ 7.5 %	+ 11.6 %
49	+ 2.8 %	+ 1.7 %

TABLE 9-15

Test Results for Case XIII-4

Strategy: British Standards 1042

# Probes	Error (ε) Computed by Program	
	$\varepsilon_{emission}$	$\varepsilon_{ave.\ velocity}$
48	+ 4.1 %	+ 3.5 %

Strategy: Equal Area

# Probes	Error (ε) Computed by Program	
	$\varepsilon_{emission}$	$\varepsilon_{ave.\ velocity}$
1	+ 3.0 %	+ 7.1 %
9	+ 16.5 %	17.9 %
16	+ 15.1 %	16.0 %
49	+ 7.0 %	+ 7.2 %

Strategy: Circular Analog-Equal Area

# Probes	Error (ε) Computed by Program	
	$\varepsilon_{emission}$	$\varepsilon_{ave.\ velocity}$
8	+ 11.4 %	+ 11.0 %
16	+ 2.1 %	+ 1.4 %
24	+ 1.1 %	+ 0.6 %

Strategy: Chebyshef

# Probes	Error (ε) Computed by Program	
	$\varepsilon_{emission}$	$\varepsilon_{ave.\ velocity}$
9	+ 15.4 %	+ 17.5 %
16	+ 10.1 %	+ 11.6 %
49	+ 1.2 %	+ 1.7 %

TABLE 10-1

Average Errors for Four Rectangular Duct Sample Cases

Strategy: British Standards 1042

# Probes	Error (ε) Computed by Program			
	$\varepsilon_{emission}$		$\varepsilon_{ave.\ velocity}$	
48	1.6	1.8	2.2	2.4

Strategy: Equal Area

# Probes	Error (ε) Computed by Program			
	$\varepsilon_{emission}$		$\varepsilon_{ave.\ velocity}$	
1	59.3	59.3	46.7	46.7
9	16.3	16.3	15.5	15.5
16	10.3	10.3	11.4	11.4
49	4.3	4.3	4.7	4.7

Strategy: Circular Analog-Equal Area

# Probes	Error (ε) Computed by Program			
	$\varepsilon_{emission}$		$\varepsilon_{ave.\ velocity}$	
8	0.8	4.1	2.7	5.3
16	5.5	10.7	5.0	6.5
24	4.5	10.5	3.9	6.

Strategy: Newton-Cotes*

# Probes	Error (ε) Computed by Program			
	$\varepsilon_{emission}$		$\varepsilon_{ave.\ velocity}$	
9	-81.1	81.1	-82.8	82.8
16	-62.5	62.5	-64.2	64.2
49	-33.8	33.8	-35.3	35.3

* Points weighted equally not by appropriate weighting factors

TABLE 10-1. (cont.)

Strategy: Gauss*

# Probes	Error (ε) Computed by Program			
	$\varepsilon_{emission}$		$\varepsilon_{ave.\ velocity}$	
9	-5.7	9.3	-3.	9.6
16	-20.9	23.6	-18.	19.9

Strategy: Chebyshef

# Probes	Error (ε) Computed by Program			
	$\varepsilon_{emission}$		$\varepsilon_{ave.\ velocity}$	
9	9.3	9.3	9.3	9.3
16	3.1	3.1	4.1	4.1
49	1.8	3.3	1.0	1.0

* Points weighted equally not by appropriate weighting factors

TABLE 10-2

Average Error for Six Circular Ducts; Diameter Locations Segregated

Strategy: Centroid

# Probes	Error (ε) Computed by Program			
	εemission		εave. velocity	
1	326.3	343.4	180.8	184.1

Strategy: Log Linear

# Probes	Error (ε) Computed by Program			
	εemission		εave. velocity	
4 probes/diameter-2 diameters*	-15.3	15.3	-12.4	12.4
4 probes/diameter-4 diameters**	- 4.5	8.5	- 6.	6.
6 probes/diameter-2 diameters*	-14.9	14.9	-10.1	10.1
6 probes/diameter-4 diameters**	- 5.4	5.4	-4.7	4.7
8 probes/diameter-2 diameters*	-11.5	11.6	-7.5	7.5
8 probes/diameter-4 diameters**	- 1.9	3.2	-2.1	2.2
6 probes/diameter-2 diameters (30° and 120°)	2.5	5.	0.03	1.4
6 probes/diameter-2 diameters (45° and 135°)	4.1	5.2	0.7	2.1
6 probes/diameter-2 diameters (60° and 150°)	0.5	7.9	-1.5	4.5

Strategy: Tangential

# Probes	Error (ε) Computed by Program			
	εemission		εave. velocity	
2 probes/diameter-2 diameters*	2.5	21.2	7.5	7.6
2 probes/diameter-4 diameters**	9.8	21.4	10.8	10.9
4 probes/diameter-2 diameters*	-6.9	8.3	-3.7	5.1
4 probes/diameter-4 diameters**	2.9	4.4	1.7	2.9
6 probes/diameter-2 diameters*	-9.	9.9	-5.3	6.2
6 probes/diameter-4 diameters**	0.8	2.6	0.1	2.2
6 probes/diameter-2 diameters(30° and 120°)	9.2	9.2	5.	5.
6 probes/diameter-2 diameters(45° and 135°)	10.5	10.5	5.5	5.5
6 probes/diameter-2 diameters(60° and 150°)	6.3	11.4	3.2	5.5

* 0° and 90° ** 0°, 45°, 90°, 135°

TABLE 10-3

AVERAGE ERRORS FOR SIX CIRCULAR DUCTS
REGARDLESS OF STRATEGY AND DIAMETER LOCATION

# PROBES	εEMISSION		εVELOCITY	
1	326.3	343.4	180.8	184.1
4	2.5	21.2	7.5	7.6
8	-4.1	15.0	-1.8	9.5
12	1.1	9.3	-0.3	5.1
16	-4.4	8.2	-3.9	5.5
24	-2.3	4.0	-2.3	3.5
32	-1.9	3.2	-2.1	2.2

TABLE 10-4

AVERAGE ERRORS FOR FOUR RECTANGULAR DUCTS

REGARDLESS OF STRATEGY

# PROBES	εEMISSION		εVELOCITY	
1	59.3	59.3	46.7	46.7
8	0.8	4.1	2.7	5.3
9	-15.3	2.9	-15.3	29.3
16	-12.9	22.	-12.3	21.2
24	4.5	10.5	3.9	6.
48	1.6	1.8	2.2	2.4
49	-9.3	13.8	-9.9	13.7

TABLE 10-5

AVERAGE ERROR FOR TEN DUCTS

REGARDLESS OF STRATEGY, GEOMETRY AND LOCATION

# PROBES	εEMISSION		εVELOCITY	
1	219.5	229.7	127.1	129.1
4	2.5	21.2	7.5	7.6
8	-3.2	13.0	-1.	8.7
9	-15.3	29.	-15.3	29.3
12	1.1	9.3	-0.3	5.1
16	-8.9	15.5	-8.3	13.8
24	-0.6	5.6	-.7	4.1
32	-1.9	3.2	-2.1	2.2
48	1.6	1.8	2.2	2.4
49	-9.3	13.8	-9.9	13.7

TABLE 10-6

AVERAGE ERROR FOR SIX CIRCULAR DUCTS

BY STRATEGY AND PROBE NUMBER

REGARDLESS OF DIAMETER LOCATION

# PROBES	εEMISSION		εVELOCITY	
CENTROID				
1	326.3	343.4	180.8	184.1
LOG LINEAR				
8	-15.3	15.3	-12.4	12.4
12	-1.9	8.3	-2.7	4.6
16	-8.	10.	-6.7	6.8
24	-5.4	5.4	-4.7	4.7
32	-1.9	3.2	-2.1	2.2
TANGENTIAL				
4	2.5	21.2	7.5	7.6
8	1.4	14.9	3.5	8.
12	4.2	10.3	2.1	5.6
16	2.9	4.4	1.7	2.9
24	0.8	2.6	0.1	2.2

TABLE 10-7

AVERAGE ERROR FOR SIX CIRCULAR DUCTS

BY DIAMETER LOCATION AND PROBE NUMBER

REGARDLESS OF STRATEGY

# PROBES		εEMISSION		εVELOCITY	
4	(0°,90°) 2 diameter	2.5	21.2	7.5	7.6
8	(0°,90°) 2 diameter	-11.1	11.8	-8.1	8.8
12	(0°,90°) 2 diameter	-12.	12.4	-7.7	8.2
16	(0°-90°) 2 diameter	-11.5	11.6	-7.5	7.5
12	(30°,120°) 2 diameter	5.9	7.1	2.5	3.2
12	(45°,135°) 2 diameter	7.3	7.8	3.1	3.8
12	(60°,150°) 2 diameter	3.4	9.6	0.9	5.0
8	(0°,45°,90°,135°) 4 diameter	9.8	21.4	10.8	10.9
16	(0°,45°,90°,135°) 4 diameter	-.8	6.5	-2.2	4.5
24	(0°,45°,90°,135°) 4 diameter	-2.3	4.0	-2.3	3.5
32	(0°,45°,90°,135°) 4 diameter	-1.9	3.2	-2.1	2.2

TABLE 11-1

EMISSION ERROR VS. NUMBER OF PROBES
USING DIFFERENT METHODS FOR TRAVERSING RECTANGULAR DUCTS

Number of Probes	Case Number	Strategy % Error			
		Equal Area	Circular Analog	Chebyshef	British Standard
8, 9	IV	8.4	- 2.8	8.0	
	V	21.8	- 0.72	16.9	
	X	14.3	- 3.1	1.8	
	XI	20.7	9.7	10.4	
16	IV	13.4	- 2.6	11.4	
	V	11.4	- 7.8	0.63	
	X	6.2	19.8	0.19	
	XI	10.3	12.6	0.074	
24	IV		- 3.6		
	V		- 8.4		
	X		18.4		
	XI		11.7		
48, 49	IV	7.7		4.0	5.4
	V	6.0		6.3	1.15
	X	1.33		- 1.32	- 0.4
	XI	2.3		- 1.8	0.2

TABLE 11-2

PERCENT AVERAGE EMISSION ERROR
AND STANDARD DEVIATION
VS. NUMBER OF PROBES

Number of Probes	From All Strategies	
	% Average Emission	Standard Deviation
8, 9	8.78	8.67
16	6.30	8.13
24	4.52	12.61
48, 49	2.57	3.22

TABLE 11-3

EMISSION ERROR VS NUMBER OF PROBES USING DIFFERENT METHODS FOR TRAVERSING CIRCULAR DUCTS

Total Number of Probes	Case Number	STRATEGY % ERROR									
		Log Linear					Tangential				
		2 Diameter (1)	4 Diameter (2)	2 Diameter (3)	2 Diameter (4)	2 Diameter (5)	2 Diameter (1)	4 Diameter (2)	2 Diameter (3)	2 Diameter (4)	2 Diameter (5)
4	II						26.1				
	III						10.1				
	VI						24.9				
	VII						10.1				
	VIII						- 36.4				
	IX						- 19.7				
8	II	- 23.1					- 1.24	31.3			
	III	- 1.6					4.2	12.0			
	VI	- 24.5					- 6.3	35.4			
	VII	- 11.1					- 1.82	15.2			
	VIII	- 13.0					- 19.3	- 19.6			
	IX	- 18.3					- 17.2	- 15.2			
12	II	- 18.4		3.8	2.5	- 21.0	- 7.2		15.5	12.8	- 15.2
	III	- 1.62		0.48	0.137	- 1.17	2.7		5.2	4.8	3.5
	VI	- 15.9		- 4.7	- 2.3	+ 1.66	- 7.9		4.7	7.4	11.8
	VII	- 9.9		- 2.7	- 1.1	4.3	- 3.7		4.1	5.9	11.8
	VIII	- 23.0		17.4	20.5	18.7	- 20.1		22.4	25.0	23.5
	IX	- 20.7		1.0	4.8	0.52	- 18.0		3.5	7.0	2.6
16	II	- 15.9	- 11.1					8.2			
	III	- 0.145	- 0.91					5.4			
	VI	- 9.5	- 18.3					1.68			
	VII	- 5.8	- 6.6					3.1			
	VIII	- 19.4	12.1					3.5			
	IX	- 18.8	- 2.1					4.7			

TABLE 11-3 (Cont.)

EMISSION ERROR VS NUMBER OF PROBES USING DIFFERENT METHODS FOR TRAVERSING CIRCULAR DUCTS

Total Number of Probes	Case Number	STRATEGY % ERROR									
		Log Linear					Tangential				
		2 Diameter (1)	4 Diameter (2)	2 Diameter (3)	2 Diameter (4)	2 Diameter (5)	2 Diameter (1)	4 Diameter (2)	2 Diameter (3)	2 Diameter (4)	2 Diameter (5)
24	II		- 7.9					2.8			
	III		- 0.74					3.8			
	VI		- 9.1					0.27			
	VII		- 5.5					1.11			
	VIII		- 1.24					2.4			
	IX		- 7.9					- 5.5			
32	II		- 5.2								
	III		1.08								
	VI		- 2.3								
	VII		- 1.26								
	VIII		2.7								
	IX		- 6.5								

(1) 0°, 90°
(2) 0°, 45°, 90°, 135°
(3) 30°, 120°
(4) 45°, 135°
(5) 60°, 150°

TABLE 11-4

PERCENT AVERAGE EMISSION ERROR
AND
STANDARD DEVIATION VS. NUMBER OF PROBES

Number of Probes	From All Strategies	
	% Average Emission Error	Standard Deviation
4	2.52	25.22
8	- 4.12	17.84
12	1.15	12.13
16	- 4.39	9.57
24	- 2.29	4.64
32	- 1.91	3.54

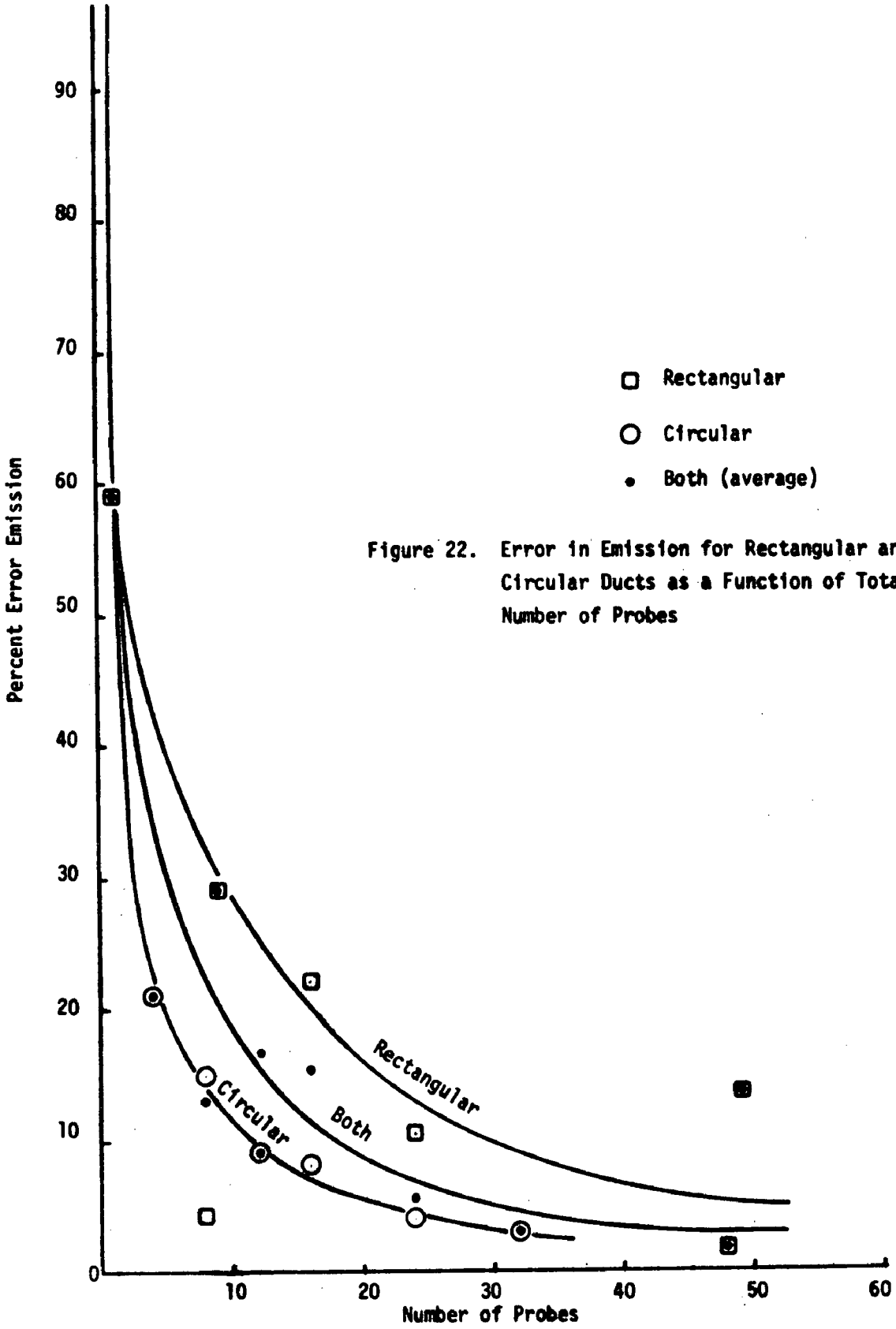

Figure 22. Error in Emission for Rectangular and Circular Ducts as a Function of Total Number of Probes

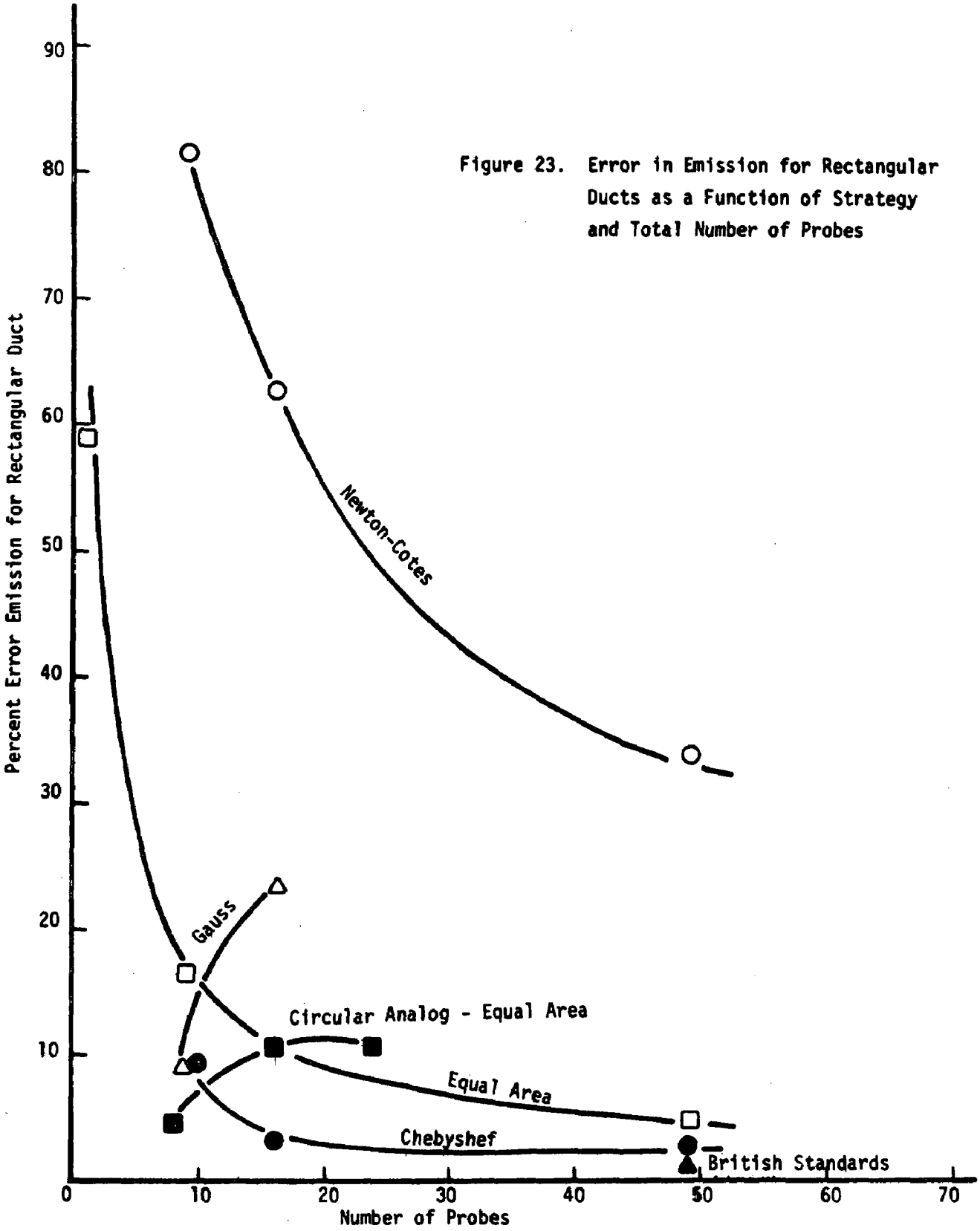

Figure 23. Error in Emission for Rectangular Ducts as a Function of Strategy and Total Number of Probes

Figure 24. Error in Emission for Circular Ducts as a Function of Strategy and Total Number of Probes.

Curve 1	Log Linear	△
Curve 2	Tangential	□
Curve 3	2 diam. (0°, 90°)	●
Point 4	1 diam. (30°, 120°)	•
Point 5	2 diam. (45°, 135°)	•
Point 6	2 diam. (60°, 150°)	•
Curve 7	4 diam. (0°, 45°, 90°, 135°)	○

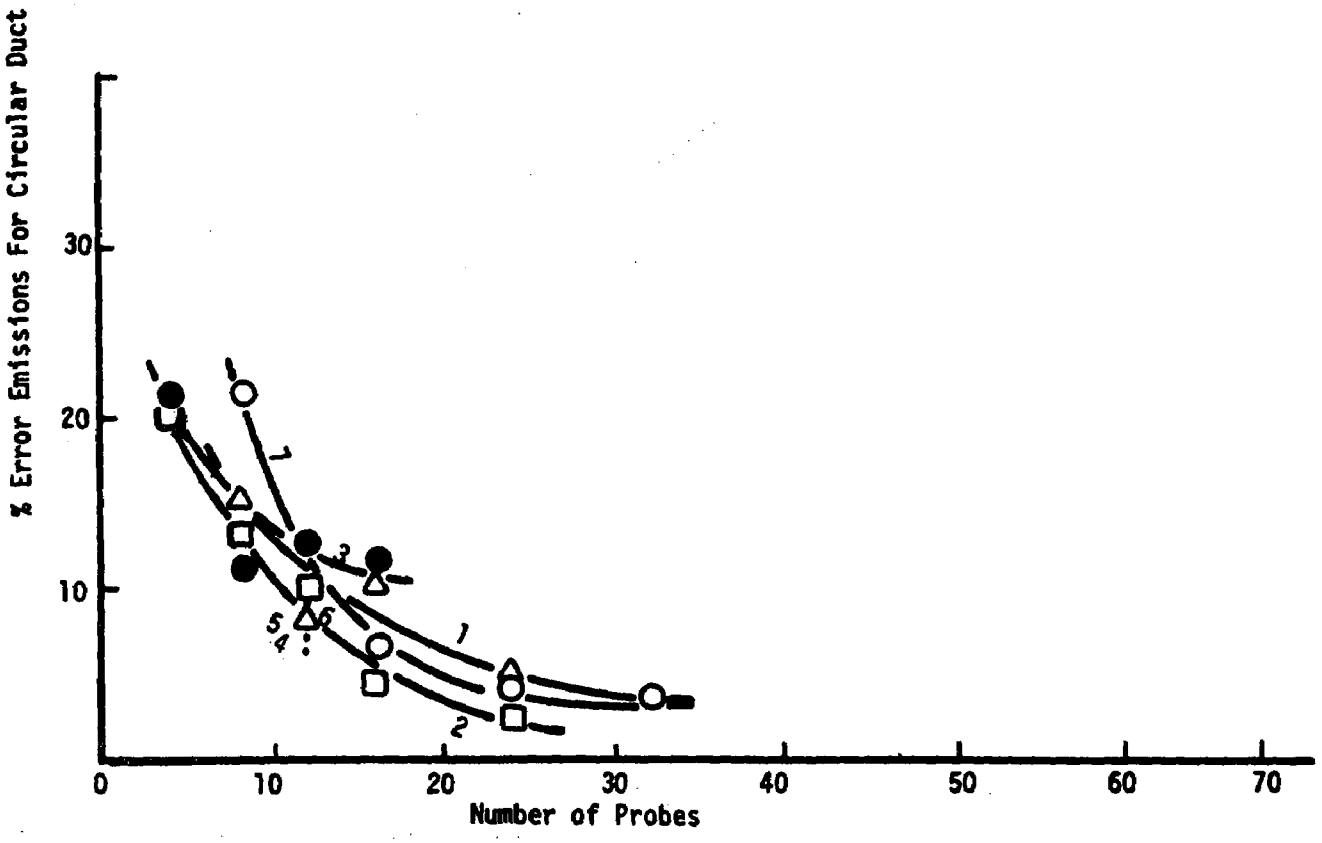

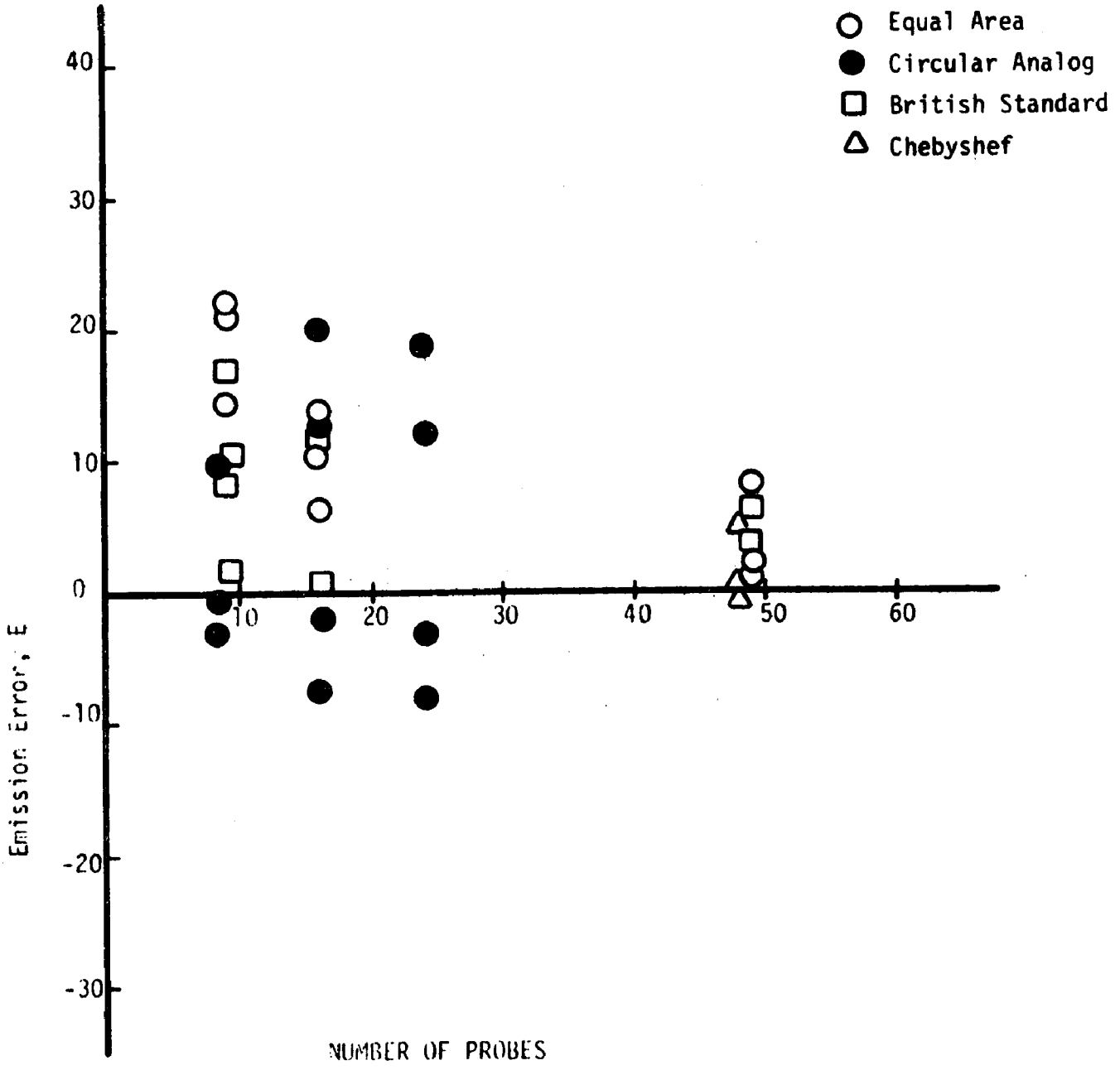

Figure 25. Emission Error vs. Number of Probes for Different Probe Locations in Rectangular Ducts

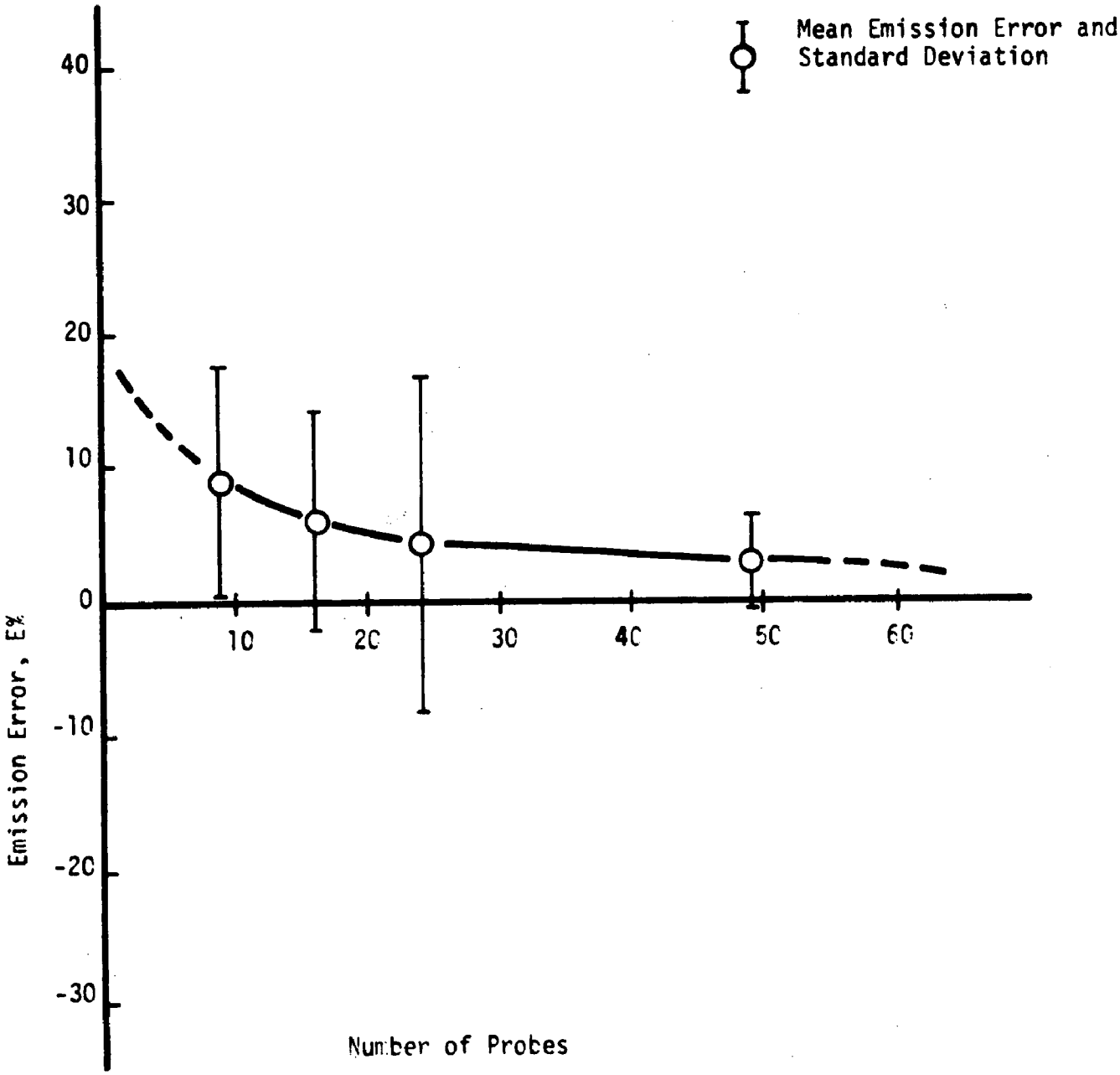

Figure 26. Mean Emission Error vs. Number of Probes for Different Probe Locations in Rectangular Ducts

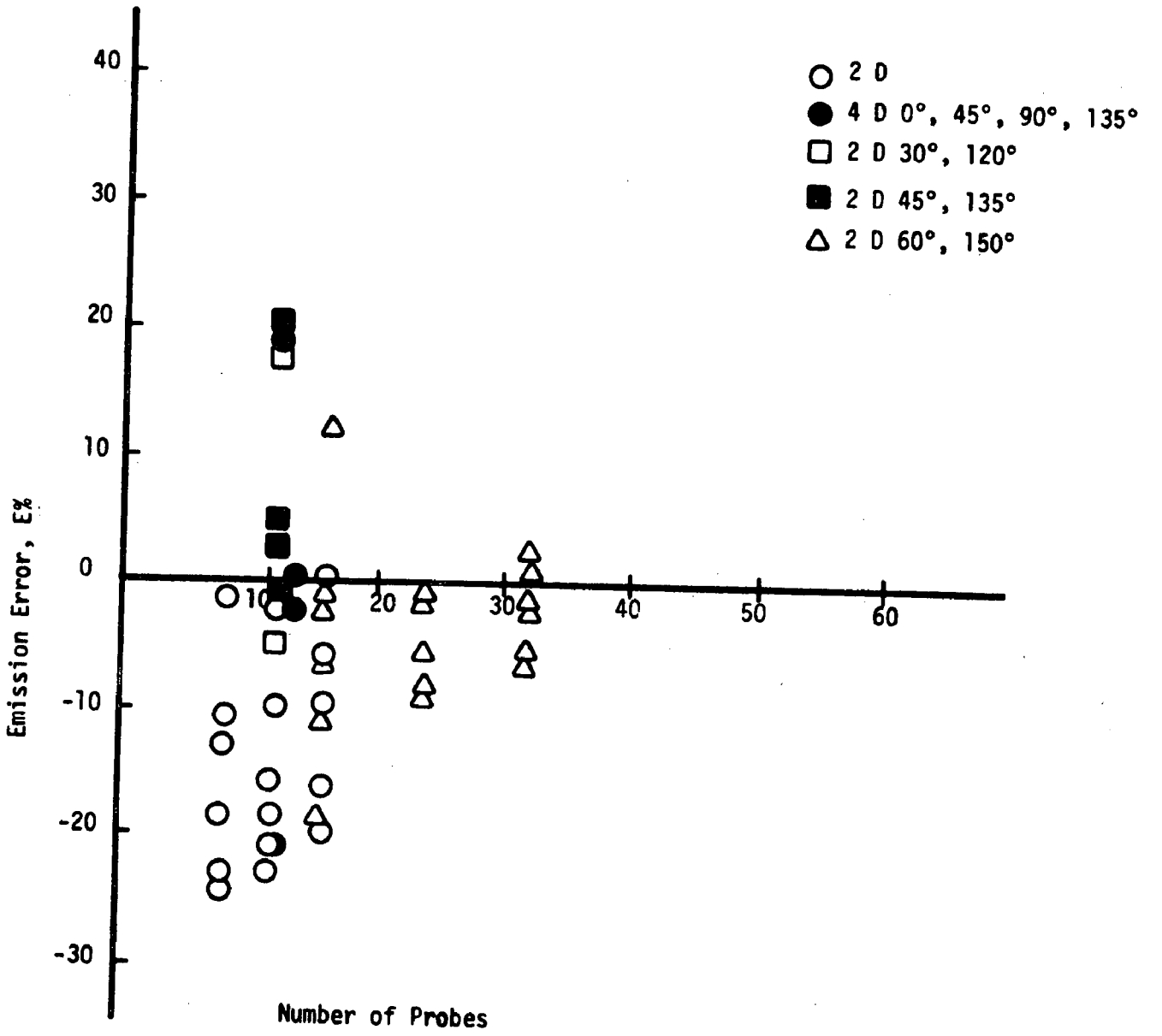

Figure 27. Emission Error vs. Number of Probes For Log Linear Method For Probe Locations in Circular Ducts

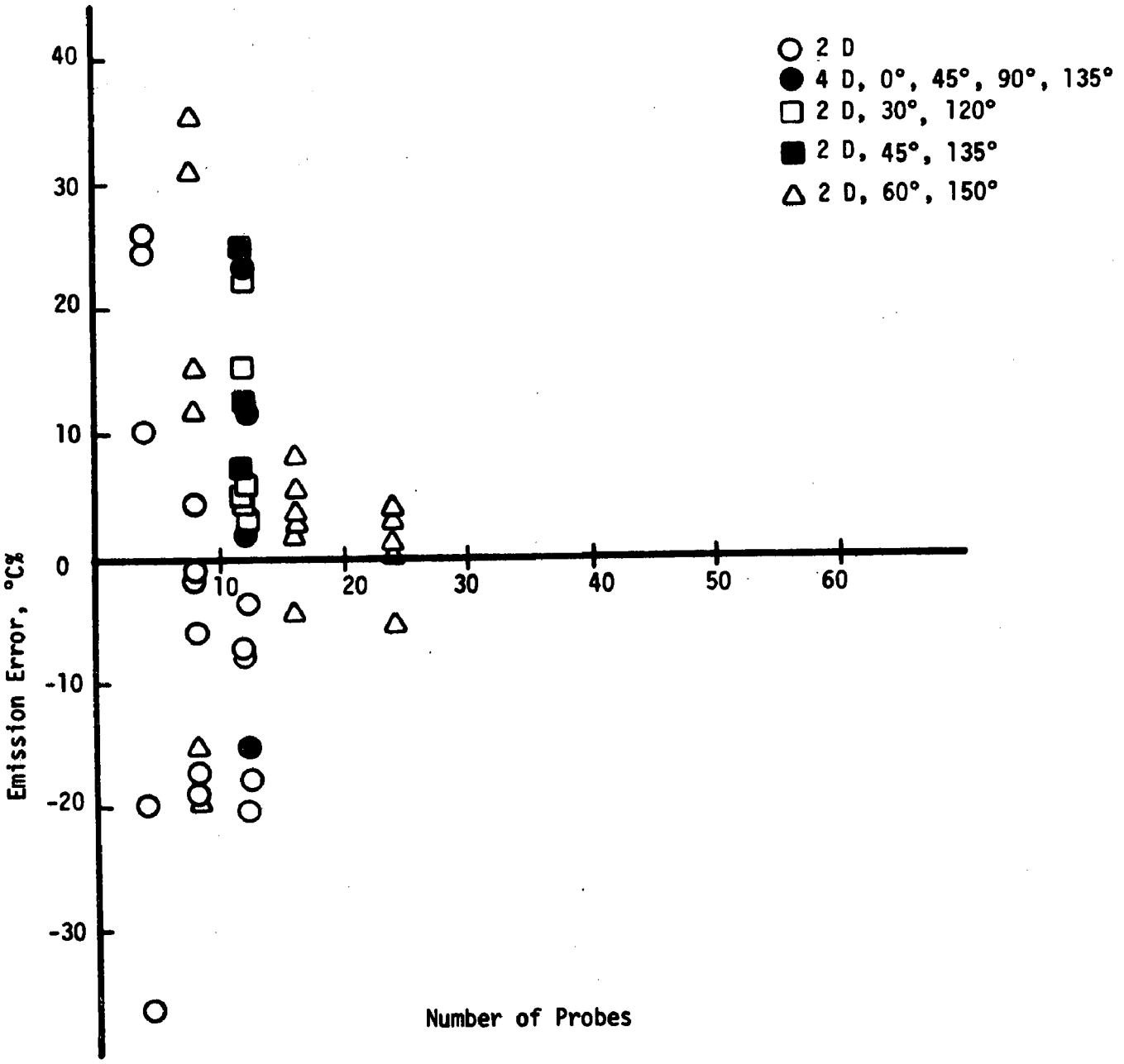

Figure 28. Emission Error vs. Number of Probes For the Tangential Method For Probe Locations In Circular Ducts

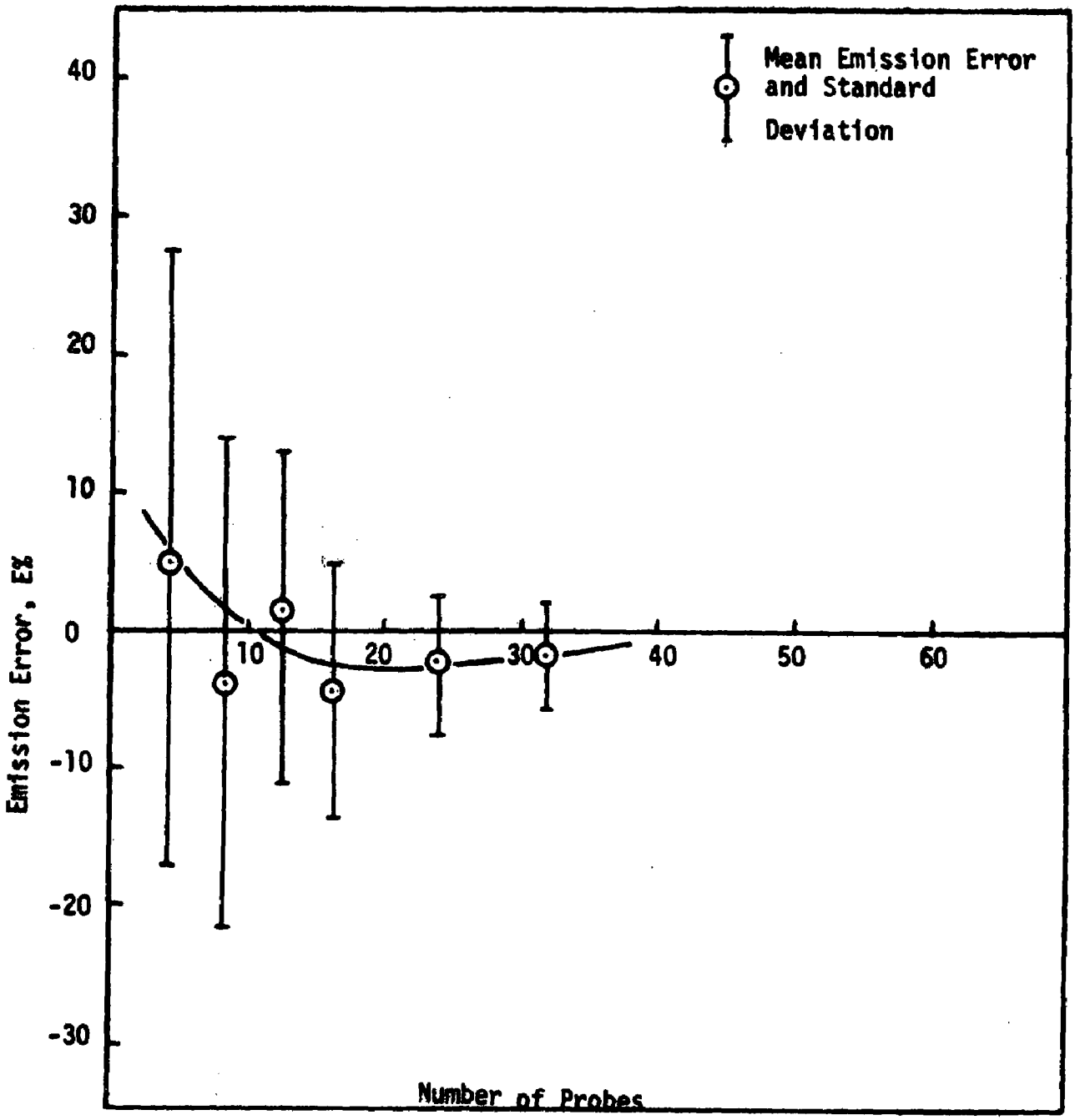

Figure 29. Mean Emission Error vs. Number of Probes For Different Probe Locations in Circular Ducts

TABLE 12-1

AVERAGE ERRORS FOR EIGHT RECTANGULAR DUCT SAMPLE CASES

Strategy: British Standards 1042

# Probes	Error (ε) Computed by Program			
	$\varepsilon_{emission}$		$\varepsilon_{ave.\ velocity}$	
48	2.5	2.6	3.0	3.1

Strategy: Equal Area

# Probes	Error (ε) Computed by Program			
	$\varepsilon_{emission}$		$\varepsilon_{ave.\ velocity}$	
1	32.4	32.4	27.0	27.0
9	15.4	15.4	15.6	15.6
16	12.4	12.4	13.4	13.4
49	6.1	6.1	6.2	6.2

Strategy: Circular Analog-Equal Area

# Probes	Error (ε) Computed by Program			
	$\varepsilon_{emission}$		$\varepsilon_{ave.\ velocity}$	
8	4.1	5.7	5.6	6.9
16	3.0	7.2	2.8	4.3
24	2.3	7.1	2.1	4.0

Strategy: Newton-Cotes*

# Probes	Error (ε) Computed by Program			
	$\varepsilon_{emission}$		$\varepsilon_{ave.\ velocity}$	
9	-81.1	81.1	-82.8	82.8
16	-62.5	62.5	-64.2	64.2
49	-33.8	33.8	-35.3	35.3

* Points weighted equally not by appropriate weighting factors.

TABLE 12-1. (cont.)

Strategy: Gauss*

# Probes	Error (ε) Computed by Program			
	εemission		εave. velocity	
9	- 5.7	9.3	- 3.0	9.6
16	-20.9	23.6	-18.0	19.9

Strategy: Chebyshef

# Probes	Error (ε) Computed by Program			
	εemission		εave. velocity	
9	11.7	11.7	12.4	12.4
16	6.9	6.9	8.1	8.1
49	2.6	2.6	1.8	1.8

* Points weighted equally not by appropriate weighting factors

TABLE 12-2

AVERAGE ERRORS FOR EIGHT RECTANGULAR DUCTS
REGARDLESS OF STRATEGY

Number of Probes	$\varepsilon_{emission}$		$\varepsilon_{velocity}$	
1	32.4	32.4	27.0	27.
8	4.1	5.7	5.6	6.9
9	- 7.4	22.3	- 7.	22.7
16	- 4.9	17.4	- 3.9	17.0
24	2.3	7.1	2.1	4.0
48	2.5	2.6	3.0	3.0
49	- 3.3	10.2	- 3.9	10.3

TABLE 12-3

AVERAGE PERCENT ERROR FOR FOURTEEN DUCTS

REGARDLESS OF STRATEGY, GEOMETRY AND LOCATION

Number of Probes	$\varepsilon_{emission}$		$\varepsilon_{velocity}$	
1	158.3	165.7	92.9	94.3
4	2.5	21.2	7.5	7.6
8	- 1.6	12.1	- 1.2	6.6
9	- 7.4	22.3	- 7.	22.7
12	1.1	9.3	- 0.3	5.1
16	- 1.9	13.4	- 3.9	2.3
24	- 0.46	5.2	- 5.4	3.7
32	- 1.9	3.2	- 2.1	2.2
48	2.5	2.6	3.	3.
49	- 3.3	10.2	- 3.9	10.3

TABLE 12-4

EMISSION ERROR VS. NUMBER OF PROBES
USING DIFFERENT METHODS FOR TRAVERSING RECTANGULAR DUCTS

Number of Probes	Case Number	Strategy percent error			
		Equal Area	Circular Analog	Chebyshef	British Standard
8, 9	IV	8.4	- 2.8	8.0	
	V	21.8	- 0.72	16.9	
	X	14.3	- 3.1	1.8	
	XI	20.7	9.7	10.4	
	XII	58.9	78.4	59.6	
	XIII-1	16.5	4.1	16.8	
	XIII-2	16.5	11.4	15.4	
	XIII-3	15.5	10.3	14.1	
	XIII-4	9.9	3.5	9.9	
16	IV	13.4	- 2.6	11.4	
	V	11.4	- 7.8	0.63	
	X	6.2	19.8	0.19	
	XI	10.3	12.6	0.074	
	XII	68.6	113.0	65.7	
	XIII-1	18.6	- 6.6	16.4	
	XIII-2	15.1	2.1	10.1	
	XIII-3	12.8	1.2	7.5	
	XIII-4	11.2	5.3	8.7	
24, 25	IV		- 3.6		
	V		- 8.4		
	X		18.4		
	XI		11.7		
	XII	64.5		61.4	
	XIII-1		- 7.4		
	XIII-2		1.1		
	XIII-3		0.33		
	XIII-4		6.3		

TABLE 12-4 (Cont.)

Number of Probes	Case Number	Strategy percent error			
		Equal Area	Circular Analog	Chebyshef	British Standard
48, 49	IV	7.7		4.0	5.4
	V	6.0		6.3	1.15
	X	1.33		- 1.32	- 0.4
	XI	2.3		- 1.8	0.2
	XII				
	XIII-1	10.2		2.8	4.6
	XIII-2	7.0	1.2	4.1	
	XIII-3	6.4	2.8	2.5	
	XIII-4	7.9		6.6	2.2

TABLE 12-5

PERCENT AVERAGE EMISSION ERROR

AND STANDARD DEVIATION VS. NUMBER OF PROBES FOR RECTANGULAR DUCTS

Number of Probes	From All Strategies	
	% Average Emission rate	Standard Deviation
8, 9	16.5	19.1
16	15.7	26.1
24	14.4	26.9
48, 49	3,7	3.1

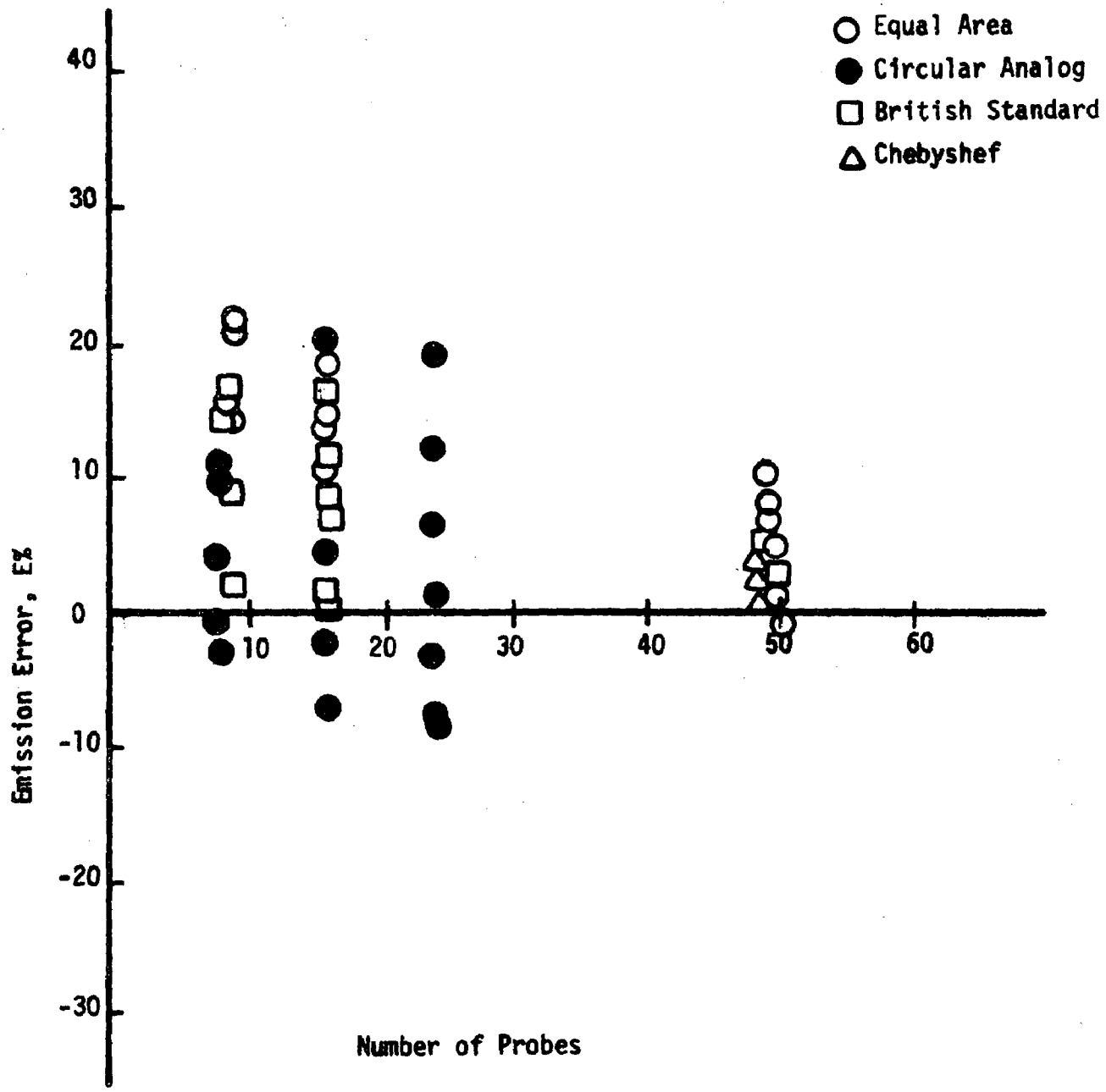

Figure 30. Emission Error vs. Number of Probes for Different Probe Locations in Rectangular Ducts

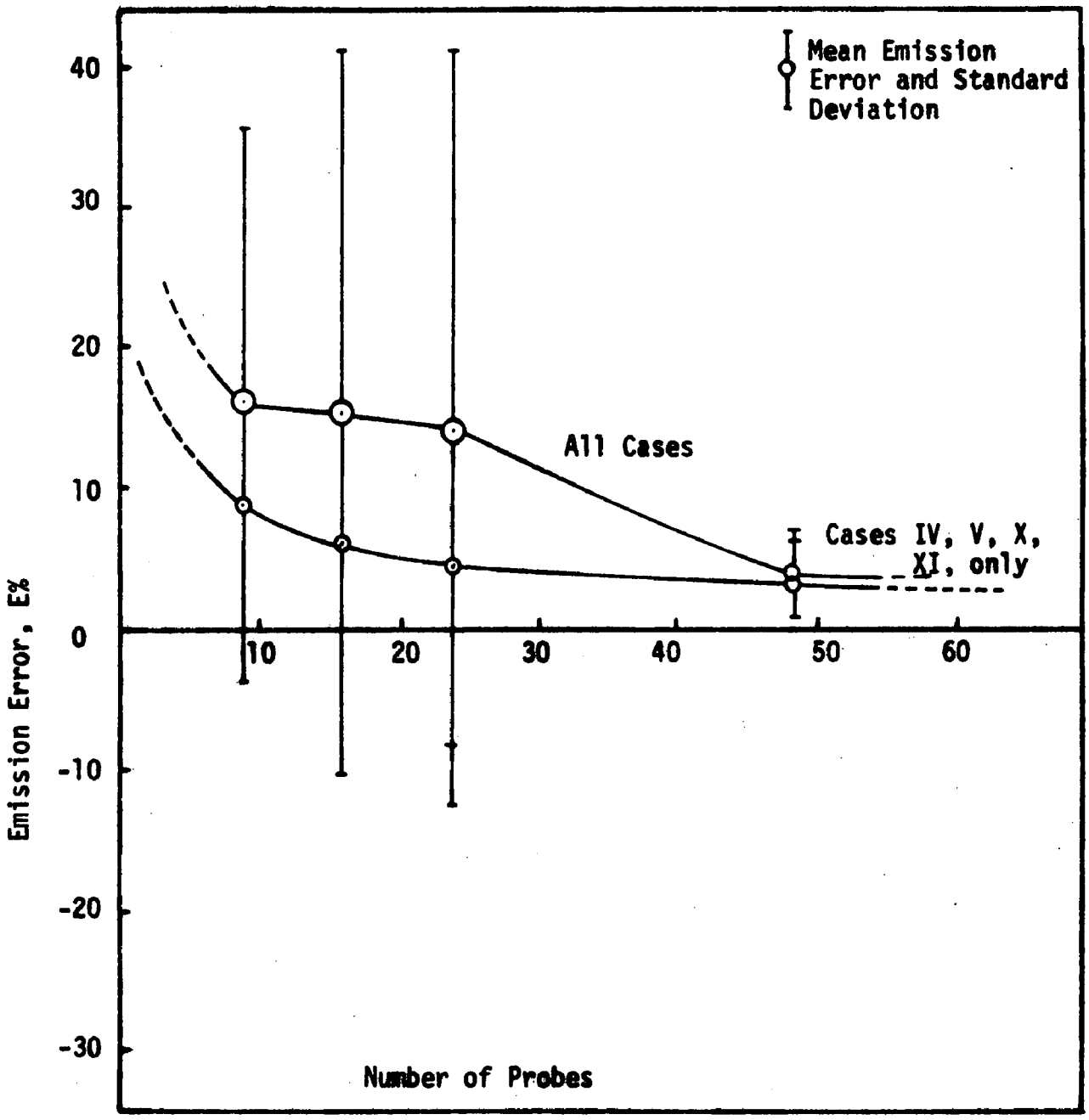

Figure 31. Mean Emission Error vs Number of Probes for Different Probe Locations in Rectangular Ducts

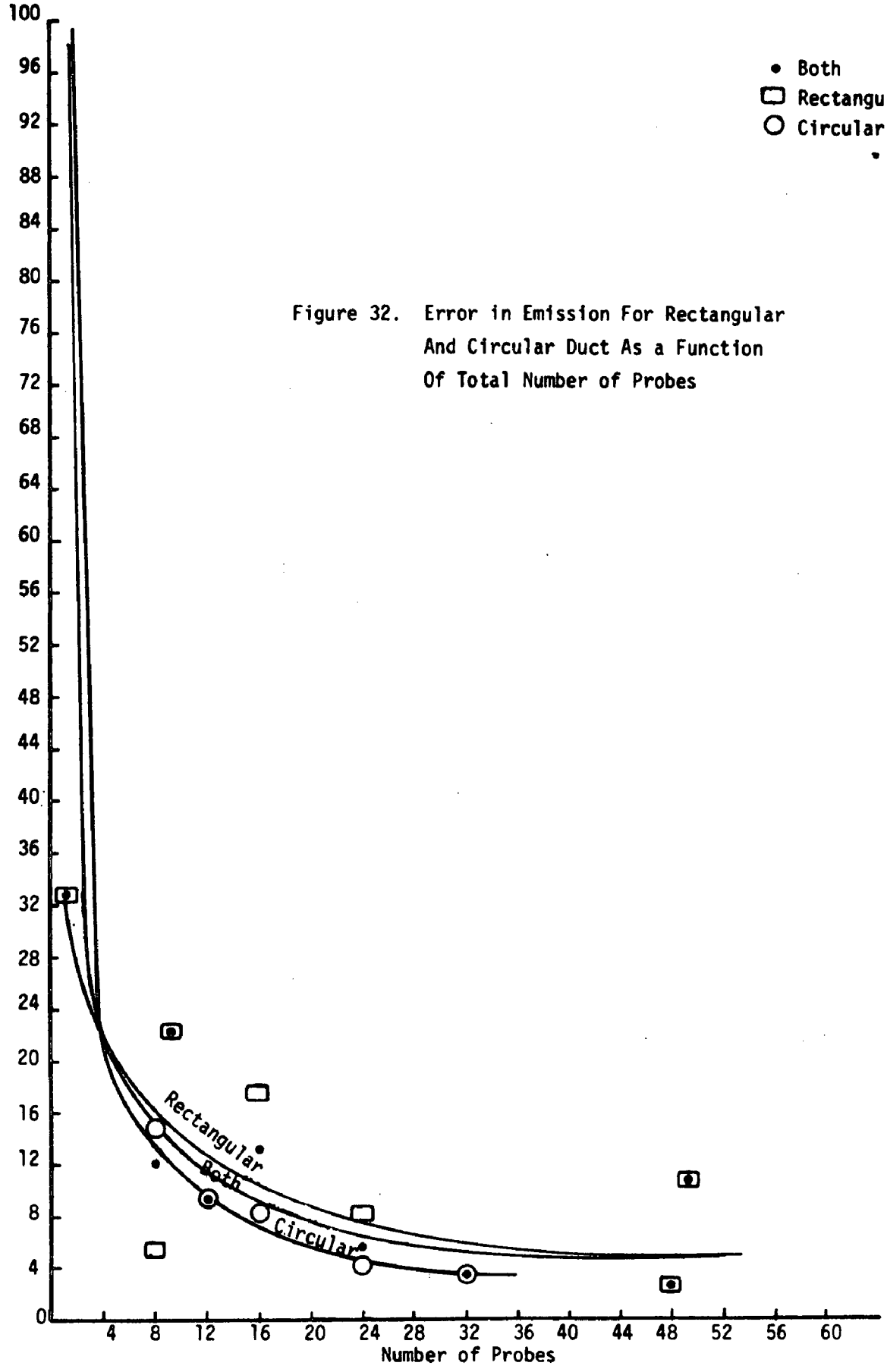

Figure 32. Error in Emission For Rectangular And Circular Duct As a Function Of Total Number of Probes

Figure 33. Error in Emission for Rectangular Ducts as a Function of Strategy and Total Number of Probes

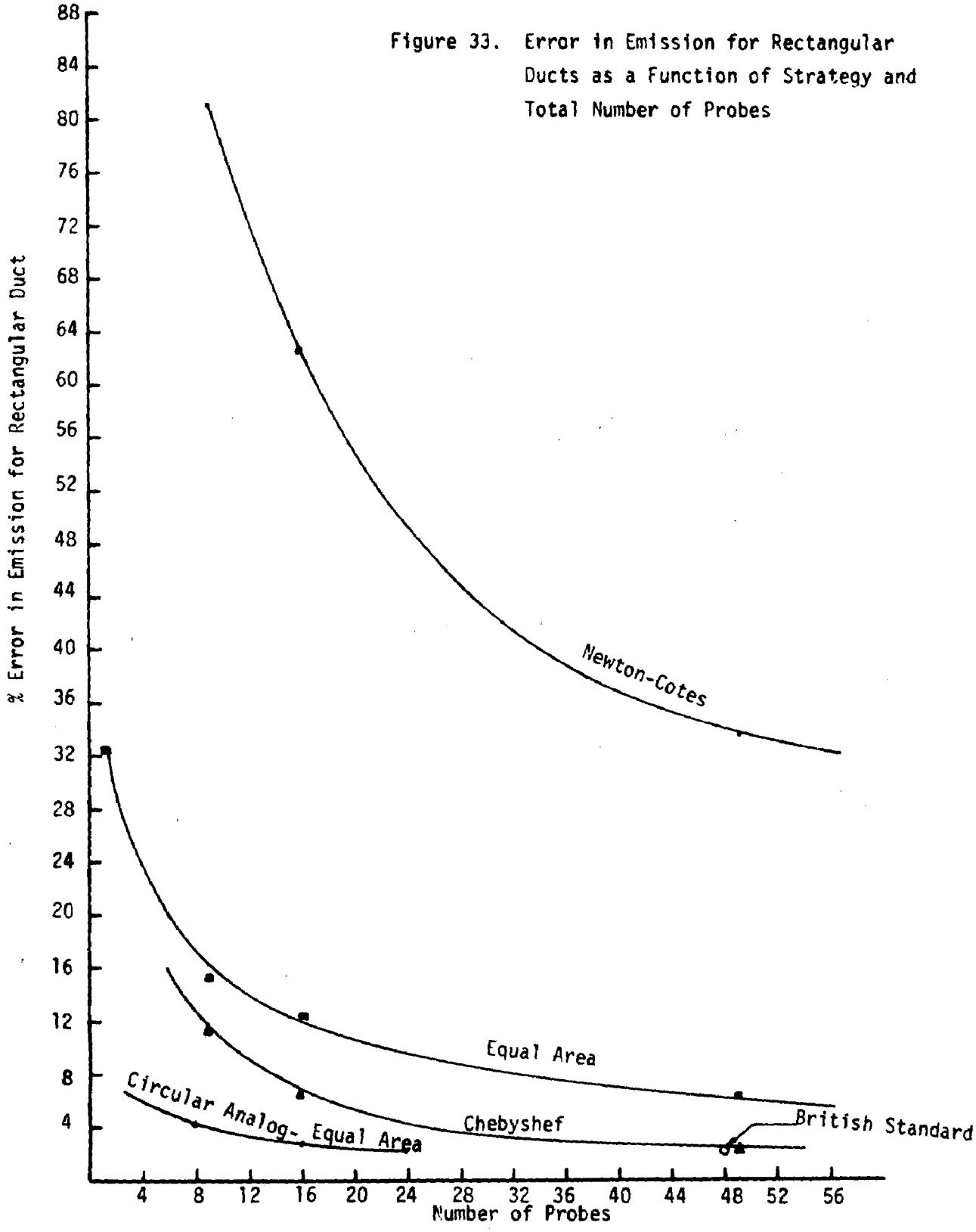

computed by summing actual errors; the rightmost entry for the average error in emission or velocity has been computed by summing the absolute values of the errors. In Tables 11-1 thru 11-4 all of the entries for average error are calculated by a summation of actual errors, i.e. allowing the positive and negative errors to cancel in the summation. Figures 22 thru 29 are derived from Tables 10-1 thru 11-4 while Figures 30 thru 33 are derived from Tables 10-1 thru 12-5.

Our evaluation of these results follows. Note that these results are based on very limited data (9 rectangular and 6 circular ducts). A principal finding of our study is that many more test cases are required before reliable conclusions can be reached. All conclusions are therefore based on the assumption that the 16 cases analyzed thus far represent good samples of the broad range of actual industrial velocity-concentration stratification profiles.

a.4 Conclusions and Recommendations

In general, increasing the number of probes for a given strategy would increase the probability of determining average velocity or emissions. Figures 22, 23, 24 and 26, and Figures 31, 32, 33 indicate that this is the case for all strategies except the modified Gauss and the Circular Analog-Equal Area strategies for the first four rectangular ducts that were studied. These two exceptions are probably due to the small number of cases studied. We therefore postulate that the error limits in sampling under stratified conditions decrease with an increasing in the number of probes. However, the magnitude of error for a particular case may increase by increasing the number of sample probes. For an extreme example, consider the case where a single probe yields a zero percent error while four sample probes yield results that are 10% in error. Obviously, one does not conclude from this that using one probe is a better general sampling procedure than using four probes, but only that it is possible for the correct result to be obtained with one probe. Therefore, intuition indicates that, in general, the

magnitude of probable error will decrease with an increase in the number of samples. Furthermore, it is postulated that the magnitude of probable error will decrease with an increase in the number of samples at a faster rate for some methodologies than for others.

For circular ducts, the log-linear technique tends to underpredict average emissions while the tangential strategy tends to overpredict. For the same number of probes and diameters the tangential strategy is slightly better than the log-linear technique in error magnitude; however, as the probes are oriented through an axis of flow symmetry the log-linear technique appears to be somewhat superior. The high mean error of the centroid strategy (1 probe in the center of the duct) indicates how poor this method is for emission measurements in stratified gases.

Generally speaking, for circular ducts, for the same number of probes, the number of diameters and diameter locations may have a significant effect on the emissions measurement. For example, consider the case where $C = f(r,\theta)$ while the concentration dependency is "greater" on r than θ. Here 8 probes on 2 diameters will likely be as, or more, effective a strategy than 8 probes on 4 diameters. However, if the dependency were reversed, i.e., the concentration were more dependent on θ than on r, 8 probes on 4 diameters would be more effective than 8 probes on 2 diameters. Clearly, it would seem that an initial detailed characterization of the shape of the concentration and velocity profiles is necessary to determine the most effective measurement strategy for a given duct sampling location. Without this a priori knowledge, the tangential strategy with 16 probes should provide a good indication of mean emissions from a circular duct (see Table 11-4) which indicates a mean error of 4.4% for the cases analyzed.

In contrast to the strategies that have been evaluated for circular ducts, different strategies give substantially different results for rectangular ducts. For the first 4 cases analyzed, the modified Newton Cotes technique gives the highest mean error while the Chebyshef technique gives the lowest. Note, however, that the British Standards technique using

48 probes has a lower mean error (1.8%) than the 49 point Chebyshef technique (3.3%), even though the size of the area segments are substantially greater than the recommended 36 in^2. Preliminary results show that 16 probes located in accord with the Chebyshef strategy should provide a satisfactory indication of mean emissions from a rectangular duct. (See Figure 23 which indicates a mean error of 3.1% for the cases analyzed.)

For rectangular ducts, the "circular analog" technique also appears to be a rather good strategy; however, its effectiveness clearly depends on the existence of flow symmetry within the duct.

As was the case with the circular ducts, a single probe located at the center of a rectangular duct yields a higher average error in predicted emissions (59.3%). Since in practical cases it would be highly desirable to measure average emissions with a single probe, it would be useful to develop a technique with which to determine the focus of points within ducts that would lead to "zero error" in emission prediction. By applying such a technique to a large group of sample concentration-velocity profiles, one could develop sets of curves, the study of which could lead to the development of an acceptable single point measurement strategy. Such an approach could be developed through modification of the existing analysis computer program.

The results from the experimental wind tunnel tests shown in Table 9-11 indicate an extermely poor measurement accuracy for all strategies using less than 25 probes. However, experimental results have not duplicated the error magnitudes suggested by the computer analysis. It is our judgment that these differences may be associated with a difficulty in fitting the usually irregular profile data of Table 6. That is, the computer fit may tend to mask some of the extreme variations in the raw data which would, of course, not happen in experimental tests. This suggests that extremely stratified flows must be measured with a large number of probes (~50) to assure reasonable measurement accuracy. Also, the simulation program should be modified to allow extreme profiles to be adequately represented.

The addition of the four TVA ducts (Cases XIII-1 to XIII-4) increased the data base for our earlier conclusions and added considerable weight to their reliability. We still believe that many more cases should be analyzed to insure that our selected profiles are indeed representative of the broad range of actual velocity-concentration stratification profiles.

These results have confirmed our earlier assessment that the circular-analog-equal area strategy is extremely effective for cases exhibiting flow symmetry. The additional data have flattened the summary curve for this strategy (Figure 33) so that increasing the number of probes now appears to yield a reduction in sampling error. In fact, the equal area strategy now appears to be the most effective strategy analyzed to date for rectangular ducts.

Figure 33 indicates that, in general, irrespective of strategy (random probe location), there appears to be no significant difference in measurement accuracy between the circular and rectangular strategies that have been evaluated in this program.

These new results do not differ substantially from earlier findings except in regard to estimated error magnitude. For example, the error in emission measurement associated with a single probe located at the center of a rectangular duct has been reduced in our calculations from 59.3% to 32.4%. However, considering the range of values making up this average, it must be concluded that a single point strategy is a poor choice unless one has prior knowledge of the flow characteristics.

Note also that the 16 point Chebyshef procedure now indicates a mean error of 6.9% rather than the 3.1% reported earlier. However, the circular analog strategy now appears to be superior with a 16 probe mean error of 3.0% and an 8 probe mean error of 4.1%.

b. Sampling Methodologies

In heterogeneous sampling, it is generally not possible to obtain a representative sample from a single arbitrary sampling location. In order to study the different strategies for obtaining a representative sample from stack gases, a mathematical analysis of the emission rate general equation was performed and different sampling methodologies were derived.

Analysis: The emission of material from a combustion source is equal to:

$$E_a = \int_A Ca\ v \cdot \vec{n} dA \qquad (1)$$

where: Ca = concentration of species (a)
v = flue gas velocity along the duct
$\vec{n}$ = unit vector normal to A
A = cross sectional area of a duct
E_a = emission rate of specie

Assuming the velocity vector is perpendicular to area (A), we can also write for species (a)

$$E_a = \int_A \frac{w}{qt} v\ dA \qquad (2)$$

where: w = mass of species (a) measured during time (t)
t = sampling time
q = volumetric sampling rate

We can approximate (2) by writing the integral as a finite sum, viz.,

$$E = \sum_{i=1}^{i=n} \frac{w_i}{q_i t_i} v_i A_i \qquad (3)$$

where: n = number of sampling locations

A_i = area of sampling, where $\sum_{i=1}^{i=n} = A$

v_i = average velocity in sampling area A_i

Therefore:

$$E = \frac{w_1 v_1 A_1}{q_1 t_1} + \frac{w_2 v_2 A_2}{q_2 t_2} + \ldots + \frac{w_n v_n A_n}{q_n t_n} \qquad (4)$$

Equation (4) is the general equation that can be used to determine the emission rate from a finite number of measurements. It is obvious that in the limit of an infinite number of sampling points, an accurate answer is obtained.

Table 13 shows that by placing special conditions or constraints on the parameters of equation (3) a simplified expression is derived and a sampling method(s) suggested. The different methods presented in Table 13 make up the group of sampling strategies which may be implemented to obtain a representative gas sample from a process stream.

c. Jet Mixing of Flue Gas Streams

From information obtained in the literature search, we concluded that in-the-stack mixing devices are not suitable for practical reasons, i.e., for mechanical installation (retrofit) and/or adverse pressure drops in the process streams. A scheme which may avoid both of these probelems involves the use of gas jets to mix the process stream (See Figure 34). In this scheme, a slip-stream from the flue gas is withdrawn from the duct and then pumped back into the duct as a mixing jet.

TABLE 13

APPROACHES BASED ON THE GENERAL EQUATION FOR FINITE SAMPLES

$$E = \sum_{i=1}^{i=n} \frac{w_i}{q_i t_i} v_i A_i$$

Special Cases and Conditions	Applicable Equation	Sampling Methods
For Steady State		
1. $A_1 = A_2 = \ldots A_n = A_i$ $t_1 = t_2 = \ldots t_n = t$ $v_1 \neq v_2 \neq \ldots v_n$ $q_1 \neq q_2 \neq \ldots q_n$	$E = \frac{A_i}{t}\left[\frac{w_1 v_1}{q_1} + \frac{w_2 v_2}{q_2} + \ldots \frac{w_n v_n}{q_n}\right]$ Concentration, velocity and sampling rate must be known at each sampling position	a. Automatically traversing with one probe b. Using several probes with sequential sample analysis
2. $A_1 = A_2 = \ldots A_n = A_i$ $t_1 = t_2 = \ldots t_n$ $\frac{v_1}{q_1} = \frac{v_2}{q_2} = \ldots \frac{v_n}{q_n} = K$ where K is a known constant	$E = A_i \; K \; Cav \sum_{i=1}^{i=n} q_i$ The proportional constant K must be known and the average concentration of the mixed samples, also the total sampled volume per unit time	a. Automatically traversing and automatically adjusting the sampling flow rate b. Use one probe or several probes with one mixed sample analysis c. For v/q to equal a constant either the velocity at the entrance of the sampling nozzle* is adjusted equally or proportionally to the velocity of the flue gas at the sampling location
3. $A_1 = A_2 \ldots A_n = A_i$ $v_1 \neq v_2 \neq \ldots v_n$ $t_1 \neq t_2 \neq \ldots t_n$	$E = A_i\left[\frac{w_1 v_1}{q_1 t_1} + \frac{w_2 v_2}{q_2 t_2} + \ldots + \frac{w_n v_n}{q_n t_n}\right]$ Concentration, velocity, sampling time and flow rate for each sample location must be known	a. Automatically traversing with one probe b. Using several probes with sequential sample analysis

TABLE 13. (Cont.)

Special Cases and Conditions	Applicable Equation	Sampling Methods
4. $A_1 = A_2 = \ldots A_n = A_1$ $q_1 = q_2 = \ldots q_n$ $\frac{v_1}{t_1} = \frac{v_2}{t_2} + \ldots \frac{v_n}{t_n} = K_1$ where K_1 is a known constant	$E = A_1 K_1 Cav \sum_{i=1}^{i=n} t$ The proportional constant K_1 must be known and the average concentration of the mixed samples, also the sampling time for each sample location	a. Automatically traversing and sampling at constant flow rate only automatically adjusting sampling time for each sampling position b. Use one probe or several probes with one mixed sample analysis
5. $A_1 = A_2 = \ldots A_n = A_1$ $q_1 = q_2 = \ldots q_n = q$ $t_1 = t_2 = \ldots t_n = t$ $v_1 \neq v_2 \neq \ldots v_n$	$E = \frac{A_1}{tq} \left[w_1 v_1 + w_2 v_2 + \ldots + w_n v_n \right]$ Concentration and velocity must be known at each sample position	a. Automatically traversing and sampling at constant flow rate b. Use one probe or several probes with sequential sample analysis
6. $A_1 = A_2 = \ldots A_n = A_1$ $v_1 = v_2 = \ldots v_n = v_1$ $q_1 = q_2 = \ldots q_n$ $t_1 = t_2 = \ldots t_n$	$E = nA_1 v_1 Cav$ The velocity being uniform over the cross section of the duct, only one measurement is needed; the average concentration of the mixed samples must be known	a. Automatically traversing with one probe or using several probes with one mixed sample analysis
7. $A_1 = A_2 = \ldots A_n = A_1$ $\frac{w_1}{q_1} = \frac{w_2}{q_2} = \ldots \frac{w_n}{q_n}$ $t_1 = t_2 = \ldots t_n$	$E = A_1 C \left[v_1 + v_2 + \ldots v_n \right]$ or= $nA_1 Cvav$ The concentration being uniform over the cross section of the duct, only one measurement is needed; the velocity of each sampling position must be known	a. Automatically traversing with one probe or using several probes for velocity measurement, with one sampling position

TABLE 13 (Cont.)

Special Cases and Conditions	Applicable Equation	Sampling Methods
8. $A_1 = A_2 = \ldots A_n = A_1$ $\frac{w_1}{q_1} = \frac{w_2}{q_2} = \ldots \frac{w_n}{q_n}$ $t_1 = t_2 = \ldots t_n$ $v_1 = v_2 = \ldots v_n$	$E = nA_1Cv$ The concentration and velocity being uniform over the cross section of the duct	a. Sampling with one probe for sample analysis
9. $A_1 = A_2 = \ldots A_n = A_1$	$E = nA_1\ Cav\ Vav$ The concentration and velocity averages must be known	a. Sampling with many probes and averaging

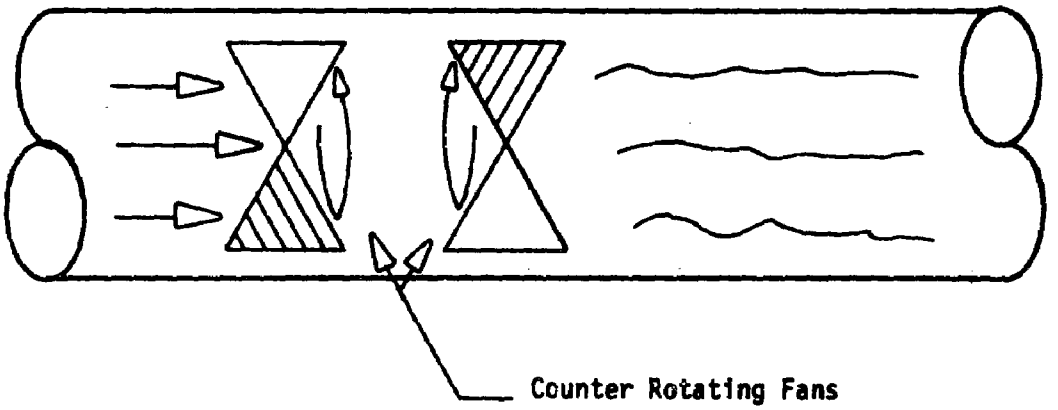

a. Fan or Turbine Mixer

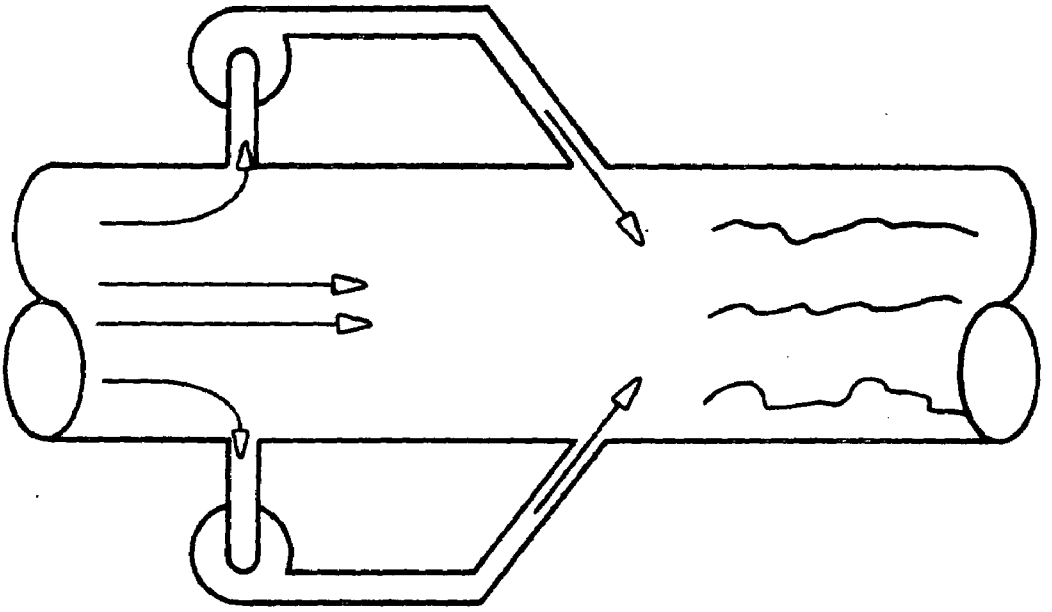

b. Gas Dynamics Mixer

Figure 34. Gas Jet Mixer

The problem of in-the-stack mixing was formulated analytically. The formulation for the two dimensional case (a tractable example) is presented in Appendix H-1. A less rigorous analysis was also performed and is presented in Appendix H-2. Calculations based on this analysis were performed on the problem of mixing flue gas by jets, and are presented in a following section, (See c.2).

c.1 Background

In principle, with the flattening of the concentration profile, the problem of extracting a representative sample becomes trivial, since a single point sample may be taken at any sampling rate; i.e., non-proportional sampling. Thus, a method which flattens (equal to a constant) the concentration profile is a very powerful method, and any reasonable scheme to achieve this should be fully investigated.

Concentration profiles can be flattened by mixing the gas stream. In any gas stream, diffusional mechanisms tend to reduce small-scale stratification; thus the role of any mixing approach should be to promote large-scale (relative to duct size) mixing. Schemes to promote mixing fall into two classes, viz.:

- Passive
- Active

Passive mixing schemes extract energy from the gas stream to promote mixing and, hence, necessarily introduce a pressure drop in the system. While it is theoretically attractive to think of using this pressure drop as a flowmeter, passive mixing elements are impractical for retrofit to full-scale systems for the reasons of excessive pressure drop. However, for new plant designs, passive mixing methods might be considered. Some examples of passive mixing schemes are:

- mixing orifices (Figure 35-a)
- mixing disks or plates (Figure 35-b)
- swirl vanes (Figure 35-c)

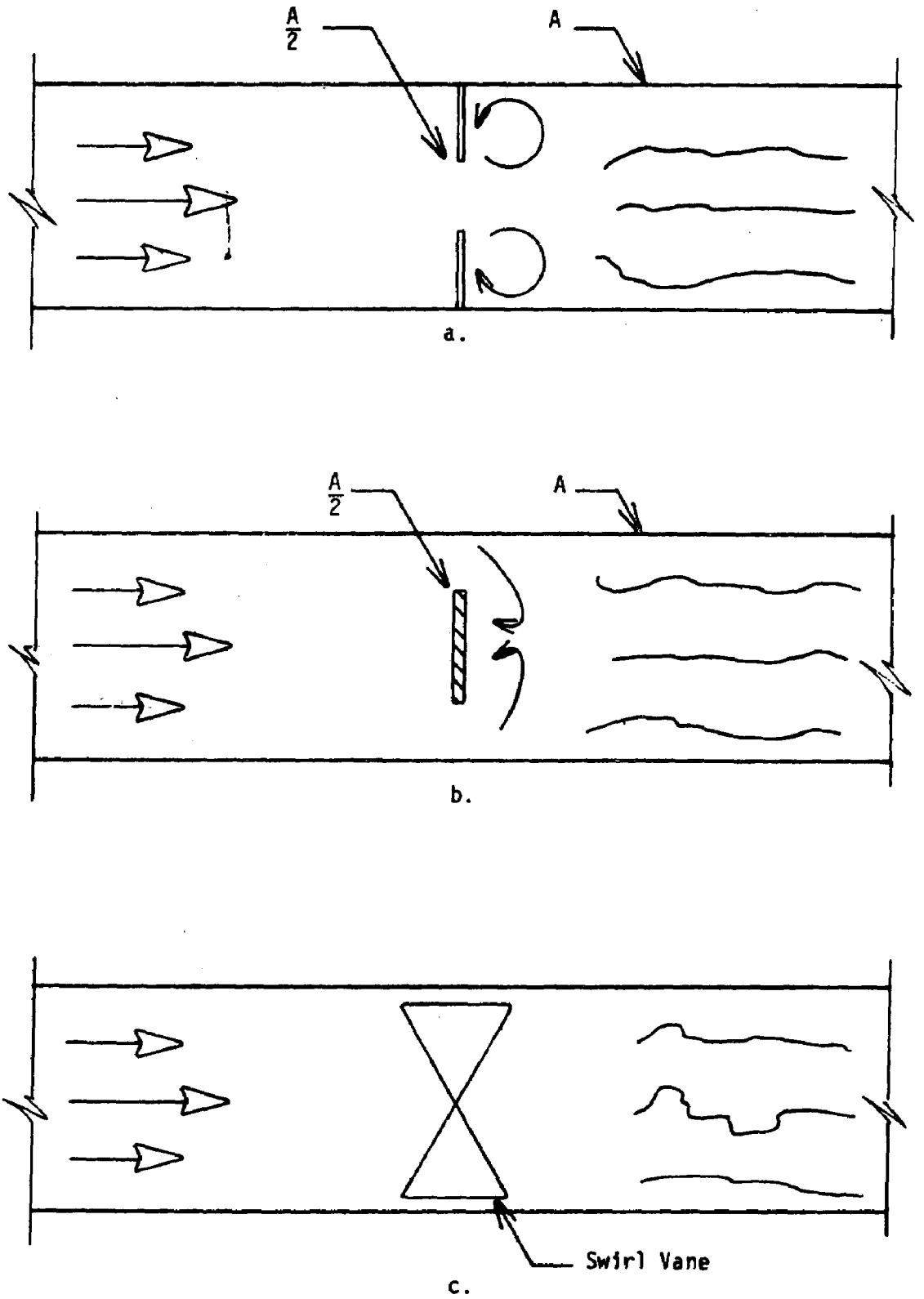

Figure 35. Passive Mixing Schemes

Active mixing elements take a variety of forms. These do not necessarily cause a pressure drop in the system; in principle, they can cause a pressure increase in the system. For these reasons, active mixing is a viable approach.

Some active mixing schemes are as follows:

- fan or turbine mixers (Figure 34-a)
- gas jet mixer (Figure 34-b)

c.2 Calculations and Results

Ideal fan power for mixing flue gas by a jet was calculated for different duct sizes. Duct diameters ranged from 2.4 m (8) to 9.1 m (30); the flue gases were assumed to be at 150°C (300°F) and one atmosphere. The ideal fan power for the jet was calculated by using the following equation:

$$P = WQH$$

where:

P = theoretical power, watts
W = specific weight of fluid, N/M^3
Q = volumetric flow rate, m^3/s at flue condition
H = developed head, m

The developed head of the jet was assumed to equal the velocity pressure head, i.e., $\frac{V^2}{2g}$. Frictional and other losses were not accounted for. It was also assumed that good mixing in the flue would be obtained when the following is met (See Appendix H-2 for the theoretical development of this analysis):

$$\frac{VD}{Ud} = 1$$

where:

v = velocity of the flue gases in the flue (m/s)
D = diameter of flue (m)
U = velocity of the jet stream at the orifice (m/s)
d = diameter of jet duct (m)

Tables 14-1 and 14-2 and Figures 36 and 37 show results for cases in which the jet inlet orifice is 1/10 the duct diameter.

In order to appreciate the power required under actual power plant conditions, the following examples are given:

Example 1 Potter, P.J., "Power Plant Theory and Design", p. 322, The Roland Press Co., N. Y., 2nd Edition, 1959.

Given: an induced draft fan designed at 193.5 m^3/s (410,000 ACFM). When the gas flow is equal to 89.7 m^3/s (190,000 ACFM) the static pressure is equal to 3.14×10^3 N/m^2 (12.6 in. of water). If an inlet damper control is used to control the gas flow, 72.5% of the outlet damper power is used. The efficiency of the fan is equal to 0.7, and the shaft hoursepower becomes:

for outlet control:

$$\text{Shaft hp} = \frac{89.7 \times 3.14 \times 10^3}{0.7} = 402 \times 10^3 \text{ W (539 HP)}$$

for inlet control:

$$\text{Shaft hp} = 402 \times 10^3 \times .725 = 291 \times 10^3 \text{ W (391 HP)},$$

and the developed pressure will equal 7×10^2 N/m^2 (2.8 in., varies as the square of the flow). Therefore, the theoretical fan power is equal to $291 \times 10^3 \times 0.7 = 205 \times 10^3$ W (275 HP).

TABLE 14-1

IDEAL FAN POWER FOR FLUE GAS JET AT ~150°C (300°F) AND 101.32 N/m^2 (1 ATM)

Diameter Of Flux (m)	Area of Flue (m^2)	Velocity In Flue (m/s)	Flow Rate In Flux (m^3/s)	Ratio of Flue to Jet Diameter	Diameter Of Jet (m)	Velocity In Jet (m/s)	Jet Area (m^2)	Flow Rate In Jet (m^3/s)	Developed Head $-u^2/2g$ (m)	Power = Qj x H x w* w = 8.48 N/m^3 (W)	(H.P)
2.4 (8')	4.67	3.0	14.01	10	0.24	30	0.0467	1.401	47.24	560	0.75
		6.1	28.49			61		2.849	189.28	4,474	
		12.2	56.97			122		5.697	757.12	35,868	48.1
		18.3	85.46			183		8.546	1703.8	121,176	162.5
		24.4	113.95			244		11.395	3029.10	287,169	85.1
		30.5	142.43			305		14.243	4732.93	560,915	752.2
3.6 (12')	10.52	3.0	31.56		0.36	30	0.1052	3.156	47.24	1,268	1.7
		6.1	64.17			61		6.417	189.28	10,067	13.5
		12.2	128.34			122		12.834	757.12	80,759	108.3
		15.2	159.90			152		15.990	1183.2[illegible]	157,715	211.5
6.1 (20')	29.18	3.0	87.54		0.61	30	0.2918	8.754	47.24	3,505	4.7
		6.1	178.0			61		17.800	189.28	28,038	37.6
		9.1	265.54			91		2.655	425.81	94,629	126.9
7.6 (25')	45.61	3.0	136.83		0.76	30	0.4561	13.683	47.24	5,444	7.3
		6.1	278.22			61		27.822	189.28	43,847	58.8
9.1 (30')	65.68	3.0	197.05		0.91	30	0.6568	19.705	47.24	7,904	10.6
		6.1	400.65			61		40.065	189.28	63,086	84.6

* Specific weight at 150°C and 101.32 $N/m^2 \times 10^3$

TABLE 14-2

IDEAL FAN POWER FOR FLUE GAS JET AT ~150°C (300°F) and 101.32 N/m^2 (1 ATM)

Diameter Of Flux (m)	Area of Flue (m^2)	Velocity In Flue (m/s)	Flow Rate In Flux (m^3/s)	Ratio of Flue to Jet Diameter	Diameter Of Jet (m)	Velocity In Jet (m/s)	Jet Area (m^2)	Flow Rate In Jet (m^3/s)	Developed Head $u^2/2g$ (m)	Power = Qj x H x w* w = 8.48 N/m^3 (W)	(H.P.)
2.4 (8')	4.67	5.1	23.6 (50,000)**	10	0.24	51	0.0467	2.36	131	2,535	(3.4)
		20.2	94.4 (200,000)			202		9.44	2080	163,532	(219.3)
		30.3	146.6 (300,000)			303		14.16	4685	552,340	(740.7)
		45.5	212.4 (450,000)			455		21.24	10539	1,863,504	(2499)
3.6 (12')	10.52	2.2	23.6		0.36	22	0.1052	2.36	25	500	(0.67)
		8.9	94.4			89		9.44	409	32,140	(43.1)
		13.4	141.6			134		14.16	916	107,977	(144.8)
		20.2	212.4			202		21.24	2080	367,854	(493.3)
6.1 (20')	29.18	0.8	23.6		0.61	8	0.2918	2.36	3	62	(0.084)
		3.2	94.4			32		9.44	53	4,175	(5.6)
		4.8	141.6			48		14.16	120	14,094	(18.9)
		7.2	212.4			72		21.24	268	47,426	(63.6)
7.6 (25')	45.61	0.5	23.6		0.76	5	0.4561	2.36	1	22	(0.03)
		2.0	94.4			20		9.44	21	1,640	(2.2)
		3.1	141.6			31		14.16	48	5,667	(7.6)
		4.6	212.4			46		21.24	109	19,313	(25.9)
9.1 (30')	65.68	0.3	23.6		0.91	3	0.6568	2.36	0.6	11	(0.015)
		1.4	94.4			14		9.44	10	820	(1.1)
		2.1	141.6			21		14.16	23	2,759	(3.7)
		3.2	212.4			32		21.24	53	9,396	(12.6)

* Specific weight at 150°C and 101.32 N/m^2 X 10^3

** ft^3/min.

Figure 36. Ideal Fan Power for Jet vs Average Flue Gas* Velocity For Different Flue Diameter At Diameter of Flue Duct/ Diameter of Jet Orifice = 1.0

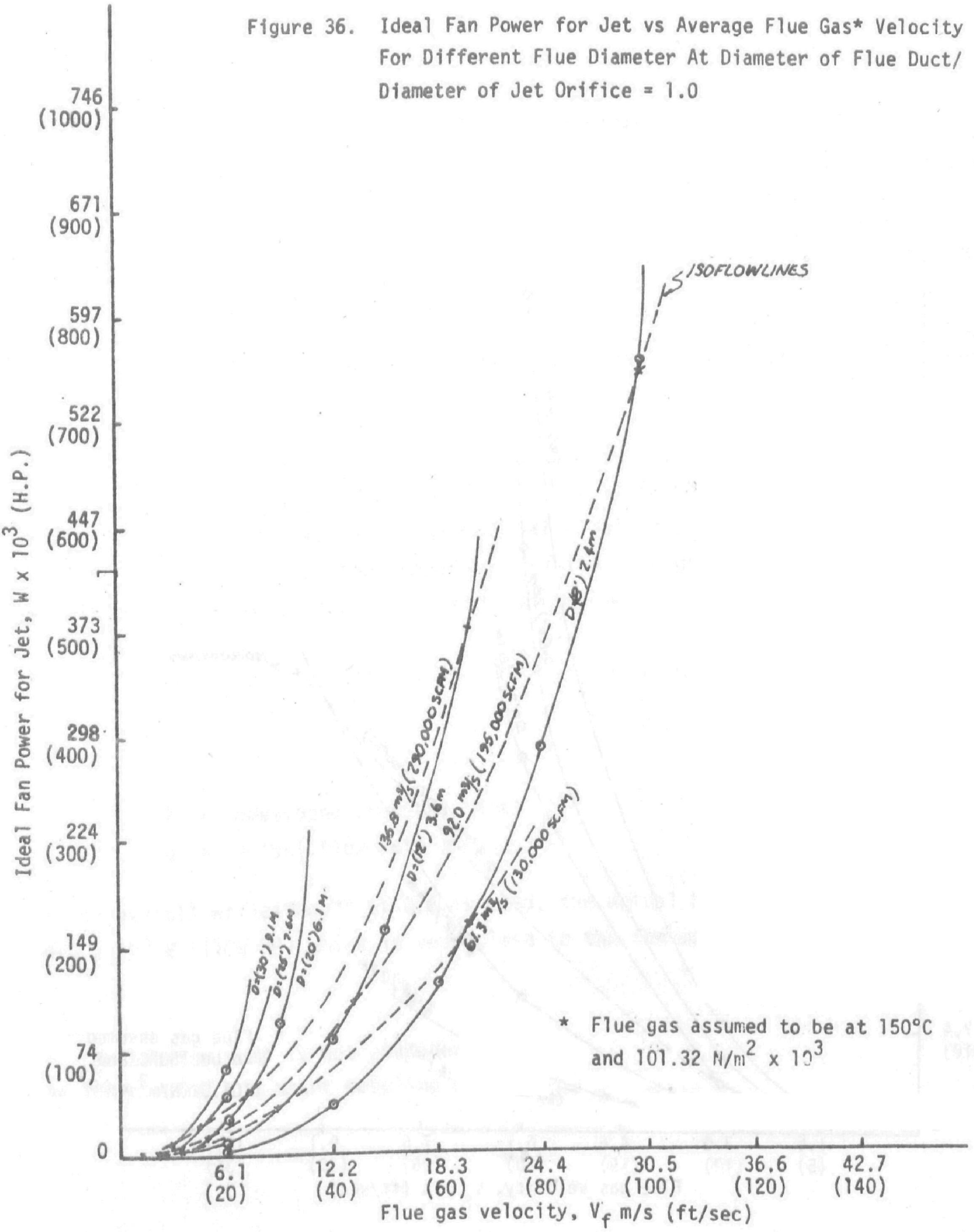

Figure 37. Ideal Fan Power for Jet vs Average Flue Gas* Velocity For Different Flue Diameter at Diameter of Flue Duct/ Diameter of Jet Orifice = 1.0

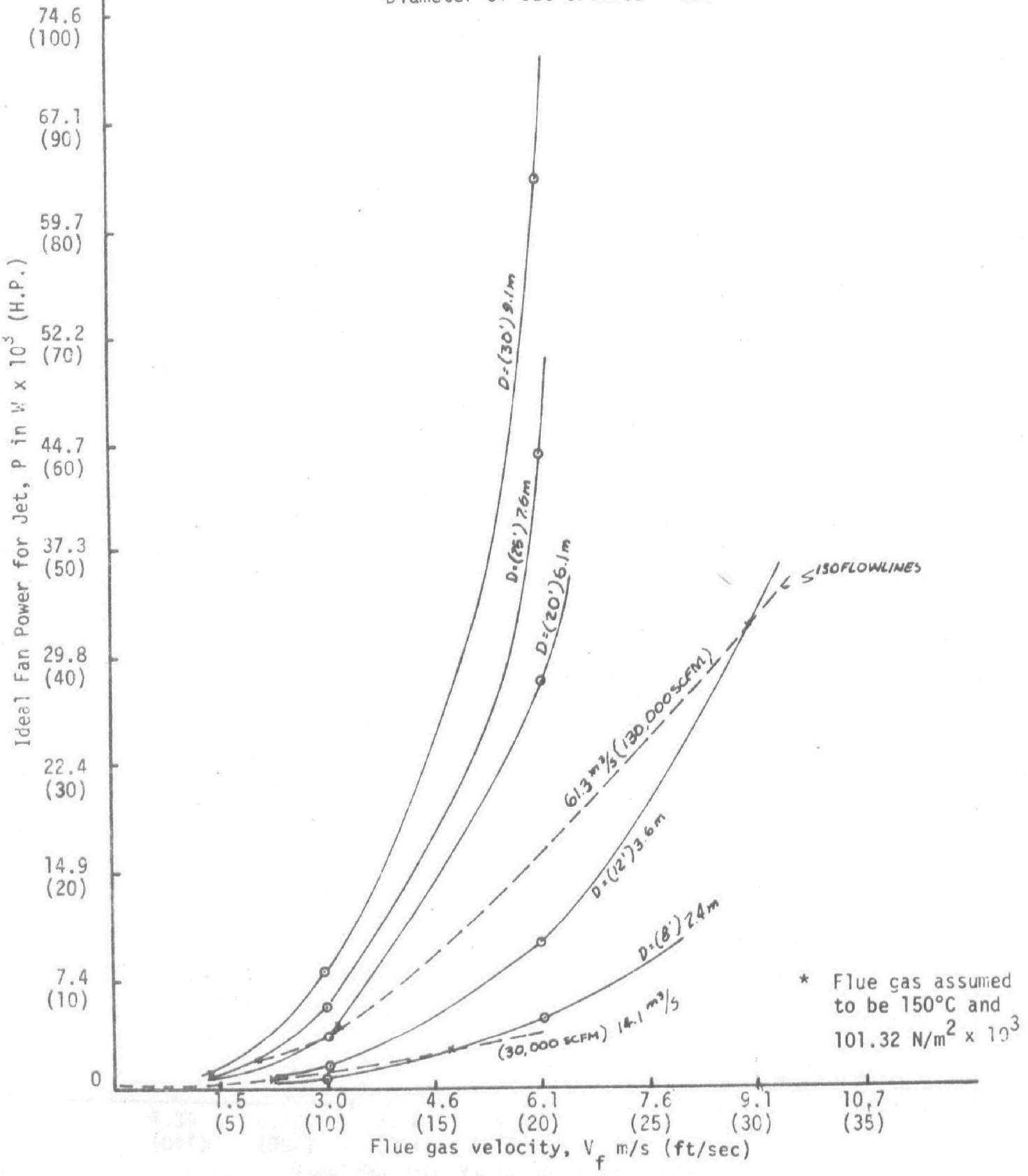

A jet used to mix 89.7 m^3/s (190,000 ACFM) flowing through a 3.0 m (12 ft.) diameter flue at 9 m/s (30 ft/sec) would need an ideal fan power for jet mixing of about 37×10^3 W (50 HP) (See Figure 36). This is approximately equal to a fifth of the power used to drive the flue gases. A quick estimate of the electrical cost per year can be obtained if we assume 4000 hrs/yr operation at 2¢/kw hour, giving a cost of electricity equal to:

$$\frac{37 \times 10^3 \times 10^{-3} \times 4000 \times 2}{100} = \$3,000$$

Example 2 Boston Edison Mystic River Power Plant, from personal communication.

A flow of 141.6 m^3/s (300,000 ACFM) is driven by a fan* with a motor of maximum rating equal to 932×10^3 W (1250 HP), at an inlet pressure of 35×10^2 N/m^2 (14" W.G.) vacuum and with a delivery pressure of about 101.33 N/m^2 (1 atm). If the temperature of the flue gases is assumed to be equal to 150°C (300°F) the ideal fan power becomes

$$Q \times P = 141.6 \times 35 \times 10^2 = 495 \times 10^3 \text{ W}$$

where

P = developed pressure, N/m^2
Q = actual flow rate m^3/s

If an overall efficiency** of 0.6 is used, the actual horsepower equals 820×10^3 W (1100 HP) which is very close to the fan motor rating.

---

* the booster pump is not considered
** fan $\eta = 0.7$ and motor coupling $\eta = 0.85$

If one considers jet mixing in the precipitator outlet duct, 7.3 m x 4.9 m (24' x 16'), the equivalent diameter is calculated to be close to 6.1 m (20'). At 92 m^3/s (195,000 SCFM) 141.6 m^3/s (-300,000 ACFM at ~150°C and 101.33 N/m^2), the ideal fan power for the jet is equal to 14.2 x 10^3 W (19 HP) (See Figure 36). The jet opening is equal to 0.61 M (2') with a jet velocity of 48.8 m/s (160 ft/sec).

In the case of jet mixing in the after preheater section with an equivalent diameter approximately equal to 3.6 M (12'), the ideal fan power for the jet is equal to 108 x 10^3 W (145 HP) (See Figure 36). The jet opening is equal to 0.37 m (1.2') with a jet velocity of 134 m/s (440 ft/sec).

From this it is concluded that, according to the jet mixing site, the power needed can range from as low as 1/20 of the total ideal fan power used in the main flue to as high as 1/5 of the total ideal fan power.

It is significant to note that the fan power varies inversely with the absolute temperature (speed and capacity being constant). In the last example the flue gases are assumed to be at ~150°C (300°F); if lower temperatures are used, more power will be required for the same actual flow rate.

The results of this analysis imply that the power requirements for the mixing jet can be modest compared to the power required to drive flue gas through the duct. While this approach cannot be considered a general solution for the problem of obtaining representative samples from all stratified gas streams, it is likely to be applicable to some particular stratified stream. However, scaled laboratory experiments should be performed to test the results indicated herein before any full-scale application is attempted. In summary, this approach now appears to be more promising than at the beginning of this program.

2. LABORATORY EXPERIMENTS

Tests with velocity and concentration traveses in square and round sections of a wind tunnel were conducted and the results are presented below. Different sampling methods are also discussed.

a. Wind Tunnel and Test Set Up

The installation of the wind tunnel equipment was first completed as shown in Figure 38. Ports and probe holders were installed at two test sections, a circular section and a square section. The plan view of the installation shows the approximate locations of the planned test sections. An additional 0.61 m (2') length of circular duct was introduced for the Annubar element, following the pitot tube traversing port. Aluminum honeycomb cores (See Figure 39) were used in the round section following the 90° bend to produce a more uniform flow.

Provisions were made for metering ethane from a 1-A cylinder into the tunnel as the test gas. Analysis of ethane from gas extracted from the test sections was by FID. The average concentration of ethane was held below the lower limit of flamability in air (LEL in air 3%). Gas velocity* was measured by a standard pitot static tube using a MKS, Inc. Baratron instrument. Control of the velocity stratification and test gas stratification was by use of a damper following the fan and a baffle[28] introduced at the entrance of the wind tunnel and by position of gas injection respectively. The referee method of measurement for the emission of ethane through the test section was by rotameter reading of the ethane supply.

---

* when air is used at temperature T_s (K°) and 101.33×10^3 N/m^2 the velocity Vs(m/s) is given by:

$$Vs = 0.87 \sqrt{\frac{\Delta h \times T_s}{1.333 \times 10^2}}$$

where Δh = differential pressure in N/m^2 (1 mm Hg = 1.333×10^2 N/m^2)

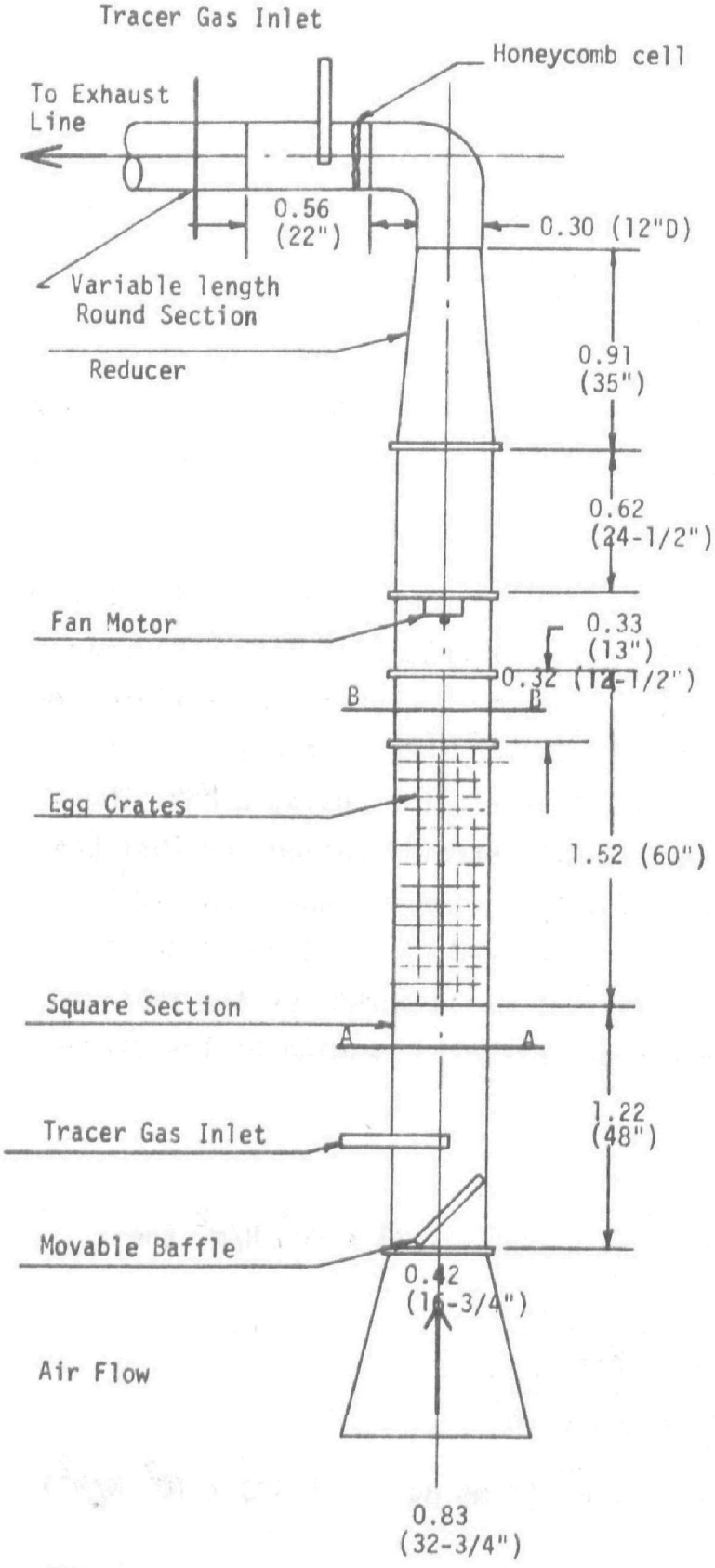

Figure 38. Wind Tunnel Plan View (One Fan)

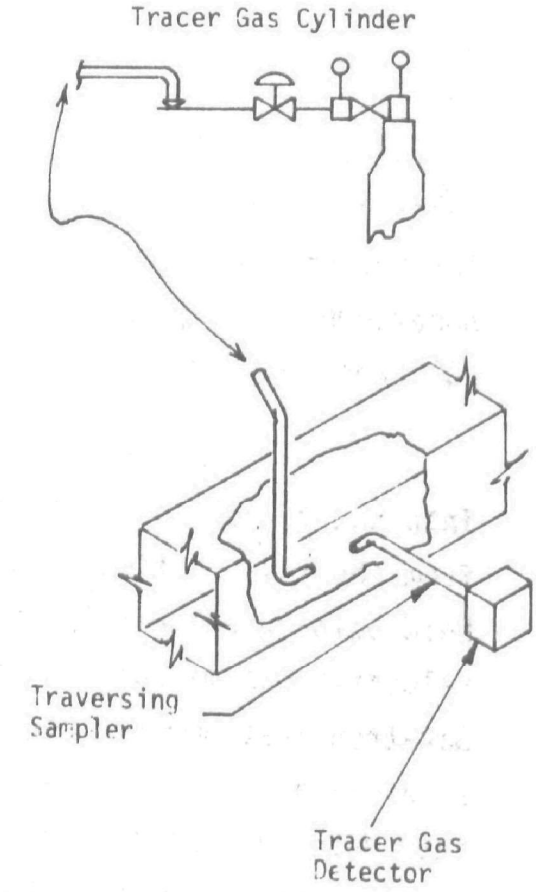

Experimental Ducts Showing Tracer Gas Set Up

Scale: ~1:40 Dims. Meters	
Sections	Material
Square	Plywood
Round	Galvanized Steel

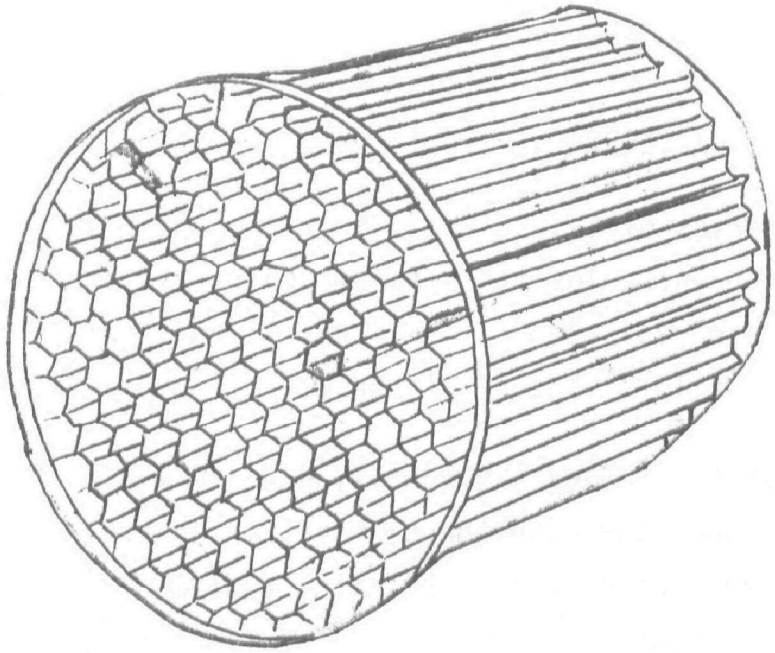

Figure 39. Aluminum Honeycomb Cells

In the most recent experiments, the wind tunnel was modified to increase the maximum flow rate. A fan the same size as the original fan was installed in series (see Figure 40). The blades were installed to operate in counter-rotation to the original fan in order to increase efficiency. This modification provided a 2.9% increase in maximum flow or a maximum average velocity of 8.3 m/s (27.3 ft/sec) in the circular section and 3.5 m/s (11.6 ft/sec) in the square section.

b. Testing Program

A series of tests (Test No. 2 through Test No. 13) were conducted with different velocities and concentration profiles. Several sampling methods were evaluated. In all cases, the tracer gas was introduced at about 16.2 x 10^{-6} m^3/s (~1 liter/min).

Test No. 2 (see Figures 41, 42, and 43) is an evaluation of the air flow through the wind tunnel measured by traversing the square as well as the round section using the pitot tube and also using the Annubar element in the round section. The calculated flow was surprisingly very close in all cases, as shown in Table 15.

Test Nos. 3 and 5 were conducted on the square and the round sections of the wind tunnel, respectively, in both cases almost all conditions were kept the same. The calculated flow from both traverses agreed within 3.5%

The total emission as calculated from the round section was about 6% higher than expected and from the square section about 10% lower than expected. This discrepancy may be due to the values of the velocities obtained when reverse conditions predominated. Results are shown in Figures 44-a, b, c and 45-a, b, c and Table 16.

Table 16 compares the value of the total emission obtained from Test No. 6 by using the 'ANNUBAR' sampling port (see Figure 46 a and b) for sampling vs. the ethane introduced. An error of about -34% was observed.

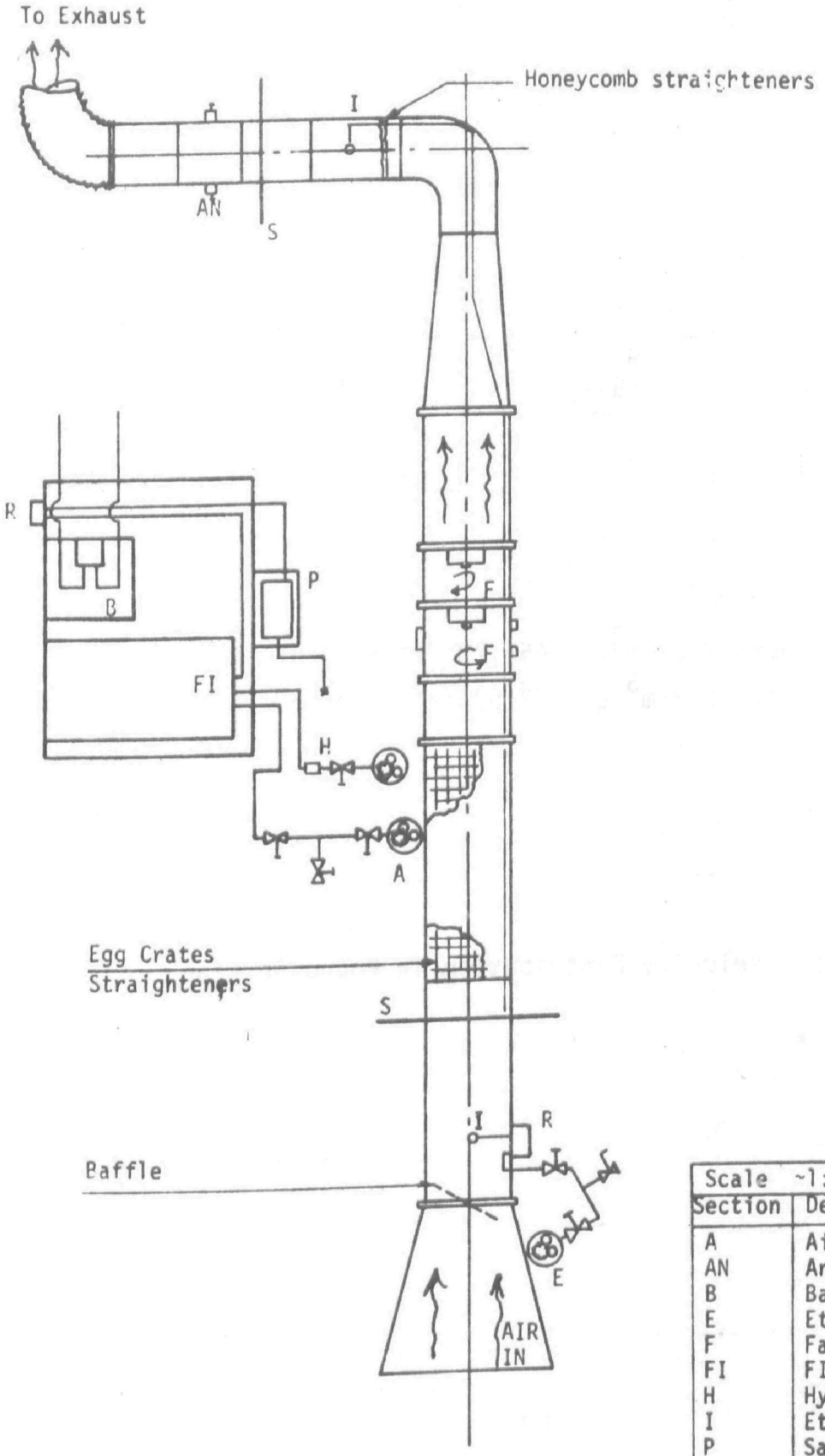

Scale ~1:40	
Section	Description
A	Air tank
AN	Annubar Element
B	Baratron
E	Ethane Tank
F	Fan
FI	FID
H	Hydrogen Tank
I	Ethane Injection Port
P	Sampling Pump
R	Rotameter
S	Sampling Ports

Figure 40. Wind Tunnel Plan View (Two Fans)

TEST NO. 2

Conditions: Baffle: Inclined ~22.5° to horizontal
Flow Area: 0.073 m^2 (0.7854 ft^2)
Temperature: 18°C

*	1	2	3	4
A	1.5 (4.86)	3.1 (10.31)	4.1 (13.31)	2.3 (7.68)
B	1.3 (4.21)	3.9 (12.86)	4.8 (15.75)	2.9 (9.41)
C	1.3 (4.35)	3.1 (10.31)	4.4 (14.58)	2.6 (8.42)

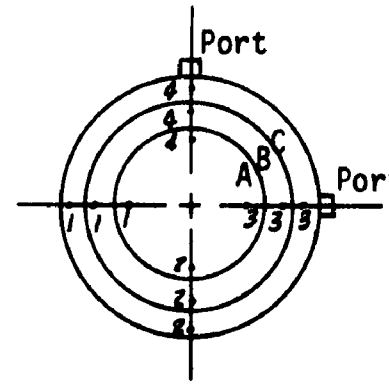

* Velocity in m/s

Total flow: 0.21 m^3/s (455.73 ft^3/min) at 18°C
or 0.2 m^3/s (427.57 ft^3/min) at 0°C

Figure 41. Velocity Distribution in Round Section

TEST NO. 2

CONDITIONS: Baffle: Inclined ~22.5° to horizontal
Flow area: 0.7854 (ft^2)
Temperature: 18°C

Annubar reading ΔP (mmHg)	0.085
Temperature $T_{°R}$	524.4
γf $\frac{0.0765 \times 520}{T}$	0.07585
Element Constant S	0.68
Formula Used	$Qn = \frac{585.24}{S} \times S \times \frac{1}{\sqrt{\gamma f}} \times \sqrt{\frac{\Delta P}{1.8663}}$
Total Flow Qn, ft^3/min	453.48 or 427.5 at 32°F
Total Flow m^3/s	0.21 0.20 at o°C

Figure 42. Average Velocity Using the Annubar Element in Round Section

TEST NO. 2

CONDITIONS: Baffle: Inclined ~22.5° to horizontal
Flow Area: 0.18 m^2 (280 in^2)
Temperature: 20°C

*	1	2	3	4	5	6	7
A	1.5	1.7	1.8	2.0	2.2	2.0	2.0
B	1.8	1.8	1.9	2.1	2.2	2.1	2.2
C	1.8	2.0	2.0	2.3	2.5	2.3	2.2
D	1.6	2.0	2.2	2.3	2.1	1.6	1.8
E	1.3	1.8	2.1	2.1	1.4	0.8	~0
F	~0	1.1	1.4	1.8	1.2	~0	-2.8
G	-5.9	-1.5	1.3	1.5	0.8	-1.0	-5.1

* Velocity in m/s
Total flow 0.217 m^3/s (459.10 ft^3/min) at 20°C
or 0.20 m^3/s (427.80 ft^3/min) at 0°C

Figure 43. Velocity Distribution in Square Section

TABLE 15

Traverse Section	Air Flow Reduced To 0°C m^3/s (32°F ft^3/min)		Remarks
Square	0.20	(428)	Pitot tube traverse, reverse flow was accounted for by subtracting
Circular	0.20	(428)	Pitot tube traverse
Circular	0.20	(428)	Average velocity is obtained using the ANNUBAR element

TABLE 16

Traverse Section	Air Flow Reduced To 0°C m^3/s (32°F ft^3/min)		Ethane Introduced kg/s	Emission Rates Calculated kg/s
Square	0.197	(418)	20.370×10^{-6}	18.240×10^{-6}
Circular	0.205	(435)	20.370×10^{-6}	18.640×10^{-6}
Circular using "ANNUBAR" element*	0.202	(427)	20.370×10^{-6}	18.517×10^{-6}

* Sampling from high pressure side tube or sampling from sampling tube - See Figure 9-b for details.

TEST NO. 3

CONDITIONS: Baffle: Inclined 22.5° to horizontal
Ethane Flow rate: 0.97 l/min = 20.3 x 10^{-6} kg/s
injected after baffle in square section
Temperature: 20°C
Flow Area: 0.18 m^2 (280 in^2)

*		1	2	3	4	5	6	7
A	V*	1.4	1.6	1.8	1.9	2.1	1.9	1.9
	C**	288	290	305	295	330	338	248
B	V	1.7	1.6	1.8	2.1	2.3	2.2	2.2
	C	293	280	265	250	275	198	148
C	V	1.8	1.8	2.0	2.3	2.4	2.3	2.0
	C	268	265	230	180	210	208	138
D	V	1.7	1.8	2.1	2.2	2.2	1.7	1.5
	C	218	205	165	120	130	128	128
E	V	1.3	1.8	2.0	1.8	1.5	0.8	0
	C	158	155	120	95	105	113	128
F	V	0	1.1	1.4	1.4	1.4	0	-2.3
	C	143	135	120	100	110	113	168
G	V	-5.1	-1.5	1.3	1.1	1.1	-1.1	-4.9
	C	183	145	140	115	130	148	203

* Velocity in m/s
** concentration must be multiplied by 0.3347 to convert to ppm ethane
Total Flow = 0.212 m^3/s (448.67 ft^3/min) or 0.197 m^3/s (418.07 ft^3/min) at 0°C
Total Emission 18.240 x 10^{-6} kg/s

Figure 44a. Velocity and Concentration Distribution Data in Square Section

TEST CONDITIONS: Baffle: Inclined 22.5°
Total Flow: 0.21 (~450 ft^3/min) at 20°C
Flow Area: 0.18 m^2 (280 in^2)

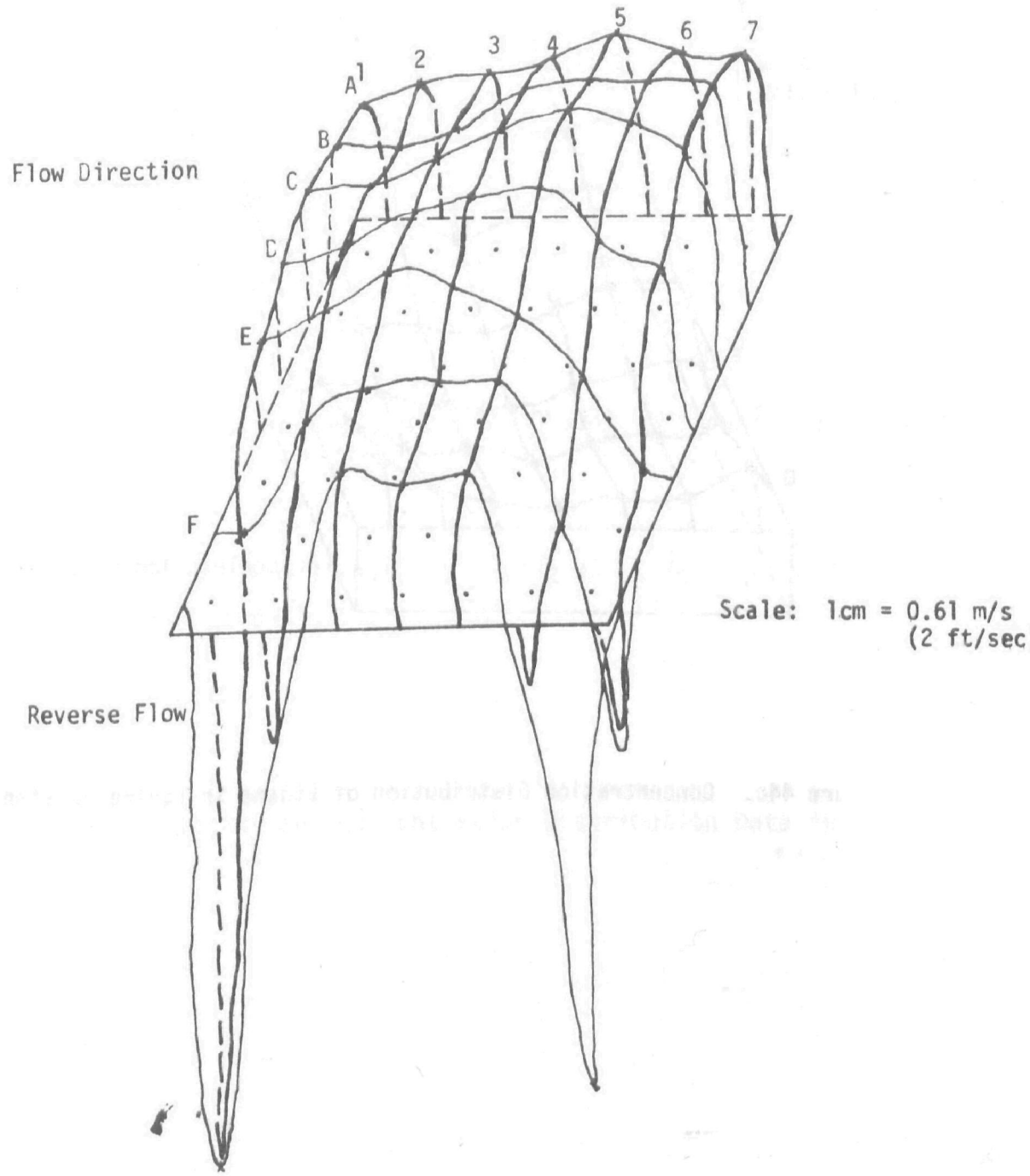

Figure 44b. Velocity Distribution in Square Section

TEST CONDITIONS: Baffle: Inclined 22.5°

Total Flow: 0.2 m^3/s (~450 ft^3/min) at 20°C

Flow Area: 0.18 m^2 (280 in^2)

Ethane Flow Rate: 16.2 x 10^{-6} m^3/s (0.97 l/min)

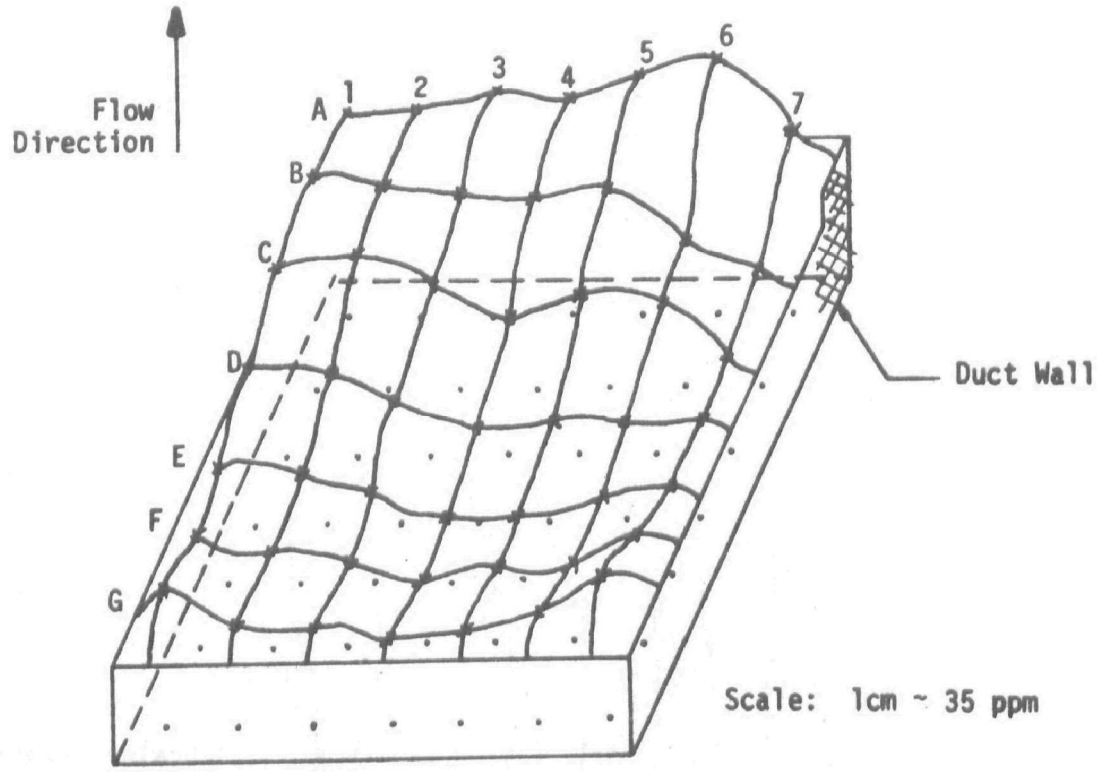

Figure 44c. Concentration Distribution of Ethane in Square Section

TEST NO. 5

Conditions: Baffle: Inclined 22.5° to horizontal
Ethane Flow rate = 0.97ℓ/min ≡ 20.37 x 10^{-6} kg/s injected after honeycomb in round section
Temperature = 18°C
Flow Area = 0.073 m^3 (.07854 ft^2)

		1	2	3	4
A	V*	1.4	3.3	3.9	2.7
	C**	540	90	130	340
B	V	1.2	3.9	4.8	2.8
	C	740	45	125	470
C	V	1.2	3.4	4.6	2.7
	C	790	40	110	500

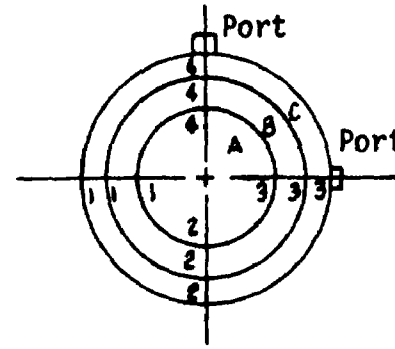

* Velocity in m/s

** Concentration must be multiplied by 0.3347 to convert to ppm ethane

Total Flow = (464.40 ft^3/min) or (435.20 ft^3/min) at 0°C
Total Emission = 21.64 kg/s

Figure 45a. Velocity and Concentration Distribution Data in Round Section

TEST CONDITIONS: Baffle: Inclined 22.5°
Total Flow: 0.219 m^3/s (465 ft^3/min)
Flow Area: 0.073 m^2 (0.7854 ft^2)

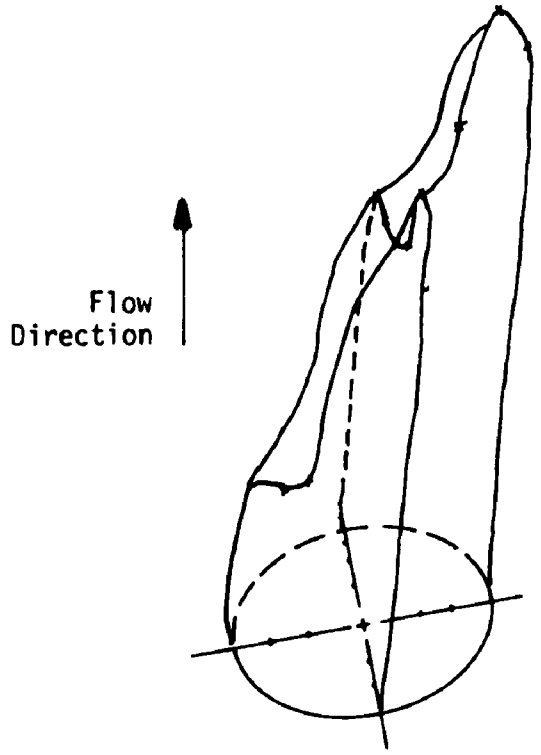

Scale: 1 cm = 0.61 m/s
(2 ft/sec)

Figure 45b. Velocity Distribution in Round Section

TEST CONDITIONS: Baffle: Inclined 22.5°
Total Flow: 0.219 m^3/s (465 ft^3/min)
Flow Area: 0.073 m^2 (0.7854 ft^2)
Ethane Flow Rate: 16.2 x 10^{-6} m^3/s (0.97 l/min)

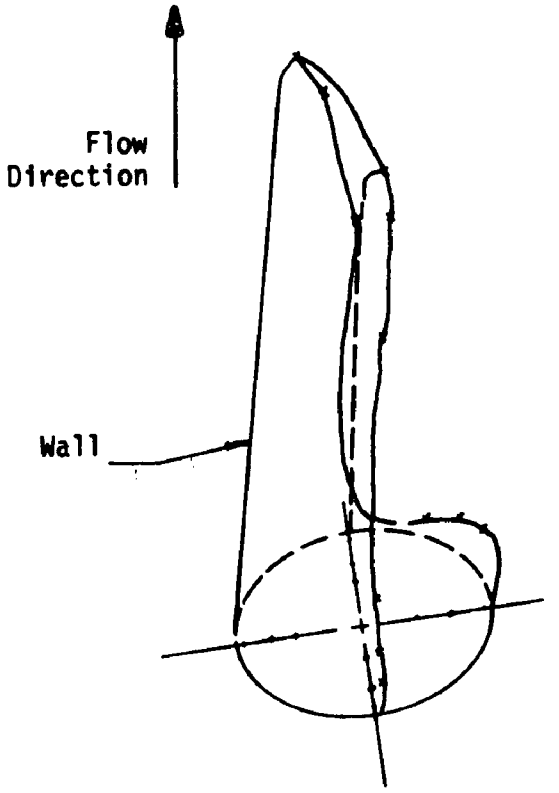

Scale: 1 cm = ~ 35 ppm.

Figure 45c. Concentration Distribution of Ethane in Round Section

TEST NO. 6

Conditions: Baffle: Inclined 22.5° to horizontal
Ethane Flow Rate = 0.97ℓ/min ≡ 20.370 x 10^{06} kg/s
Temperature 18°C
Flow area = 0.073 m^2 (0.7854 ft^2)
Flow rate = 0.21 m^3/s (454 ft^3/min)

Special Condition	Concentration*
Well mixed sample	220
Sampling from cap (No. 1)	150
Sampling from H. press	150
**	1
Sampling position No. 2	160
2-3	220
3	290
4	370
5	330
6	340
7	310
8	340
9	330
10	300
11	155
12	145

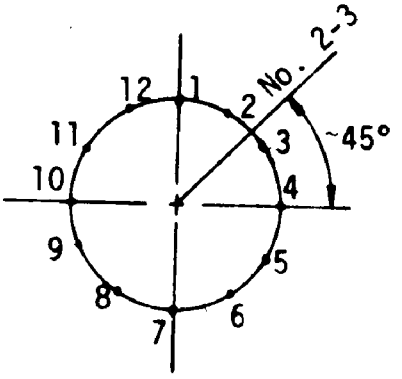

* Concentration must be multiplied by 0.3347 to convert to ppm ethane

** Sampling position No. 1 is holes facing stream flow as in Figure other positions, holes facing stream at an angle

Figure 46a. Average Concentration Using the "Annubar Element"

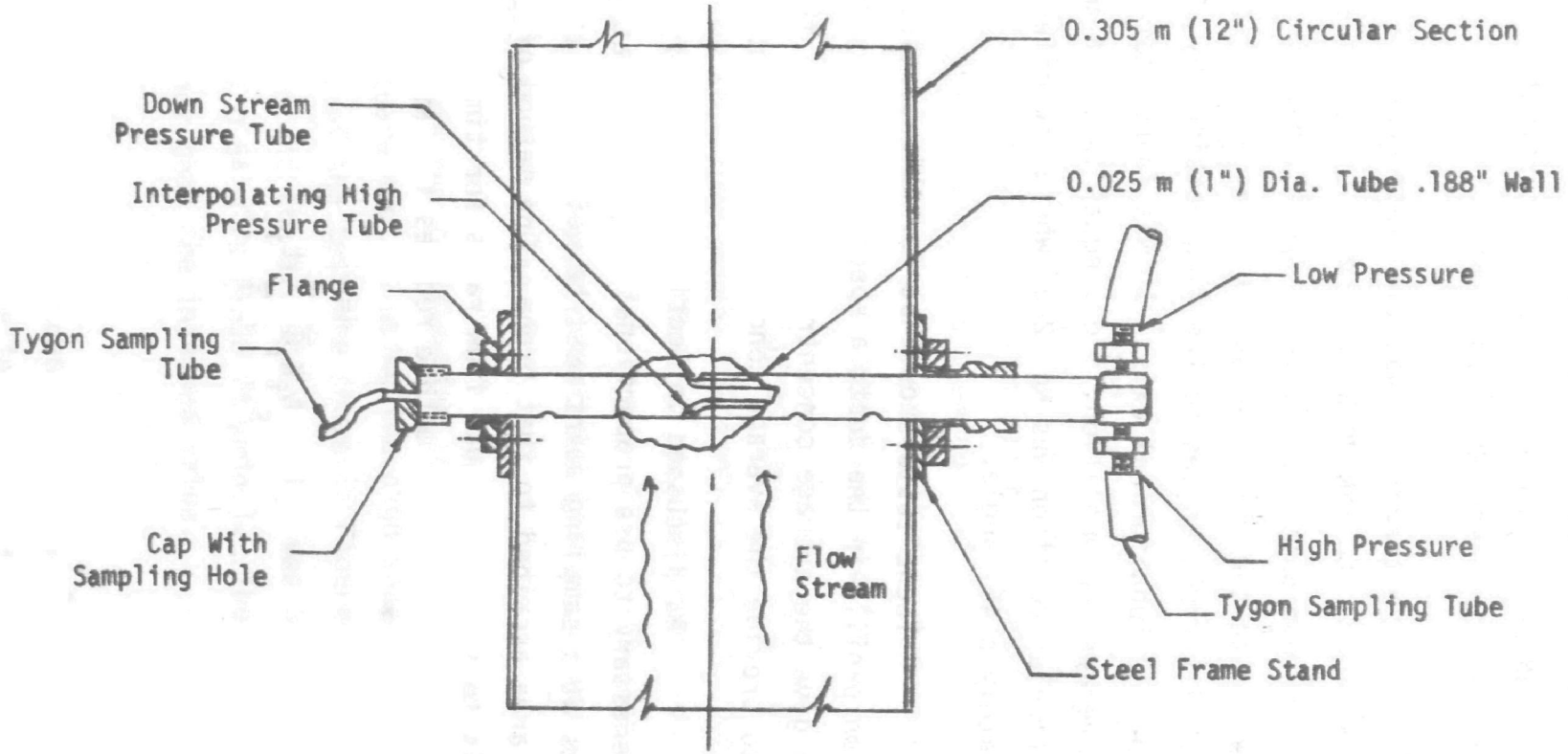

Figure 46b. Annubar Flow Element

In Test No. 6, ethane was well mixed by introducing it into the square section port and sampling in the round section after the fan using the 'ANNUBAR' element. Since no concentration stratification existed, the correct emission was obtained as expected.

The tracer gas was then introduced after the honeycomb in the round section and the 'ANNUBAR' element was used as a sampling probe to obtain an average sample at different positions. The first position of the element was with the holes facing the flow; other positions were with the element at different angles to the flow obtained by rotating the element 360° about the longitudinal axis. It was found that one position gave the correct average concentration, i.e., equal to the mixed sample concentration. This particular position was No. 2-3, where the holes faced the stream at approximately a 45° angle.

These tests show that for this particular velocity and concentration profile in the duct, a specific position of the Annubar was found to give the average concentration. However, this position is not expected to provide the average concentration for another set of profiles

As discussed in Section IV .B.1.b. of this report, it is generally necessary to use proportional samplers. That is, gas concentration measurements at a sampling point must be weighted by the local gas velocity and the area ascribed to that probe. One method of satisfying this condition is to sample at equal flow rates for times proportioned to the local stack gas velocity. This method reduces the emission rate equation to:

$$E = A_i K_1 \bar{C} \sum_{i=1}^{i=n} t_i$$

where:

E = emission rate

A_i = area ascribed equally to all probe's location

K_1 = proportional constant equal to $\frac{V_1}{t_1} = \frac{V_2}{t_2} = \cdots = \frac{Vn}{tn}$

$\bar{C}$ = average concentration of the mixed samples

t_i = sampling time for each sample location

Test Nos. 7 and 8 were conducted to demonstrate this method. The sampling set up is sketched in Figure 47-a. Sampling from all locations was done sequentially at an equal rate. A stop watch was used to measure the sampling time which had been calculated previously from velocity profile data. The average concentration was obtained by collecting the total sample in a mylar bag and then sampling the mixed contents with a F.I.D.

Test results are given in Figures 47-b and 47-c. Both tests were performed at the same locations across a traversing port of the square section of the wind tunnel; the only difference was the proportionality constant K. Results from Test Nos. 7 and 8 show a +2% and -6% discrepancy in emission rate respectiyely, from that calculated from each sampling location velocity and concentration traverse.

Test No. 9-1 was run to determine the velocity and concentration profiles generated in the square section using the high speed wind tunnel as shown in Figure 40. Results of the test are shown in Figures 48-a,b. A 91 point traverse* was performed and the average velocity was 3.5 m/s (11.6 ft/sec ft/sec) with a total flow of 0.64 m^3/s (1356 ft^3/min.). The calculated total emission was 1.9% higher than the injected value.

---

* Numbers 1,2,3,...7 are the original 49 centroid of equal area sampling locations. Number 1-2, 3-3, .. 6-7 are located respectively mid-way between 1 and 2, 2 and 3 .. 6 and 7.

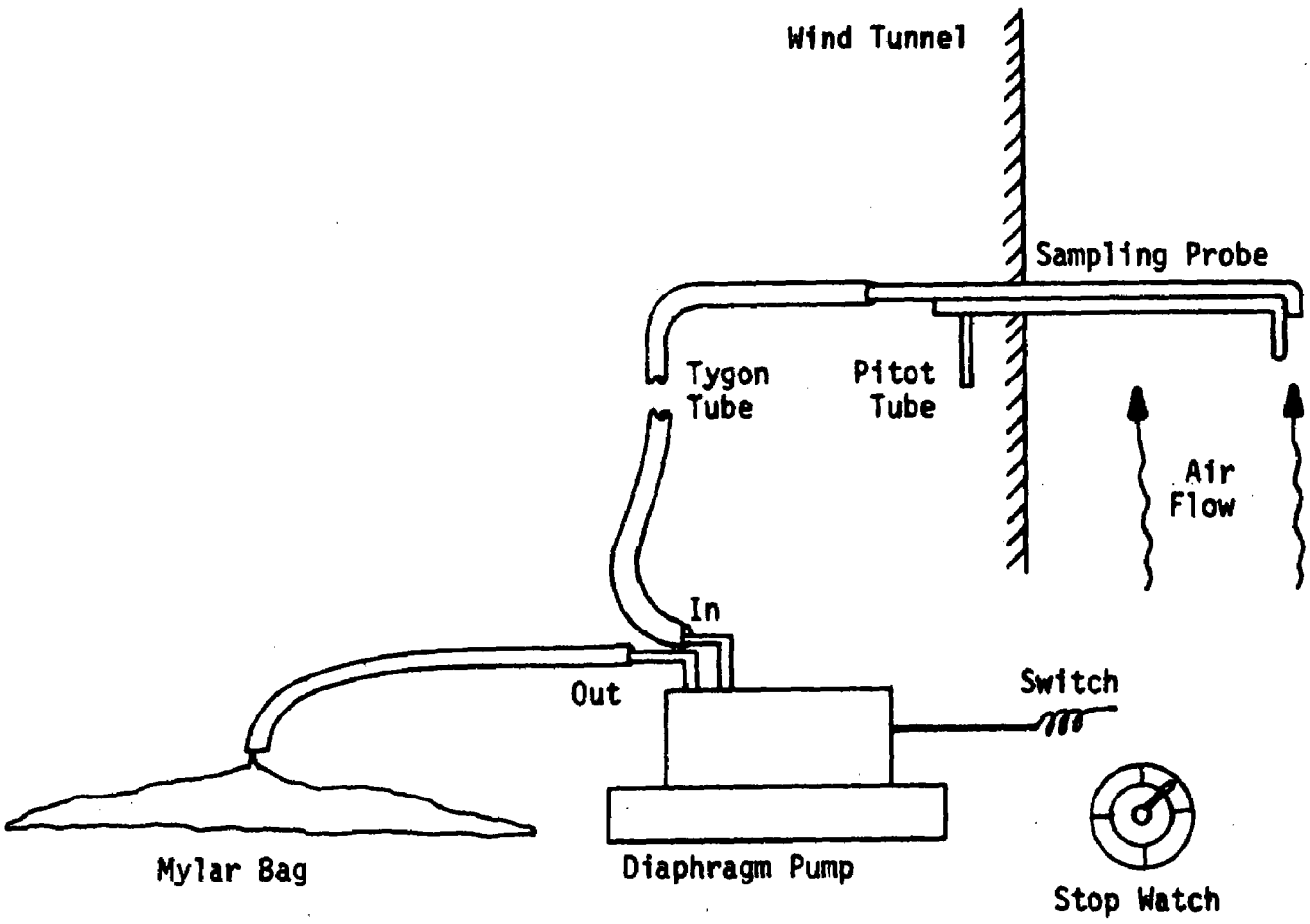

Figure 47a. Experimental Set-up for Manually Adjusting Sampling Time At Each Sampling Position

TEST NO. 7

Conditions: Baffle: inclined 22.5° to horizontal
Ethane Flow Rate: 16.2 x 10^{-6} m^3/s (0.97ℓ/min)
Temperature: 16°C
Flow Area 0.18 m^2 (280 in^2)

	Port No. 5	t_i [c]	$v_i c_i$
A V [a] / C [b]	2.10 / 330	27.60	693
B V / C	2.26 / 280	29.60	632
C V / C	2.44 / 205	32.00	500
D V / C	2.10 / 135	27.60	283
E V / C	1.49 / 115	19.50	171
F V / C	1.41 / 120	18.50	168
G V / C	1.15 / 130	15.10	150
$\sum_{i=1}^{i=7}$		169.10	2597
prom bag C_{au}	205		
K	1/4		
E^d = $K+\Sigma t_i x C_{au}$ or $\Sigma v_i c_i$		2654	2597

Discrepancy + 2%

Footnotes

a velocity m/s

b concentration must be multipilied by 0.337 to convert to ppm ethane

c time in seconds

d emission rate (not converted

Figure 47b. Sampling in Square Section at Constant Flow Rate With Manually Adjusting-Sampling Time for Each Position

TEST NO. 8

Conditions: B Baffle: inclined 22.5° to horizontal
Ethane Flow Rate: 16.2×10^{-6} m/s
Temperature: 16°C
Flow Area: 0.18 m^2 (280 in^2)

	Port No. 5	t_i [c]	$v_i c_i$
A V [a] C [b]	2.10 335	55.1	703
B V C	2.25 280	59.2	630
C V C	2.44 2.5	64.1	500
D V C	2.10 135	55.1	284
E V C	1.49 115	39.0	171
F V C	1.41 125	37.0	176
G V C	1.15 135	30.2	155
$\sum_{i=1}^{i=7}$		339.8	
from bag C_{au}	190		
K	1/8		
E [d] = $K+\Sigma t_i x C_{au}$ or $\Sigma v_i c_i$		2460	2619

Footnotes

a velocity m/s

b concentration

c time in seconds

d emission rate (not converted)

Discrepancy - 6%

Figure 47c. Sampling in Square Section at Constant Flow Rate With Manually Adjusting Sampling Time For Each Position

Figure 48a. Velocity and Concentration Distribution Data in Square Section

TEST NO. 9

		1	1-2	2	2-3	3	3-4	4	4-5	5	5-6	6	6-7	7
A	V[1]	2.1	2.1	2.1	3.0	4.1	3.1	3.5	3.5	3.5	3.0	2.8	2.3	2.3
	C[2]	85	90	85	95	105	110	110	115	120	95	100	85	95
B	V	2.6	2.1	2.8	3.0	3.1	3.6	3.7	3.8	3.6	3.5	3.2	3.0	3.0
	C	95	95	106	115	120	120	120	115	110	90	85	65	75
C	V	2.8	2.8	2.6	3.1	3.1	3.8	4.0	3.9	4.1	4.2	4.1	4.3	4.0
	C	105	115	125	125	130	130	130	120	116	90	90	65	65
D	V	2.3	2.6	2.6	3.0	3.3	3.9	4.2	4.4	4.5	4.9	4.9	4.7	4.7
	C	120	115	125	125	130	125	120	105	105	80	70	60	55
E	V	2.3	2.3	2.8	3.0	3.3	3.4	3.8	3.9	4.4	4.6	5.1	5.0	4.7
	C	100	105	110	120	115	115	100	95	85	65	50	35	35
F	V	2.6	3.0	3.2	3.3	3.6	3.4	3.8	3.9	4.1	3.9	4.6	4.9	4.6
	C	80	80	85	90	90	100	105	90	70	60	45	30	25
G	V	2.9	3.5	4.0	4.0	4.0	4.0	4.0	3.9	3.6	3.6	3.8	3.8	3.8
	C	60	55	55	60	60	65	70	70	60	50	45	30	25

CONDITIONS: Baffle: Inclined 22.5° to horizontal
Flow Area: $0.18 m^2$ ($280 m^2$)
Ethane Flow Rate: 20.23×10^{-6} kg/s
Number of Fans: 2 fans in series
Temperature: 20°C

[1] velocity m m/s

[2] concentration must be multiplied by 0.298 to convert to ppm ethane: Average Velocity = 3.5 m/s (11.6 ft/sec)
Total Flow = 0.64 m^3/s (1356 ft^3/min) at 20°C Total Emission = 20.62×10^{-6} kg/s

TEST CONDITIONS:

Baffle: Inclined 22.5°

Total Flow: 0.64 m^3/s (1355 ft^3/min)

Flow Area: 0.18 m^2 (280 in^2)

Average Velocity: 3.5 m/s (11.6 ft/sec)

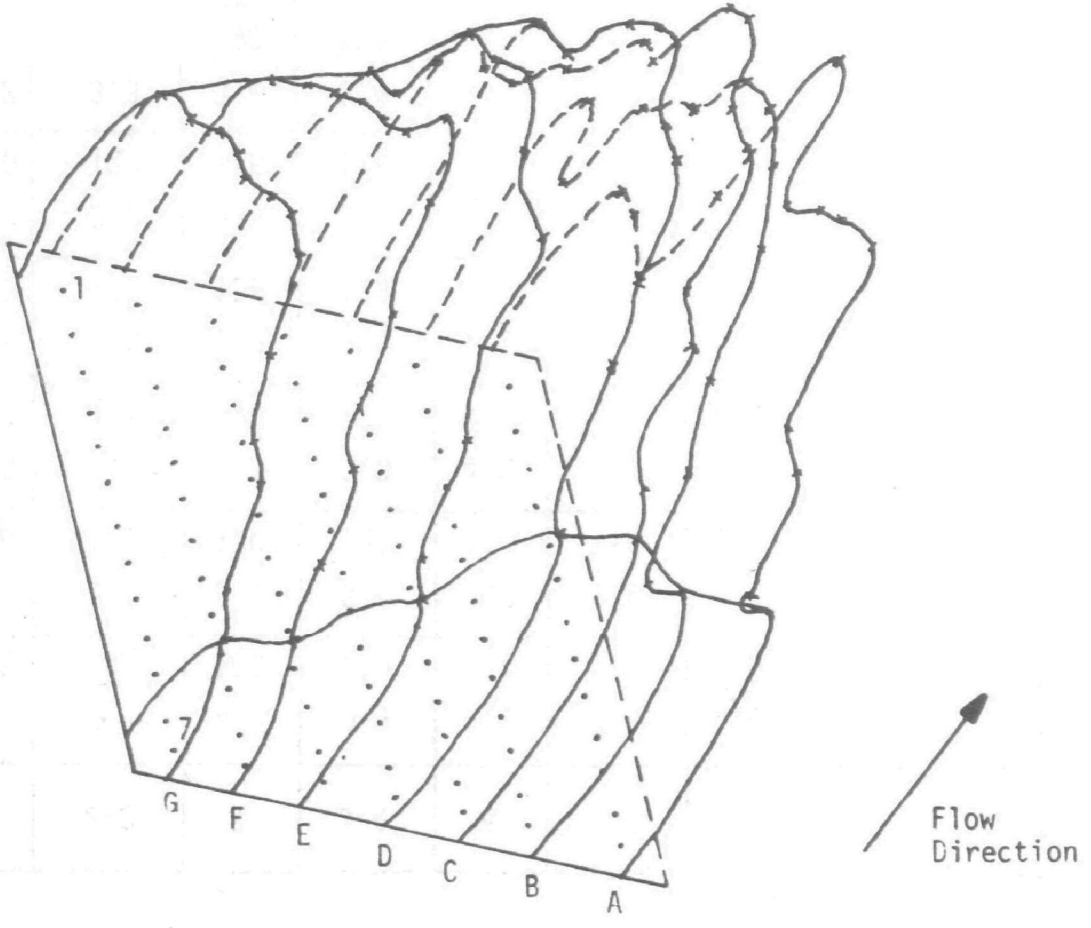

Scale:

1 cm ~ 45.05 x 10^{-9} kg/s

Figure 48b. Velocity and Concentration Distribution In Square Section

Test No. 9-2 was run on the circular section of the wind tunnel using the traversing ports and locations* as shown in Figure 49-a. The velocity and concentration distributions are shown in Figures 49-b,c respectively. The calculated average velocity was 7.9 m/s (26 ft/sec), giving a total flow of 0.575 m^3/s (1218 ft^3/min) which is approximately 10% less than the calculated flow from the square section. The total emission rate was 23.66 x 10^{-6} kg/s (0.02366 gm/sec), about 17% higher than the real value.

Because of the considerable disagreement between these and the square section results, Test No. 9-3 was run using the traversing ports rotated at a 45° angle as shown in Figure 50-a using the same radial locations. The velocity and concentration distrubutions are shown in Figures 50-b,c, respectively. The calculated average velocity was 8.2 m/s (27 ft/sec), giving a total flow of 0.606 m^3/s (1284 ft^3/min), which is about 5% less than the calculated flow from the square section. The total emission rate was 25.06 x 10^{-6} kg/s (0.02506 gm/sec.), about 24% higher than the real value.

The results of Test No. 9-4 using the Annubar element are shown in Figures 51-a,b. The total flow was equal to 0.515 m^3/s (1092 ft^3/min), approximately 19% lower than the value obtained from the square section. During this test, the tracer gas was injected before the fan location to obtain a mixed sample. After a concentration profile was generated, the tracer gas was injected after the fan location. Sampling from the Annubar element was done through the tap opposite the pressure taps at a rate of about 50 x 10^{-6} m^3/s (3 liters/min).

---

* Radii to stations in zone A, b and C respectively are 0.063 m (2.5"), 0.108 m (4.25"), and 0.140 m (5.5"). Stations locations in zone ℄-A, A-B and B-C are located mis-way between ℄ and A, A and B, and, B and C.

TEST NO. 9-2

Conditions: Baffle: Inclined 22.5° to horizontal
Ethane Flow Rate = 0.97 ℓ/min ≡ 20.23 x 10^{-6} kg/s
Temperature = 20°C
Flow Area = 0.073 m^3 (0.7854 ft^2)
No. of Fans in Series = 2

	1	2	3	4
℄A V*	6.1	10.0	9.0	℄ 8.1-8.3
C**	195	5	15	℄50-85
A V	4.9	10.7	9.2	8.2
C	160	0	5	260
A-B V	4.3	11.1	8.3	8.4
C	20	0	0	460
B V	4.2	11.6	7.7	8.2
C	20	0	0	560
B-C V	4.2	11.1	7.3	8.1
C	10	0	0	425
C V	4.1	9.5	6.7	7.8
C	5	0	4	260

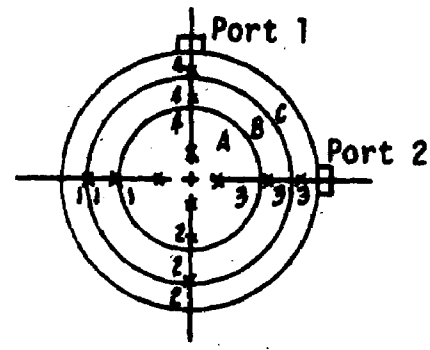

* Velocity in m/s

** Concentration must be multiplied by 0.298 to convert to ppm ethane

1 Disreguard significant figures in table

Total flow = 0.515 m^3/s (1218 ft^3/min)

Total emission = 23.66 x 10^{-6} kg/s

Figure 49a. Velocity and Concentration Distribution Data in Round Section[1]

TEST CONDITIONS:

Baffle: Inclined 22.5°

Total Flow: 0.57 m^3/s (1218 ft^3/min)

Flow Area: 0.073 m^2 (0.7854 ft^2)

No. of Fans in Series: 2

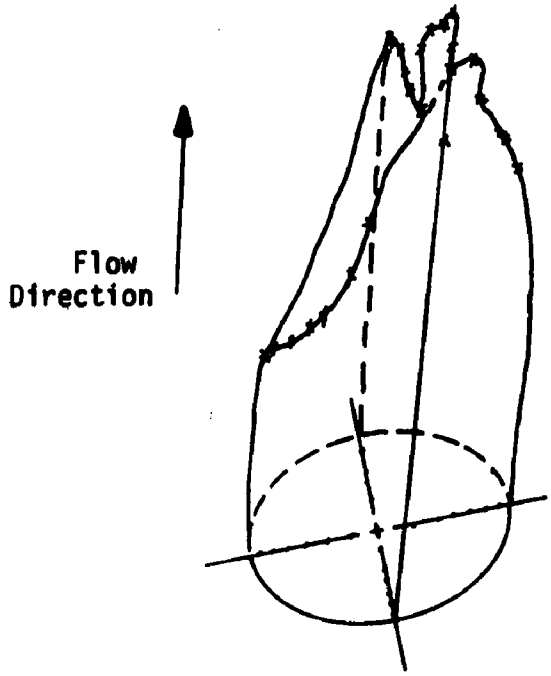

Scale: 1 cm = 1.5 m/s (5 ft/sec)

Figure 49b. Velocity Distribution in Round Section

TEST CONDITIONS:

Baffle: Inclined 22.5°

Total Flow: 0.575 m^3/s (1218 ft^3/min)

Flow Area: 0.073 m^2 (0.7854 ft^2)

Ethane Flow Rate: 16.2 x 10^{-6} m^3/s (0.97 ft/min)

No. of Fans in Series: 2

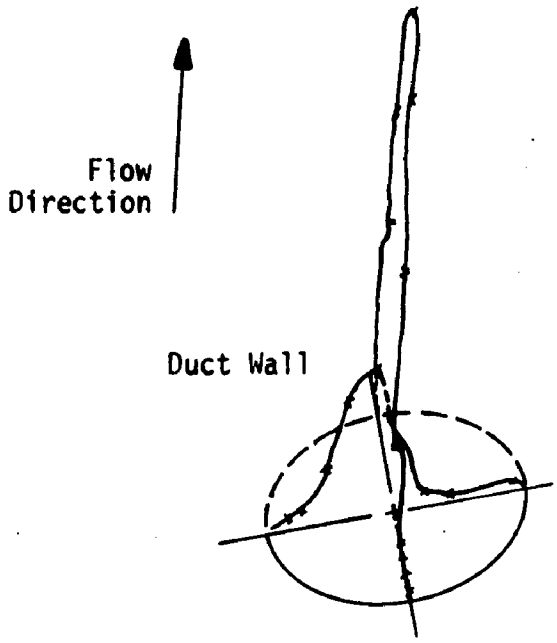

Scale: 1 cm = ~ 35 ppm

Figure 49c. Concentration Distribution of Ethane in Round Section

TEST NO. 9-3

Conditions: Baffle: Inclined 22.5° to horizontal
Ethane Flow Rate = 0.97 ℓ/min = 20.23 x 10^{-6} kg/s
Temperature 20°C
Flow Area 0.073 m^2 (0.7854 ft^2)
No. of Fans in Series = 2

		1	2	3	4
℄A	V*	7.5	9.8	8.6	℄8.1-7.1
	C**	50	3	25	℄50-270
A	V	7.4	10.7	8.6	6.6
	C	30	0	10	750
A-B	V	7.7	11.1	8.1	6.3
	C	7	0	2	870
B	V	8.3	11.1	7.9	6.2
	C	2	0	2	650
B-C	V	8.1	11.3	8.0	6.3
	C	0	0	1	370
C	V	7.6	10.6	8.2	6.2
	C	0	0	0	150

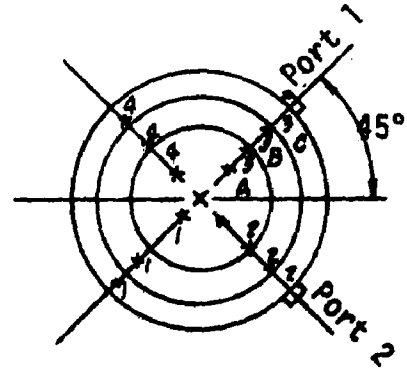

* Velocity in m/s

** Concentration must be multiplied by 0.298 to convert to ppm ethane

1 Disregard significant figures in table

Total flow = 0.606 m^3/s (1284 ft^3/min) using 25 points traverse
Total emission = 26.06 kg/s

Figure 50a. Velocity and Concentration Distribution Data in Round Section[1]

TEST TEST CONDITIONS:

Baffle: Inclined 22.5°

Total Flow: 0.606 m^3/s (1284 ft^3/min)

Flow Area: 0.073 m^2 (0.7854 ft^2)

No. of Fans in Series: 2

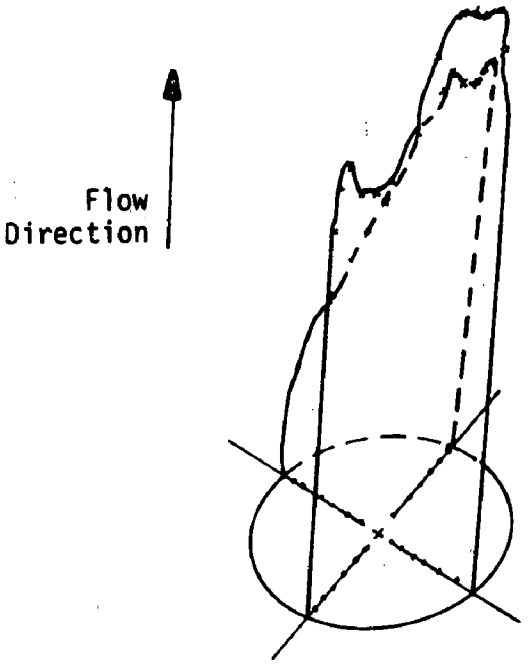

Scale: 1 cm = 1.52 m/s (5 ft/sec)

Figure 50b. Velocity Distribution in Round Section

TEST CONDITIONS:

Baffle: Inclined 22.5°

Total Flow: 0.606 m^3/s (1284 ft^3/min)

Flow Area: 0.073 m^2 (0.7854 ft^2)

Ethane Flow Rate: 16.2 x 10^{-6} m^3/s (0.97 l/min)

No. of Fans in Series: 2

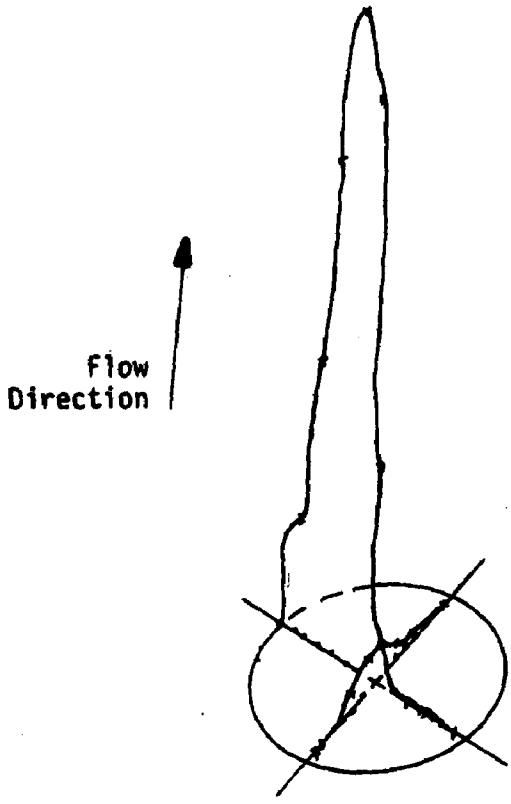

Scale: 1cm = ~ 35 ppm

Figure 50c. Concentration Distribution Of Ethane In Round Section

TEST NO. 9-4

Conditions: Baffle: inclined 22.5° to horizontal
Flow Area: 0.073 m^2 (0.7854 ft^2)
Temperature: 20°C
No. of Fans in Series = 2

Annubar reading ΔP (mm Hg)	0.49
Temperature T_{o_R}	528
$\frac{\gamma f}{0.0765 \times 520}$	0.07534
Element Constant S	0.58
Formula Used*	$Qn = \frac{585.24}{S} \times S \times \frac{1}{\sqrt{\gamma f}} \times \sqrt{\frac{\Delta P}{1.8663}}$
Total Flow at T° Qn, ft^3/min	1092
m^3/s	0.515

* $Qn = 7.897 \times S \times 0.7676 \times (11.994)^2 \times 1.0 \times 1.0 \times \frac{1}{\sqrt{\gamma f}} \times \sqrt{\frac{\Delta P(mmHg)}{1.8663}}$

Figure 51a. Average Velocity Using the Annubar Element in Round Section

TEST NO. 9-4.

Conditions: Baffle: Inclined 22.5° to horizontal
Flow Area: 0.073 m^2 (0.7854 ft^2)
Temperature: 20°C
No. of Fans in Series: 2

No. of Fans	Sample*	Velocity press. head N/m^2 (mm Hg)		Conc. of Tracer Gas**	Approx. angle of rotation of element to obtain Av. Conc.
1	Mixed	28.67	(0.215)	110	0°
	Not Mixed	28.67	(0.215)	10	0°
	Not Mixed	7.33	(0.055)	110	55° upward
	Not Sampling	8.00	(0.060	-	55° upward
2	Mixed	62.67	(0.47)	85	0°
	Not Mixed	62.67	(0.47)	10	0°
	Not Sampling	65.33	(0.49)	-	0°
	Not Mixed	32.00	(0.24)	85	45° upward
	Not Sampling	33.33	(0.25)	-	45° upward

* Sampling rate ~ 50 x 10^{-6} m^3/s (3 liters/min)

** To convert to ppm multiply by 0.298

Figure 51b. Average Velocity and Concentration Using an Annubar Element For Sampling

As shown in Figure 14b, the Annubar element was also used for sampling. When the element was not rotated, the total emission rate was about 88% lower than the real value. By rotating the element, the average concentration was obtained at an angle of approximately 45° upward, while using the two fans in series. It is significant that the value of the velocity head (in mm Hg) measured from the Annubar element was virtually unaffected by simultaneously sampling from the reference tap. This indicates that for special cases of flow and concentration profiles, this instrument can be used to obtain a representative gas sample and total flow simultaneously. However, since in all cases the Annubar was rotated to obtain the correct average concentration value (as determined by total gas flow and tracer injection rate), this approach is applicable only in cases where the profiles remain constant and the apparatus can be aligned on the basis of an independent knowledge of the correct average concentration.

Results of Test Nos. 10-1 through 10-3 are shown in Figures 52-a through Figure 54-b. A 16 point traverse was done on the square section using 3 different sampling methods. The Chebyshef method gave an average velocity approximately 2% higher than the 91 point traverse method, and an emission rate of 3% less. The Centroid of equal area method gave an average velocity of 2% less and an emission rate of 6% less. The Circular analog method gave a much higher average velocity as well as emission rate, 17% and 21% higher, respectively, than the 91 point traverse method.

Three sets of tests were run for different velocity and concentration profiles. These profiles were generated by operating one or both fans and/or changing the wind tunnel damper position. In two sets of tests, three methods of sampling were investigated in the square section: the Chebyshef method, the Centroid of Equal Area method and the Circular Analog method, for a 16 point traverse. The data from the first set of tests, Test No. 11, are shown in Figures 55a, b, and c. The emission rate as calculated from the Chebyshef method for the 16 point traverse was about 8% less than the injected amount, while the average velocity was about

TEST NO. 10-1

Conditions:
Baffle: Inclined 22.5° to horizontal
Damper: fully open
Temperature: 22°C
Flow Area: 0.18 m^2 (280 in^2)
Ethane Flow Rate: 0.97 ℓ/min = 20.096 x 10^{-6} kg/s
No. of Fans in Series: 2
Average Velocity: 3.6 m/s (11.8 ft/sec)
Emission Rate: 19.49 x 10^{-6} kg/s

	1	2	3	4
A V*	3.3	3.3	3.9	2.1
A C**	100	125	90	60
B V	3.4	3.9	4.4	4.5
B C	120	130	105	55
C V	2.2	3.8	4.4	4.8
C C	90	110	90	35
D V	1.1	4.2	4.2	4.2
D C	75	60	60	15

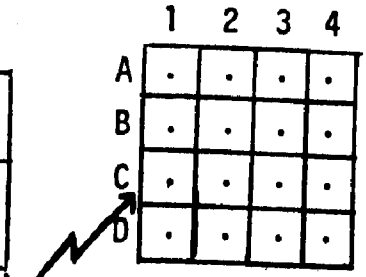

Percent Distance	Distance (m)	
10.27	0.044	(1.72")
40.72	0.173	(6.82")
59.28	0.252	(9.92")
89.73	0.382	(15.03")

* Velocity in ft/sec
** Concentration must be multiplied by 0.298 to convert to ppm

1 Disregard significant figures in Table

Figure 52a. Velocity and Concentration Distribution Data in Square Section Using the Chebyshef Method for Sixteen Point Traverse[1]

TEST CONDITIONS:

Baffle: Inclined 22.5°

Total Flow: 0.65 m^3/s (1380 ft^3/min)

Flow Area: 0.18 m^2 (280 in^2)

Average Velocity: 3.6 m/s (11.8 ft/sec)

Scale:

1 cm ~ 45.05 x 10^{-9} kg/s

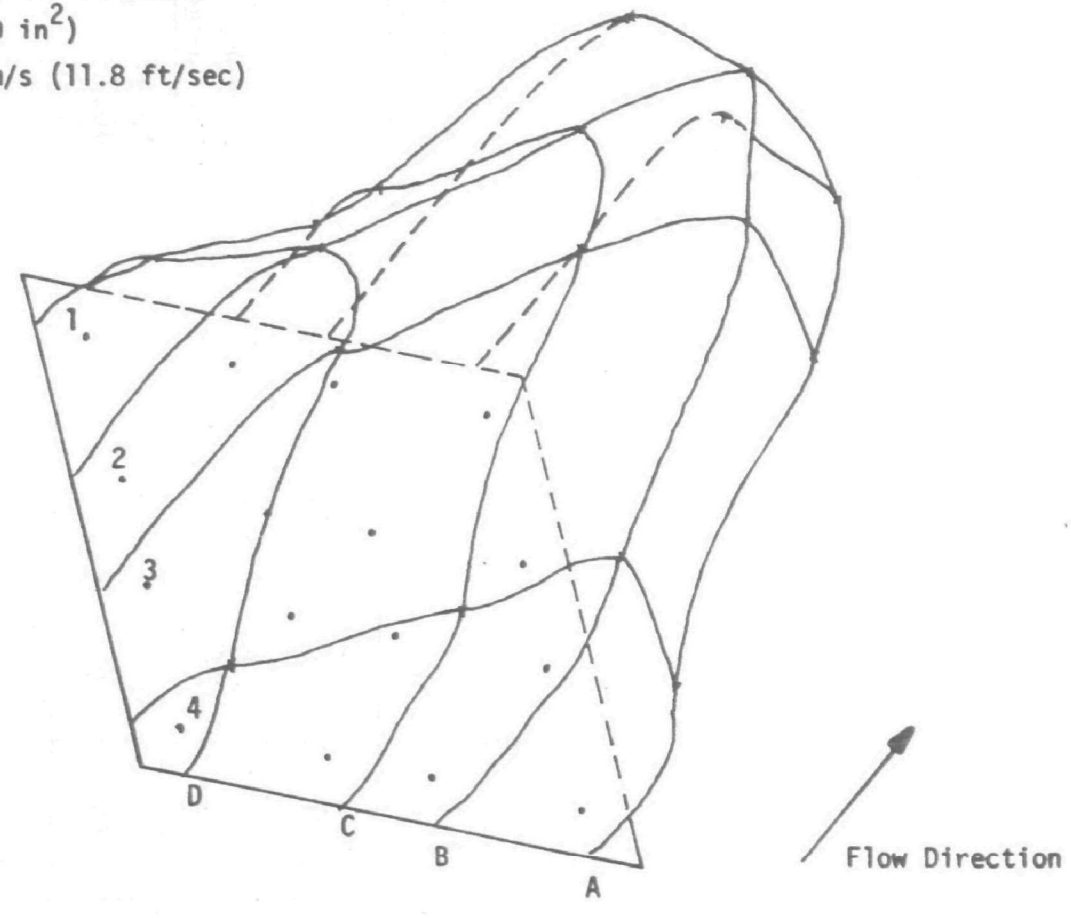

Figure 52b. Velocity * Concentration Distribution in Square Section Using the Chebyshef Method

TEST NO. 10-2

Conditions: Baffle: Inclined 22.5° to horizontal
Damper: Fully open
Temperature: 22°C
Flow Area: 0.18 m^2 (280 ft^2)
Ethane Flow Rate: 0.97 ℓ/min ≡ 20.096 x 10^{-6} kg/s
No. of Fans in Series: 2
Average Velocity: 3.5 m/s (11.40 ft/sec)
Emission Rate: 18.85 x 10^{-6} kg/s

	1	2	3	4
A V*	3.2	3.4	3.5	2.1
A C**	95	130	90	70
B V	3.2	3.5	4.1	4.1
B C	125	135	100	55
C V	1.5	3.7	4.7	4.9
C C	85	100	80	45
D V	0.7	4.1	4.3	4.6
D C	70	65	70	20

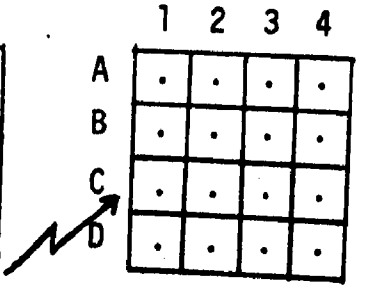

* Velocity in ft/sec
** Concentration must be multiplied by 0.298 to convert to ppm

1 Disregard significant figures in Table

Figure 53a. Velocity and Concentration Distribution Data in Square Section Using the Centroid of Equal Area Method for Sixteen Points Traverse[1]

TEST CONDITIONS:

Baffle: Inclined 22.5°

Total Flow: 0.63 m^3/s (1335 ft^3/min)

Flow Area: 0.18 m^2 (280 in^2)

Average Velocity: 3.5 m/s (11.40 ft/sec)

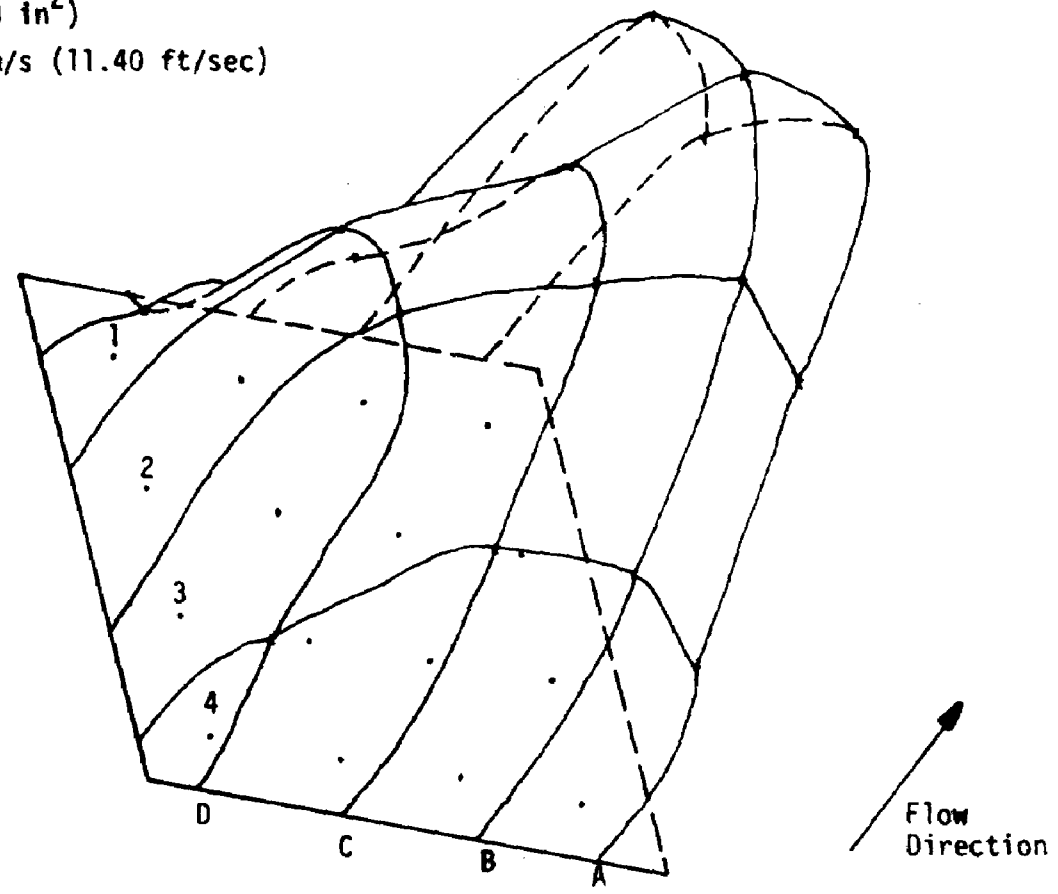

Scale:

1 cm ~ 45.05 x 10^{-9} kg/s

Figure 53b. Velocity * Concentration Distribution in Square Section Using the Centroid of Equal Area Method

TEST NO. 10-3

Conditions: Baffle: Inclined 22.5° to horizontal
Damper: Fully open
Temperature: 22°C
Flow Area: 0.18 m^2 (280 ft^2)
Ethane Flow Rate: 0.97 ℓ/min.≡ 20.096 x 10^{-6} kg/s
No. of Fans in Series: 2
Average Velocity: ~ 4 m/s (13.00 ft/sec)
Emission Rate: 24.15 x 10^{-6} kg/s

		1	2	3	4	5	6	7	8
A	V*	3.2	3.3	4.1	3.9	4.1	4.2	4.5	3.8
	C**	115	120	120	120	105	85	65	60
B	V	3.3	3.1	3.2	3.8	4.5	4.9	4.9	4.5
	C	100	110	115	120	100	75	60	30

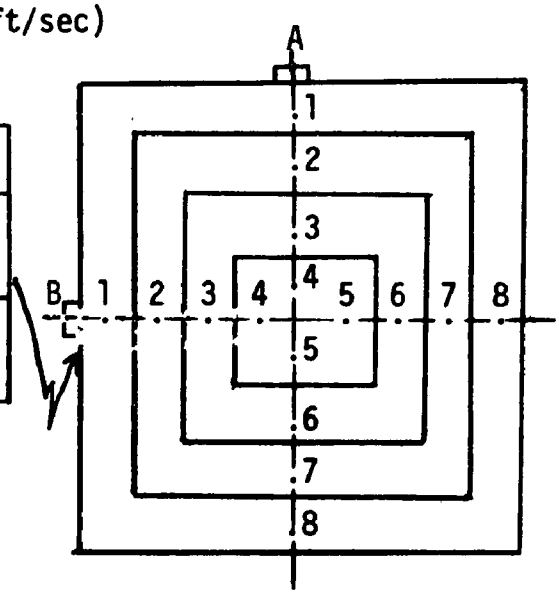

* Velocity in m/s

** Concentration must be multiplied by 0.298 to convert to ppm ethane

1 Disreguard significant figures in table

% Distance Across Duct	Distance (m)	
3.4	0.014	(0.57")
10.7	0.045	(1.80")
19.8	0.084	(3.30")
36.0	0.914	(6.00")
64.0	0.272	(10.70")
80.2	0.340	(13.40")
89.3	0.380	(14.96")
96.6	0.411	(16.20")

Figure 54a. Velocity and Concentration Distribution Data in Square Section Using the Circular Analog Method for Sixteen Points Traverse

TEST CONDITIONS:

Baffle: Inclined 22.5°

Total Flow: 0.717 m^3/s (1520 ft^3/min)

Flow Area: 0.18 m^2 (280 in^2)

Average Velocity: ~ 4 m/s (13.0 ft/sec)

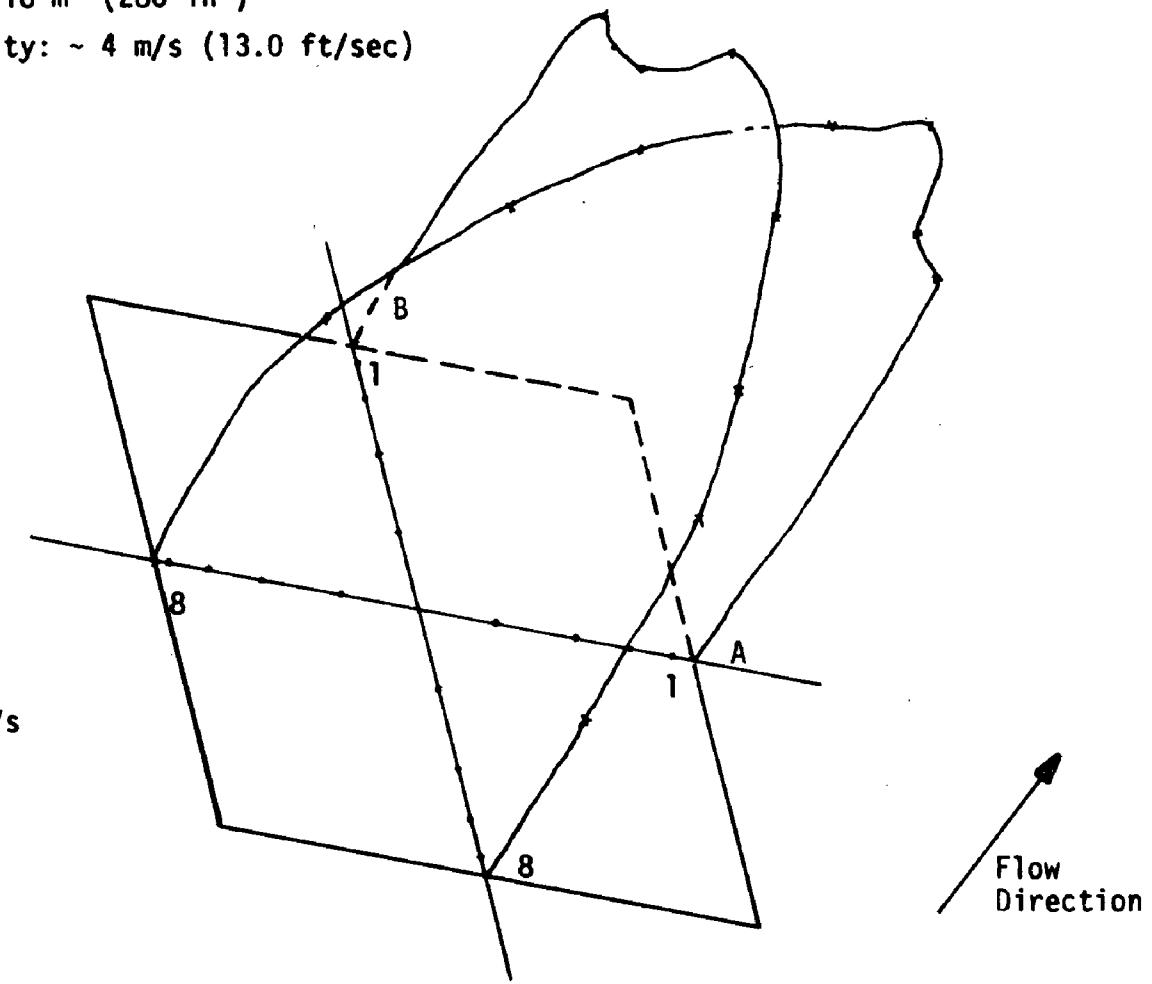

Scale:

1 cm ~ 45.05 x 10^{-9} kg/s

Figure 54b. Velocity * Concentration Distribution in Square Section Using The Circular Analog Method

TEST NO. 11-1

Conditions: Baffle: Inclined 22.5° to horizontal
Damper: Fully open
Temperature: 20°C
Flow Area: 0.18 m^2 (280 in^2)
Ethane Flow Rate: 0.97 ℓ/min ≡ 20.23 x 10^{-6} kg/s
No. of operating fans: 1
Average velocity: 2.6 m/s (8.4 ft/sec)
Emission rate: 18.57 x 10^{-6} kg/s

		1	2	3	4
A	V*	-8.3	0.0	2.9	3.3
	C**	115	145	120	105
B	V	2.3	4.1	4.5	4.3
	C	160	155	120	75
C	V	2.7	3.8	4.5	4.9
	C	170	130	85	40
D	V	3.0	4.1	2.1	2.6
	C	110	105	85	90

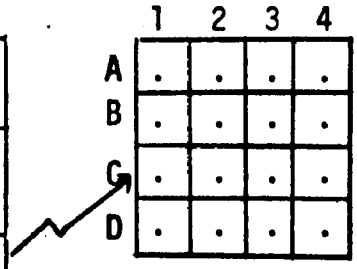

Percent Distance	D Distance (m)	
10.27	0.044	(1.72")
40.72	0.173	(6.82")
59.28	0.252	(9.92")
89.73	0.382	(15.03")

* Velocity in m/s

** Concentration must be multiplied by ~0.31 to convert to ppm

Note: expected average velocity from average concentration measurement of a mixed sample equal to 2.6 m/s (8.5 ft/sec)

Figure 55a. Velocity and Concentration Distribution Data in Square Section Using the Chebyshef Method for Sixteen Point Traverse

TEST NO. 11-2

Conditions: Baffle: Inclined 22.5° to horizontal
Damper: Fully open
Temperature: 20°C
Flow Area: 0.18 m^2 (280 in^2)
Ethane Flow Rate: 0.97 ℓ/min ≡ 20.23 x 10^{-6} kg/s
No. of Operating Fans: 1
Average Velocity: 2.6 m/s (8.5 ft/sec)
Emission Rate: 19280 x 10^{-6} gm/sec

		1	2	3	4
A	V*	-7.4	1.1	3.3	3.6
	C**	120	150	120	100
B	V	2.0	3.9	4.5	3.9
	C	155	150	105	95
C	V	2.6	3.5	4.3	4.9
	C	165	140	80	45
D	V	2.9	4.1	2.1	2.1
	C	120	115	85	100

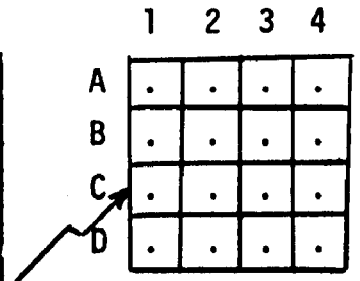

* Velocity in m/s

** Concentration must be multiplied by ~0.3 to convert to ppm

Note: expected average velocity from average concentration measurement of a mixed sample equal to 8.5 ft/sec.

Figure 55b. Velocity and Concentration Distribution Data in Square Section Using the Centroid of Equal Area Method for Sixteen Points Traverse

TEST NO. 11-3

Conditions: Baffle: Inclined 22.5° to horizontal
Damper: Fully open
Temperature: 20°C
Flow Area: 0.18 m^2 (280 in^2)
Ethane Flow Rate: 0.97 ℓ/min ≡ 20.23 x 10^{-6} kg/s
No. of Operating Fans: 1
Average Velocity: 3.7 m/s (12.2 ft/sec)
Emission Rate: 27.03 x 10^{-6} kg/s

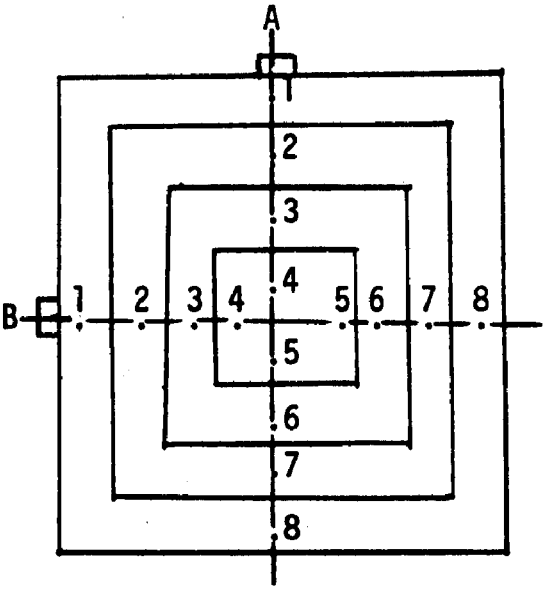

		1	2	3	4	5	6	7	8
A	V*	0.7	2.6	3.8	4.5	4.1	4.2	4.1	4.2
	C**	135	140	140	145	100	100	90	75
B	V	2.4	2.7	3.0	3.8	4.9	5.0	4.9	4.5
	C	170	170	165	150	90	65	50	35

* Velocity in m/s

** Concentration must be multiplied by ~0.30 to convert to ppm.

Note: expected average velocity from average concentration measurement of a mixed sample equal to 2.6 m/s (8.5 ft/sec)

% Distance Across Duct	Distance in Inches	
3.4	0.014	(0.57")
10.7	0.046	(1.30")
19.8	0.084	(3.30")
36.0	0.914	(6.00")
64.0	0.272	(10.7")
80.2	0.34	(13.4")
89.3	0.38	(14.96")
96.6	0.411	(16.2")

Figure 55c. Velocity and Concentration Distribution Data in Square Section Using the Circular Analog Method for Sixteen Points Traverse

the same as that calculated from the known value for the total flow through the square section. The Centroid of equal area method gave an emission rate of 5% less than the injected amount, while the average velocity was practically the same as in the provious method. By using the Circular analog method for 16 point traverse, the emission rate was found to be higher than the known value by approximately 34% and the average velocity was over-estimated by about 43%. This considerable agreement is due partially to the inadequacy of the Circular analog method in accounting for the reverse flow occurring near the corner of the square duct.

The data summarized for the second set of tests, Test No. 12, are shown in Figures 56a, b, and c. The emission rate calculated from the Chebyshef, the Centroid of equal area and the Circular analog methods differed by -42%, -32%, and +28%, respectively, with the known value of the injected tracer gas. The average velocity calculated from the Chebyshef traverse method was 65% less than the actual average velocity and 50% less when the Centroid of equal area method was used, but exceeded by 18% the actual value when the Circular analog method was used. This large discrepancy is probably due to highly reversed flow conditions in the duct.

Test No. 13 was run on the circular section with the damper partially open. A 25 point traverse, on two diameters including the center line value, was sampled, and results are given in Figure 57. The calculated emission rate was about the same as the known injection value, although the average velocity was found to be 25% less than the expected average value.

TEST NO. 12-1

Conditions: Baffle: Inclined 22.5° to horizontal
Damper: Partially open
Temperature: 20°C
Flow Area: 0.18 m^2
Ethane Flow Rate: 0.97 ℓ/min ≡ 20.23 kg/s
No. of Operating Fans: 2
Average Velocity: 1.1 m/s (3.6 ft/sec)
Emission Rate: 11.7 x 10^{-6} kg/s

		1	2	3	4
A	V*	-8.2	2.1	3.8	0.7
	C**	100	115	150	115
B	V	3.6	4.2	4.1	1.6
	C	115	140	140	80
C	V	~0.0	3.9	4.1	1.1
	C	105	130	110	40
D	V	-8.9	4.5	3.9	-2.6
	C	85	100	90	35

* Velocity in m/s
** Concentration must be multiplied by ~0.3 to convert to ppm

Note: expected average velocity from average concentration measurement of a mixed sample equal to 7.6 m/s (25 ft/sec)

Figure 56a. Velocity and Concentration Distribution Data in Square Section Using the Chebyshef Method for Sixteen Point Traverse

TEST NO. 12-2

Conditions: Baffle: Inclined 22.5° to horizontal
Damper: Partially open
Temperature: 20°C
Flow Area: 0.18 m^2 (280 in^2)
Ethane Flow Rate: 0.97 ℓ/min ≡ 20.23 x 10^{-6} kg/s
No. of Operating Fans: 2
Average Velocity: 1.6 ms/ (5.3 ft/sec)
Emission Rate: 13.78 x 10^{-6} kg/s

		1	2	3	4
A	V*	-5.8	2.1	3.6	0.9
	C**	100	115	155	130
B	V	3.9	4.1	4.1	1.6
	C	115	140	140	70
C	V	0.0	3.8	4.1	1.1
	C	105	125	100	40
D	V	-5.9	4.6	3.6	0.0
	C	85	85	95	35

* Velocity in m/s
** Concentration must be multiplied by ~ 0.3 to convert to ppm

Note: expected average velocity from average concentration measurement of a mixed sample equal to 7.6 m/s (25 ft/sec)

Figure 56b. Velocity and Concentration Distribution Data in Square Section Using the Centroid of Equal Area Method For a Sixteen Point Traverse

TEST NO. 12-3

Conditions: Baffle: Inclined 22.5° to horizontal
Damper: Partially open
Temperature: 20°C
Flow Area: 0.18 m^2 (280 in^2)
Ethane Flow Rate: 0.97 ℓ/min ≡ 20.23 x 10^{-6} kg/s
No. of Operating Fans: 1
Average Velocity: 3.6 m/s (11.8 ft/sec)
Emission Rate: 25.92 x 10^{-6} kg/s

		1	2	3	4	5	6	7	8
A	V*	3.5	3.3	3.9	4.3	4.0	3.9	3.9	4.1
	C**	150	120	140	145	120	110	105	80
B	V	0.4	2.3	3.6	4.1	4.3	4.3	3.9	3.6
	C	115	110	120	135	120	85	40	35

* Velocity in m/s
** Concentration must be multiplied by ~ 0.3 to convert to ppm

Note: expected average velocity from average concentration measurement of a mixed sample equal to 7.6 m/s (25 ft/sec)

Figure 56c. Velocity and Concentration Distribution Data in Square Section Using the Circular Analog Method for Sixteen Points Traverse

TEST NO. 13

Conditions: Baffle: Inclined 22.5° to horizontal
Damper: Partially open
Temperature 20°C
Flow Area: 0.073 m^2 (0.7854 ft^2)
Ethane Flow Rate[a]: 0.97 ℓ/min ≡20.23 x 10^{-6} kg/s
No. of Operating Fans: 2
Average Velocity: 5.9 m/s (19.4 ft/sec)
Total Emission: 20.46 x 10^{-6} kg/s

		1	2	3	4
℄-A	V*	℄4.9-4.1	7.0	5.8	4.3
	C**	℄235-225	210	235	220
A	V	3.6	8.0	6.6	3.8
	C	210	120	210	190
A-B	V	4.1	8.9	7.3	3.8
	C	195	55	145	155
B	V	4.7	9.7	7.4	3.8
	C	165	15	85	130
B-C	V	5.1	9.4	7.4	3.8
	C	150	5	40	115
C	V	5.2	8.3	7.0	3.6
	C	135	5	20	105

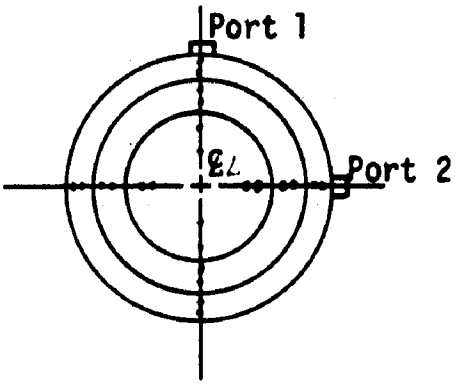

a injection port was changed to previous the honeycomb section

* Velocity in m/s

** Concentration must be multiplied by 0.32 to convert to ppm ethane

Figure 57. Velocity and Concentration Distribution Data in Round Section

c. Results and Conclusions

Different sampling methods were investigated in Test Nos. 2 through 13. These included: sampling from the round and the square section and the annubar at low airflow rate; sampling with proportional time; directional sampling in the round section; directional sampling from the Annubar element; and sampling from the square section using the 16 point traverse by the use of either the Chebyshef method, the Centroid of equal area method, or the Circular analog method. The calculated flow from traversing both the square and circular sections as well as from using the Annubar element closely agreed when the average velocity was low. A good estimate of the emission rate was also obtained from both round and square sections at lower flow rates. When sampling time from different locations was proportioned to the local air velocity in Test Nos. 7 and 8, a good agreement in emission rate was obtained compared to the calculated emission rate using velocity and concentration measurement from each location.

The proportional time method has potential application in non-reverse stratified gas flow when a true total emission rate is desired. The application of a continuous automatic method for proportional sampling is also possible by automating the above procedure.

The most recent results (at higher air flow rate), obtained from traversing the square and circular sections, showed a good agreement between the calculated air flow from each section only when the traversing ports of the round section were rotated by an angle of about 45°. These results demonstrate the inability of the perpendicular (2 diameters) traverse method to account for certain velocity profiles with azimuthal dependence. By rotating the traversing scheme, a more accurate flow rate may be obtained. This indicates that a knowledge of the flow and emission profiles is helpful in selecting the optimum orientation of the sampling diameters.

The total emission rate obtained from the square section using the 91 point traverse was very close (~1%) to the real value (no reverse flow existed in this section). This is in accord with the intuitive notion that the error should decrease with an increase in the number of samples.

The emission rate calculated from the circular section in Test No. 9 differed substantially from the known injected value. Because the average velocity was increased about three fold using the two fans in series, the lateral diffusion of the tracer gas was limited by reduced residence time and only a high concentration spike was obtained. This spike-like profile slipped through the sampling mesh; hence, traversing methods did not lead to the correct answer. It is significant to note that by comparing the velocity and concentration profiles one could see a greater diffusion of tracer gas in areas where the velocity was lower. When the tracer gas injection port and the injection tube in the circular section were modified (Test No. 14), less stratification occurred and the emission rate agreed closely with the known value. However, in this test, the calculated air flow differed considerably (-25%) from the known value. This implies that the traversing procedure was adequate only for the combined velocity and concentration profiles. Thus, without a previous knowledge of the velocity and concentration profiles, the actual value of the emission rate as well as total flow can only be assured by a minimum of traverses along 4 diameters, 45° apart, with at least 8 sampling points/diameter.

Results from the 'Annubar Element' tests showed a substantial error in the flow rate measurement in one test and good agreement in another test, but in all cases showed a much larger error than that observed in the circular section traverse runs. The Annubar element was observed to give the average concentration only when rotated, which shows the inability of this element to measure the flow and average concentration when interpolation occurs in a line where no average velocity or concentration

exists. It is suggested that perpendicularly positioned 'Annubars' could be used for better results, which would increase the probability of obtaining a reliable answer. Also, in high air flows, i.e., 3.3 m/s (11 ft/sec), the Annubar could be used simultaneously for sample extraction and as a flow sensor.

The average velocity and total emission rate, calculated from the Chebyshef and Centroid of equal area methods for two sets of tests using only 16 points for traversing in the square section, were very close to the values obtained from the 91 point traverse method. When a highly reversed flow was generated (Test No. 12), both methods failed to give the actual value of the emission rate or the total air flow; instead, a much lower value was given. In contrast, the Circular analog method for the square section using 16 traverse points gave a much higher average velocity and emission rate in all cases. The latter method is expected to give larger errors in cases where no average emission rate exists in the 2 perpendicular traversing planes. Therefore, it is recommended that one use either the Chebyshef or the Centroid of equal area method for a 16 point traverse in cases where highly reversed flow is not present. For reverse flow conditions, a much higher number of sampling points is recommended (see Table 17).

TABLE 17.

VARIATION OF PERCENT ERROR IN EMISSION RATE AND TOTAL FLOW
AS CALCULATED FROM DIFFERENT TRAVERSING TECHNIQUES USED IN THE SQUARE SECTION

Test No.	No. of Fans In Operation	Damper Position	No. of Traversing Points	% ERROR*						Flow Condition
				Centroid of Equal Area		Chebyshef		Circular Analog		
				Emission	Av. Velocity	Emission	Av. Velocity	Emission	Av. Velocity	
9-1	2	fully open	91	1.9						no reverse
9-1	2	fully open	49	<1	<1					no reverse
10	2	fully open	16	-6	-2	-3	2	21	17	no reverse
11	1	fully open	16	-5	<1	-8	<1	34	43	reverse
1212	2	partially open	16	-32	-50	-42	-65	28	18	highly reverse

* within ±3% reproduceability

TEST CONDITIONS:

Baffle: Inclined 22.5° horizontal

Ethane Flow Rate: 0.97 l/min = 2023 x 10^{-6} kg/s

Flow area: 0.18 m^2 (280 in^2)

Temperature: 20°C

C. TASK III - FIELD DEMONSTRATION

Boston Edison's Mystic Station power plant was the site of field experiments during the final task of this program. Three locations in the plant duct work were first considered in an attempt to find gas stratification: the after air preheater ducts, the after precipitator duct, and the inlet ducts to the scrubber of Unit No. 6. Table 1 summarizes the conditions of these locations.

The air preheater outlet ducts and the south inlet duct to the scrubber were surveyed. Because air in leakage was likely to occur in the air preheaters, gas stratification was found in a preliminary survey at the air preheater outlet ducts. The demonstration test was therefore run at this location.

The sampling train, sampling procedures and results for both the preliminary survey and final demonstration test are discussed below.

1. SAMPLING SYSTEM AND CALCULATION PROCEDURES

a. Sampling System Arrangement

The sampling system was prepared according to the schematic arrangement shown in Figure 1-a through 1-d.

S-type pitot tubes heads (about 0.3 m (1') long), sampling probes and dust filters were constructed of 316 stainless steel. Extensions were provided so that probes and pitot tube lengths could be varied from 2.13 m (7') to 3.66 m (12') according to the sample location requirement. Because of subsequent delays in delivery of stainless steel tubes for S-Pitot tubes, extensions were made of hard copper 0.057 m O.D. (3/16" O.D.). The connections of the sample line to the probe tube as well as manometer outlet lines to the S-pitot tube were all Swagelock quick disconnects. This arrangement simplified and expedited the sampling procedure from different probe sets since only one sampling train were available.

TABLE 1

	Air Preheater Outlet Duct	Electrostatic Precipitator Outlet Duct	Scrubber Inlet Duct
No. of Ducts	2	1	2
No. of Ports/Duct	3	12	5
Diameter of Port	0.076 m (3")	0.076 m (3")	0.12 m (4")
Ports Location	nearly centroid of equal area locations	symmetrically located on both sides of the duct	centroid of equal area locations
Duct Dimensions [width x heighth]	3.1m x 3.3m (10'4" x 11')	14.8m x 5.1m (48'6" x 16'8")	2.1m x 3.7m (7' x 12')
Ports Elevation From Ground Level	3m (10')	13.1m (43')	24m (~80')
Duct Location	Indoors	Outdoors	Outdoors
Pressure	Negative	Negative	Positive

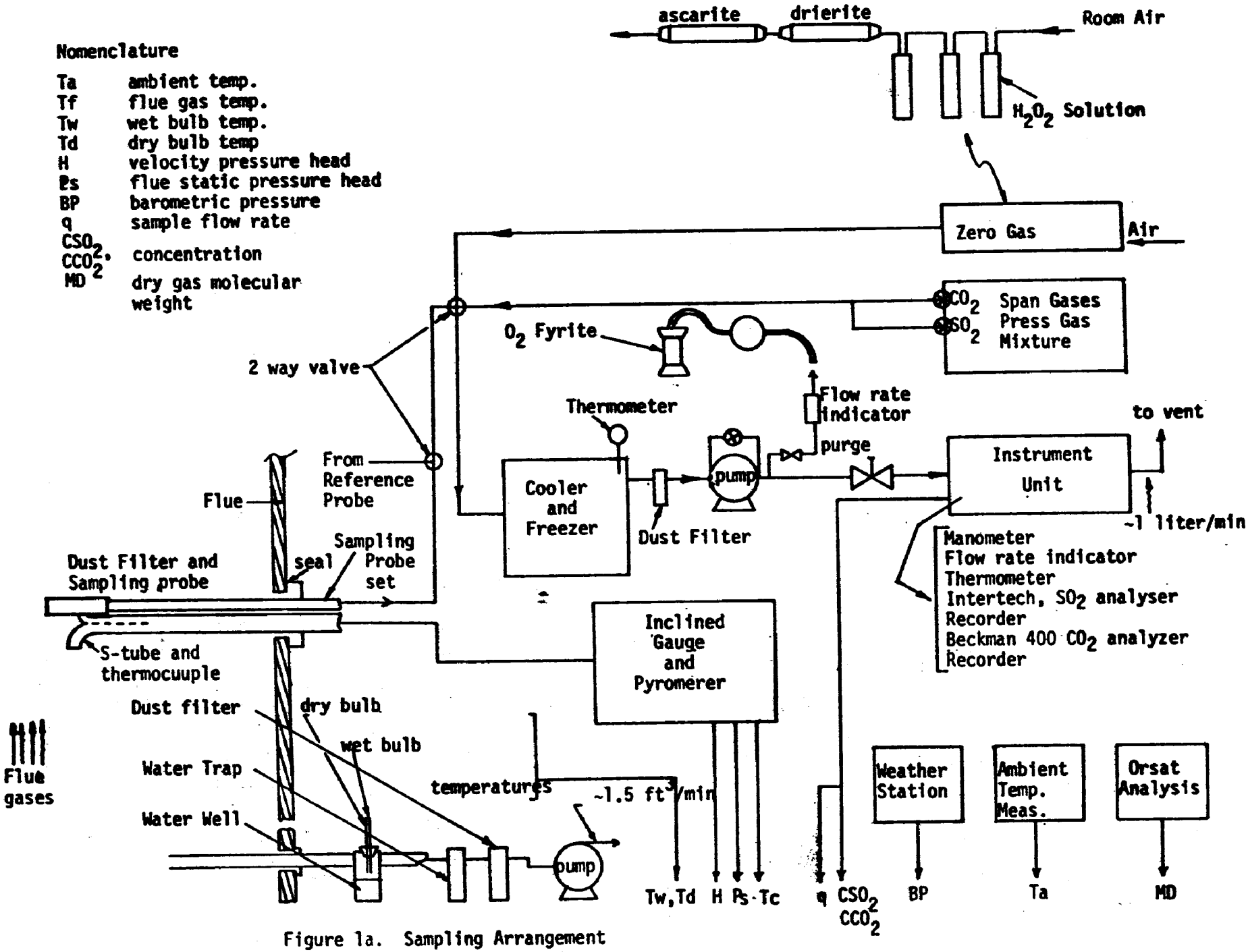

Figure 1a. Sampling Arrangement

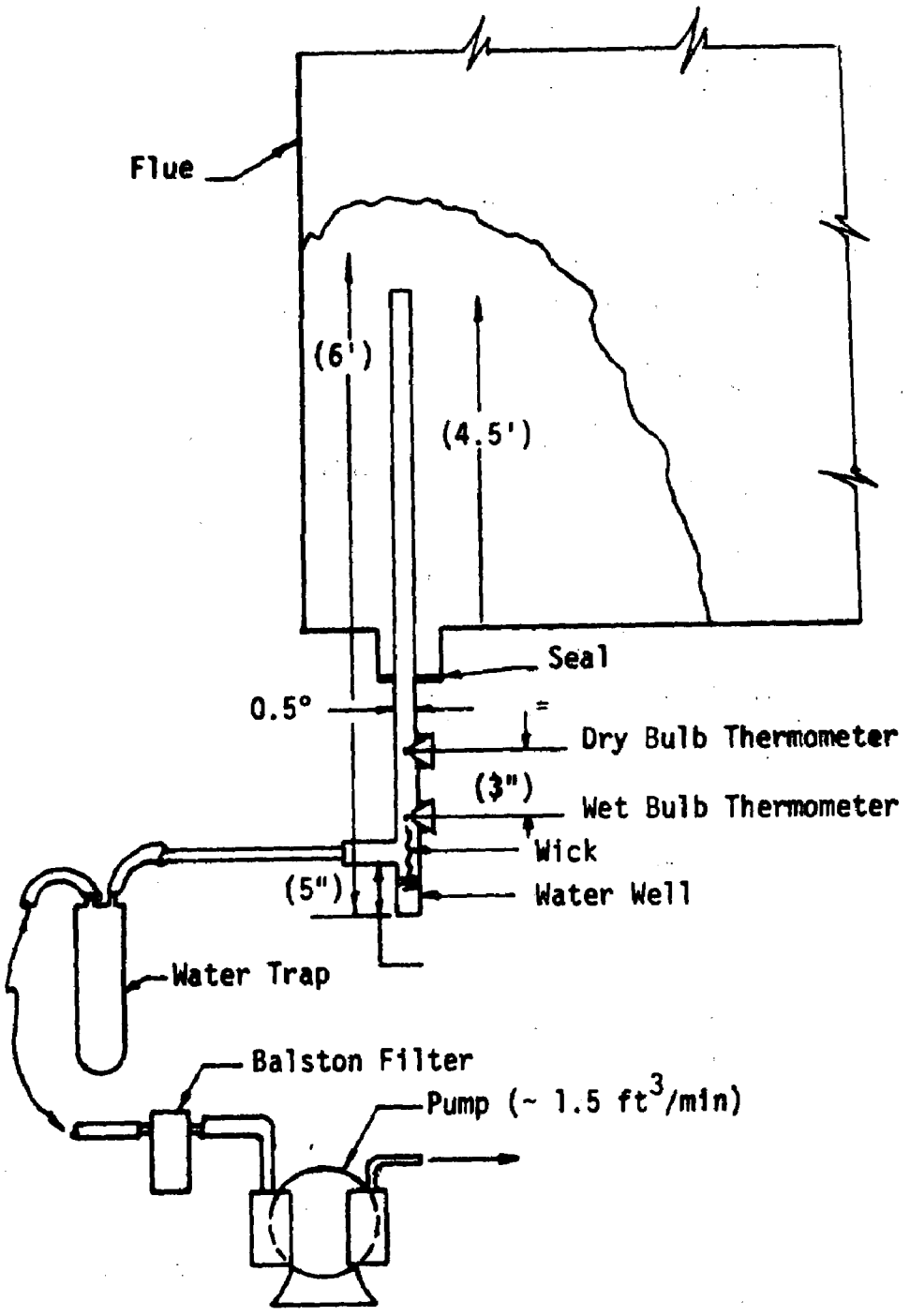

Figure 1b. Humidity Test Arrangement

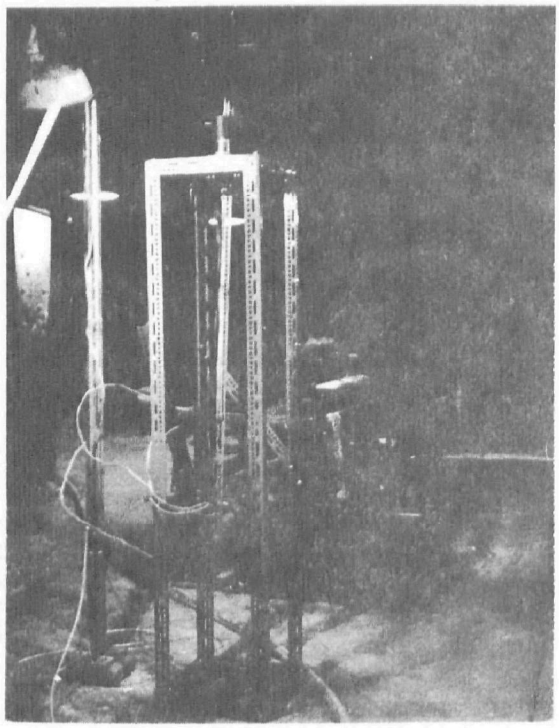

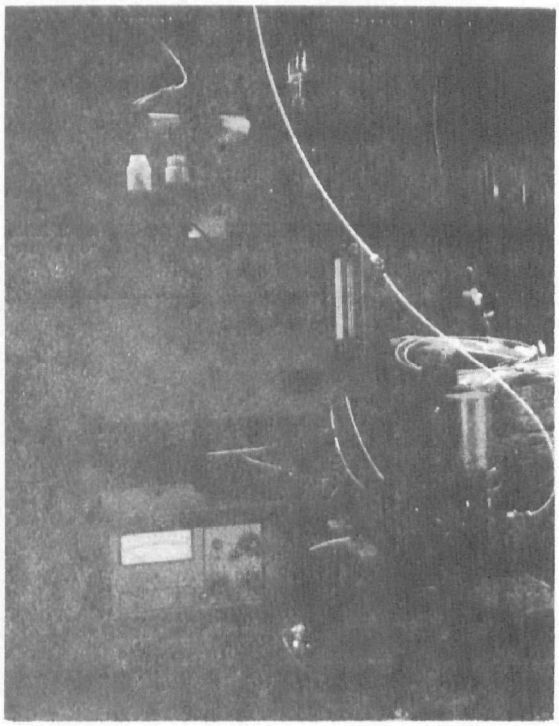

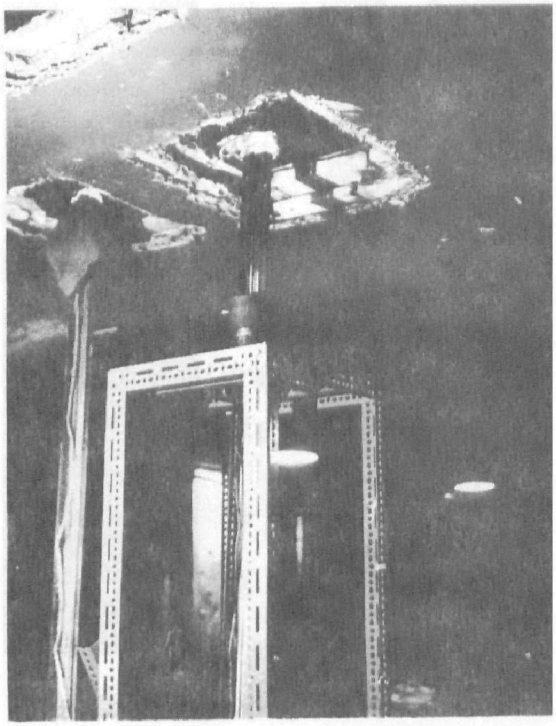

Figure 1c.

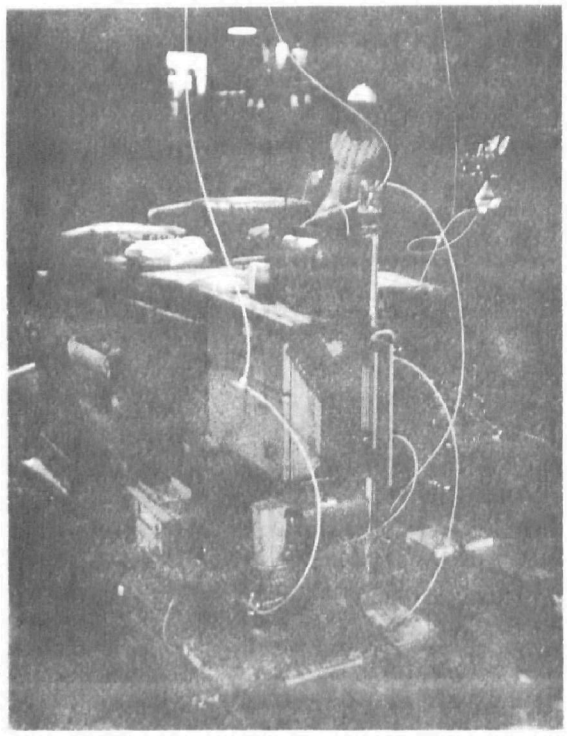

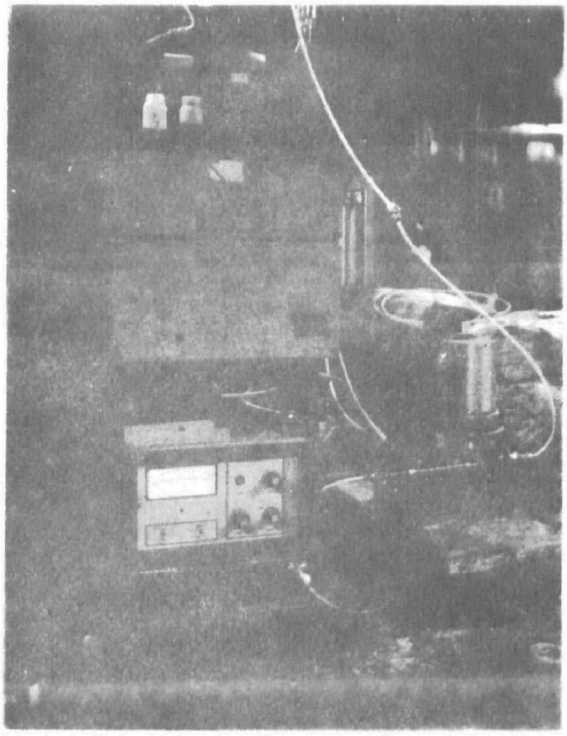

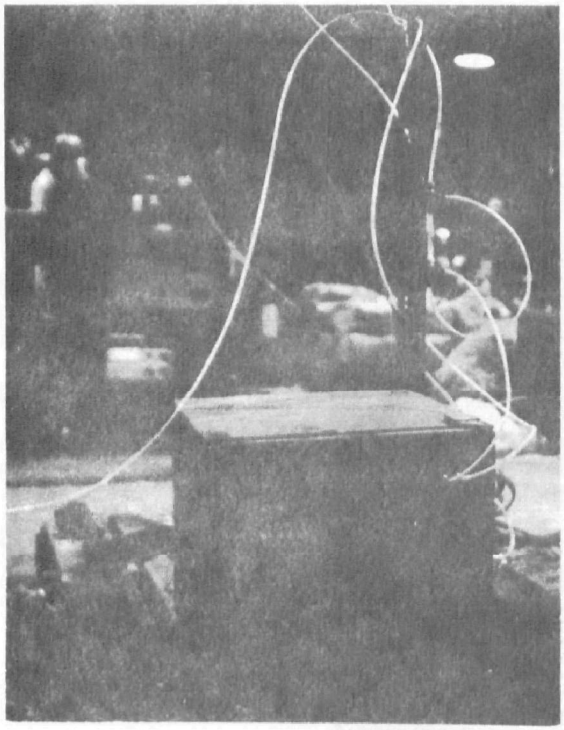

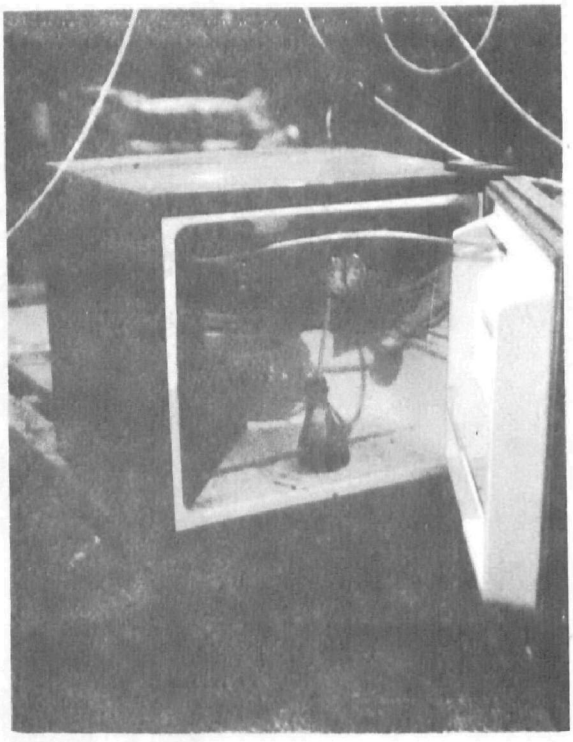

Figure 1-d

All thermocouples were made of iron/constantin wires. To keep the wires resistant to a maximum of 2.2 ohms (maximum calibration setting for pyrometer), 6 m (~20') of 14 gage insulated wire was used to fabricate each thermocouple. For each thermocouple, the hot junction was silver soldered, then covered lightly with Teflon tape and finally shielded with stainless steel tube (about 0.3 m (1') of the thermocouple wire was shielded). An Alnor pyrometer was used to read the flue gas temperature.

A refrigerator of 0.043 m^3 capacity (~1.5 ft^3) was used to cool the sample prior to analysis. Two small holes were drilled in the refrigerator door for the inlet and outlet flue gas lines. The flue gas sampling line in the refrigerator was made of approximately 1.8 m (6') of stainless steel (1/4" tube) followed by 6 m (~20') of poly-flo tube (1/4"). This line was shaped in a large coil form and was reinforced in position with 2 steel Dexxion angle irons. The water vapor and other condensables were trapped in a 250 x 10^{-6} m^3 (250 cc) Pyrex vial introduced into the refrigerator. The temperature inside the refrigerator was kept near freezing (~3°C). The freezer section was used to remove most of the remaining moisture content of the sampled flue gas stream in a plastic trap. All connections were perfectly sealed.

Specifications for the major pieces of equipment are given in Table 2.

The percent moisture was calculated from wet and dry bulb temperatures measured by a separate sampling train, as shown in Figure 1-b.

The pressure in the line near the flow meter and the measuring instruments for CO_2 and SO_2 gases were kept nearly atmospheric by using a short vent line opened to atmosphere (the CO_2 analyzer was followed by the SO_2 analyzer).

TABLE 2

MAJOR EQUIPMENTS SPECIFICATION

Equipment	Specification and Manufacturer
Dwyer gage	Model 400, Dwyers
SO_2 Gas Analyzer	Infra Red, Uras 2, Intertech Co.
CO_2 Gas Analyzer	Infra Red, Beckman Model No. 864, Beckman Instruments, Inc.
O_2 Fyrite	Bachareh Industrial Instrument Co., Pittsburgh, Pa.
Refrigerator	(1.5 ft^3) Sears Cat. No. 3467370N, Sears Roebuck and Co.
Pyrometer	Alnor No. 1500, Alnor Instruments
Pump	Flue Gas Pump No. T-5 (prototype), Metal Bellows Corp., Sharon, Mass.
Dust Filter	Balston Filter 95-S, Balston Inc., Lexington, Mass.
Filter Element	Filter tube Grade A, Balston Inc., Lexington, Mass.

Sufficient sample line was used from the refrigerator to the analyzers, and the temperature of the sample gas equilibrated to room temperature. In all sampling cases, the same flow rate (~2 liters/min) was maintained; about 16.6 x 10^{-6} m^3/s (1 liter/min) only went to the analyzers; the remainder was purged. The purge line was provided to increase the response time of the system by rapidly flushing the lines ahead of the pump. It was also used for the Fyrite analysis of O_2 in the gas sample.

Chart recorders (Texas Instruments Inc.) were provided for each analyzer for recording data on a continuous basis.

b. Calculation Procedures

The method used for calculating the emission rates from traverses is outlined in the flow sheet shown in Figure 2. The data sheet used in data collection is shown in Figure 3.

2. PRELIMINARY SURVEY TESTS

The following is a discussion of preliminary survey tests conducted on the exhaust ducts of Unit No. 6 at the Mystic Station. During the preliminary survey, the outlet ducts of the air preheaters (See Figure 4) and the south inlet duct to the scrubber were examined for gas stratification. Oxygen and carbon dioxide were sampled at different locations in the ducts and analyzed by Fyrites.

Oxygen and carbon dioxide stratification was found in the air preheater outlet duct (north side), while no stratification was found at the scrubber's inlet duct. On the basis of this evidence, it was decided to survey both outlet air preheater ducts for SO_2, CO_2 (NDIR) and velocity.

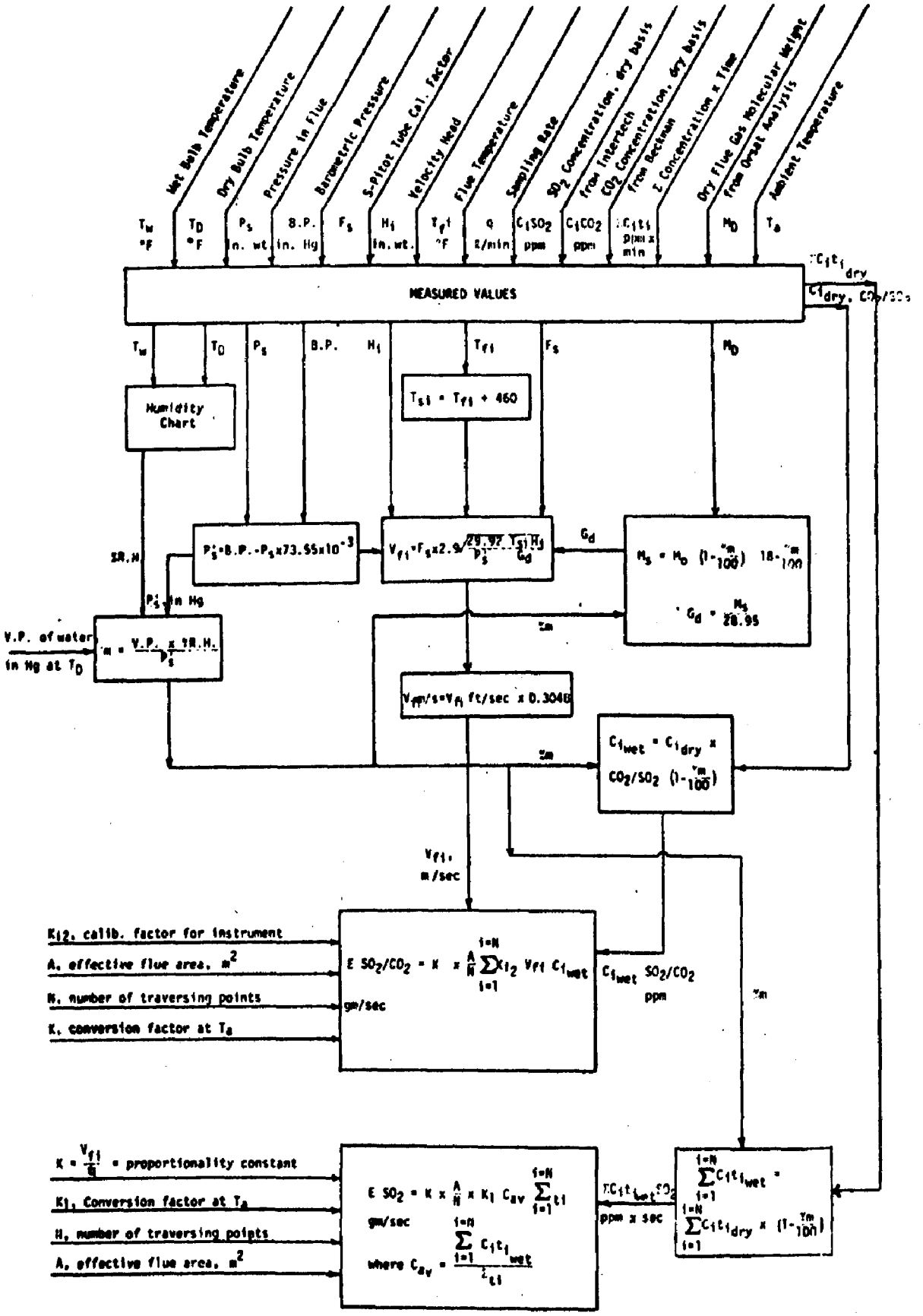

Figure 2. Emission Rate Calculation Procedure

Figure 3

TEST UNIT _____ STATION _____

TEST NUMBER _____ DATE _____

TEST LOAD _____

	PORT _____								PORT _____							
Position	T °C	Vh	Vel	FR	O_2	CO_2	SO_2	Time	T °C	Vh	Vel	FR	O_2	CO_2	SO_2	Time

WET BULB TEMP _____ DRY BULB TEMP

AMBIENT AIR TEMP _____ °F

AVERAGE F.G. TEMP _____ °F

AVERAGE STATIC PRESS. _____ IN. WATER

AVERAGE VELOCITY _____ F.P.S.

BAROMETRIC PRESS. _____ IN. Hg

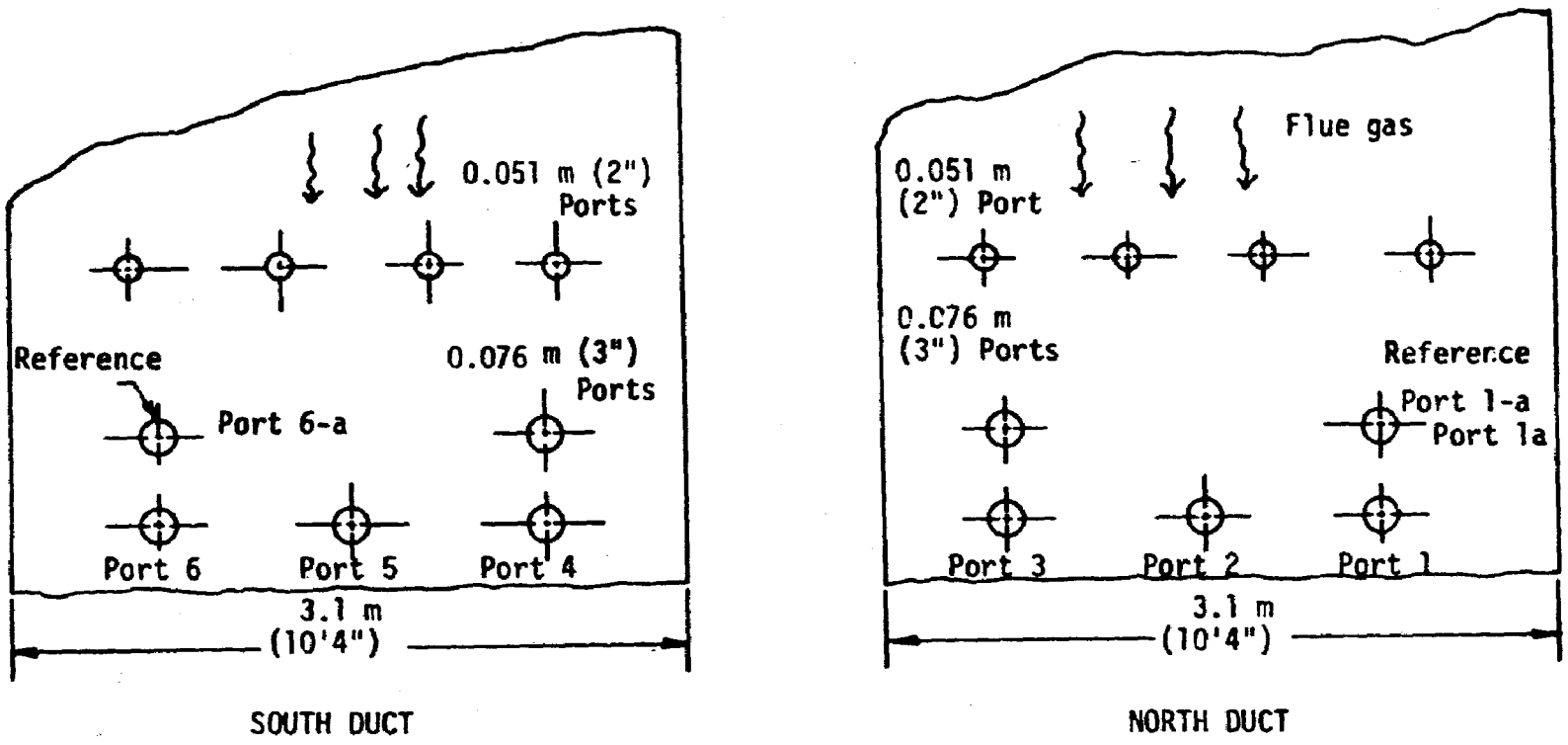

Figure 4. After Air Preheaters Ducts - Plan View

a. Sampling Procedure

The sampling train described in the previous section was used in these tests.

The after air preheater ducts were surveyed using one sampling probe set which kept the reference probe set at a constant position. Because the location was "indoors" a heated sampling tube was not required to prevent freezing.

Since the 0.076 m (3") dia. ports were less than 2.7 m (9 feet) above floor level, some difficulty was encountered in introducing a longer length probe. A 0.9 m (3 foot) extension was used with a 2.7 m (9 foot) probe to sample at locations 2.4 m (8 feet) and 3.0 m (10 feet) inslide the ducts. This extra length was connected after the 2.7 (9 foot) probe was introduced about 1.2 m (4 feet) inside the duct.

To assure a vertically straight probe assembly in the duct, the sampling tube, the S-tube and the thermocouple were secured firmly to a Dexxion No. 225-S angle iron. The whole assembly was introduced into the port and fixed in position by a specially fabricated stand, as shown in Figure 1-c. A tight seal was obtained by closing the port with asbestos tape, wrapped in aluminum foil.

When sampling at the inlet duct to the scrubber, a 2.7 m (9 foot) stainless steel tube (1/4" O.D.) was used to collect the gas sample. A Dexxion steel angle iron was used to give horizontal support to the sampling tube. A 2.7 m (9 foot) extension was provided for both the sampling tube and the steel support and an asbestos rag sealed the port. O_2 and CO_2 analyses of the gas sample were performed by using the Fyrites.

b. Results

Test results from surveying the south inlet duct to the scrubber did not show any gas stratification (see Figure 5).

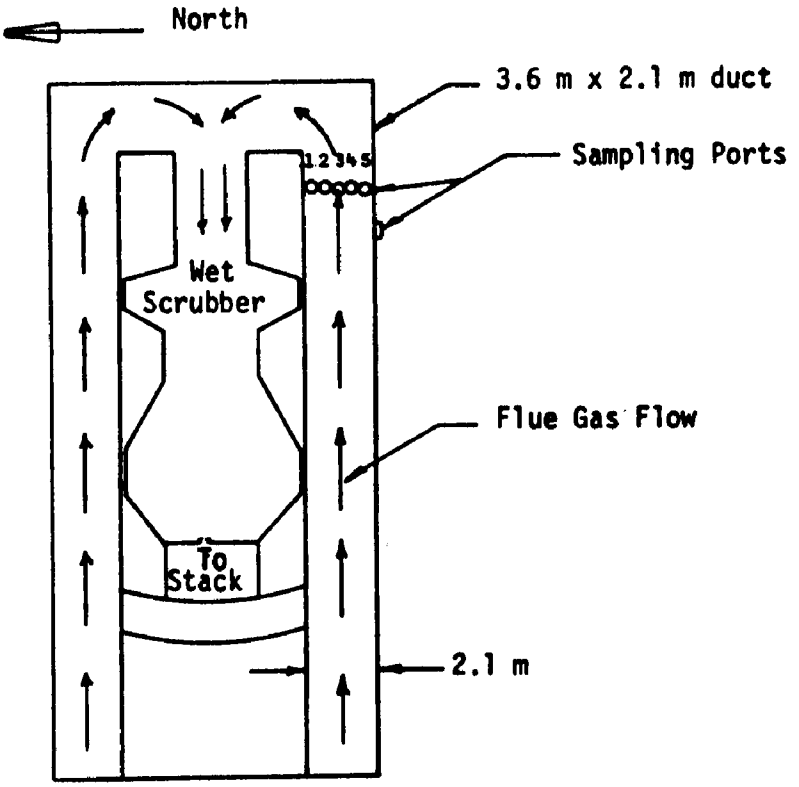

Test Run Using Fyrites For CO_2 and O_2 Content

Port 4 (m) x 10^{-1}	% CO_2	% O_2	Port 3 (m) x 10^{-1}	% CO_2	% O_2
6	11.0, 11.5	6.0	6	11, 11.5	6.5, 6.0
12	10.5, 11.0	6.5	12	11.0, 11.5	6.5, 6.0
18	11.0, 11.5	6.0	18	11.0, 11.5	6.5
24	11.0, 11.5	6.0, 6.0			
30	11.0	6.0, 6.0			

* On April 16, 1974 a constant load on the scrubber was kept as well as constant gross MW output during the testing period.

Figure 5. Results From Test Run* At The Scrubber South Inlet Duct

Port 4 was surveyed at five locations, from 0.6 m to 3 m in the duct, and Port 3 was surveyed for three locations, from 0.6 m to 1.8 m in the duct. In all cases, the percent CO_2 was equal ~11% ± 0.5% and the percent O_2 was equal ~6% + 0.5%. Since gas concentration stratification was not observed, further tests at this location were not attempted.

Test results from the preliminary survey showed gas stratification in the ductwork after the air preheaters in all cases. Results from the Fyrite tests run on the north duct are presented in Figures 6-a and 6-b. At Port No. 3 the oxygen content varied from 4.5% at 0.6 m (2 feet) to about 7.5% at 2.9 m (9.5 feet), and the CO_2 content decreased from 10.5% at 0.6 m (2 feet) to 8.5% at 2.9 m (9.5 feet).

Results from Test Nos. 3 and 4, using the NDIR analyzers for flue gas analysis, are presented in Figures 7 a through 8 d. The after air preheater duct (north side) was surveyed at 130 mw gross output. For all locations in the duct, the SO_2 concentration was sampled as well as the SO_2 concentration from a reference point. The velocity and temperature at the reference and sampling points were also measured. The reference SO_2 concentration varied ±11 ppm around a mean value of 749 ppm, while the values at the different sampling locations varied ±47 ppm around a mean value of SO_2 concentration equal to 680 ppm. The velocity in the duct ranged from as low as 8 m/s (28 ft/sec) to as high as 15 m/s (48 ft/sec). Lower values were generally obtained near the top of the duct at a probe insertion of 2.4 m (8 feet) and 3.0 m (10 feet). The SO_2 concentration times velocity term (which is proportional to the emission rate) varied ±26% about the mean value, with a lower value of 35% below the mean and the highest 43% above the mean. Temperature stratification was also observed to vary from 120°C to 155°C near the center of the duct.

Figure 6a

TEST UNIT No. 6, After Air Preheater STATION _____

TEST NUMBER 1 DATE 3/18 and 3/19, 1974

TEST LOAD ~150 MW

	PORT								PORT							
Position	T °C	Vh	Vel	FR	O_2	CO_2	SO_2	Time	T °C	Vh	Vel	FR	O_2	CO_2	SO_2	Time
0.6m (2')	130	1.0			7.5	9.0										
1.2m (4')	145	1.0			7.0	9.5										
						10.0										
1.8m (6')	140	0.9			6.5	9.5										
					7.0											
2.0m (6 3/4')	135	0.6			6.5	9.5										
						9.5										
2.4m (7 3/4')	145	0.7			6.0	9.5										
					6.5	10.0										
0.6m (2')									145	1.7			7.0	10.0		
													6.0	10.5		
1.2m (4')									145	1.7			5.0	11.0		
1.8m (6')									145	1.5			5.0	10.5		
													5.5			
2.4m (8')									140	1.4			7.0	10.0		
													6.5			
2.9m (9.5')									135	1.0			6.5	10.0		
													7.0			

WET BULB TEMP	DRY BULB TEMP
AMBIENT AIR TEMP	°F
AVERAGE F.G. TEMP	°F
AVERAGE STATIC PRESS.	IN. WATER
AVERAGE VELOCITY	F.P.S.
BAROMETRIC PRESS.	IN. Hg

Figure 6b

TEST UNIT No. 6, After Air Preheater STATION Mystic

TEST NUMBER 2 DATE 3/19/74 @ ~3:30

TEST LOAD Peak Load ~154 MW

	PORT								PORT							
Position	T °C	Vh	Vel	FR	O_2	CO_2	SO_2	Time	T °C	Vh	Vel	FR	O_2	CO_2	SO_2	Time
0.6m (2')	130	2.0			4.5	10.5										
					4.5											
1.2m (4')	150	2.0			5.0	11.0										
					5.5											
1.8m (6')	150	1.6			5.5	10.0										
					5.5											
2.4m (8')	145	0.9			6.5	8.5										
					7.0	8.5										
2.9m(9.5')	140	0.6			7.0	8.5										
					7.5											
REPEAT (AT 4:45)																
1.2m (4')	150	2.0			5.5	10.5										
					5.5											

WET BULB TEMP DRY BULB TEMP

AMBIENT AIR TEMP °F

AVERAGE F.G. TEMP °F

AVERAGE STATIC PRESS. IN. WATER

AVERAGE VELOCITY F.P.S.

BAROMETRIC PRESS. IN. Hg

Figure 7a. After Air Preheater Duct (North Side) Velocity, SO_2 Concentration and Temperature Traverse at ~ 130 MW Gross Output*

TEST NO. 3

	C_m		C_r**		$C_N = \frac{C_m}{\bar{C}_r} \times \bar{C}_r$		Ratio $R = SO_2/CO_2$	H_s	T_s	V	B.P.	P_s	$C_{N_{SO_2}} \times V$
	SO_2 (ppm)	CO_2 (%)	SO_2 (ppm)	CO_2 (%)	SO_2 (ppm)	CO_2 (%)	x 10^4	x 10^2 (N/m^2)	(°C)	(m/s)	N/m^2	N/m^2	(ppm x m/s)
PORT NO. 1			0.6 m (2') inside								103.30×10^3	2.74×10^3	
0.6m (2')	705		745		709		0.30		120	11			7,800
1.2m (4')	720		750		719		0.32		145	11			7,910
1.8m (6')	630		750		629		0.25		140	10			6,290
2.4m (8')	630		745		633		0.20		140	9			5,700
3.0m (10')	645		740		653		0.25		135	10			6,500
PORT NO. 2													
0.6m (2')	735		745		739		0.52		150	15			11,080
1.2m (4')	760		735		774		0.50		155	15			11,610
1.8m (6')	730		760		719		0.38		150	12			8,630
2.4m (8')	675		750		674		0.32		145	12			8,090
3.0m (10')	645		750		644		0.23		140	10			6,440
PORT NO. 3													
0.6m (2')	705		735		718		0.47		125	14			10,050
1.2m (4')	705		735		718		0.44		140	14			10,050
1.8m (6')	690		765		675		0.37		145	12			8,100
2.4m (8')	615		765		602		0.18		140	8			4,820
3.0m (10')	615		765		602		0.20		135	9			5,420
σ std. dev.	47		11		52				3	1.8			2,080
$\bar{V}$, $\bar{C}$ or $\bar{T}_{mean}$	680		749		680				140	12			7,900

* Preliminary survey at the Mystic Station power plant on March 25, 1974, Unit No. 6
** Tr = 130°C; Hr ~ 0.8×10^2 N/m^2

Figure 7b. After Air Preheater North Duct Velocity, SO_2 Concentration and Temperature Profile* At ~ 130 MW Gross Output

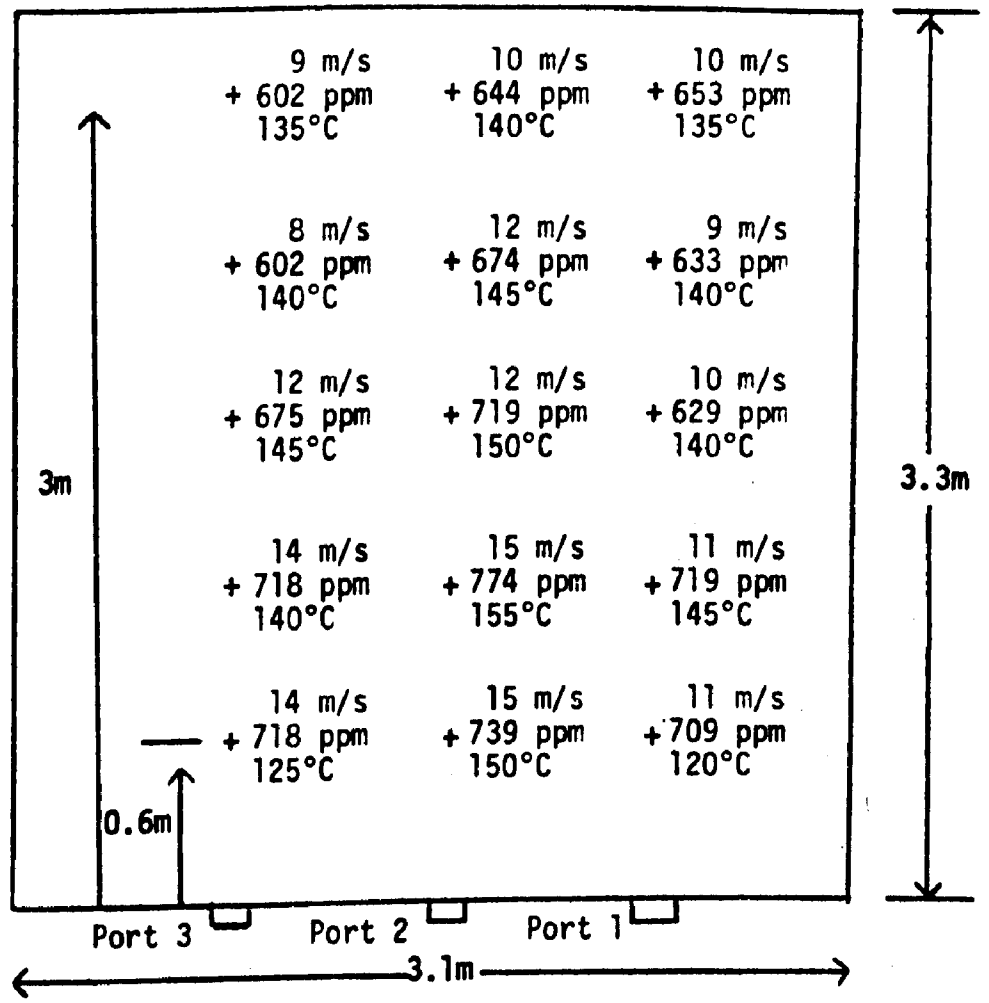

* from preliminary survey

Figure 8a. After Air Preheater Duct (South Side) Velocity, SO_2 and CO_2 Concentration and Temperature Traverse At ~ 150 MW Gross Output*

TEST NO. 4

	C_m		C_r**		$C_N = \frac{C_m}{C_r} \times C_r$		Ratio $R = SO_2/CO_2$	H_s	T_s	V	B.P.	P_s	$C_{N_{SO_2}} \times V$
	SO_2 (ppm)	CO_2 (%)	SO_2 (ppm)	CO_2 (%)	SO_2 (ppm)	CO_2 (%)	$\times 10^4$	$\times 10^2$ (N/m^2)	(°C)	(m/s)	N/m^2	N/m^2	(ppm x m/s)
PORT NO. 4			0.6 m (2') inside								101.9×10^3	3.1×10^3	
0.6m (2')	900	12.3	855	11.3	908	12.3	73.8	1.5	125	15			13,620
1.2m (4')	850	11.8	870	11.3	843	11.8	71.4	1.5	125	15			12,650
1.8m (6')	825	11.3	840	11.4	848	11.4	74.4	1.2	130	14			11,870
2.4 (8')	810	10.8	870	11.3	803	10.8	74.3	1.0	130	13			10,440
3.0m (10')	810	10.8	870	11.3	803	10.8	74.3	0.7	130	11			8,830
PORT NO. 5													
0.6m (2')	910	12.6	855	11.3	918	12.6	72.8	1.8	130	17			15,610
1.2m (4')	915	12.6	865	11.3	913	12.6	72.5	1.8	140	17			15,520
1.8m (6')	855	11.7	870	11.3	848	11.7	72.5	1.7	130	17			14,420
2.4m (8')	855	11.3	870	11.3	848	11.3	75.0	1.5	130	15			12,720
3.0m (10')													
PORT NO. 6													
0.6m (2')	840	11.5	870	11.3	833	11.5	72.4	1.0	120	13			10,830
1.2m (4')	910	12.2	860	11.3	913	12.2	74.8	1.1	130	14			12,780
1.8m (6')	885	12.1	860	11.3	888	12.1	73.4	0.8	140	11			9,770
2.4m (8')	855	12.0	870	11.2	848	12.1	70.1	0.6	140	10			8,480
3.0m (10')	860	12.0	860	11.3	863	12.0	72.0	0.9	140	12			10,360
σ Std. Dev.	36	0.6	9	0.0	39	0.6	1.4		11	2.4			2,310
$\bar{V}$, $\bar{C}$ or $\bar{T}_{mean}$	863	11.8	863	11.3	863	11.8	73.1			14.0			11,990

* Preliminary Survey at the Mystic Station Power Plant on March 28, 1974, Unit No. 6

** Tr = 125°C, Hr=0.45 in water, ϵ_m = 9.5%

Figure 8b. After Air Preheater South Duct Velocity, SO_2 and CO_2 Concentration and Temperature Profile* At ~150 MW Gross Output

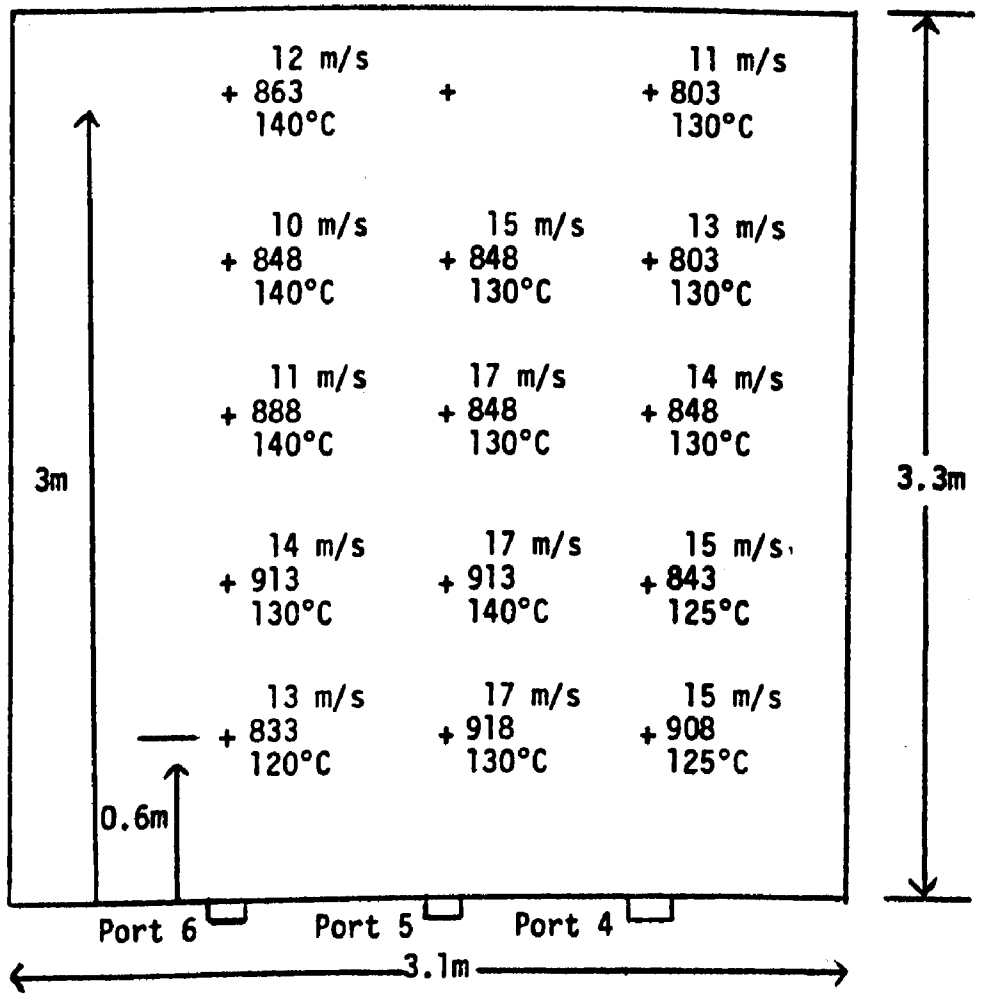

* from preliminary survey

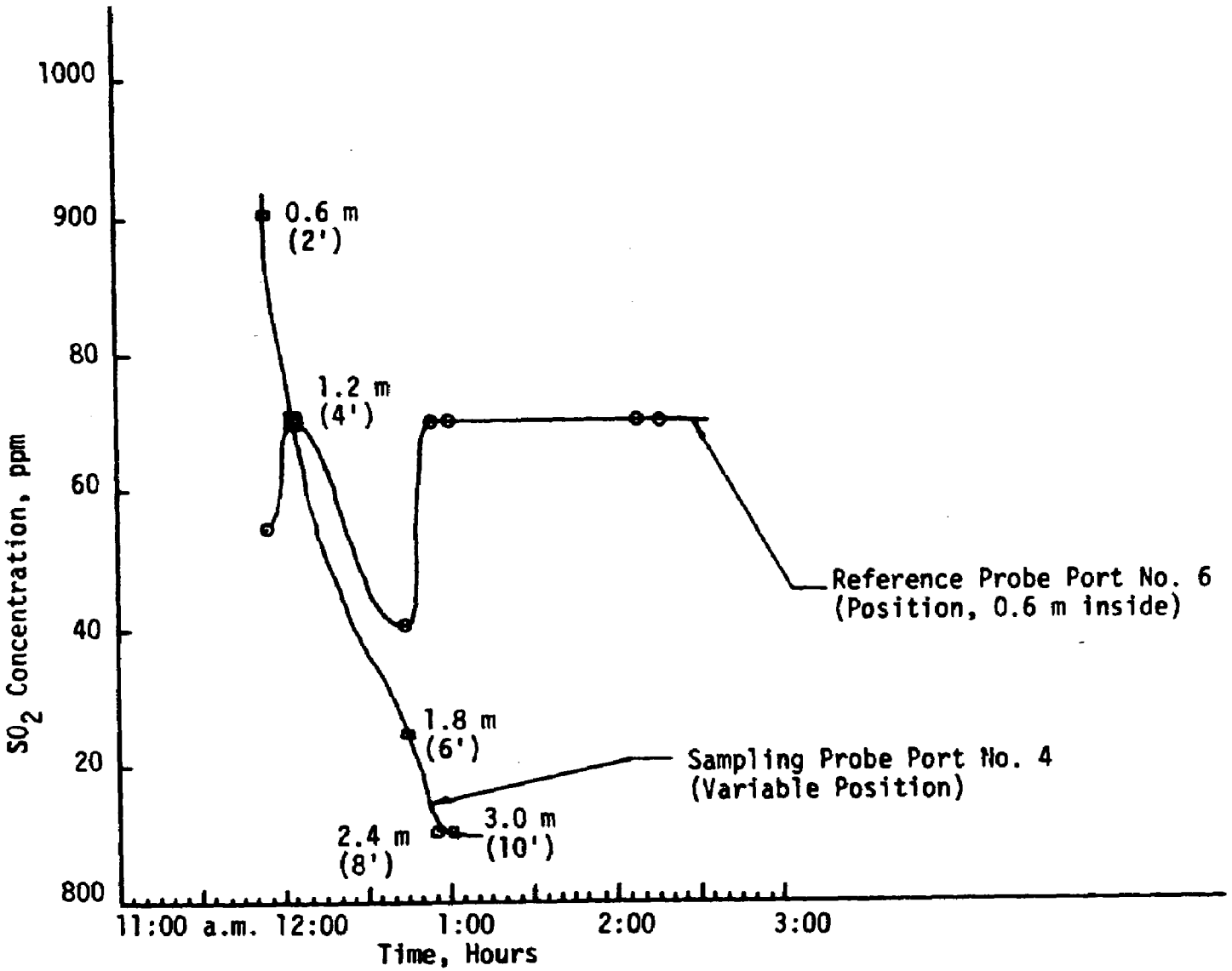

Figure 8c. After Air Preheater Duct (South Side), Port No. 4 Traverse With Fixed Reference Probe Fcr ~ 150 MW Gross Output

Velocity Profile

Velocity Scale:
1 cm = 3m/sec

SO_2 Concentration Profile

SO_2 Concentration Scale:
1 cm = 200 ppm

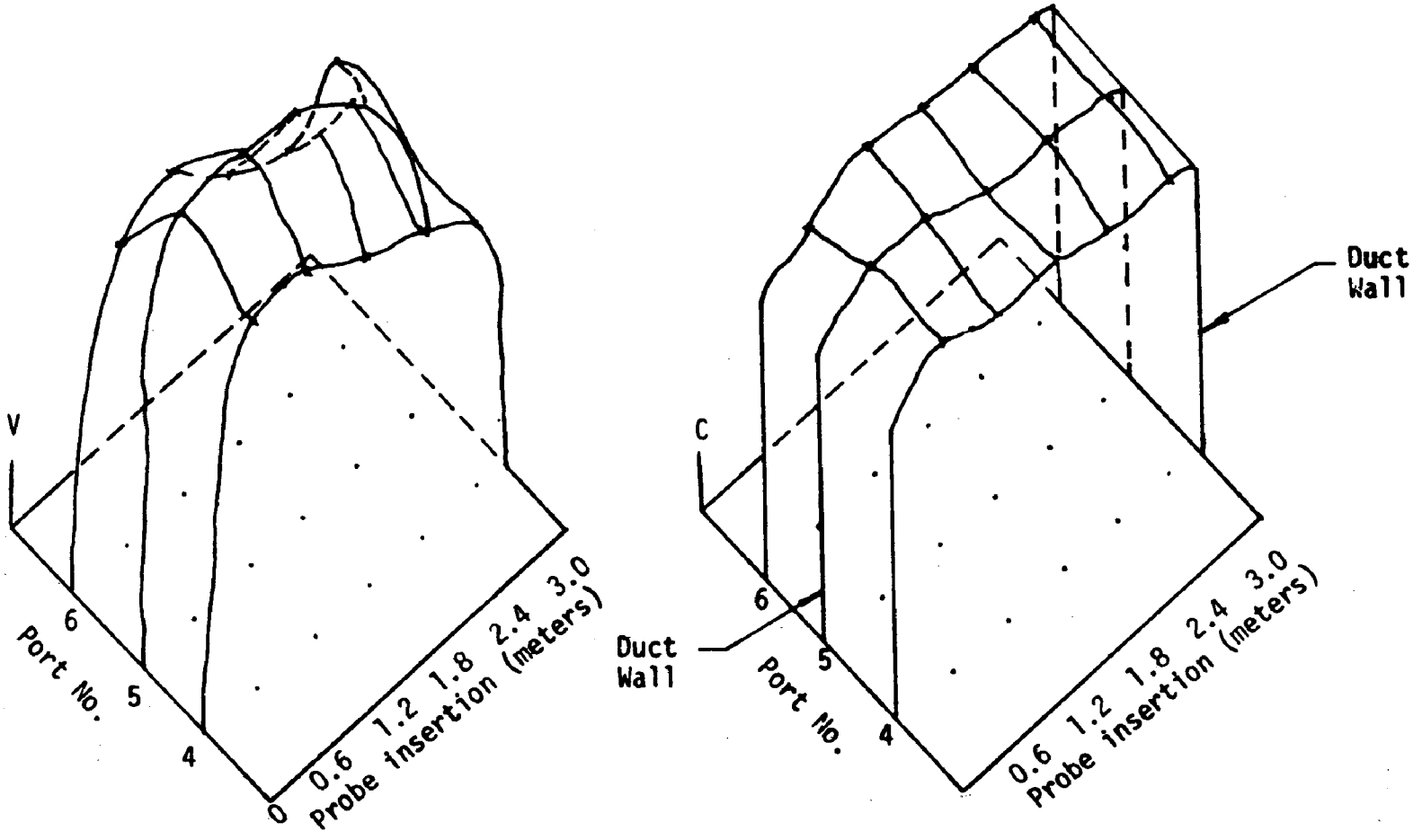

Figure 8d. After Air Preheater Duct (South) Velocity and SO_2 Concentration Profiles At ~ 150 MW Gross Output

Results from Test No. 4 were obtained from testing at the south duct after the air preheater at ~150 mw gross output. SO_2 and CO_2 concentrations were reported for both the sampling probe and the reference probe gas samples. The reference SO_2 concentration varied ±9 ppm about a mean value of 863 ppm, while the reference CO_2 concentration held steady at 11.3% CO_2. The sample concentration values at the different locations in the duct varied for both SO_2 and CO_2. A standard deviation of ±36 ppm about a mean of 863 was obtained for SO_2 concentrations, and a variation of ±0.6% about a mean of 11.8% was obtained for CO_2 concentrations. The ratio of SO_2/CO_2 concentrations had a mean value of 73.1×10^{-4} with a standard deviation of $\pm 1.4 \times 10^{-4}$.

The reference sample held a reasonably steady value for SO_2 and CO_2 concentrations in the flue gas during the traversing in Port No. 4. (See Figure 4-c). The velocity in the duct varied from as low as 110 m/s (34 ft/sec) to a high of 17 m/s (57 ft/sec) near the center of the duct. The SO_2 concentration times velocity term varied ±19% about the mean value, with a lower value of 28% below the mean and the highest 43% above the mean. Temperature in the duct varied from 120°C (248°F) to 140°C (284°F). The velocity and SO_2 concentration profiles are both displayed in Figure 8-d.

c. Discussion of Results and Conclusions

The north and south ducts following the air preheater outlet were surveyed for gas stratification, using three ports equally separated on the width of the duct and at locations inside the duct ranging from 2 feet to 10 feet. The gas samples were first analyzed for oxygen and carbon dioxide using the Fyrites. Stratification of both O_2 and CO_2 was observed in the north duct for about 150 mw gross load; this was confirmed at 130 mw gross output using the analyzer to detect SO_2 concentrations. A lower degree of SO_2 and CO_2 stratification was observed at the south duct at 150 mw, indicating that the conditions in the two ducts are not similar. The c.v. for SO_2 concentrations in the ducts is less than 10%, on an average, but the c.v. in the velocity time SO_2 concentration term is about 25% at ~130 mw gross output.

These results show a greater emission rate stratification than SO_2 concentration stratification, which is due to the low velocity value observed at the same location where a low SO_2 concentration value was found. Confidence in these results depend upon the knowledge that during sampling, the reference samples maintained a nearly steady value for SO_2 and CO_2 concentrations. Also, the concentration ratios of SO_2 and CO_2, for the points associated with the whole sampling plane, did not vary more than ~2%, which is consistent with the expected precision of the analyzers, i.e. ±1%. This result is in accord with the hypothesis which predicts that SO_2 and CO_2 are stratified in the same way.

Based on the stratification data obtained initially, the south duct test results were further analyzed. Interpolated and extrapolated values for velocity and SO_2 concentrations, for 9 to 15 probes equal area strategy, were taken from actual data profiles and the CV term calculated (See Table 3-a to 3-c and Figures 9-a thru 9-c).

The average values for velocity, SO_2 concentration and the CV term, for the 9 and 15 equal area strategy and for the actual data, are tabulated in Table 4 with the standard deviation and the coefficient of variation. Practically speaking, the CV term (concentration x velocity) can be considered to be the same for all cases and therefore the 9 probe equal area strategy is comparable to the 16 probe equal area strategy.

If 9 probes were used, the average concentration times velocity term is equal to 12100 (ppm x m/sec). One could attempt to compare the measured emission value to the actual emission value based on 9989×10^{-6} m^3/s* of residual fuel oil used at 1.9% S*. The specific gravity of the oil may be taken as 0.96.

---

* From Boston Edison operating data, expected fuel flow rate at 150 mw equal 9500 gallons/hr.

TABLE 3-a

VALUES FOR SO_2 CONCENTRATION AND VELOCITY FOR THE ACTUAL 15 POINTS TRAVERSE*

AT 150 MW

		C ppm SO_2	V m/s	CV ppm x m/s
PORT 4	4-1	908	15	13,620
	4-2	843	15	12,650
	4-3	848	14	11,870
	4-4	803	13	10,440
	4-5	803	11	8,830
PORT 5	5-1	918	17	15,610
	5-2	913	17	15,520
	5-3	848	17	14,420
	5-4	848	15	12,720
	5-5			
PORT 6	6-1	833	13	10,830
	6-2	913	14	12,780
	6-3	888	11	9,770
	6-4	848	10	8,480
	6-5	863	12	10,360
$\bar{V}$, $\bar{C}$ or $\overline{CV}$		863	14	11,990
σ		39	2.4	2,300
CV** (%)		4.5	17.4	19.2

* At (2'), (4'), (6'), (8') and (10') inside the duct

** Coefficient of variation

TABLE 3-b

INTERPOLATED VALUES FOR SO_2 CONCENTRATION AND VELOCITY
FOR 15 PROBES EQUAL AREA

		C ppm SO_2	V m/s	CV ppm x m/s
PORT 4	4-1	908	14	12,450
	4-2	865	15	13,440
	4-3	850	14	12,170
	4-4	810	13	10,860
	4-5	803	11	9,050
PORT 5	5-1	918	15	13,710
	5-2	915	17	15,340
	5-3	865	17	14,760
	5-4	848	16	13,440
	5-5	848	13	10,850
PORT 6	6-1	833	11	9,140
	6-2	880	13	11,800
	6-3	900	12	10,970
	6-4	850	10	8,810
	6-5	860	12	10,480
$\bar{V}$, $\bar{C}$, or $\overline{CV}$		863	14	11,800
σ		35	2.1	2,000
CV* (%)		4.0	15.2	17.3

* Coefficient of variation

TABLE 3-c

EXTRAPOLATED AND INTERPOLATED VALUES
FOR SO_2 CONCENTRATION AND VELOCITY
FOR 9 PROBES EQUAL AREA

		C ppm SO_2	V m/s	CV ppm x m/s
PORT 4	4-1	908	15	14,110
	4-2	850	14	12,170
	4-3	803	12	9,540
PORT 5	5-1	918	16	15,390
	5-2	865	17	14,760
	5-3	848	14	11,890
PORT 6	6-1	833	12	10,410
	6-2	900	12	10,970
	6-3	855	11	9,900
$\bar{V}$, $\bar{C}$, $\bar{CV}$		865	14	12,100
σ		38	2.1	2,160
CV* (%)		4.0	15.2	17.8

* Coefficient of variation

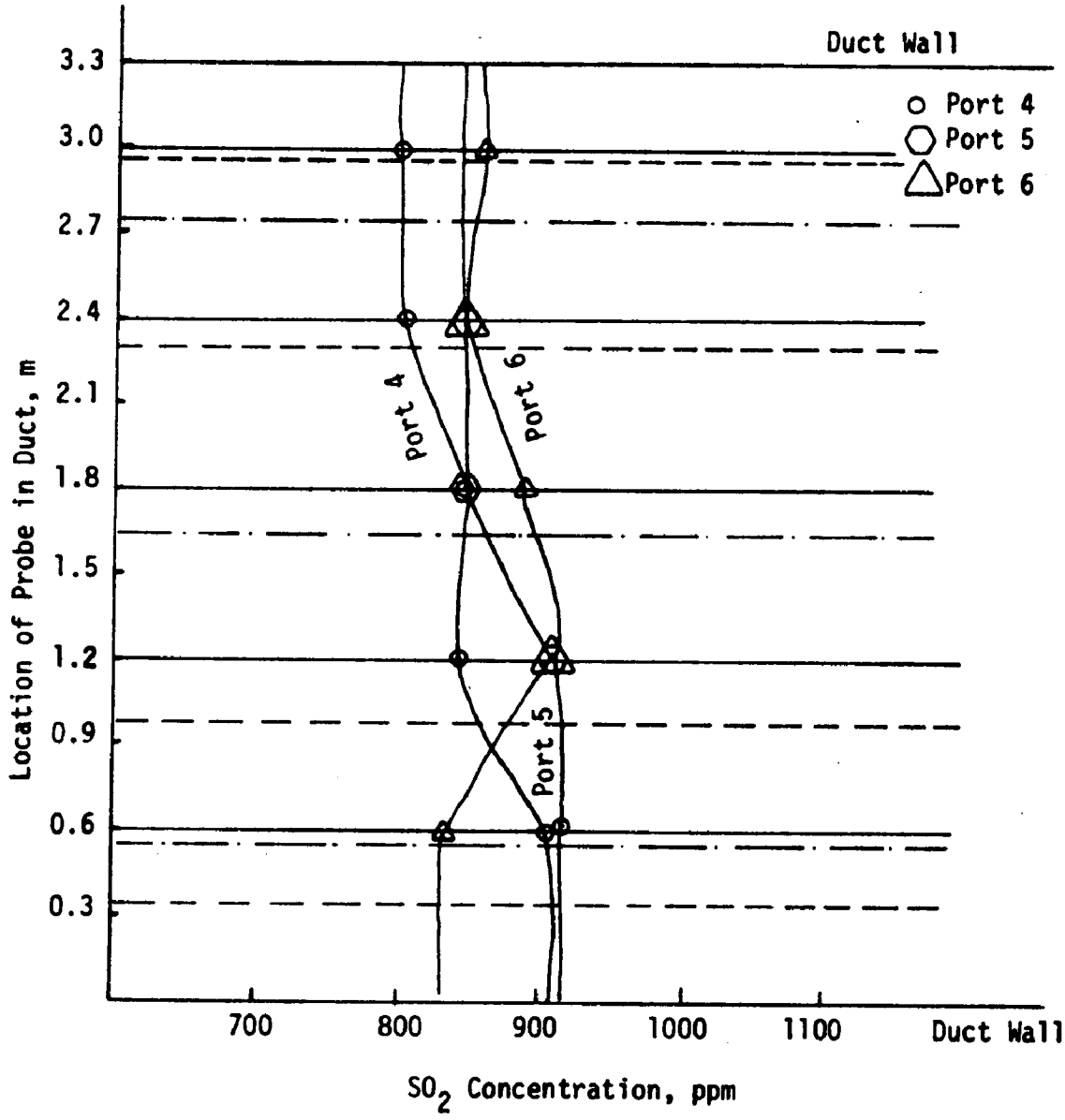

Figure 9a. South Duct SO_2 Concentration at 150 MW for 1.9% Sulfur Oil

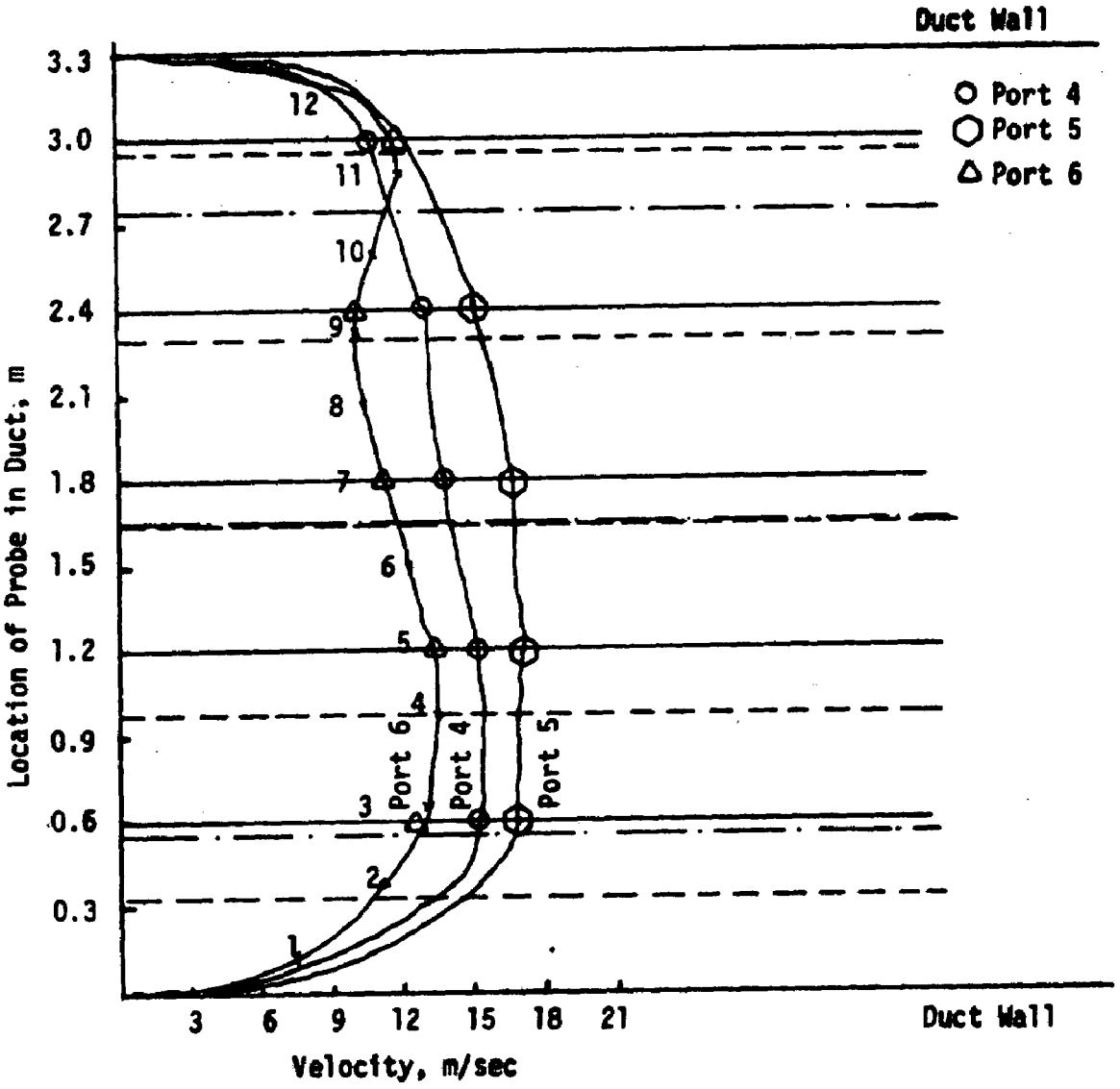

Figure 9b. South Duct Velocity Profile at 150 MW

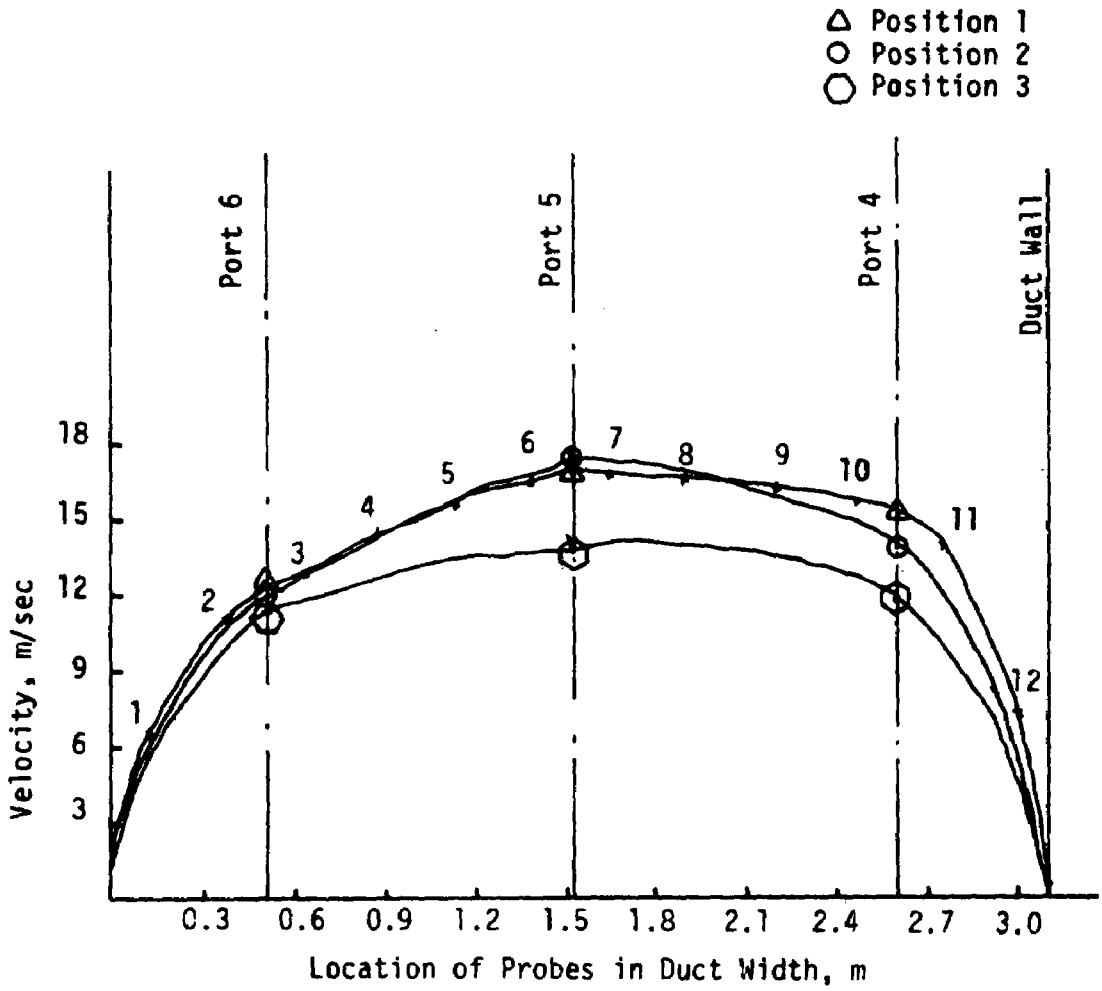

Figure 9c. South Duct Velocity Profile at 150 MW

TABLE 4

SOUTH DUCT (PORT 4, 5, 6) AT 150 MW*

COMPARING DIFFERENT SAMPLING METHODS

Method and No. of Probes	$\bar{C}$ ppm SO_2	σ	C.V.** (%)	$\bar{V}$ m/s	σ	C.V.** (%)	$\overline{CV}$ ppm x m/s	σ	C.V.** (%)
15 probes *** (real data)	863	39	4.5	14	2.4	17.4	11,990	2,300	19.2
15 probes (equal area)	863	35	4.0	14	2.1	15.2	11,800	2,000	17.3
9 probes (equal area)	865	38	4.0	14	2.1	15.2	12,100	2,160	17.8

* percent sulfur in fuel = 1.9%
** Coefficient of variation
***Average temperature ~130°C
% moisture = 9.5% (measured)

The expected emission of SO_2 (assuming 3% of the sulfur in the oil converts to SO_3) based on the sulfur content in the oil is equal to:

$$\frac{1 \times 10^3 \times 9989 \times 10^{-6} \times 0.96 \times 1.9 \times 64 \times 0.97}{32 \times 100} \sim 355 \times 10^{-3} \text{ kg/s}$$

For the actual data, if one assumes that the north duct will behave similarly, we obtain:

$$2\left[\text{Area} \times C \times V \times \left(1 - \frac{\%m}{100}\right) \times \frac{64}{34 \times 10^{-3}}\right]$$

$$\therefore \frac{2 \times 10.5\ m^2 \times 12100 \times 10^{-6} \times 64 \times (1-0.095)}{34 \times 10^{-3}} = 430 \times 10^{-3} \text{ kg/s}$$

The percent difference between the actual and the expected emission is equal to +21%. The difference may be due to difficulties encountered in measuring the pulsating flow in the duct and/or failure to consider the boundary layer effort on the flue gases flow rate. It is also possible that this difference is based on the reported value of the fuel flow rate which has not been verified.

By attempting to extrapolate more points near the boundary (see Figure 10), the mean value for the velocity was found to be equal to 13 m/sec, about 8% lower than the measured value. It is therefore expected that the calculated percent error in emission rate will include at least +8% error due to boundary layer effect.

Based on these results and analyses, a nine probe equal area strategy was planned for the final demonstration test.

3. DEMONSTRATION TEST

Based on the stratification data collected in the preliminary survey, plans were made for the demonstration test at the locations after the air preheaters for a 9 equal area strategy for each duct, i.e., a total of 18 sampling

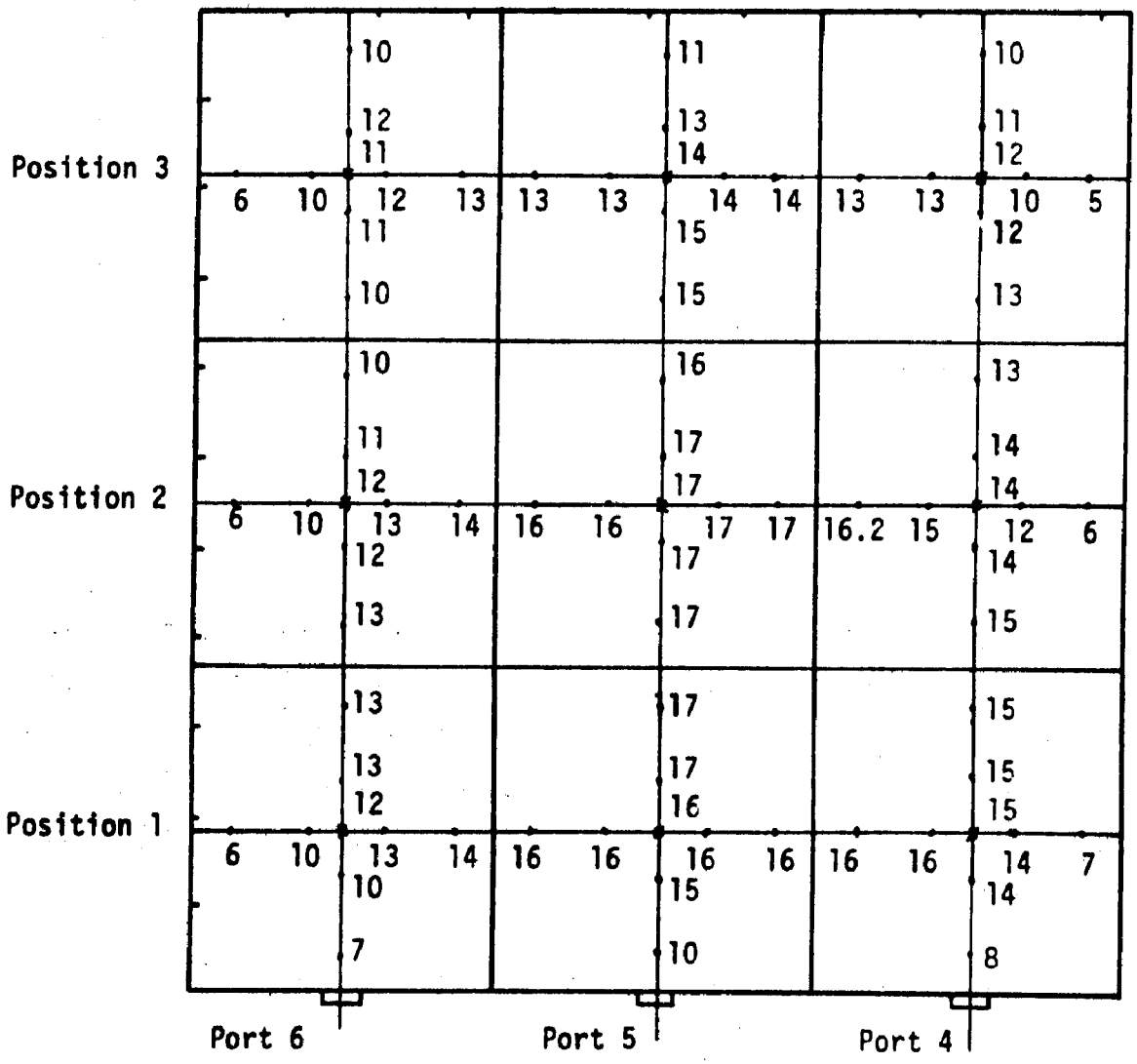

* Dimension in m/sec

Figure 10. South Duct Velocity Profile at 150 MW

points for both ducts. The set up included 6 sets of probes, one for each sampling port and 2 sets of probes for the two reference ports (one reference probe for each duct). At each location SO_2, CO_2 (NDIR) and O_2 (Fyrite) concentrations plus temperature and velocity were measured. Methods of data collection and test results are discussed below.

a. Sampling Procedure

The sampling train arrangement was as described in Section IV.C.1.a., shown in Figures 1-a through 1-d.

A schematic diagram of the set up of probes and stands is shown in Figure 11. The reference probe assembly was maintained at 10.6 m (2') inside the duct, and each duct has one reference assembly. The probe tip assembly at each port was placed into the duct in three different positions, i.e., about 0.6 m 1.7 m and 2.7 m into the duct (duct dimensions are 3.1 m wide and 3.3 m high).

A gauge was used to monitor the high sulfur fuel oil tank during the test period. The test ran from about 11 o'clock in the morning until 4 o'clock in the afternoon. During the test, a constant load (~144 mw gross output) was maintained on the boiler unit No. 6 as well as the scrubber unit. The latter was checked by running Fyrites tests on both CO_2 and O_2 analyses at the inlet south duct to the scrubber.

Sampling proceeded as follows:

1. Calibration of analyzers using both zero and span gases
2. Sampling from Reference 1a at the north duct
3. Sampling from Port No. 1 at the first position
4. Sampling from Reference 1a
5. Sampling from Port No. 2 at the first position

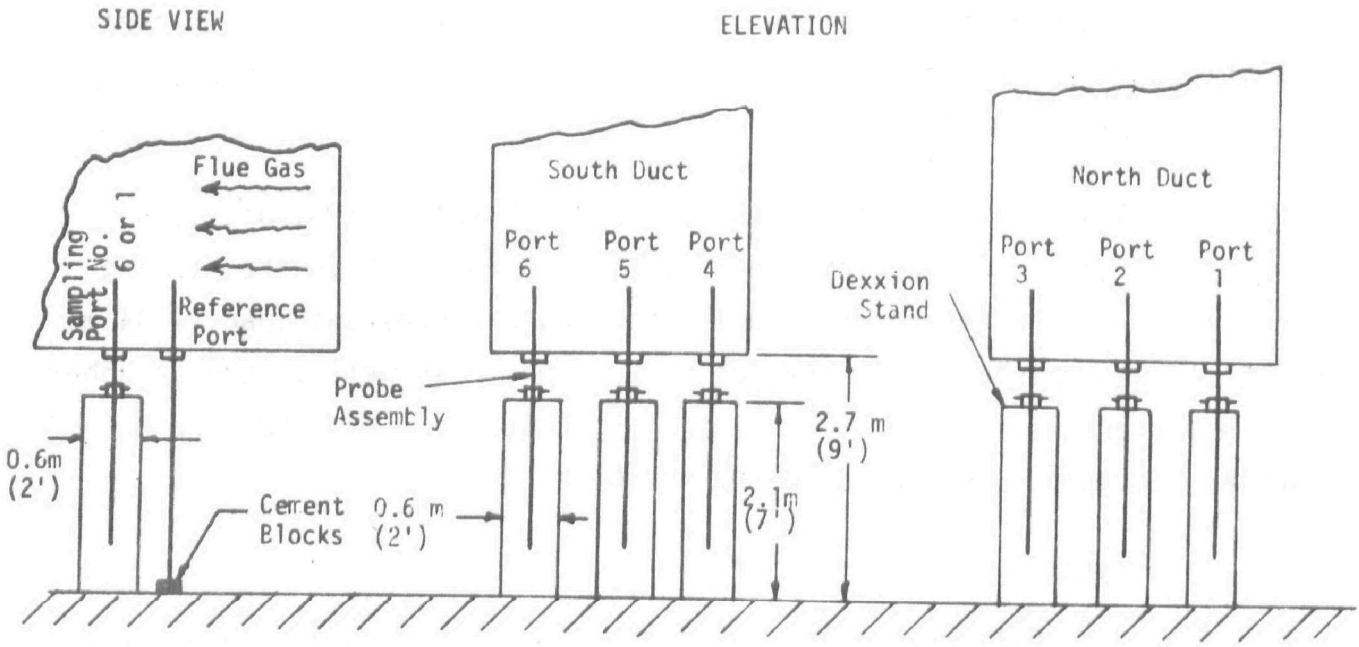

Figure 11. After Air Preheater Sampling Arrangement

This sequence was followed for all points at the first position. The probe assembly was adjusted for the second position as soon as sampling from the first position was completed. The same sampling procedure was then repeated for the second position and the third position. At the termination of a run the analyzers were calibrated.

About 36 samples were analyzed, involving 18 sampling points, centroid of equal areas, and 18 reference points. At each location SO_2, CO_2 (NDIR) and O_2 (Fyrite) concentrations plus temperature and velocity were measured. SO_2 and CO_2 data were recorded continuously.

When O_2 analysis was performed (by Fyrite), the sample was taken from the purge line while the flue gas stream leading to the analyzers was closed. This was done because hand pumping to the Fyrite causes pressure fluctuations which effect the analyzers output signal, specifically the Intertech SO_2 analyzer.

The purge stream as well as the analyzer flue gas stream were adjusted (same setting for each sampling point) by checking the flow measuring elements (rotameters).

The sampled gas temperature (equal to room temperature) and humidity (controlled by refrigerator temperature) were also kept constant for all sampling points. Therefore, equal volumes per unit time were sampled from each location.

Humidity tests were run separately, twice for each duct. The sampling arrangement shown previously in Figure 1-b was used.

Sampling at the inlet south duct to the scrubber was performed at a constant location, about 1.2 m inside the duct at Port No. 4, using the same arrangement described in the preliminary survey section (see Section IV .C.1.b.).

b. Results

Test results from surveying the south and north ducts after the air preheaters showed CO_2, O_2, and SO_2 gas stratification while the test load was kept constant at 144 mw gross output from Unit No. 6. The reference sample from each duct held a reasonably steady value for SO_2 and CO_2 concentrations in the flue gas during the whole traversing period. The CO_2 and O_2 concentrations, at the inlet south duct to the scrubber, also held a steady value during the test period (See Figure 12). Test results are presented in Tables 4-a thru 5-b and Figures 12 and 13. All calculations made are included in Appendix I.

The reference SO_2 concentration at the north duct varied ±12 ppm from a mean value of 943 ppm; the CO_2 concentration varied ±0.2% from a mean value of 11.9%, while the O_2 concentration did not show any variation. The normalized values at the different sampling locations varied for SO_2 concentration by ±52 ppm from a mean value of 917 ppm with a low value of 840 ppm and a high value of 990 ppm; for CO_2 concentration by ±0.9% from a mean value of 11.6% with a low value of 10.4% and a high value of 12.8%; and for O_2 concentration by ±0.4% from a mean value near 6.5% with a low value of 6% and a high value of 7%. The velocity in the duct ranged from as low as 10 m/s to as high as 18 m/s with an average value of 15 m/s and a standard deviation of ±2.5 m/s. Temperature stratification was also observed varying from 130°C to 150°C.

The coefficient of variation of the concentration times velocity term (which is proportional to the emission rate) was ±22%, ±24%, ±16% for SO_2, CO_2 and O_2, respectively; the lowest and highest deviation from the mean was -37% and + 24% for SO_2, -39% and +35% for CO_2, -24% and and + 27% for O_2. The average SO_2/CO_2 concentration ratio was equal to 79.1×10^{-4} with a coefficient of variation of 2.1%.

The reference SO_2 concentration at the south duct varied ±8 ppm from a mean value of 1042 ppm. The variation of CO_2 concentration was negligible, while the O_2 concentration varied ±0.2% from a mean value of 4%.

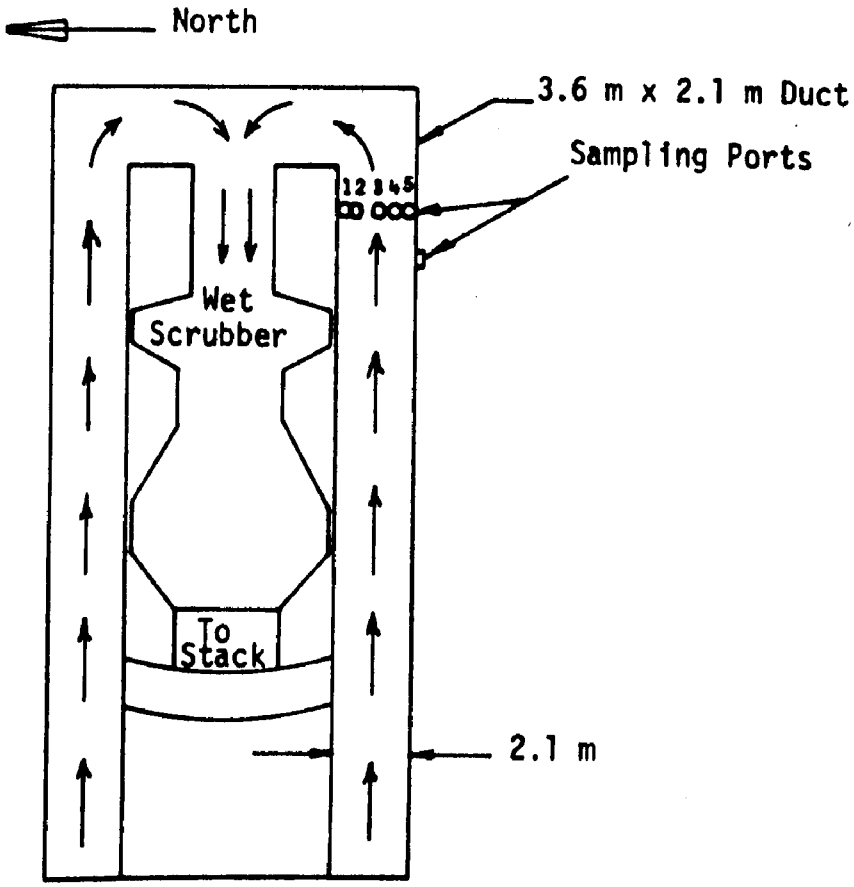

Position	% CO_2	% O_2	Time
Port No. 4	10.5	6.0	11:05
1.2 m	10.0	6.0	11:35
Inside	10.0	6.0	12:05
	10.0	6.0	12:45
	10.0	5.5	1:30
	10.0	6.0	2:15

* On April 24, 1974 from 11:00 a.m. to 2:30 p.m.

Figure 12. CO_2 And O_2 Concentrations At The Inlet South Duct To the Scrubber Using the Fyrites*

TABLE 4-a

NORTH DUCT DATA REDUCTION AT ~144 MW GROSS OUTPUT

Position	T_s (°K)	H x 10^2 (N/m^2)	$V=F_s \times 3.9 \times C_1 \sqrt{\frac{B.P. \times H \times T_s}{P_s' \times Gd}}$ $C_1=0.19$ (m/s)	C_M O_2 %	C_M CO_2 %	C_M SO_2 ppm	C_R O_2 %	C_R CO_2 %	C_R SO_2 ppm	$C_N = \frac{C_M C_R}{C_R}$ O_2 %	C_N CO_2 %	C_N SO_2 ppm	$C_N V$ (ppm x m/s) O_2 (x 10^4)	CO_2 (x 10^4)	SO_2	$\frac{CNSO_2}{CNCO_2}$ x 10^{-4}
PORT NO. 1																
1-1	408	1.37	15	6.0	11.8	945	6.0	11.6	930	6.0	12.1	960	90	181	14,400	79.3
1-2	413	0.87	12	6.0	11.6	915	6.0	12.1	960	6.0	11.4	900	72	137	10,800	78.9
1-3	403	0.62	10	7.0	10.6	855	6.0	12.1	960	7.0	10.4	840	70	104	8,400	80.8
PORT NO. 2																
2-1	423	1.99	18	6.5	12.5	960	6.0	11.6	930	6.5	12.8	975	117	230	17,550	76.1
2-2	408	1.37	15	6.0	11.6	915	6.0	12.0	945	6.0	11.5	915	90	172	13,725	79.5
2-3	408	1.25	14	7.0	10.9	870	6.0	12.0	945	7.0	10.8	870	98	151	12,180	80.5
PORT NO. 3																
3-1	418	1.87	18	6.0	12.5	975	6.0	11.6	930	6.0	12.8	990	108	230	17,820	77.3
3-2	413	1.37	15	6.0	12.0	930	6.0	12.0	945	6.0	11.3	930	90	178	13,950	78.1
3-3	408	1.25	14	6.5	10.9	870	6.0	12.1	945	6.5	10.7	870	91	150	12,180	81.3
σ	6.0		2.5				0.0	0.2	12.0	0.4	0.9	52	15	41	3,000	1.7
$\bar{V}$ or $\bar{C}$	411		15				6.0	11.9	943	6.3	11.6	917	92	170	13,445	79.1
CV**(%)	1.5		17				0.0	1.8	1.2	6.8	7.5	5.6	16.3	24.1	22.4	2.1

CONDITIONS: B.P. = 100.9 N/m^2 (29.8" Hg) x 10^3
P_s' = 97.2 N/m^2 (28.7" Hg) x 10^3
T_sAV = 411°K
Gd = 0.99
F_s* = 0.835

* Average value of S-tube calibration factor
** Coefficient of variation

TABLE 4-b

SOUTH DUCT DATA REDUCTION AT ~144 MW GROSS OUTPUT

Position	T_s (°K)	H x 10^2 (N/m^2)	$V=F_s \times 3.9 \times C_1 \sqrt{\frac{B.P. \times H \times T_s}{P_s' \times Gd}}$ $C_1=0.19$ (m/s)	C_M O_2 %	C_M CO_2 %	C_M SO_2 ppm	C_R O_2 %	C_R CO_2 %	C_R SO_2 ppm	$C_N = \frac{C_M \bar{C}_R}{C_R}$ O_2 %	C_N CO_2 %	C_N SO_2 ppm	$C_N V$ (ppm x m/s) O_2 (x 10^4)	CO_2 (x 10^4)	SO_2	$\frac{CNSO_2}{CNCO_2}$ x 10^{-4}
PORT NO. 4																
4-1	403	1.62	16	7.0	12.8	960	4.0	13.5	1035	7.0	12.8	965	112	205	15,440	75.4
4-2	403	1.37	15	5.5	12.5	990	4.0	13.4	1050	5.5	12.6	980	82	189	14,700	77.8
4-3	393	0.99	12	6.0	11.8	930	4.0	13.5	1035	6.0	11.8	935	72	142	11,220	79.2
PORT NO. 5																
5-1	403	1.62	16	6.0	13.9	1050	4.0	13.5	1035	6.0	13.9	1055	96	222	16,880	75.9
5-2	403	1.49	15	5.0	13.4	975	4.0	13.5	1035	5.0	13.4	980	75	201	14,700	73.1
5-3	393	1.18	14	5.5	12.3	975	4.0	13.5	1035	5.5	12.3	980	77	172	13,720	79.7
PORT NO. 6																
6-1	413	1.37	15	4.5	13.5	1050	4.5	13.5	1050	4.0	13.5	1040	60	202	15,600	77.0
6-2	408	0.99	13	4.0	1-.4	1020	4.0	13.5	1050	4.0	13.4	1010	52	174	13,130	75.4
6-3	403	0.62	10	4.5	13.0	1005	4.5	13.5	1050	4.0	13.0	995	40	130	9,950	76.5
σ	6.3		2.0				0.2	-0	8	1.1	0.7	37	22	30	2,200	2.0
$\bar{V}$ or $\bar{C}$	403		14				4.1	13.5	1042	5.2	13.0	993	74	182	13,900	76.7
CV** (%)	4.9		14.3				5.3	-0	0.7	21.1	5.3	3.7	30	16	16	2.6

CONDITIONS: B.P. = 100.9 N/m^2 (29.80 Hg)
P_s' = 97.6 N/m^2 (28.84 Hg)
$T_s AV$ = 403°K
$\bar{Gd}$ = 1.01
F_s* = 0.835

* Average value for S-tube Calibration factor
** Coefficient of variation

TABLE 4-c

AVERAGE CONCENTRATIONS FROM BOTH DUCTS

	O_2 (%)	CO_2 (%)	SO_2 ppm	SO_2/CO_2 $\times 10^{-4}$
σ	1.0	1.0	59	2.2
C^*_{mean}	5.8	12.3	955	77.9
C.V.**	17%	8%	6%	2.8%

	O_2 ($\times 10^4$)	CO_2 ($\times 10^4$)	SO_2 ppm
σ	20	36	2,600
$(CxV)_{mean}$	83	176	13,600
C.V.**	25%	20%	19%

* C_{mean} was also found to be equal to (ALL DRY BASIS)

$$\frac{\sum_{i=1}^{i=18} C_i V_i}{\sum_{i=1}^{i=18} V_i}$$

** Coefficient of variation

TABLE 5

5-a TEST NO. 1

NORTH DUCT		SOUTH DUCT	
T_D(°C)	T_W(°C)	T_D(°C)	T_W(°C)
54.4	47.8	48.9	44.4
57.2	47.8	50.6	45.6
57.8	48.3	52.2	46.1
58.9	48.9	53.3	46.7
60.0	48.9	54.4	46.7
61.1	48.9	56.1	47.2
62.2	48.9	57.2	47.2
63.3	49.4	59.4	47.8
64.4	49.4		
65.6	49.4		
66.7	50.0		

5-b TEST NO. 2

NORTH DUCT		SOUTH DUCT	
T_D(°C)	T_W(°C)	T_D(°C)	T_W(°C)
53.9	47.2	46.1	44.4
57.2	47.8	48.9	45.0
59.4	48.3	51.1	46.1
61.1	48.9	52.2	46.1
63.3	48.9	54.4	46.7
64.4	48.9	56.1	47.2
65.5	48.9	57.2	47.8
66.6	48.9	58.9	47.8
67.8	49.4	60.0	47.8
68.9	49.4	62.2	47.8

Figure 13

Recorder Output

13-a. SO_2 Recorded Output Signal at 0.5 in/min - Response Curves

13-b. CO_2 Recorded Output Signal at 0.5 in/min - Response Curves

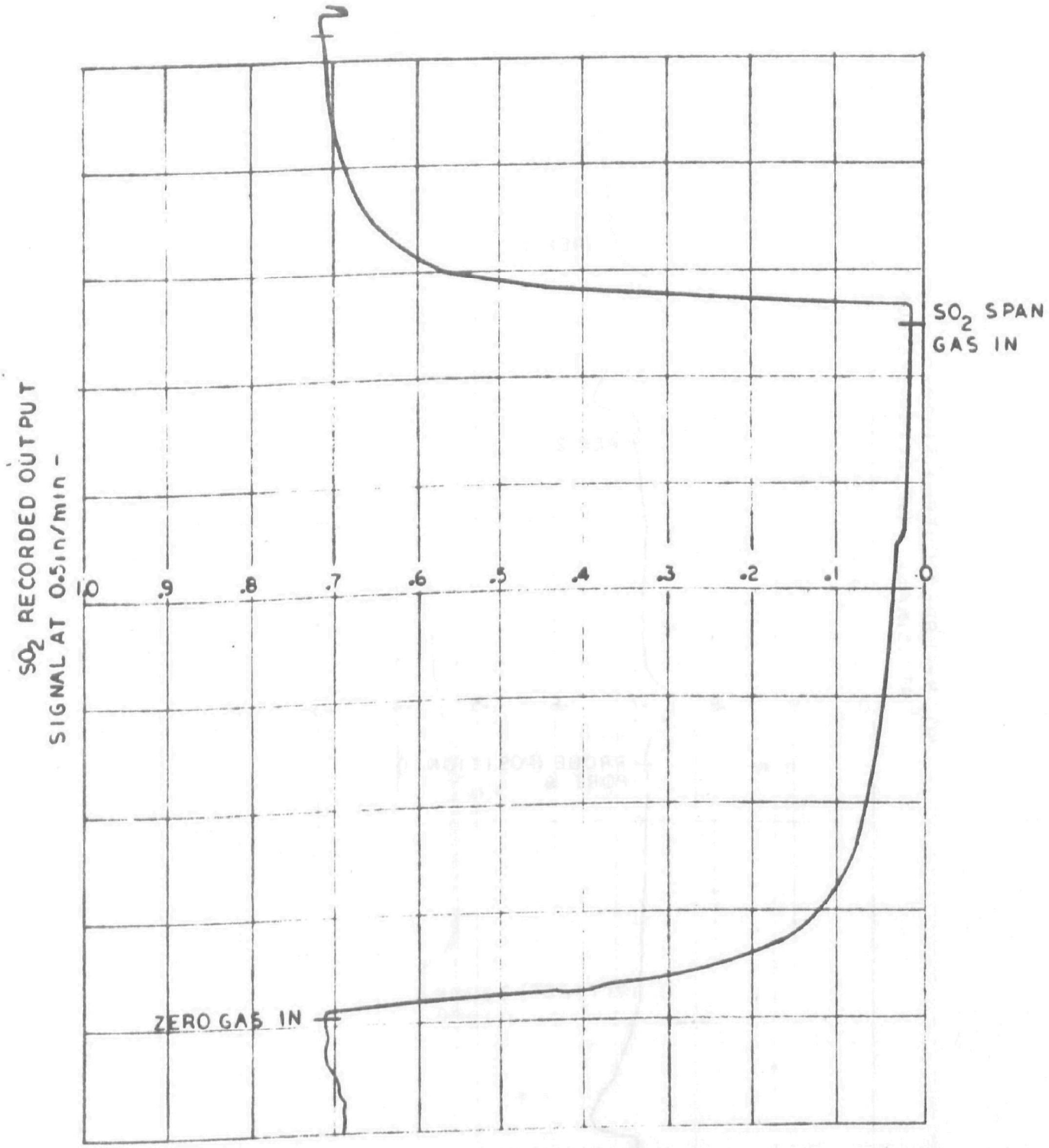

Figure 13a. SO_2 Recorded Output Signal at 0.5 in/min - Response Curves

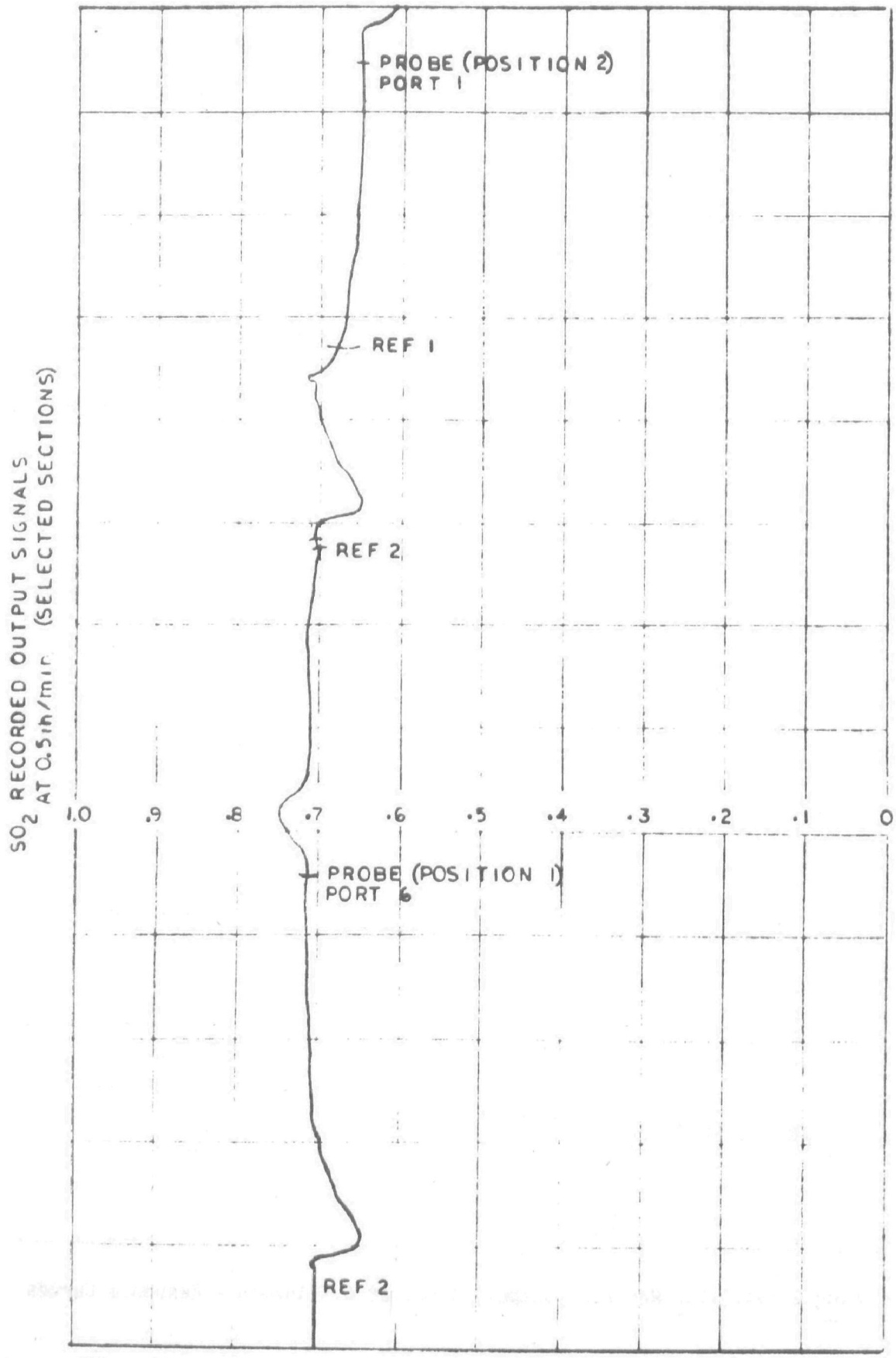

Figure 13a. SO_2 Recorded Output Signal at 0.5 in/min - Response Curves

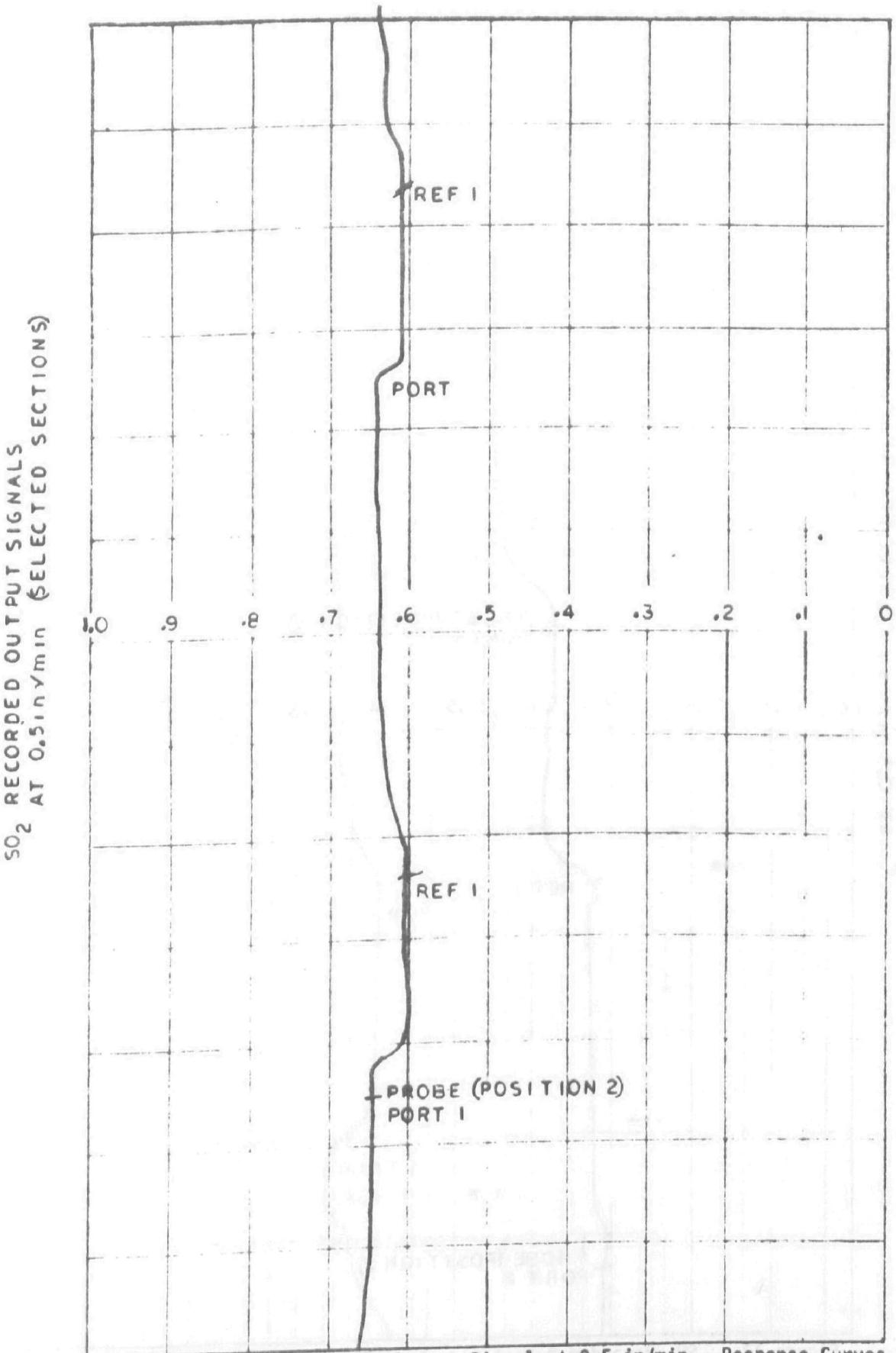

Figure 13a. SO_2 Recorded Output Signal at 0.5 in/min - Response Curves

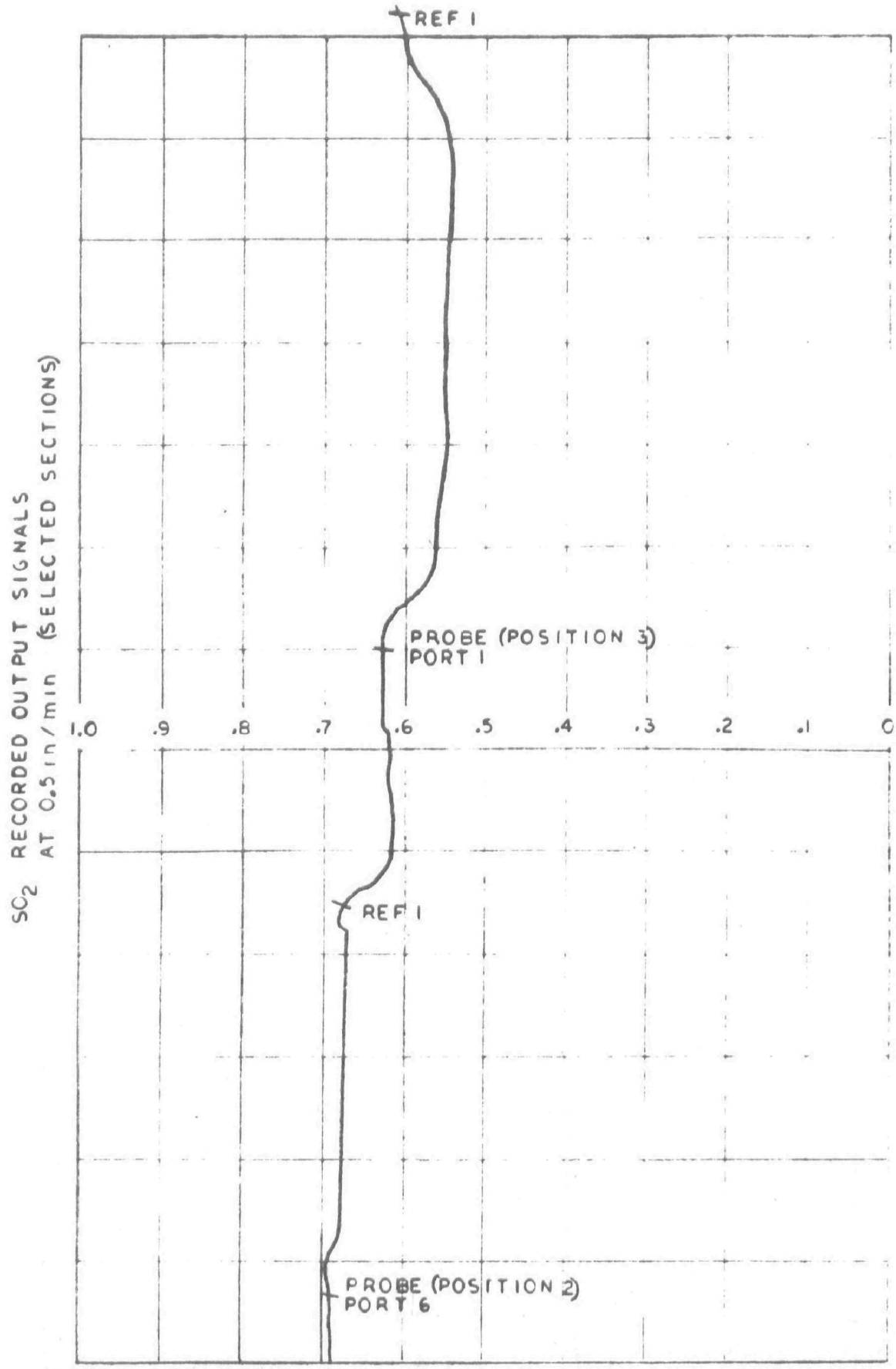

Figure 13a. SO_2 Recorded Output Signal at 0.5 in/min - Response Curves

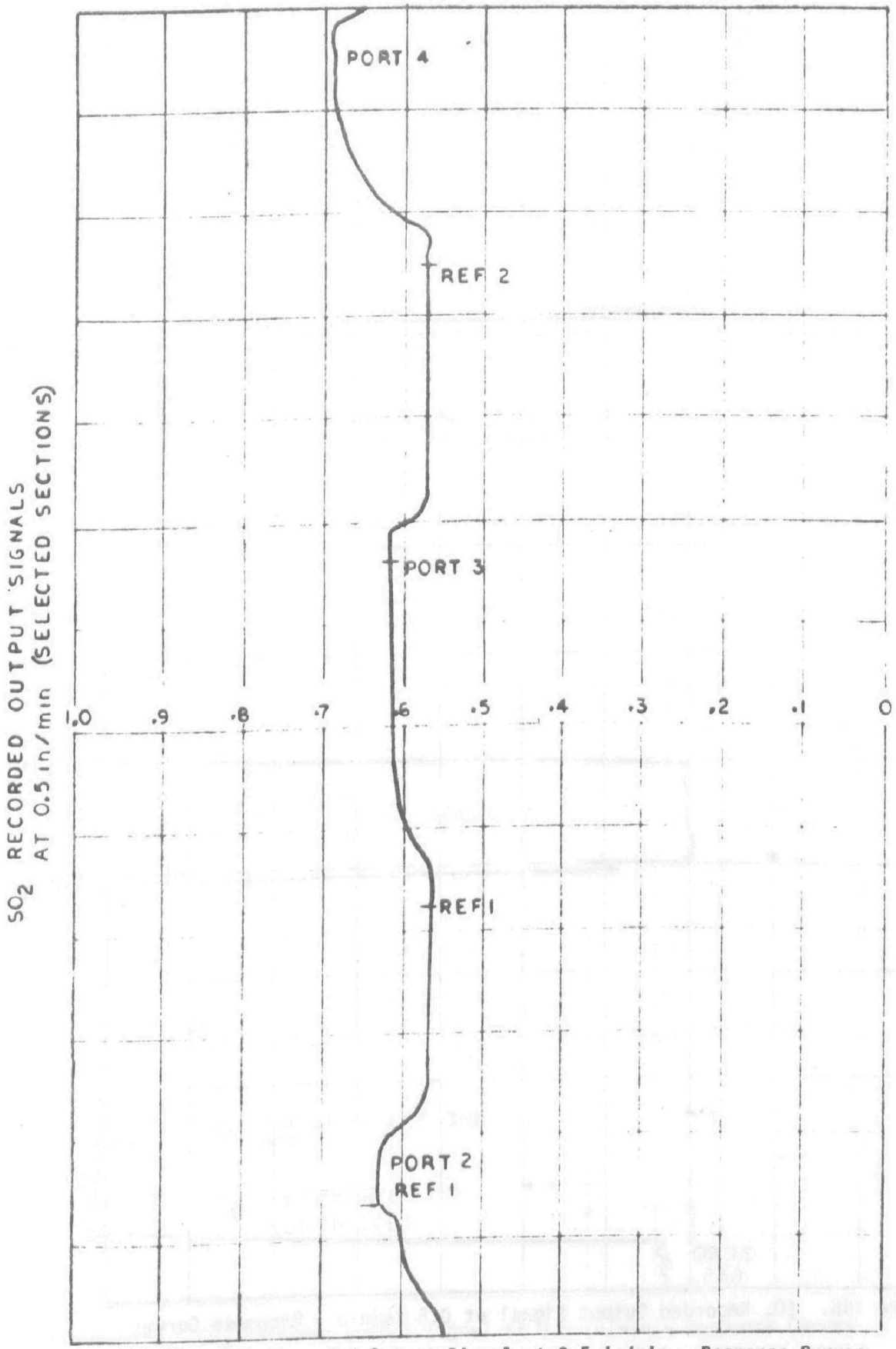

Figure 13a. SO_2 Recorded Output Signal at 0.5 in/min - Response Curves

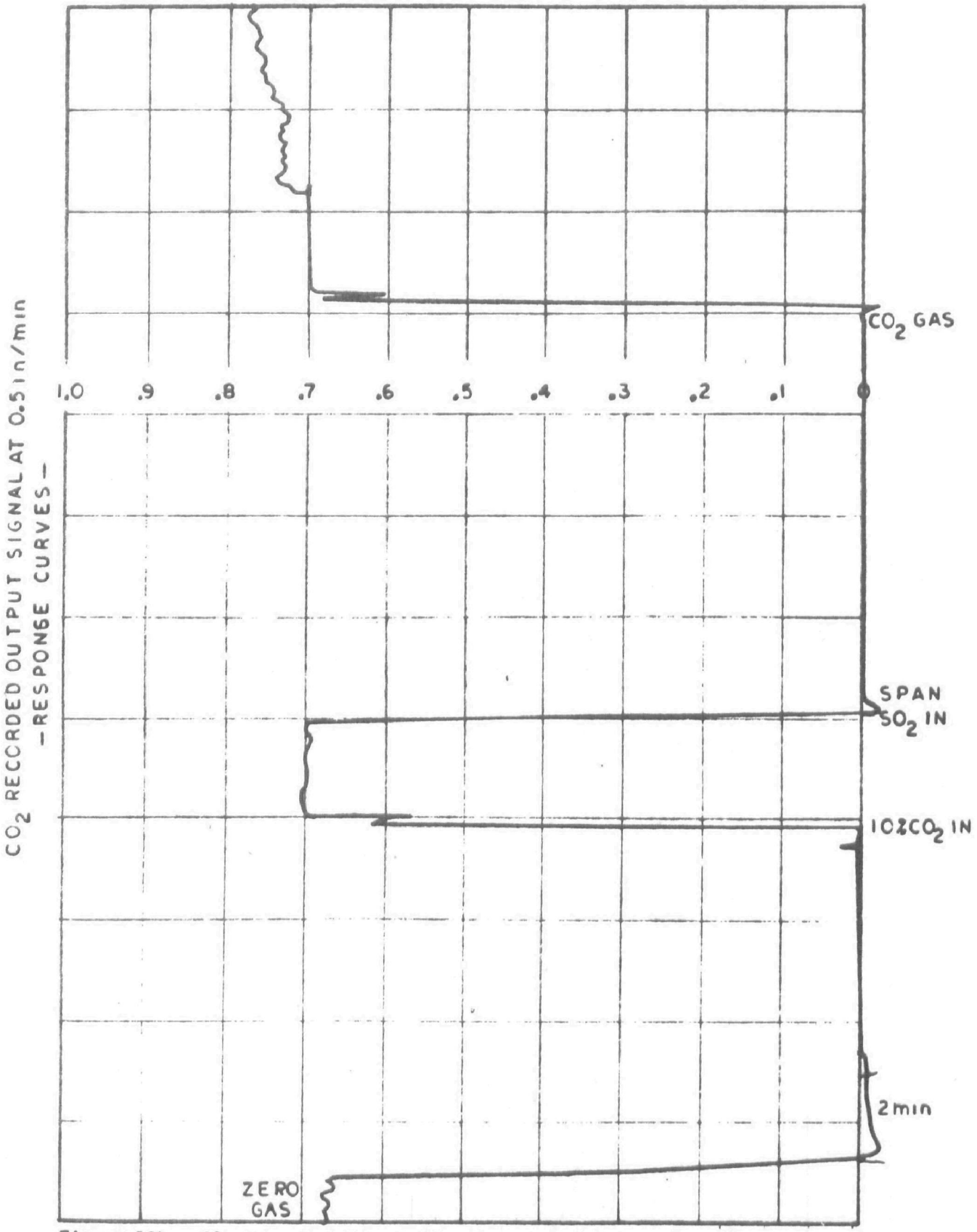

Figure 13b. CO_2 Recorded Output Signal at 0.5 in/min - Response Curves

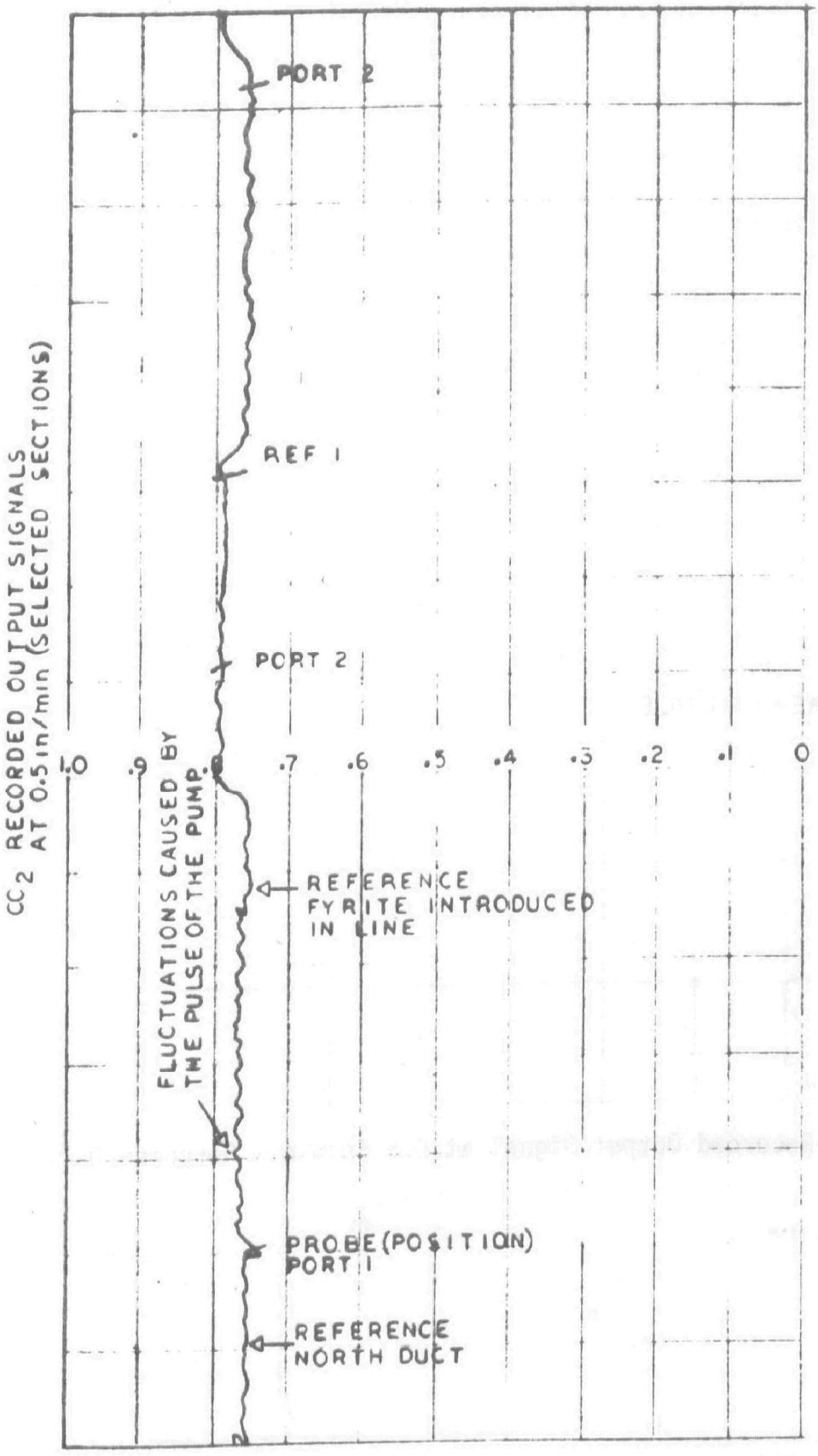

Figure 13b. CO_2 Recorded Output Signal at 0.5 in/min - Response Curves

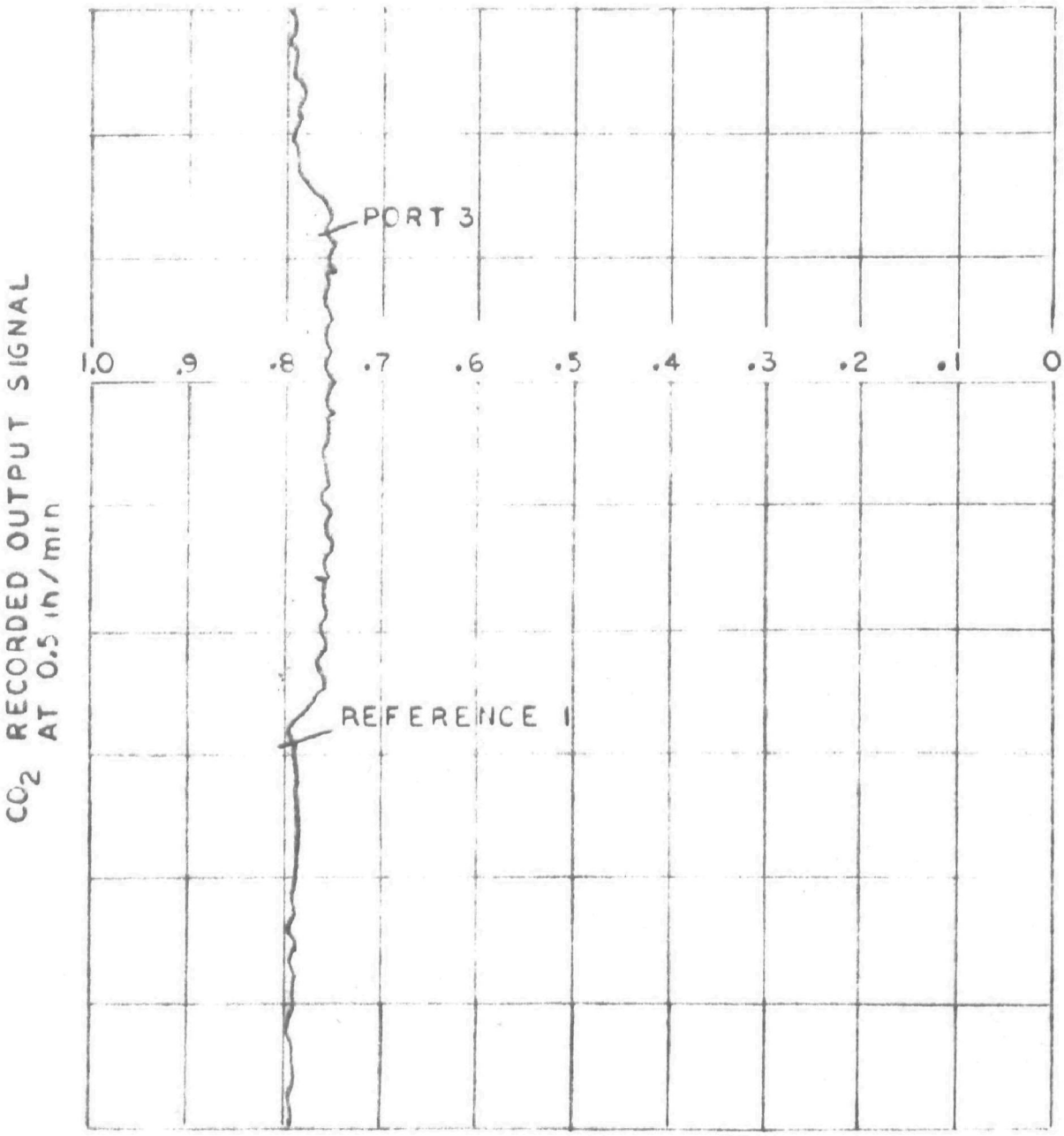

Figure 13b. CO_2 Recorded Output Signal at 0.5 in/min - Response Curves

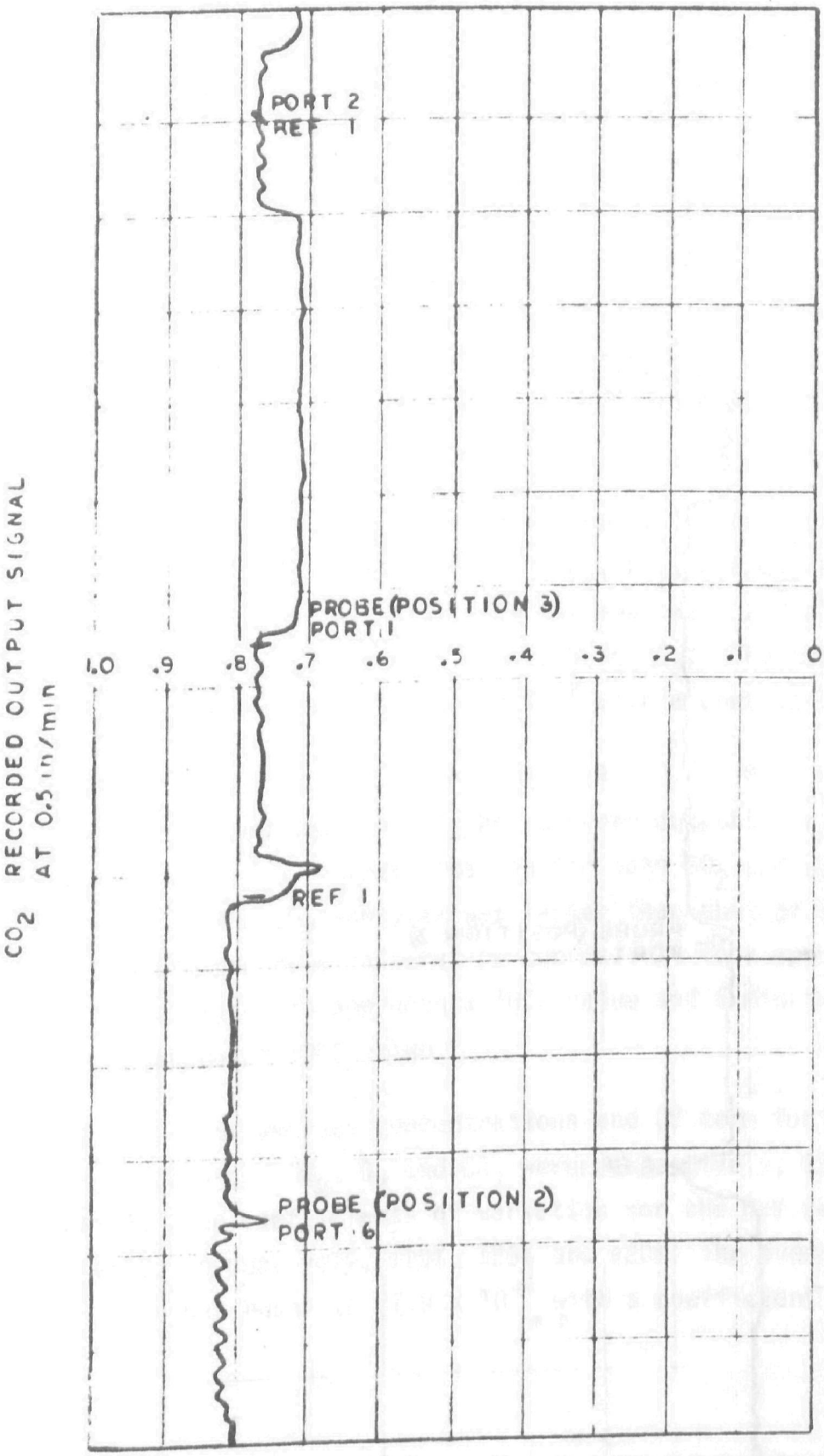

Figure 13b. CO_2 Recorded Output Signal at 0.5 in/min - Response Curves

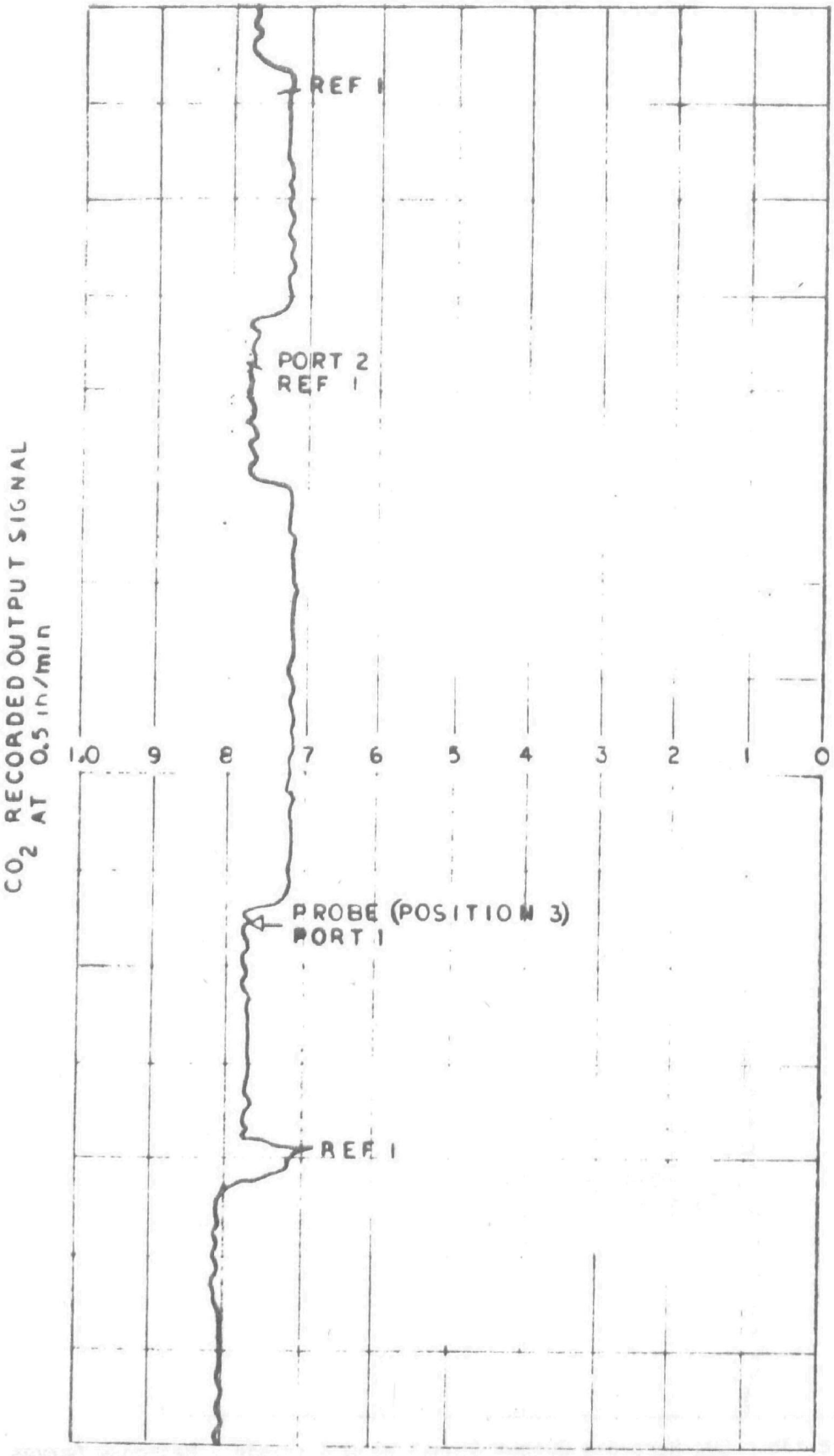

Figure 13b. CO_2 Recorded Output Signal at 0.5 in/min - Response Curves

The normalized values at the different sampling locations varied for SO_2 concentration by ±37 ppm from a mean value of 993 ppm (with a lowest value of 935 ppm and a highest value of 1055 ppm); for CO_2 concentration by ±0.7% from a mean value of 13.0% (with a lowest value of 11.8% and a highest value of 13.9%); and for O_2 concentration by ±1.1% from a mean value of 5.2% (with a lowest value of 4% and a highest value of 7%).

The velocity measured in the duct ranged from as low as 10 m/s to as high as 16 m/s with an average value of 14 m/s and a standard deviation of ±2.0 m/s. Temperature stratification was also observed varying from 120°C to 140°C.

The coefficient of variation of the concentration times velocity term was ±16%, ±16%, ±30% for SO_2, CO_2, and O_2, respectively; the lowest and highest deviation from the mean was -28% and +21% for SO_2, -28% and + 21% for CO_2, and -45% and +51% for O_2. The average SO_2/CO_2 concentration ratio was equal to 76.7×10^{-4} with a coefficient of variation of 26%.

A few sections of the recorder outputs are displayed in Figures 13-a and 13-b. Stratification for both SO_2 and CO_2 was recorded. The response of the CO_2 analyzer was faster than that of the SO_2 analyzer, as shown in the recorded calibration curves. It took approximately 3 minutes for the CO_2 analyzer to approach a 100% value and 6 minutes for the SO_2 analyzer to approach 100% value.

The average concentrations and CV term for both ducts are given in Table 4-c. SO_2, O_2 and CO_2 were respectively, 955 ppm, 5.8%, 12.3% (dry basis). The coefficients of variation for the CxV term for SO_2, O_2, and CO_2 were, respectively, ±19%, ±25% and ±20%. The average SO_2/CO_2 concentration ratio was equal to 77.9×10^{-4} with a coefficient of variation of 2.8%.

Humidity test results are shown in Table 5-a. The percent moisture calculation, based on average values for wet and dry bulb temperatures from both tests, is given in Appendix I, Calculation A. The percent moisture in the north and south ducts was equal to 11% and 10%, respectively. The molecular weight of the flue gas stream is calculated in Appendix I, Calculation B. The relative gas density for the north and south ducts was equal to 0.99 and 1.01 respectively. Emission calculations and total flue gas flow rate are given in Appendix I, Calculation C. The estimated SO_2 emission from both north and south ducts was equal to 475 x 10^{-3} kg/s, 17% higher than the calculated amount from fuel oil analysis (see Appendix I, Residual Fuel Oil Analysis). The CO_2 emission from both ducts was equal to 42 kg/s, 35% higher than the calculated amount from fuel oil analysis. The total flow measured was equal to 176 m^3/s at standard conditions (273°K and 101.33 N/m^2), which is equivalent to 373,000 SCFM (dry basis) or 573,000 ACFM (dry basis). An analysis of these results is presented in the following section.

c. Discussion of Results and Conclusions

Actual concentration and velocity data, describing stratification in a flue gas stream have been recorded at Boston Edison's Mystic Station for the air preheater outlet ducts for the higher sulfur oil fired Unit No. 6, immediately downstream of a 90° bend. A 9 probe equal area strategy was used. A summary of the results of the demonstration test is given in Table 6.

The expected emissions of SO_2 and CO_2, based on the residual fuel oil analysis (as shown in Appendix I), were equal to 405 x 10^{-3} kg/s and 31.0 kg/s, respectively. The total SO_2 and CO_2 emissions from the south and north ducts as calculated in Appendix I, Calculation C are equal to 475 x 10^{-3} kg/s and 42 kg/s, respectively. This implies a +17% error on SO_2 emission and a +35% error on CO_2 emission. The total measured flow rate was equal to 176.0 m^3/s (dry basis) at STP*.

* 273°K and 101.33 N/m^2

TABLE 6

SUMMARY OF THE DEMONSTRATION TEST
RESULTS FROM BOTH DUCTS

Test Load	144 mw gross output	
Fuel Consumption	9.92 kg/s (9820 gallons/hr, sp. gr. 0.96)	
Fuel Oil Analysis	2.1% S, 85.36% C, 11.45% H	
	(North Duct)	(South Duct)
Average SO_2 Concentration	917 ppm	993 ppm
Average CO_2 Concentration	11.6%	13.0%
Average O_2 Concentration	6.3%	5.2%
Average SO_2/CO_2 Concentration	79.1×10^{-4}	76.7×10^{-4}
Average Velocity	15 m/s	14 m/s
Average % Moisture	11%	10%
Average Temperature	138°C	130°C
Average Static Pressure	$97.2\ N/m^2 \times 10^3$	$97.6\ N/m^2 \times 10^3$
Effective Area of Duct	$10.5\ m^2$	$10.5\ m^2$
SO_2 Emission	229×10^{-3} kg/s	246×10^{-3} kg/s
CO_2 Emission	19.9 kg/s	22.1 kg/s
Flow Rate (DRY BASIS) At 273°K and $101.33\ N/m^2 \times 10^3$	$89.5\ m^3/s$	$86.5\ m^3/s$

The system was further analyzed in an attempt to discover the source of the error. Theoretical combustion based on 18% excess air (Calculation D) forcasted 12.08 m^3 of dry gases/kg of oil at standard conditions.* The estimated sulfur dioxide concentration was equal to 1180 ppm (dry basis) and the estimated carbon dioxide concentration was equal to 13.2% (dry basis). Because air in leakage occurred at the air preheater, the excess dilution caused by air was calculated from an oxygen balance (see Calculation E, Appenidx I); the expected SO_2 and CO_2 concentrations after dilution were found to be equal to 1055 ppm and 11.8% respectively. The average SO_2 concentration from measured values was equal to 955 ppm, i.e., 9% lower than expected. The average CO_2 concentration from measured values was equal to 12.3%, i.e., 4% higher than expected.

An analysis of the dry flue gas volumetric rate was performed (Appendix I, Calculation E). Based on the assumption that a +26% error originates from the flow rate measurements (+17% - (-9%)), air in leakage was estimated to be equal to 19.9 m^3/s (42,000 SCFM). As a result of this analysis, the oxygen concentration balance closed to within 9% and the CO_2 emission error to within 5%. Therefore, it is concluded that the large error in measuring the emission rate originated from an inadequate flow measurement.

It was previously stated[55] that "an accurate determination of the quality of gas flow is a prerequisite to a realistic evaluation of the total pollution effluent". The flow conditions at the after air preheater ducts were severe. The ducts followed a 90° bend, and a pulsating flow was encountered. The probable flow pattern is shown in Figure 14a and 14b. By using the S-pitot tube as a measuring device in a pulsating flow and not attempting to measure the velocity near the walls, additive errors were generated. The boundary layer error had already been estimated from preliminary test results to be near +8%; however, larger errors can also be expected[55]. Consequently, the true flow is less than the measured flow, as was discovered in this experimental test.

---

* 273°K and 101.33 N/m^2

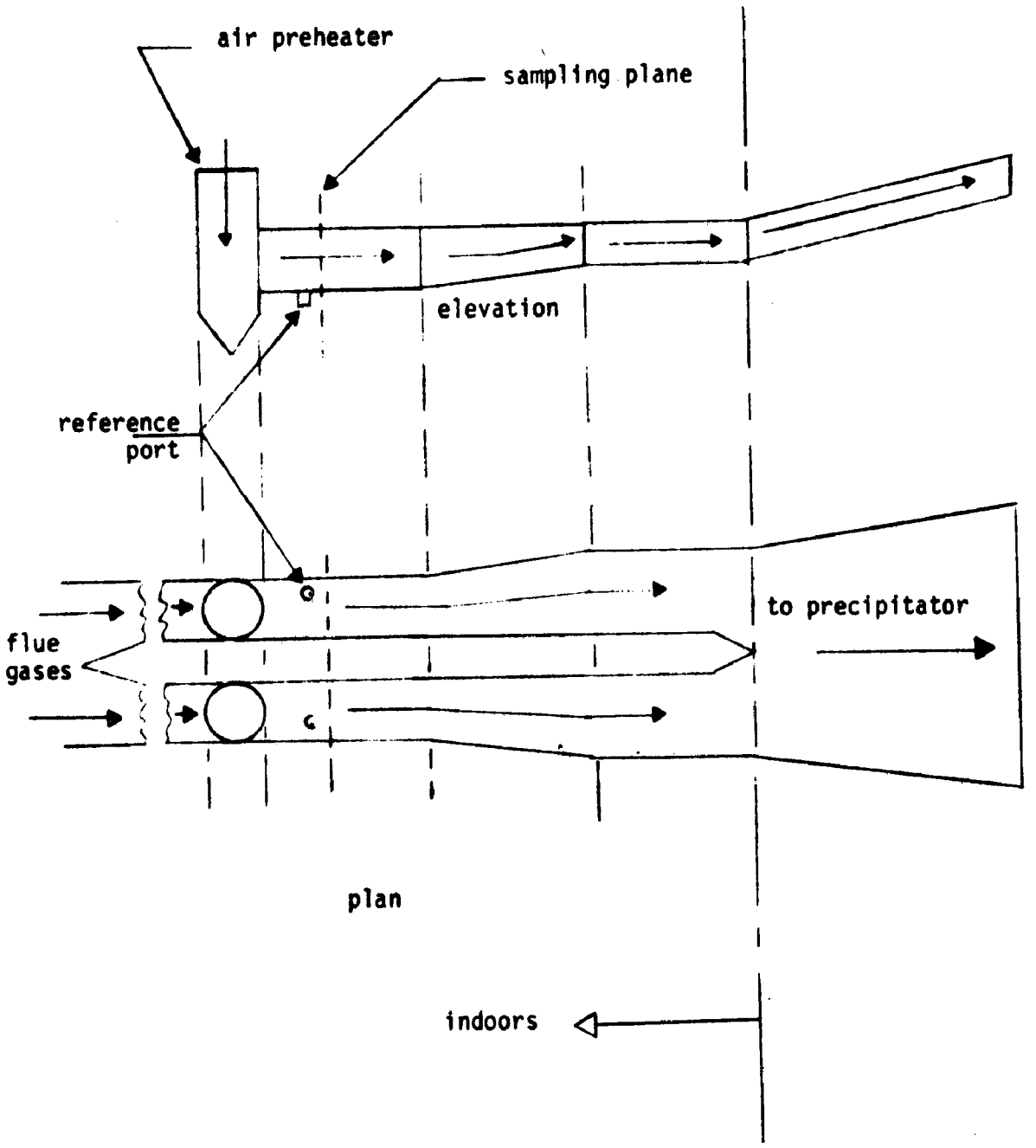

figure 14a. Schematic of Sampling Plane Position Relative to Air Preheater

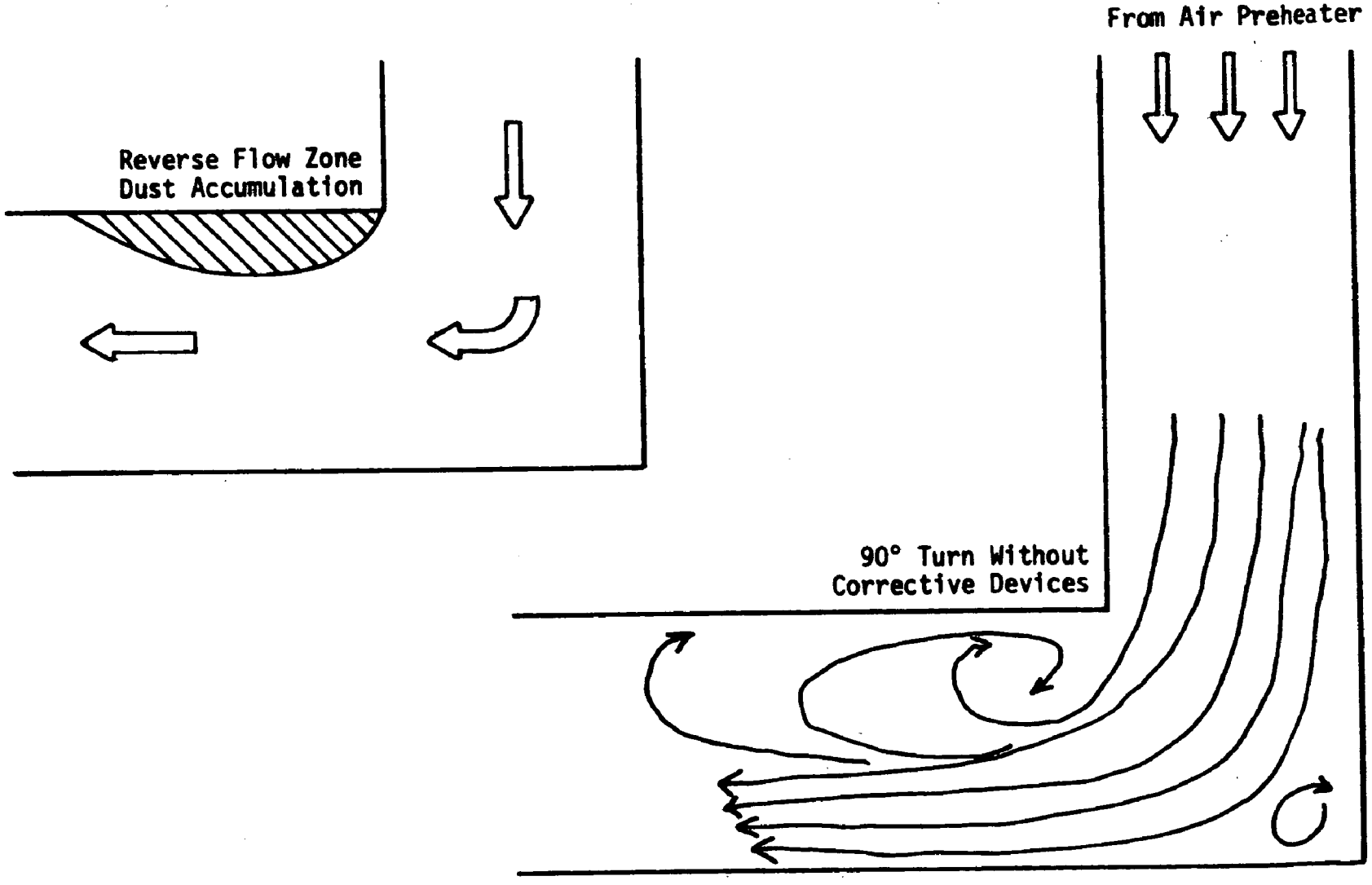

Figure 14b. Probable Flow Pattern At the After Air Preheater Ducts

To improve the accuracy and reliability of flow measurements in severe flow conditions (reverse flow, pulsating flow, etc.), new flow measuring devices have to be developed to handle all these flow conditions. Also, the boundary layer must be elevated in detail or its error accounted for in the analysis.

Because of the errors involved in the instrumental measurement and sampling, the SO_2/CO_2 concentration ratio technique can not be evaluated to better than experimental errors, i.e., analyzer accuracies, boiler feed rate, fuel composition, etc., (see estimations in Appendix I).

V. DISCUSSION AND RECOMMENDED PROCEDURES

A. GENERAL

At the conclusion of the three tasks in this program, two approaches can be identified which may be applied as the present state-of-the-art for extracting a representative gas sample from stratified process streams. These approaches are:

1. Single point sample extraction and analysis for the ratio of the test gas species, e.g., SO_2, to a reference species which is an intrinsic tracer of the process, e.g., CO_2.

2. Multi-point sample extraction of sample gas.

In our opinion, approach 1 is generally preferred over approach 2, on the basis of instrumental simplicity and absence of possible flow measurement problems.

At this time the exact accuracy of each method can not be specified in general terms. In the demonstration task (Task III), we found that it was not possible to close the material balance using approach 2 because of suspected error in the flow/velocity measurement, which was estimated at about 26% from the stoichiometry of the process. (This problem is explained in greater detail in the previous section and Appendix I.) The results from the intrinsic tracer or reference gas technique were encouraging, although there are still uncertainties associated with the gas analyzer measurement and the measurements for process parameters such as fuel rate. The instrumental advantage of this procedure is that a single extraction probe may be used and proportional sampling is not required.

B. PROCEDURES FOR REPRESENTATIVE SAMPLING USING AN INTRINSIC TRACER OR REFERENCE GAS

A reference tracer gas, produced during the process which produces the pollutant gas, may be used with process rate data to determine the mass flow or emission of the pollutant species. For example, in a combustion system such as described in Task III of this program, the mass flow of SO_2 was determined from the ratio of the concentration of SO_2 to the concentration of CO_2 in the flue gas, while the mass flow of CO_2 was calculated for fuel firing rate and fuel analysis, viz.:

$$\dot{M} = \frac{C}{C'} \dot{M}'$$

where: $\dot{M}$ is the pollutant gas mass flow
$\dot{M}'$ is the reference gas mass flow
C is the pollutant concentration
C' is the reference concentration.

Before applying this procedure, the test plane should be checked for gas stratification by surveying with a gas analyzer for the pollutant species desired or by Orsat or Fyrite for CO_2 or O_2. As a rule of thumb, about 16 samples well dispersed over the test plane should be taken. If stratification is not present, a stratified gas procedure is not necessary. If stratification is present, the intrinsic tracer/reference gas procedure may be applicable. In order to determine whether or not this procedure is applicable, a survey should be made by traversing the sample probe from the sampling system over the test plane, incorporating the two analyzers. This check is necessary to assure that the test gases and reference gases are stratified in the same manner. If it is known that the process stream is a mixture from two or more units manifolded together and the fuel in each unit is not identical, this method will not be applicable.

The survey data indicate that the set of ratios of test gas concentration to reference gas concentration should be within ±10% of the mean value for approximately 16 measurements. If this condition is met, the probe should be fixed for operation at or near a location giving the mean value.* An example of a typical sampling system for a test gas and a reference gas is given in Section IV under the equipment description for Task III.

At the same time that the gas concentration ratio is monitored, it is necessary to obtain process data on the fuel rate and the composition of the fuel, e.g., carbon content. From this data the mass flow of the reference gas can be calculated.

This approach is particularly interesting for the special application of determining the pollutant removal efficiency of a gas control system when the inlet and/or outlet gas streams are stratified. The fraction passed through the control device may be represented in the form of the previous equation by the following:

$$\frac{\dot{M}_o}{\dot{M}_i} = \frac{C_o/C_o'}{C_i/C_i'} \frac{\dot{M}'_o}{\dot{M}'_i}$$

where the subscripts o and i denote outlet and inlet, respectively. To be valid, the reference gas species must not have been removed by the control device, i.e., $\dot{M}'_o \approx \dot{M}'_i$. The fractional efficiency of the control system is given by the following:

$$\left[1 - \frac{C_o/C_o'}{C_i/C_i'}\right]$$

---

* These specifications are arbitrary; however, they are in accord with the procedures used in the field demonstration program. In our demonstration, this procedure predicted the SO_2 emission at 9% less than the value predicted stoichiometrically.

This technique requires only a single point gas extraction in the ductwork before and after the control device. The sampling system should be of the type described for SO_2 and CO_2 in Section IV, Task III of this report. If two sets of analyzers are used to determine the ratio of C_i/C_i' and Co/Co' (inlet and outlet), real-time efficiency measurements can be determined for the control device, thus allowing the device to be adjusted for optimum operation. This is similar to the approach one would use if the gases were unstratified; of course, only the pollutant species would be measured in this case.

This special procedure obviates the problems of obtaining fuel rate and fuel analysis data as well as total gas flow information. For these reasons, it is a very attractive procedure for measuring removal efficiencies of gas scrubbers.

C. SAMPLING ARRAY PROCEDURE

Sampling array concepts have been discussed earlier in Section IV. The sampling array procedure is generally applicable to all stratified streams. However, in some cases, the effort required to implement this procedure can be unattractively high. In addition, as discussed in Section IV, Task III, problems associated with measuring gas flow/velocity appear to adversely effect the measurement of the pollutant mass flow or emission. For this reason, sampling arrays are considered to be a "second choice" method to be used when the intrinsic tracer method is not applicable.

1. Pre-Survey to Assess Degree of Stratification

A preliminary investigation of the degree of gas and velocity stratification is necessary. The gas stream is surveyed at different locations in one plane of the duct, using Orsat or Fyrites for analysis of O_2 and CO_2 and S-pitot tubes for measurement of velocity. The survey is valid only if a constant process load is monitored. In this case, spatial variations are independent of time variations (unsteady state operations), thus allowing

the spatial variations to be fully evaluated. To check the stability of the operation during testing, a reference probe must be kept at a constant location in the duct while gas is withdrawn for analysis. Sequential analysis of gas and velocity measurements from a reference probe and a sampling point probe is recommended. When gas stratification is identified, a more rigorous survey must follow. If insignificant stratification is observed, it is not necessary to use a stratified gas procedure.

2. Rigorous Survey and Selection of Sampling Points

In order to obtain the complete velocity and concentration profiles of a gas stream section, the manual methods for traversing rectangular and circular ducts are recommended.

The 48 point equal area method or the 49 British Standard Methods may be used for rectangular duct traverses. For circular ducts, the cross section may be divided into 32 equal areas; this method traverses 4 diameters with 8 sampling points per diameter. As shown in Section IV, this number of samples with these locations provides a high probability of estimating the true emission.

When the velocity and concentration profiles are established for a given process load, these data can be used to determine an appropriate simplified sampling method which may be employed to obtain the emission rate to within an acceptable deviation from the real value. These data should be used in order to select a reduced number of sampling points from the rigorous survey data which give results that are equal or nearly equal to the results obtained from the rigorous survey. The possible methods may be selected from the following:

a. Use the computer program procedures detailed in Appendix J.

b. Generate expected values for a selected number of points, by manual interpolation between the data points, and then compare the mass flow from the summation of the generated points to the results from the rigorous survey. When an acceptable estimation, e.g. 5% is achieved with a minimum number of points, this number can be implemented in the measurement array.

It is likely that 9 or 16 points will be required for the equal area strategy for rectangular ducts. For circular ducts, the probable requirement will be 16 points obtained from 4 diameters, i.e. 4 points per diameter for high azimuthal stratification, or 16 points on two diameters for high radial stratification. If a reverse flow is encountered, a larger number of sampling points is recommended. When the appropriate number of sampling points is determined, based on the knowledge of the flow and concentration conditions, one can then proceed to design the appropriate sampling system and array.

3. Design, Construct and Install an Automatic Array of Proportional Samplers

The design of a sampling system is dependent mainly on the nature of the flow and concentration conditions. For non-reverse flow conditions and highly stratified concentration conditions, two alternative methods may be used to adjust sampling flow in proportion to gas velocity at the sampling points. One method would involve sampling from each point with a flow rate proportional to the velocity at the sampling point. A schematic diagram of this sampling system is shown in Figure 1. An alternative method would be to sample sequentially from each point for times proportional to the velocity at that point. The schematic diagram of this system is shown in Figure 2.

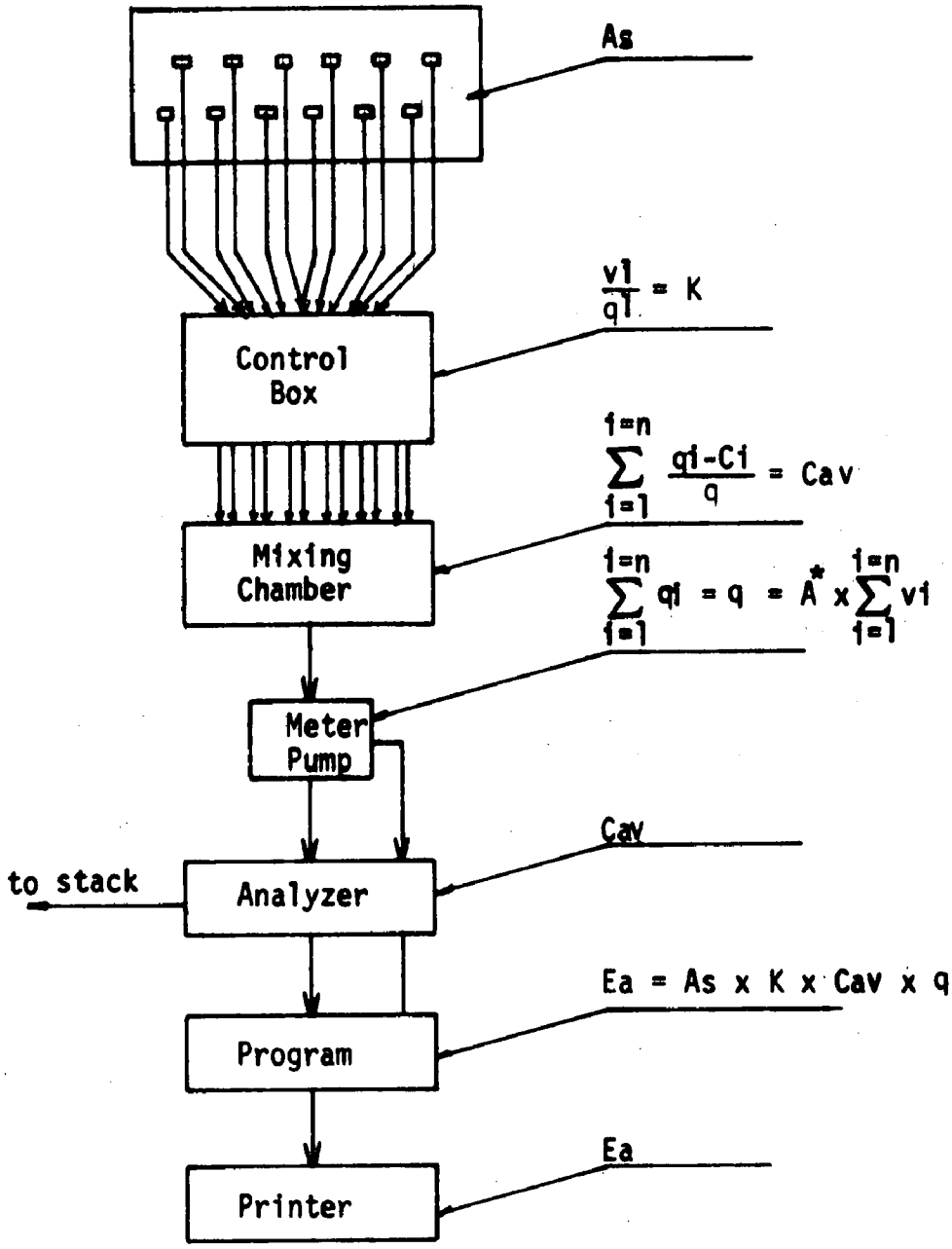

* A = area of sampling nozzle

Figure 1. For Non-Reverse Flow in Ducts

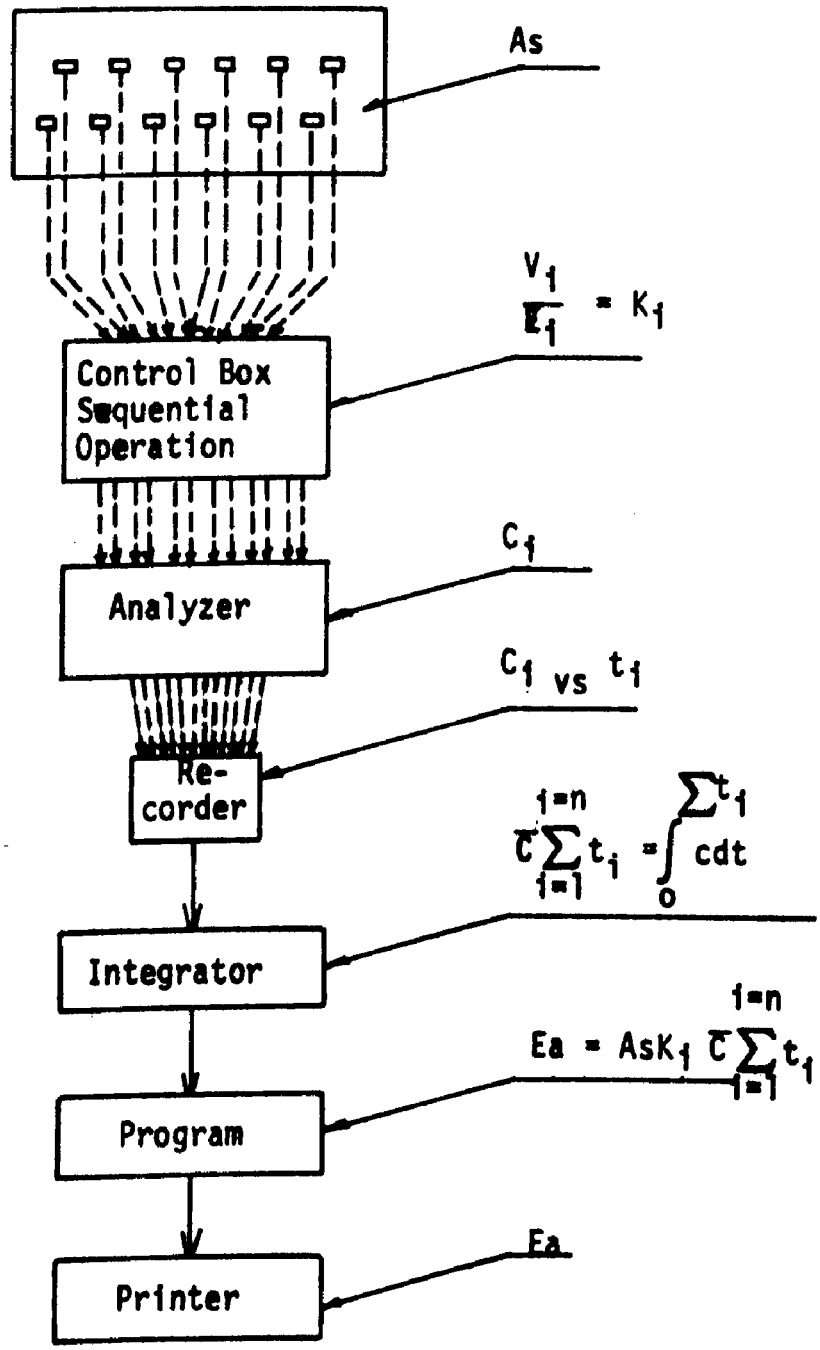

Figure 2. For Non-Reverse Flow In Ducts

When spatial concentration stratification is negligible and/or velocity stratification (C.V.* $\leq$ 10%), one can obtain an average concentration value by directly sampling with equal flow rates from each sampling point and mixing the sampling streams. If the value of the total flow is known, a reliable estimate of the emission rate may be obtained. The schematic diagram of this system is shown in Figure 3.

When reverse flow exists in the duct, the concentration and directional velocity for each sampling point must be recorded separately for each point. The concentration times velocity values are then algebraically added to account for the direction of the flow (reverse flow is negative velocity).

* Coefficient of variation

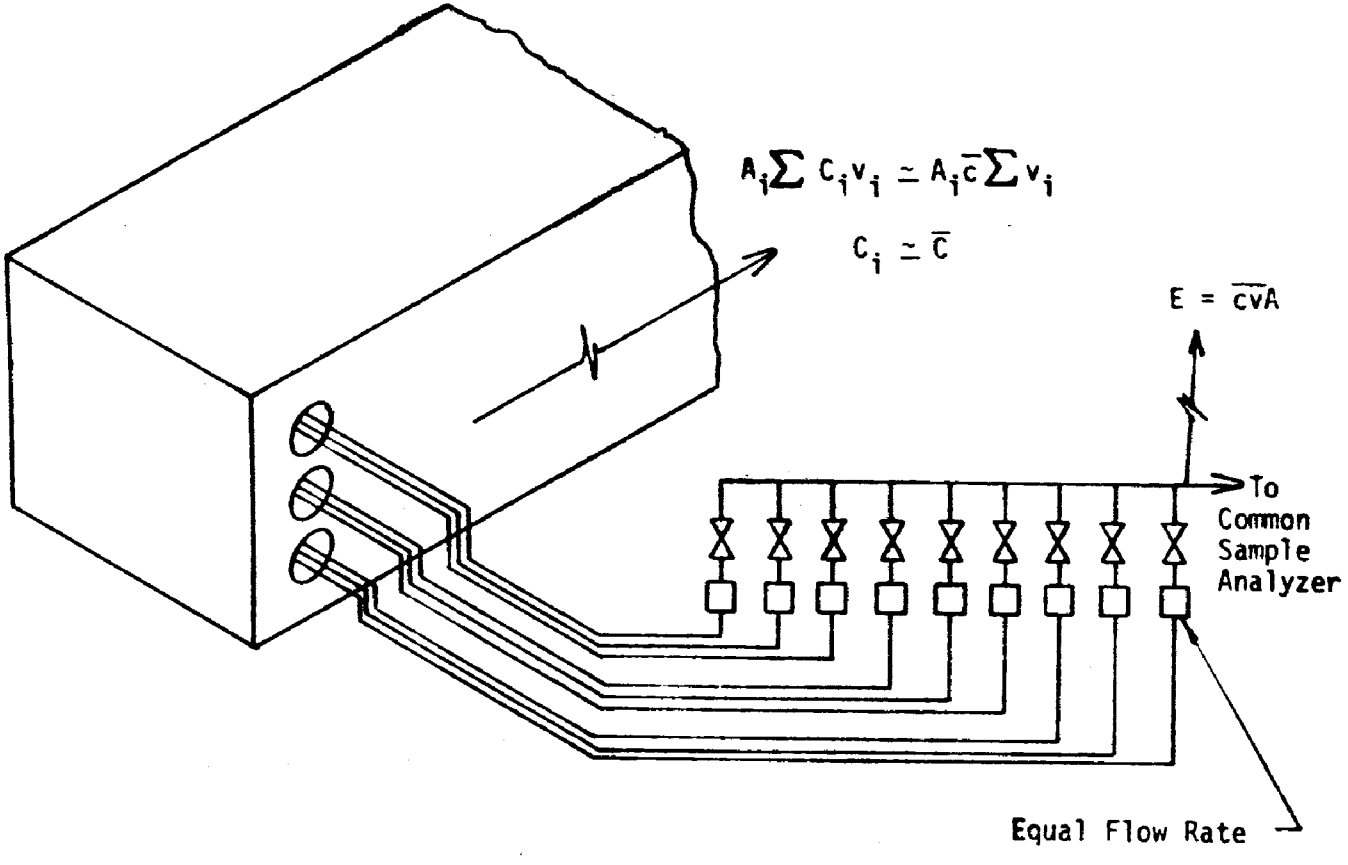

Figure 3 For Non-Reverse Flow in Ducts

SECTION VI

REFERENCES

1. Personal communication with R.W. Robinson, Manager, Field Testing and Performance Results, Combustion Engineering, Inc., Windsor, Connecticut.

2. Personal communication with K.O. Plache, Ellison Instrument Div. of Dieterich Standard Corp., Boulder, Colorado.

3. Spence, R.D., et al, and C.E. Rodes, "A Polymeric Interface for Monitoring SO_2 Emission from Stationary Sources", Paper No. 42C presented at the 74th National Meeting of the AICHE, New Orleans, Louisiana, March 1973, pp. 11-15.

4. Nieuwenhuizen, J.K. and H. Posthumus, "An Accurate Simple Method for Air-Flow Measurement in Field Tests on Air-Cooled Heat Transfer Equipment", J. Inst. Fuel, 40, 313 (1967), pp. 45-47.

5. Nonhebel, G., ed., Gas Purification Processes for Air Pollution Control. London.

6. Stairmand, C.J., "The Sampling of Dust Laden Gases", Trans. Inst. Chem. Engrs., 29 (1951), pp. 15-44.

7. Cooper, H.B.H., Jr., and A.T. Rossano, Jr., "Source Testing for Air Pollution Control", Environmental Science Services, 24 Danbury Rd., Wilton, Conn. 06897, Div. of E.R.A., pp. 63-66.

8. Hyde, P., "Particulate Sampling of Wigman Burners", Forest Research Laboratory, Oregon State University, Corvallis, Oregon, October, 1968.

9. Rosinski, J., and A. Lieberman, "An Automatic Isokinetic Sampling", Appl. Sci. Res., 6, Sec. A (1956), pp. 92-96.

10. Coenen, W., "A Simple Flow Sensitive Arrangement With a Thermistor and its Technical Application to Dust Measurement", Staub-Reinhalt Luft, 29, No. 11 (1969), pp. 16-22.

11. Grindell, D.H., "Monitoring Smoke and Flue Dust Emission", AEI Eng., 2, No. 5 (1962), pp. 229-235.

12. Gilmore, J.S., et al, "State of the Art: 1971 Instrumentation for Measurement of Particulate Emissions from Combustion Sources, Volume II: Particulate Mass - Detail Report", Thermo-Systems, Inc., St. Paul, Minnesota (PB-202-666), April 1971.

13. Granville, R.A. and W.G. Jaffrey, "Dust and Grit in Flue Gases", Engineering, Feb. 27, 1959, p. 285.

14. Wilson, K.D. and D.A. Falgout, "A New Approach to Isokinetic Null Probe Design", Environmental Engineering, Inc., Gainsville, Florida, Paper No. 72-32.

15. Edouard, L., "La Mesure des Concentrations en Poussière des Gaz à l'Entrée des Cheminées de la Centrale Thermique de Creil, Le Génie Civil, Physique Industrielle, 1961, p.270.

16. Donoso, J.J., "An Automatic Multiple Smoke Sampler", AIME TRANS., J. Metals, 188 (March 1950), pp. 610-612.

17. Hyde, P., "Particulate Sampling of Wigman Burners", Forest Research Laboratory, Oregon State University, Corvallis, Oregon, October 1968.

18. Moore, A.S., "Sampling Dust in the Bureau of Mines Coal-Fired Gas Turbine", Combustion, (October 1973), pp. 28-30.

19. Jackson, M.R., et al, "Prototype Fly Ash Monitor for Municipal Incinerator Stacks", Proc. National Incinerator Conf. (1970), p. 182.

20. "Development of an Automatic Fly Ash Monitor", report prepared by IIT Research Institute under contract to APWA Research Foundation, Chicago, Illinois.

21. Personal communication with Dr. Winston, IKOR Inc., 2nd Avenue, Burlington, Mass. 01803.

22. Bosch, J., "Device for the Continuous Determination of the Dust Flow in Flowing Gases", Staub-Reinhalt Luft, 32, No. 11 (1972), pp. 8-14.

23. Ounsted, D., "A Rapid, Multipoint, Oxygen Analyzer for Power Station Flue Gases", J. Inst. Fuel, 42 (1969), pp. 408-411.

24. Williamson, R.C. and J.A. Russell, "On-Line Gas Analysis of Jet Engine Exhaust", Society of Automotive Engineers (SAE), Combined Fuels and Lubricants, Power Plant and Transportation Meetings, Pittsburgh, Pa., October 30 - November 3, 1967. Paper No. 670945.

25. Fair, J.R., B.B. Crocker, and H.R. Null, "Sampling and Analyzing", Chem. Eng., (Sept. 18, 1972), p. 146.

26. Dresia, H. and F. Spohr, "Experience With the Radiometric Dust Measuring Unit Beta Staubmeter", Staub-Reinhalt Luft, 31, No. 6 (1971), p. 19. (English).

27. Benedict, R.P., Fundamentals of Temperature, Pressure and Flow Measurements. John Wiley & Sons, Inc. 1969. p. 129.

28. Fitton, A. and C. P. Sayles, "The Collection of a Representative Flue Dust Sample", Engineering, p. 229, Feb. 22, 1952.

29. Personal communication with Prof. Paul Giever, University of Michigan, (1969).

30. Sherwood and Pigford, Absorption and Extraction, McGraw Hill Book Co., New York (1952).

31. Luxl, F. C., "Analyzing and Control of Oxygen in Boiler Flue Gas", Paper No. 61-WA-340, ASME Annual Meeting (1961).

32. ASME, "Flue and Exhaust Gas Analysis", Report No. PTC 19.10 (1968).

33. Hawksley, P. G. W., et.al., "Measurement of Solids in Flue Gases", British Coal Utilization Research Association, Leatherhead (1961).

34. Personal communication with R. Larkin, NAPCA, Cincinnati, Ohio, (1969).

35. Ower, E. and R. C. Pankhurst, Measurement of Air Flow, Pergamon Press (1966).

36. Federal Register, Vol. 36, No. 247, EPA, Standards of Performance for New Stationary Sources, (December 23, 1971).

37. "Determining Dust Concentration in a Gas Stream", PTC 27-1957, The Amer. Soc. of Mech. Engineers, New York (1957).

38. "Methods of Testing Fans for General Purposes", Part I, B. S. 848, British Standards Institution, London, (1963).

39. "Flow Measurement", B. S. 1042: 1943, British Standards Institution, London (1951).

40. Haaland, H. H., Editor, "Methods for Determination of Velocity, Volume, Dust and Mist Contents of Gases", Bulletin WP-50, 7th Ed., Western Precipitation Div., Joy Manufacturing Co., Los Angeles (1968).

41. ASTM D-22 Subcommittee VI, Tentative Standard Method for Sampling Stacks, (1970).

42. ASME, Fluid Velocity Measurement, PTC 19.5.3-1965.

43. Keffer, J. F. and Baines, W. D., "The Round Turbulent Jet in A Cross Wind", Journal of Fluid Mechanics, Vol. 15, Pt. 4, pp. 481-496, (1963).

44. Platten, J. L. and Keffer, J. F., "Deflected Turbulent Jet Flows", Journal of Applied Mechanics, Vol. 38, No. 4, pp. 756-758, (1971).

45. Pratte, B. D. and Baines, W. D., "Profiles of the Round Turbulent Jet In A Cross Flow", Journal of the Hydraulics Division, ASCE, Vol. 92, No. HY6, pp. 53-64, (1967).

46. Wu, J., "Near-Field Trajectory of Turbulent Jets Discharged at Various Inclinations into a Uniform Cross Flow", AIAA Journal, Vol. 11, No. 11, pp. 1579-1581, (1973).

47. Chilton, T. H., Genereaux, R. P., "The Mixing of Gases for Reaction", AIChE Trans., 25, (1930).

48. Hoult, D. P., Weil, J. C., "Turbulent Plume in a Laminar Cross Flow", Atmospheric Environment, 6, (1972).

49. Deutsche, N., DIN 4702 Blattz, Seite 16, Beuthvertrieb GmbH, Berlin 30, Koln, (December 1967).

50. B. P. Research Centre, Sunbury on Thames, Middlesex, R. W. Butcher, "Continuous Combustion Equipment", Tech Memo No. 120496 Project No. 106, 15.1.68.

51. B. P. Research Centre, Petroleum Div. Sunbury on Thames, "The Sampling of Gases from Ducts, Design of Multihole Sampling Probes", Tech Memo No. 110030, Project No. 110, 7.3.60.

52. Personal communication with Dr. A. Oring, Pittsburgh Energy Research Center, Pennsylvania.

53. Personal communication with Falkenberry, TVA, Chatanooga, Tennessee.

54. Prepared for Environmental Protection Agency under Contract No. 22-69-95.

55. Burton, C. L., "Quantitation of Stack Gas Flow", Journal of the Air Pollution Control Association, Vol. 29, No. 8, p. 631, (1972).

TECHNICAL REPORT DATA
(Please read Instructions on the reverse before completing)

1. REPORT NO. EPA-650/2-74-086-a and b	2.
3. RECIPIENT'S ACCESSION NO.	
4. TITLE AND SUBTITLE Procedures for Measurement in Stratified Gases, Volumes I and II (Appendices)	5. REPORT DATE September 1974
	6. PERFORMING ORGANIZATION CODE
7. AUTHOR(S) A. Zakak, R. Siegel, J. McCoy, S. Arab-Ismali, J. Porter, L. Harris, L. Forney, and R. Lisk	8. PERFORMING ORGANIZATION REPORT NO.
9. PERFORMING ORGANIZATION NAME AND ADDRESS Walden Research Division of Abcor, Inc. 201 Vassar Street Cambridge, Mass. 02139	10. PROGRAM ELEMENT NO. 1AB013; ROAP 21ACX-092
	11. CONTRACT/GRANT NO. 68-02-1306
12. SPONSORING AGENCY NAME AND ADDRESS EPA, Office of Research and Development NERC-RTP, Control Systems Laboratory Research Triangle Park, NC 27711	13. TYPE OF REPORT AND PERIOD COVERED Final; 6/73-5/74
	14. SPONSORING AGENCY CODE
15. SUPPLEMENTARY NOTES	

16. ABSTRACT The report gives results of a program to develop methods for the continuous extraction of representative gas samples from gas streams that exhibit compositional stratification. The program considered available data in the literature, as well as field data generated during the program. Wind tunnel tests and mathematical modeling were used to develop sampling methodologies which are recommended. Data from the literature, as well as program data, indicate that stratification exists, although it is unlikely that gas stratification is as widespread or as severe as particulate stratification. Depending on conditions, two different methods are recommended. The first method involves monitoring the ratio of SO2, NOx, etc. to CO2 at a single location. Then, from the measured fuel flow and chemistry of the process, the mass flow of CO2 can be predicted. The product of the measured ratio and the predicted mass flow of CO2 is the mass flow of the pollutant. Where conditions do not permit using this method, it is recommended that a schedule of manual surveys be conducted followed by installation of a multi-element proportional sampler and gas velocity array.

17. KEY WORDS AND DOCUMENT ANALYSIS

a. DESCRIPTORS	b. IDENTIFIERS/OPEN ENDED TERMS	c. COSATI Field/Group
Air Pollution Measurement Gases Sampling Stratification Wind Tunnels Mathematical Models Data Carbon Dioxide	Air Pollution Control Stationary Sources Proportional Sampler Gas Velocity Array	13B, 12A 14B 07D, 07B

18. DISTRIBUTION STATEMENT Unlimited	19. SECURITY CLASS *(This Report)* Unclassified	21. NO. OF PAGES 276
	20. SECURITY CLASS *(This page)* Unclassified	22. PRICE

EPA Form 2220-1 (9-73)